Application of Remote Sensing in the Assessment of Oil Pollution Impacts on Biodiversity in Rivers State, Nigeria

A thesis submitted for the degree of Doctor of Philosophy at the University of Leicester

By

Nkeiruka Nneti Onyia (B. Agric., MPhil, AFHEA)

School of Geography, Geology and the Environment

University of Leicester

January 2020

Abstract

Application of Remote Sensing in the Assessment of Oil Pollution Impacts on Biodiversity in Rivers State, Nigeria

Nkeiruka Nneti Onyia

Biodiversity loss remains a global challenge, and monitoring methods are often limited in their coverage. Rivers State is a biodiversity hotspot because of the high number of endemic species endangered by oil pollution. This thesis investigates the potential of integrating remote sensing tools for monitoring biodiversity in the State using vascular plant species as indicators. Satellite data from Hyperion, Sentinel 2A and Landsat were analysed for their usefulness. Soil samples from polluted and control transects were analysed for total petroleum hydrocarbon (TPH), phosphorus (P), lead (Pb), temperature, acidity, species diversity, abundance and leaf chlorophyll concentration. Field data results showed significant differences in all variables between polluted and control transects. Average TPH on polluted transects was 12,296 mg/kg, and on control transects was 40.53 mg/kg. 163 plant species of 52 families were recorded with *Poaceae and Cyperaceae* the most abundant. Floristic data ordinated on orthogonal axes of soil parameters revealed that TPH strongly influenced species occurrence (r = -0.42) and abundance (r = -0.39). Similarly, application of the spectral variability hypothesis (SVH) revealed the underlying environmental gradient controlling vegetation composition on polluted transects as TPH and on control transects as P. Models of relationship between spectral metrics and soil properties estimated soil TPH (R^2 = 0.45) and P (R^2 = 0.62) with marginal errors. Hyperion data provided better insight into vegetation response to oil pollution. Continuum removed reflectance, band depths of absorption maxima, red edge reflectance all significantly differed between polluted and control vegetation. Furthermore, a new index created from TPH sensitive Hyperion wavelengths- normalised difference vegetation vigour index (NDVVI) outperformed traditional narrowband vegetation indices (NBVIs) in models estimating species diversity in Kporghor. R^2 and RMSE values for Shannon's index were 0.54 and 0.5 for NDVVI-based models and 0.2 and 0.67 for NBVI-based models respectively. This research provides evidence of oil pollution effect on vegetation composition, abundance, growth and reflectance and outlines how this information can be used for biodiversity monitoring.

Acknowledgements

Table of contents

List of Figures

List of Tables

14

15

1 Introduction

This chapter provides background information for this research, explaining the oil pollution problem and its impact on biodiversity in the study area. It also outlines the justification for the study and the potential contribution to remedying the myriad of social issues associated with oil pollution in the study area.

1.1 Research Background

The Niger Delta is one of the most extensive wetlands in the world and is Africa's largest delta. It consists of unique ecological zones, which extend from the coastal barrier ridges, inland to lowland rainforest zone. The well-endowed ecosystem is abundantly rich in biodiversity with very high densities of flora and fauna (Emoyan, Akpoborie and Akporhonor, 2008). The Niger Delta is part of the Guinean Forests Ecosystems of West Africa classified as a biodiversity hotspot (biologically rich and threatened ecological habitat). This region originally estimated to cover $1,300,000$ km^2 is fragmented and most of its tropical forest degraded due to mainly human activities. Although severely diminished (only about $140,000$ km^2 remains) the ecosystem harbours about 2000 endemic species from approximately 9000 vascular plant species (Khaligian, 2012). The significant diversity of the Niger Delta has degraded considerably due to oil-related anthropogenic activities (Agbogidi and Ofuoku, 2006).

Oil exploration in the Niger Delta commenced since the 1950s (Aroh *et al.* 2010). Over the years, the industry has expanded to include oil drilling, production, transportation, processing and storage. Accordingly, as noted by Oyinloye and Olamiju, (2013) and other researchers, oil production accounts for up to 96% of the Nigerian national economy. This growth has, however, come at an enormous cost to the environment of the Niger Delta with oil spillages, gas flaring, inappropriate waste disposal (solids and liquids), discharge of toxic chemicals, land use changes including forest fragmentation and degradation, flooding and soil erosion, and so on adversely impacting on the environment (Emoyan, Akpoborie and Akporhonor, 2008; Opukri and Ibaba, 2008).

Researchers have investigated the significant impacts of the various oil spills on the mangrove forest. Corcoran *et al.* (2007) reported a reduction of 26% in the mangrove forest within the Niger Delta since the oil boom. Similarly, Osuji *et al.* (2004) and United Nations Environmental Programme (UNEP, 2011) following a survey of different parts of the region revealed the disastrous impact of oil pollution to mangrove and other vegetation ranging from extreme stress to destruction. Several investigations such as Zabbey (2004), Osuji *et al.* (2004), Nwilo and Badejo, (2005), Opukri and Ibaba, (2008), Ugochukwu and Ertel (2008) also revealed that oil and gas operations not only cause environmental degradation in the sensitive ecosystem, they destroy the traditional livelihood of residents, whose main occupations are fishing and farming. Additionally, oil and gas operations affect weather conditions, soil fertility, waterways and habitats for wildlife; cause acid rains and drastically reduce agricultural yields. These negative impacts subsequently result in migration of endemic fauna as well as social displacements of inhabitants of the affected areas.

In the face of these concerns, and the need to sustainably meet the increasing demand for natural resources due to the population explosion in the region, policymakers, resource managers, and other stakeholders must employ appropriate tools for environmental and resource assessment, monitoring and management. As biodiversity is an essential natural resource in the Niger Delta, its conservation is a high priority but delicate due to the complexity of the concept and the global expectation of contracting parties to meet the targets of many international agreements such as the United Nations Environmental Programme Convention on Biological Diversity (UNEP-CBD). The CBD which came into force in December 1993 demands that all contracting parties develop national strategies, plans and programmes for the conservation and sustainable use of biological diversity (Article 6 of the CBD). In Article 7, it reiterates that nations are obliged to develop mechanisms to identify its components of biological diversity, monitor these components; identify processes/ activities that adversely impact on biodiversity and organise and maintain the collated data (UNEP, 1992). Thus, it is crucial for Nigeria, a party to this convention to develop a strategic and coherent approach to biodiversity management (identification, monitoring and conservation) particularly in the Niger Delta region. Presently this is not the case. Firstly, information on biodiversity across the vast and ecologically dense Niger Delta region is fragmented, incomplete, outdated, offline or even non-existent (United Nations

Development Programme UNDP, 2010). Different and sometimes conflicting organisations commonly store the available data, thereby rendering data inaccessible and non-exchangeable. The absence of reliable information has severe consequences for, not only understanding regional biodiversity but also hampers the selection and development of appropriate indicators for monitoring of temporal and spatial changes in ecosystems (Salem, 2003). It also hinders effective biodiversity-oriented decision making across the oil and gas industry in Nigeria (UNDP , 2010).

To remedy this situation, researchers have explored various data acquisition methods to determine the biodiversity status in the Niger Delta and establish links between oil exploration and biodiversity loss in the region. These include (Environmental Resources Managers Limited, (ERML), 1997; World Bank, 1995; Ohimain, 2003; Ohimain, 2004; Onwuka, 2005; Olajire *et al.* 2005; Osuji and Ezebuiro, 2006; Agbagwa, 2008; Agbagwa and Akpokodje, 2010; Agbagwa and Ndukwu, 2014). Most of these studies utilised traditional methods of data collection including sampling using quadrats or transects (line, point and Recce walk). For instance, Osuji *et al.* (2004) adopted a modified sampling technique, which involved field reconnaissance surveys, grid plots and quadrants for a post-impact assessment of oil pollution on soil, fauna and flora. Luisella and Akani (2003) working with freshwater turtles to determine the effects of oil pollution on the community adopted another traditional method which involved surveying, hoop traps, dip-netting and trawling to collect specimens for their study.

Similarly, Daniel-Kalio and Braide (2002) conducted a study of the impact of accidental oil spill on cultivated and natural vegetation in a wetland area of the Niger Delta using traditional techniques of data collection which included the establishment of transects on the oil spill sites and the surrounding areas. These traditional approaches to measuring biodiversity at local scales are time-consuming, challenging, and expensive. They are also skill and experience-dependent and often adversely affect the object and area of study. Furthermore, the methods are spatially limited and are incapable of generating relevant data at regional and global scales (Duro *et al.* 2007). With increasing global effort channeled towards reducing biodiversity loss, it is pertinent to investigate the adverse effects of oil spills on the

environment that may have escaped previous studies relying on traditional biodiversity monitoring methods.

Over the years, remote sensing (RS) have increasingly become indispensable tools in the collection, analysis and management of information about the earth's environment and resources. Various studies explored the application of RS in environmental management and conservation programmes, for instance, Duro *et al.* (2007) who examined the potential for integrating remote sensing in developing a national biodiversity monitoring system for Canada that is applicable across regions and continents. Earlier researchers such as Petit *et al.* (2001) had used remote sensing data to analyse change processes and project short-term land-cover changes in Zambia. More recent studies have successfully integrated remotely sensed data with traditional methods for the ecosystem and ecosystem service assessments (Vihervaara *et al.* 2014; Andrew, Wulder and Nelson, 2014).

There is however a paucity of literature on this subject (biodiversity monitoring) that utilises remote sensing tools in the Niger Delta region of Nigeria. A significant proportion of the available literature on the application of RS in biodiversity-related studies is from developed countries. The bulk of literature originating from Nigeria, report investigations in the Niger Delta for instance, (Fagbami, Udo and Odu, 2009; Adegoke *et al.* 2010; Adoki, 2012; Oyinloye and Olamiju, 2013; Kuenzer *et al.* 2014); but none has addressed oil pollution in the light of these technological advancements. A thorough review of related literature has hitherto failed to reveal a previous study that documented the species diversity index of the study area, investigated the impact of oil pollution on biodiversity in the Niger delta utilising RS techniques and developed prediction models using spectral metrics to estimate species richness and diversity. These knowledge gaps are what the current study aims to address using methods that are repeatable, scalable and accessible to interested parties. The study adopted an integrated approach to data generation and evaluation to achieve this aim. The integrated approach includes the use of free satellite data, open source software for image and statistical analyses, field survey applying standard sampling methods and laboratory analysis in an internationally certified laboratory.

1.2 Justification of the Study

1.2.1 Crude Oil Pollution and Effects in Rivers State

Oil pollution is the contamination of any substrate such as the soil or air with materials containing petroleum hydrocarbons. Environmental pollution is the direct or indirect alterations of the physical, thermal, biological or radioactive properties of any part of the environment in such a way as to create a hazard or potential hazard to health, safety and well-being of any living species (Oyebadejo and Ugbaja, 1995). the European Union Water Framework Directive (2000) defines pollution as the 'direct or indirect introduction, as a result of human activity, of substances or heat into the air, water or land which may be harmful to human health or the quality of aquatic ecosystems or terrestrial ecosystems'(p. L327/7). Basorun and Olamiju (2013) reported that the effects of pollution on the environment could be immediate (primary effects) or delayed (secondary effects). While primary effects occur immediately after contamination, for instance, the death of marine plants and wildlife after an oil spill at sea; secondary effects are often delayed or persist in the environment for years sometimes in negligible amounts. There are various sources of oil pollution; however, this study limits to pollution caused by crude oil spills from damaged pipelines.

Rivers State extends to slightly over 11000 km^2 in the southernmost part of the Niger Delta region. According to the National Census in 2006, the State has a population of over 5 million people administered in 23 local government areas (National Population Commission, 2015). The indigenous people of Rivers State have lived in the Niger Delta region for over 500 years in densely populated close-knit rural settings. The people are primarily farmers and anglers who depend on the natural resources within their locality. Archaeological and historical evidence showed that the people had a well-established social system that placed great value on the environment from where they derived their livelihood. This social system also, through the observance of traditions rooted in nature; ensure sustainable exploitation of natural resources and the protection of biodiversity. For instance, forests (usually communally owned) were not just perceived as a piece of land where trees and animals dwell, but as an "intrinsically sacred possession" hence indiscriminate felling of trees and hunting

animals were forbidden (The Ecumenical Council for Corporate Responsibility, (ECCR), 2010).

Before the discovery of oil, agriculture was the primary source of income for the inhabitants. More than 44 per cent of the rural population engaged in the farming of cassava, maize, yam, plantain, palm oil and scavenging for periwinkles, snails, mushrooms and artisanal fishing. About 18 per cent were involved in local trading while 10 per cent were service providers such as tailors, transporters, carpenters and so on (Alagoa and Clark, 2009). Since the 1950s, oil exploration has been ongoing in Rivers State with Shell Petroleum Development Company (SPDC) Nigeria Limited as the principal operators (Human Rights Watch, 1999; Lindén and Pålsson, 2013). Nigeria is the 5th highest exporter of crude oil in the world with about 2.524 million barrels of oil exported every day (Central Intelligence Agency, 2015). Presently all the oil comes from the Niger Delta region and accounts for 95% of the foreign exchange earnings of the country. Consequently, the region is subject to alarming levels of environmental pollution from oil spills and gas flaring (Oyeshola, Fayomi and Ifedayo, 2011). Oyinloye and Olamiju (2013) reported that in the 50 years of oil exploration in Nigeria, there are records of about 6000 spill incidents discharging over 5 million barrels of crude oil into the environment.

For several years, Rivers State was an arena of restiveness and conflict due to the impact of oil exploration activities on the environment, health and livelihood of the host communities. Oil spills from leaking pipelines (huge pipelines that carry oil to other parts of the country crisscross the region); wellheads and flow stations, transportation, oil bunkering, artisanal refineries have frequently occurred yet under-reported for decades in the Niger Delta (Mmom and Arokoyu, 2010; United Nations Environmental Programme, 2011; Lindén and Pålsson, 2013). The influence of tides and floods further exacerbate the damage by spreading the spillage over large areas of vulnerable ecosystems. What was once a significant wetland is now a region whose residents can no longer subsist on traditional fishing and farming (United Nations Environmental Programme, 2011; Oluduro, 2012). The drilling for oil has also led to gas flares where billions of cubic feet of gas is burnt daily.

Incidents of human rights abuses in the form of environmental degradation abound in the Niger Delta where the oil wealth originates. For instance, HRW (1999) documented that barely 27 per cent of the population have access to safe potable water, while only about 30 per cent enjoy electricity, usually privately sourced. They also asserted that 90 per cent of the populace lives below $2 a day while 80% are unemployed and about 30 per cent are illiterate. In the same vein, a report by the Ecumenical Council for Corporate Responsibility (ECCR) in 2010 highlighted the impact of oil and gas operations in the Niger Delta on life expectancy in the region. From about 70 years, age has markedly dropped to 45 years. It also reported that the delta, which was once a net food exporter now imports 80 per cent of its food and the health and education facilities colossally dilapidated in the rural areas (The Ecumenical Council for Corporate Responsibility, (ECCR), 2010).

This dismal situation reiterates the need for substantive change in the manner of handling environmental issues in Nigeria. The focus needs to shift from reactive to proactive if the 2020 Aichi targets of the United Nations Convention on Biodiversity (CBD), which Nigeria is party to, are to be met. The results of this study will provide relevant tools to support this change and equip stakeholders with resources that will facilitate proactive management of biodiversity.

1.2.2 Importance of Biodiversity Monitoring in the Niger Delta

Rivers State is a biodiversity hot spot with a significant concentration of various species most of which are endemic (United Nations Development Programme, 2006; Nzeadibe *et al.* 2011). The depletion of these natural resources is alarming due to a combination of several factors. In recent years, in addition to licensed oil operators, many artisanal refineries operating illegally across the region have gained a foothold in the region. Spillages have often occurred from oil exploration activities such as drilling, transportation, bunkering, burst pipes and uncleansed oil spills. The growth of the oil industry resulted in an unprecedented population explosion. A combination of both factors in concert with institutional laxity in environmental protection "led to substantial damage to Nigeria's environment" (Ngoran, 2011). The implication for the environment is massive degradation and biodiversity loss (Oluduro, 2012). Several studies report a correlation between the

wanton environmental degradation in the Niger Delta and the rise of violent conflicts in the region (Watts, 2004; Obi, 2009; Orji, 2012; Adams and Ogbonnaya, 2014).

The failure of regulatory agencies to enforce environmental laws that address the situation and offer viable remedies has been appalling and definitive (Okwoche, 2011; Orji, 2012; Odoeme, 2013). The oil companies have not helped matters due to their reluctance to own-up to spills, engage in effective clean-up procedures or pay commensurate compensation to victims. The oil companies also hoard the relevant data and fail to maintain their facilities (Adujie, 2010; Duffield, 2010; Oluduro, 2012). As reported by Adujie (2010), the oil companies have demonstrated double standards in response to environmental pollution in the Niger Delta. For instance, in the aftermath of the Gulf of Mexico spill, oil companies voluntarily carried out remediative actions and offered compensations to individuals and companies even well before the effects and consequences of pollution were visible. However, the same companies have consistently ignored and disregarded clear cases of extreme environmental pollution and degradation leading to loss of livelihoods, poverty, and even deaths in Niger Delta. Consequently, host communities through civil and militant groups resort to demonstrations, attack oil installations and disrupt oil production activities across the region. The ensuing chaos has resulted in the loss of revenues to the country of up to 543 million dollars per day at the peak of the crises (Obi, 2009; Adujie, 2010; Orji, 2012; Odoeme, 2013).

A comprehensive review of the Nigerian legal system by Oluduro (2012) confirmed that there is inadequate legislation for compensating victims of oil spills and environmental damage. He suggested that an acceptable regime is enforced to protect the environment and inhabitants of oil-rich areas. Effective enactment of such important laws demands among others, access to a reliable, valid data set portraying the before and after scenarios of the impacted area. A structured monitoring programme can only obtain such data for Nigeria as a whole and Rivers State in particular.

A well-endowed biodiversity hotspot like Rivers State in Nigeria constantly subjected to oil spillages, biodiversity monitoring is crucial for several reasons, including the need to meet the strategic goals of the Aichi Biodiversity Targets. However, conventional monitoring

method such as field survey is not sufficient due to the constraints of time, equipment and accessibility associated with the study area. Hence, the proposal for integrating remote sensing data with field data to develop prediction models for biodiversity estimation using vascular plants as surrogates. Moreover, the need to monitor the variations and patterns of ecosystem processes, structures and functions demand the integration of remote sensing and field-based management practices (Gould, 2000). Vascular plant species serve as valuable biodiversity indicators because they are identifiable, sampled, stored or transported and distributed over a wide range of habitats and environments (Faith and Walker, 1996). Pereira and Cooper (2006) asserted the suitability of vascular plants species for monitoring biodiversity.

The present study aims to investigate the most appropriate means for biodiversity monitoring in the Niger Delta using Rivers State as a case study that will reflect the devastating impact of oil pollution on the environment. Results will provide reliable and verifiable data for decision making towards achieving both national and global goals.

1.3 Summary

This chapter provided a background to the problem tackled in this research and the justification. Chapter 2 will provide a detailed review of the literature addressing the concept of remote sensing in biodiversity monitoring.

2 Literature Review

This chapter explores the literature on biodiversity monitoring, outlining the global history of conservation efforts, progress and challenges. It also provides a review of biodiversity monitoring methods, advancing from traditional field sampling practices to integrated approaches using earth observation tools. Furthermore, relevant concepts in biodiversity monitoring and conservation such as biodiversity indicators, essential biodiversity variables and vegetation indices are discussed. Finally, the chapter outlines the aim and objectives of this research as well as the thesis structure.

2.1 Timeline of Global Biodiversity Monitoring

The earth has the natural capacity to achieve and maintain a balance through the interactions and interdependency of the various species of living organisms inhabiting it. Although humans and other organisms (flora and fauna) depend on biodiversity for services such as water cycle and soil formation; biological resources such as food and medicine; and social benefits such as research, education and cultural values (Shah, 2014), the increasing pressure on these resources have negatively interfered with nature's balance. Pitman (1953) stated that human activities, particularly the introduction of alien species adversely affect the proliferation of the indigenous species and upset the equilibrium of nature.

Scientists have warned from the 1970s, that the loss of planetary biodiversity occurs at an unprecedented rate with dire consequences for the earth and all its inhabitants. Environmentalists from around the developed world gathered in the United States to show support for the concept of environmental protection. The event tagged First Earth Day was in April 1970. Also in 1971, International Institute for Environment and Development (IIED) was created with the mission to globally facilitate the scientific investigation, adoption and implementation of sustainable development principles (International Institute for Environment and Development, 1971). Following this, a United Nations Conference on the Human Environment held in Stockholm in 1972 produced a document outlining 26 guiding principles aimed at preserving and enhancing the human environment (United Nations Environment Programme, 1972). A few years later, the Convention on International Trade in Endangered Species of Wild Fauna and Flora (CITES) came into force. It aimed to protect

endangered species by participating countries (CITES, 1975). This convention was a significant achievement as ecologists had predicted the extinction of up to a million species of living organisms by the year 2000 (Franco, José Luiz de Andrade, 2013).

In the 1980s and 1990s, the international community under the guidance of the United Nations reached several milestone agreements. These include the World Conservation Strategy (1980); the UN World Charter for Nature (United Nations, 1982); and the Brundtland Commission Report (Brundtland Commission, 1987). The Global Environment Facility (GEF) established in 1991 supported the protection of the global environment and promoted environmentally sustainable development (Global Environment Facility, 2013). With mounting evidence of increased and even irreparable degradation of ecological systems, societal concerns triggered a series of regulatory, political and legal actions aimed at minimising the impact of anthropogenic disturbances (Kennish, 1991). For instance, the United Nations in June 1992 convened a Conference on Environment and Development in Rio, also known as the Earth Summit. The principal objectives of this summit were "the conservation of biological diversity, the sustainable use of its components and the fair and equitable sharing of the benefits arising out of the utilisation of genetic resources". Governments achieving these objectives required the adoption of sustainable development programs, which involved finding environmentally friendly alternatives to economic development that will protect the earth's non-renewable resources. The summit produced a plan of action document known as Agenda 21 which participating countries committed to (United Nations, 1997).

At the turn of the century, and to mark the beginning of a new millennium, the UN General Assembly in 2000 drafted a set of goals known as the Millennium Development Goals (MDG), which reiterated the need for parties to incorporate the precept of sustainable development in nation-building plans. There were set targets for various causes including the full implementation of the Convention on Biological Diversity (CBD) by 2010 (United Nations General Assembly, 2000). Furthermore, in April 2002, at The Hague, another conference of parties (COP) convened by the CBD evaluated the progress of its programmes. It focussed on achieving three additional goals namely:-controlling the distribution of invasive species; adoption of guidelines for sharing of genetic resources and attendant

benefits; and providing stronger economic incentives to reduce deforestation. In the same year, a second Earth Summit held in Johannesburg prioritised five issues including biodiversity. Participating countries agreed to reduce the extinction rate of the planet's flora and fauna by 2010. In order to achieve this, the UN commissioned the Millennium Ecosystem Assessment project to "assess the consequences of ecosystem change for human wellbeing and the scientific basis for action needed to enhance the conservation and sustainable use of those systems and their contribution to human wellbeing" (Millennium Ecosystem Assessment, 2005, page v). The report of the findings was approved and incorporated into future deliberations of the global assembly. The CBD in October 2010 adopted a series of documents including the revised and updated Strategic Plan for Biodiversity (Aichi Targets 2020, the Nagoya and the Cartagena Protocols). To mark the 20th anniversary of the Rio Conference, the UN Conference on Sustainable Development provided a forum for the evaluation of the achievements and shortfalls of previous Summit outcomes. Participating countries also reaffirmed their commitment to these agreements. Besides, member States agreed to strengthen the United Nations Environment Program and adopted the outcome document.

Before the concern for the diversity of life and its conservation gained worldwide attention, Meine *et al.* (2006) noted that ecologists and biologists together with other stakeholders made concerted efforts to confront the issue from various angles. Promoting the sometimes conflicting arguments not only expanded the scope of biological studies, but also "unfolded as colonialism, the Industrial Revolution, human population growth, expansion of capitalist and collectivist economies, and developing trade networks", thereby rapidly and significantly transforming human, social, economic and ecological relationships. Progressively, however, agitation for protection and conservation of natural resources; initially for their aesthetic values and then increasingly for their genetic reserve; gained global attention. Despite these laudable efforts, recent reports suggest that progress has been insufficient and uneven, particularly in the area of biodiversity conservation. According to the UN Millennium Development Goals Fact Sheet (United Nations, 2013), the target of significantly reducing biodiversity loss by 2010 failed. In fact, despite an increase in protected areas, many more species are at risk of extinction now than before, while the world's fisheries remain below sustainable yields due to over-exploitation. The forests are also affected as millions of

hectares of forested land are lost yearly to other uses, mainly urbanisation and agriculture. Several reports from around the globe analysing remotely sensed images have depicted such changes in land cover maps (Stow *et al.* 2004; Yuan *et al.* 2005; Shalaby and Tateishi, 2007; Xiao *et al.* 2006; Petit, Scudder and Lambin, 2001). In line with this, the international community through the Convention on Biological Diversity of the United Nations have developed new frameworks building on previous efforts. These targets known as the Aichi Biodiversity Targets are set to be accomplished by the year 2020 (Convention on Biological Diversity, 2010a).

Given this background, researchers have played and continue to play a significant role as outlined in the millennium ecosystem assessment documents, to provide the necessary data upon which any future success will rely. Earlier in history, Wallace (1862) urged scientists and researchers to educate society on the critical role of biological diversity in human wellbeing and encourage its preservation for the benefit of both the present and future generations. Carpenter *et al.* (2006) reiterated this position in their outline of the research needs of the millennium assessment project. Amongst other knowledge gaps, they noted the absence of a systematic and replicable strategy for monitoring ecosystems and biodiversity changes and the drivers. They stressed that this information is essential "to understand the limits and consequences of biodiversity loss and the actions needed to maintain and restore ecosystem functions."

2.2 Progress and Challenges

Biodiversity monitoring involves measuring species occurrence and rates of change at different scales within an ecosystem (Yoccoz, Nichols and Boulinier, 2001). Biologists, ecologists and other stakeholders worldwide agree on the significance of monitoring biodiversity at different scales of time and space in the bid to curtail biodiversity loss. Han *et al.* (2014) remarked that resource monitoring is the "cornerstone of biodiversity and conservation science." Muchoney (2008) stated that biodiversity monitoring is vital to satisfy the series of Conventions and Protocols that have been agreed upon by parties to the Convention on Biodiversity (CBD); the Convention on the Conservation of Migratory Species (CMS); the Ramsar Convention (RC); the Convention on International trade in

Endangered species (CITES), the Framework Convention on Climate Change (UNFCC) and others. Lindenmayer and Likens (2010) outlined the advantages of biodiversity monitoring to include

i. the identification and assessment of threats and uncertainties;
ii. insight into eco-evolutionary dynamism and basis for scientific research and investigations;
iii. timely intervention when necessary to mitigate ecosystem changes that may impact services;
iv. relevant data pool to support legal decisions about the environment.

Perhaps, more importantly, the need for biodiversity monitoring hinges on the fact that the ecological services that benefit humans and other organisms in a given ecosystem may become impeded and untraceable (Dobson, 2005) in the absence of an implementable monitoring programme. Methods adopted for biodiversity monitoring determine the quality and quantity of data collected as well as its usage. Pettorelli *et al.* (2014) stated that data should be accessible, reliable and globally relevant. Noss (1990) and Nagendra (2001) suggested monitoring biodiversity at "multiple levels of organisation and at multiple spatial and temporal scales" taking into consideration the various components of biodiversity. Furthermore, Hestir *et al.* (2008) opined that monitoring programmes should be systematic and comprehensive to be effective in protecting biodiversity.

There are challenges associated with biodiversity monitoring. Vihervaara *et al.* (2014) for instance questions how to measure the different components of biodiversity such as structures, functions, ecosystems, communities, species and genomes. Others argue that since only a little proportion of life on earth is actually known; (in Wilson *et al.* (1996), Stork estimated that only about 10 to 30% of the total global species numbering up to 15 million are identified, with little or no knowledge on their distribution and biology) monitoring of the known species is irrelevant since unknown species continue to go extinct. The lack of consensus on the definition and scope of biodiversity (Holt, 2006), the strategy, scale and cost also constrain effective monitoring of biodiversity. For instance, Krebs (2002) argues that monitoring will be of scientific value when factors such as environmental variations and

ecological processes are investigated. Other areas of discord include the prioritisation of conservation goals, in other words, who and what should benefit from conservation efforts (Sheil, Sayer and O'Brien, 1999), and the conflicting objectives of economic and sustainable development. Many nationally defined conservation goals are local and usually prioritised for effective management (Yoccoz, Nichols and Boulinier, 2001) with minimal consideration for the role of research in informed decision making (Han *et al.* 2014). Sheil (2001) noted that developing countries usually saddled with limited resources and sometimes bankruptcies are "easily side-tracked by initiatives that promise some support." For instance, the United Nations Collaborative Programme on Reducing Emissions from Deforestation and Forest Degradation (UN REDD+) linked to the Framework for Climate Change poses a threat to biodiversity conservation (United States Agency for International Development, 2014; Bayrak and Marafa, 2016). This threat is due to its emphasis on forest preservation for carbon sequestration and not necessarily for biodiversity conservation. A recent review of the biodiversity goals and proposed monitoring methods in national REDD+ programs in 2014 revealed that few countries have mitigating plans for the impacts of the programme on biodiversity. The review also showed that the sampled countries had commenced the implementation of the REDD+ program at subnational levels without a defined process for integrating data obtained at different scales for effective monitoring of biodiversity (United States Agency for International Development, 2014).

An important area of contention in biodiversity monitoring is the selection of appropriate indicators for assessment. Biodiversity indicators are the characteristics of the organism, and the ecosystem that are susceptible to external stimuli and that are measurable repetitively. Formulating a measurable set of biodiversity indicators is necessary for any meaningful monitoring programme (Dengler, 2009). Furthermore, Dobson (2005) outlined that the lack of a skilled workforce to conduct the necessary field collection and taxonomical classification constrained the implementation of national monitoring programmes. Lindenmayer and Likens (2010) who revealed that a vast majority of monitoring programs fail to achieve their aims due to poor planning at the initial stage or lack of focus during implementation supported this opinion. Others like Brooks *et al.* (2006); Mace and Baillie, (2007); Carwadine *et al.* (2009) and Harrop and Pritchard, (2011) reported that political,

financial, and institutional difficulties impede successful implementation of the CBD decisions at national and regional levels.

In a recent review, Chandra and Idrisova (2011) observed a vast and growing disparity in the measurable progress linked to the development status of the implementing party. They discovered that developing economies while in acute need of urgent and thorough action to halt biodiversity loss are least able to make meaningful progress in achieving the CBD targets. Although there has been notable advancement in monitoring technology, a massive database of recorded field observations as well as satellite images available; Carpenter *et al.* (2006) decried the absence of a standard, uniform and integrated procedure for monitoring biodiversity loss and ecosystem degradation across local, regional, global and temporal scales. Pereira and Cooper (2006); Scholes *et al.* (2012); Pereira *et al.* (2013) and Han *et al.* (2014) reaffirmed this in their various works. Fortunately, several national and international organisations such as the Global Biodiversity Information Facility (GBIF), the International Union for Conservation of Nature (IUCN), World Wildlife Fund (WWF), the Group on Earth Observations Biodiversity Observation Network (GEO BON) and so on, are bridging this gap. Steps taken to achieve this include digital interconnection of existing databases and further research on biodiversity monitoring and conservation (Global Biodiversity Information Facility, (GBIF), 2015; Scholes *et al.* 2012). It is imperative to mention here that a higher percentage of the efforts and successes attained concentrate in developed countries with extensive databases in the first place. It is also of significant implications that in the biodiversity-rich tropics exposed to extreme biodiversity loss (Lugo, 1988), biodiversity monitoring is minimal and conservation practices are subject to political, cultural, social and financial considerations (Stork, 1996).

2.3 Methods of Monitoring Biodiversity

The establishment of global organisations with the goal of integrating the existing local, national and regional databases of biodiversity facilitate the incorporation of this information in policy and management decision-making processes. However, it is impossible to monitor all the various life forms that inhabit any ecosystem at any given time. It is also impossible to measure and monitor the effects of various management practices on all species

(Lindenmayer, Margules and Botkin, 2000). Furthermore, there is the concern that monitoring results are open to high error percentages due to several factors that are difficult to control (Archaux, 2011).

So much has been written about the effect of sampling methods on ecological and diversity study (Stohlgren, Falkner and Schell, 1995; Dengler, 2009). Factors such as type (quadrant or transect), shape (rectangle or square), size (small or large) and number (few or numerous) have been suggested, reviewed and modified by various ecologists over the years (Sattout and Caligari, 2011). However, no single technique lends itself to universal applicability; hence, ecologists are yet to agree on a standardised sampling method for measuring species diversity at any habitat (Stohlgren, Falkner and Schell, 1995). In any case, the appropriate monitoring technique suitable for any habitat (for instance-forest, grassland, wetlands, marine or desert) depends on identifying the attributes that indicate the condition of the habitat, the broad and specific objectives of the programme as well as the available resources (Sattout and Caligari, 2011). These attributes may include the size and shape (diameter of tree species, boundaries); the soil (type and nutrient status); hydrology (watercourse configuration, flooding regime, water chemistry, water table fluctuations); composition (communities, species composition, richness and diversity); structure (age class diversity, horizontal and vertical structural diversity, deadwood) and dynamics of the system (regeneration; composition, number and distribution, planting frequency). Hence different habitats required different monitoring methods but based on structural similarities, recommended and standardised methods are transferrable across a wide range of habitats (Hill *et al.* 2005).

The most common method for monitoring biodiversity involves sampling plots. Sample plots can be fixed or non-fixed. Random sampling is highly recommended to minimise the presence of bias in the results. Samples of any medium are obtained from quadrants or transect mapped along the habitat in the desired pattern (either following an apparent physical characteristic such as precipitation gradient or following the impact of anthropogenic activities such as oil spills). (Elzinga, Willoughby and Salzer, 1998; Musila *et al.* 2005; Seak, Schmidt-Vogt and Thapa, 2012). Sample sizes range from 500 to 1000m^2 depending on the habitat condition, management objectives and available resources.

Rondeux and Sanchez (2010) recommended that the total area sampled makeup about 10% of the total study area and a minimum sample plot density of 1 plot per hectare. Measurements are taken from sample plots using various tools such as traps and nets for animals as well as through counting, visual estimation and photography for vegetation (Seak, Schmidt-Vogt and Thapa, 2012).

2.4 Biodiversity Indicators (BIs)

Biodiversity indicators are components of an ecosystem which are selected to function as proxies or surrogates for other members of the community. Assessment of BIs determines changes in the ecosystem or the effect of management strategy on protected areas (Burgman and Lindenmayer, 1998). According to Landres *et al.* (1988) an indicator species is "an organism whose characteristics (e.g. presence or absence, population density, dispersion, reproductive success) are used as an index of attributes too difficult, inconvenient, or expensive to measure for other species or environmental conditions of interest".

Clearly, it is not practicable to monitor all the elements of biodiversity at any level or scale, hence the need to select appropriate indicators that convey relevant information about other components of the ecosystem (Sparrow *et al.* 1994; McLaren *et al.* 1998; Duelli and Obrist, 2003; Canterello and Newton, 2008; Dung and Webb, 2008). The planned monitoring objectives or purposes determine the suitability of an indicator. An ideal indicator according to Duelli and Obrist (2003) should correlate linearly with the component of the biodiversity or entity assessed.

2.4.1 Habitat Records

Habitats are essential indicators of biodiversity due to the presence of particular environmental parameters associated with them. A habitat is defined as a geographical entity that supports the existence of certain species or communities, as well as, the physical dimensions such as soil type, topography and so on of the area (Bruce *et al.* 2013). Habitats, intricately link with biodiversity as the habitat heterogeneity hypothesis suggests.

The extent and status of habitats is an essential and useful measure of biodiversity and offers several practical advantages, which include interpretation of aerial and satellite data for

regular monitoring of status and trends. Furthermore, the phytosociological relationships between habitat and species composition help to identify particular species assemblages in a study transect. Bunce *et al.* (2013) affirmed that habitat condition relate to species distribution and abundance. Processes that promote habitat degradation affect the biodiversity of the habitat, and the extent of this effect is established from habitat data. Past and ongoing investigations report severe degradation of the landscape and habitat of the study area arising from oil exploration and related activities. This study aims to develop remote sensing tools that can map both spatial and temporal extents of these changes.

2.4.2 Plant Species

Plant species also serve as valuable indicators because they are more easily identified, sampled, stored or transported and distributed over a wide range of habitats and environments (Faith and Walker, 1996). Also, Pereira and Cooper (2006) affirmed that vascular plants are suitable indicators of biodiversity for global monitoring programmes.

2.4.3 Biodiversity Indicator Partnership

The Convention on Biological Diversity (CBD) in 2006 mandated the Biodiversity Indicators Partnership to facilitate the development and application of biodiversity indicators in monitoring programmes worldwide. Since the over 20 years of its existence, the BIP has attempted to coordinate a global partnership providing the essential data, analysis and professionalism needed for successful development of indicators for biodiversity monitoring. Together with the partners, they have created an extensive list of indicators some of which are fully developed globally with standardised methodologies. The Aichi 2020 targets of focus and biodiversity indicators explored in this study are shown in Table 2.1.

Table 2.1 The AICHI 2020 target and biodiversity indicators relevant to the present research

Target 5	**By 2020, the rate of loss of all natural habitats, including forests, is at least halved and where feasible brought close to zero, and degradation and fragmentation is significantly reduced**
Indicators	Trends in extent, condition and vulnerability of ecosystems.
	Extinction risk trends of habitat dependent species.
	Trends in extent of selected ecosystems and habitats
	Trends in the proportion of degraded/threatened habitats
	Trends in fragmentation of natural habitats
	Trends in the proportion of natural habitats converted.
	Trends in pressures from habitat conversion, pollution, invasive species, climate change, overexploitation and underlying drivers

2.5 Determining Species Diversity of Transects.

2.5.1 Similarity Index of Polluted and Control Transects

Prior to determining the vascular plants diversity of investigated transects, the similarity index of polluted and control transects was evaluated.Similarity index measures the degree of association or agreement of two entities or variables, in this case, vegetation data from polluted and control transects (Warrens, 2008). Similarity index of pairs of segments determines the degree of their association based on their species composition. This study utilised the abundance-based Sorenson's similarity index. Abundance data takes into account both commonness and rareness of species and places more weight on individuals of the species; and hence provide more detailed information about vegetation on the sampled area (JOSEPH *et al.* 2006; Chao *et al.* 2006). Many researchers (Sattout and Caligari, 2011; Petrovic, Jurisic and Rajkovic, 2010) have used Sorenson's coefficient as an appropriate test to determine the similarity between investigated units. To ensure that the sampled transects have common features, the Sorenson's index (IS) was calculated to determine the community similarity between segments of polluted and control transects as well as among the different locations.

The formula for Sorenson's similarity index (IS) is:

$$IS = \frac{2MW}{MA+MB} * 100 \tag{1}$$

Where

MW = Sum of the smaller numbers of plant species common to the control and test transects
MA = the sum of all plant species in the transect A
MB = the sum of plant species in the transect B

2.5.2 Richness and Diversity Indices

Species diversity measures the diversity within a habitat or ecological community classified as alpha, beta or gamma diversity. Alpha diversity (α-diversity) describes the number of species present (species richness or species abundance) and the distribution pattern of the individual members of these species (species evenness or species equitability) within an ecological unit (Hurlbert, 1971). On the other hand, beta diversity (β-diversity) is the summation of the differences among habitats. It measures the change in species composition between two or more habitats within a region or between regions (Magurran, 2010). Lastly, gamma diversity (γ-diversity) also known as regional diversity is a composite of α and β – diversities. Diversity indices were computed for each segment of polluted and control transects in order to answer the research questions. The various indices of species diversity include species richness which refers to the number of species present in a given area without reference to the abundance or distribution pattern of the species , species evenness which is the relative abundance of a species in a community. Other indices include the Simpson's diversity index and Shannon'ds diversity index; the Chao-1 richness index and the Menhinick index. Detailed description of these indices and their formuylae are provided in Appendix 8.1: Description of vegetation and biodiversity measures.

2.5.3 Beta Diversity Index of Polluted and Control Transects

Beta diversity, a term coined by R. H. Whittaker in 1960 describes 'the extent of change in community composition or degree of community differentiation in relation to a complex gradient of the environment or a pattern of environments'. According to Ricotta (2012), beta diversity quantifies the amount of variation in species composition among sampling units

such as communities, assemblages, plots and so on. Similarly, Baselga (2012) defines beta diversity as the ratio between regional (gamma) diversity and local (alpha) diversities. Beta diversity values are dependent on the extent of the study area, size of the sampling units and sampling interval (Legendre and Legendre, 2012). Quantifying the variation in species assemblages provides relevant information for understanding the ecological and environmental processes that influence biodiversity and ecosystem services. Beta diversity of ecological units provides critical information on the functioning and management of ecosystems as well as biodiversity conservation policies (Legendre, 2007). For instance, the inference of oil pollution effect on species diversity is possible from beta diversity analysis, which detects the variations between species composition and abundance on polluted and control transects. Differences in the species turnover for polluted and control transects at different locations is an indication of biodiversity response to oil pollution. The formula for calculating beta diversity is given by Jost (2010) and based on Whittaker (1960) for communities with equal weights (in this study, equal sampling units) is as follows

$$\beta = \gamma/\alpha \qquad (2)$$

Where,

β = Beta diversity,
γ = Gamma diversity (diversity of the entire study area)
α = Alpha diversity (diversity of each transect, polluted and control)

2.6 Remote Sensing in Biodiversity Monitoring

Conventional biodiversity monitoring methods are constrained by local, national and regional issues including finances, shortage of skilled staff, out of date equipment, lack of accessibility, and further threat of habitat destruction through fieldworks, questionable monitoring objectives and attendant errors (Stork, 1996; Powers *et al.* 2013). One method that has proved a hopeful remedy to these constraints is remote sensing from space-borne or airborne platforms.

Remote sensing is the science and art of obtaining information about an object, area or phenomenon through the analysis of data acquired by a device that is not in direct contact

with the target (Alcantara, 2013). Remote sensing is a viable instrument for photographing the earth surface at regular time intervals. It affords a synoptic perspective of earth features, which is not feasible through other means of observation. Remote sensing provides data on large-scale patterns, trends and interactions at desired levels particularly when combined with ground data (Schott, 2007). It generates reliable data about earth's topography and land cover, rainfall, temperature and other climatic variables, habitats and world biomes (Noss, 1999; Boyd and Danson, 2005).

For this research, remote sensing is defined as the observation of the earth's land surface utilising reflected or emitted electromagnetic radiation. It excludes remote sensing applications in other fields such as in geodesy and seismology. Used in conjunction with Geographical Information Systems (GIS), Nagendra (2001) and other researchers have studied the application of remote sensing in understanding the patterns of species distribution in an ecosystem. Boyd and Danson (2005) maintained that remote sensing offers unprecedented capabilities for global forest mapping and health assessments and may be the only practical way of monitoring earth's forested areas on a timely and consistent basis. It also allows for the mapping of large areas efficiently and more accurately (Wulder, 1998). Furthermore, progress in sensor technology and analytics enhance remote sensing application in solving environmental management problems across disciplines (Galidaki and Gitas, 2015). For biodiversity issues such as species identification and distribution, this progress is a welcome development.

Generally, data from remote sensing combined with expert knowledge enables the classification of landscapes and habitats based on predefined systems such as the Food and Agriculture Organization Land Cover Classification System (LCCS) (Lucas *et al.* 2015). Warren *et al.* (2014) observed that ecosystem heterogeneity affects species richness and abundance, suggesting that spectral diversity correlates closely with biodiversity. The approaches to the use of remote sensing in monitoring biodiversity are indirect and direct.

2.6.1 Indirect Remote Sensing (IRS)

IRS involves the measurement of environmental parameters as proxies of biodiversity trend in question. Through remote sensing, indirect indicators of diversity such as land cover maps

are analysed and combined with field data to model and predict features of biodiversity like species composition or abundance (Turner *et al.* 2003; Millennium Ecosystem Assessment, 2005; Haines-Young, Potschin and Kienast, 2012). The concepts driving this approach include

2.6.1.1 The Habitat Heterogeneity Hypothesis (HHH)

MacArthur and MacArthur (1961) proposed the hypothesis stating that increased environmental heterogeneity increases species richness. Douda *et al.* (2012) stated that the distribution of species in any habitat depends on their characteristics and environmental requirements; hence, microhabitats support different species (niche theory). It follows that the more heterogeneous a habitat is, the higher its species diversity index. Factors such as topography, soil variability, habitat disturbance, landscape structure and complexity, in turn, determine habitat heterogeneity. These factors are remotely sensed and positively correlate with species diversity in swamp forest community (Douda *et al.* 2012); in a disturbed habitat characterised by varying ecological niches (Warren *et al.* 2014); and in Savannah region (Oldeland *et al.* 2010).

2.6.1.2 The Spectral Variation Hypothesis (SVH)

The spectral variation hypothesis proposed by Palmer *et al.* (2002) suggests that spectral variations from remotely sensed images can determine plant species diversity. Palmer tested this hypothesis in 2002 using aerial images with very high spatial resolution (1m) while Rocchini *et al.* (2004) carried out similar testing using multispectral satellite image of 3m spatial resolution. In both investigations, the possibility of estimating species diversity of the study area based on the spectral variability of the remotely sensed images showed great potentials (Rocchini, Chiarucci and Loiselle, 2004). Several studies have shown that the variations in the internal structures of different species such as pigments, tissues that produce unique spectral signatures drive the relationship between spectral variability and species diversity at a particular area (Heumann, Hackett and Monfils, 2015). Hall *et al.* (2012) demonstrated that the spectral variability explained about 30-35% of species diversity in their study area. In the present research, the potential of both multispectral and hyperspectral

images for predicting the diversity of species in Rivers State is investigated using Sentinel-2 and Hyperion EO-1 images.

2.6.2 Direct Remote Sensing

Direct remote sensing involves the use of hyperspectral and hyper-spatial sensors for direct sensing of individual organisms, species assemblages or ecological communities (Turner *et al.* 2003). Presently, however, these high-resolution images are mostly commercially available and are expensive to acquire.

2.6.3 Remote Sensing Derived Indices

A third approach involves the measurement of an ecosystem's functioning and productivity variables to determine its species composition. Some researchers have successfully established a positive linear relationship between species diversity and ecosystem productivity (Waide *et al.* 1999). Clevers *et al.* (2002) and Andrew *et al.* (2014) confirmed the direct measurement of plant biophysical and biochemical characteristics and changes in these attributes by satellite sensors. These possibilities prompt the development of very high-resolution sensors to monitor biodiversity, predict species distributions and model ecosystem responses to environmental and anthropogenic changes (Turner *et al.* 2003). For instance, Thenkabail *et al.* (2004b) and Adamu *et al.* (2014) examined varying plant responses to certain stress factors; Blackburn and Ferwerda, (2008) measured chlorophyll concentration from leaf reflectance; Houborg and Boegh, (2008) and Dalponte *et al.* (2009) in their various studies determined the nitrogen and lignin content of leaves from reflectance data and so on. Recent research established strong links between species richness and spectral diversity (Warren *et al.* 2014; Aneece, Epstein and Lerdau, 2017; Peng *et al.* 2018a; Onyia, Balzter and Berrio, 2018).

2.6.4 Limitations in Biodiversity Monitoring

A common drawback to the use of remote sensing in biodiversity monitoring is the level of multidisciplinary cooperation and interaction needed to achieve realistic results. Regardless of the quality of the remotely sensed data acquired, there is a primary need for local experts including ecologists, botanists and so on to ensure accurate interpretation and classification

of the data (Lucas *et al.* 2015). In addition to this, the amount of information relevant to biodiversity retrieved from remotely sensed data depends on the size of the study area and the resolution of the remote sensor (Nagendra 2001). The choice of the sensor will ultimately depend on the availability of funds as data from higher resolution sensors (spectral and spatial) cost a lot more to obtain.

A review of available literature in remote sensing shows that both very high and very low spatial resolutions impede accurate interpretation of the images. For instance, Boyd and Danson (2005) explained that coarse spatial resolution imagery might provide inaccurate results when applied in a local context but are acceptable in large area studies. Conversely, finer spatial resolution imagery suitable for local area studies is less likely to generate accurate maps when extrapolated to regional or national scales. Furthermore, Malingreau and Tucker (1988) reported that the utilisation of higher resolutions satellite imagery is constrained by high cost, large volumes, delay in the acquisition, and particularly in the tropics; cloud cover and dense smoke from forest fires.

Although remote sensing is an effective means of spatial and temporal classification of vegetation and land cover types, there are still accuracy problems with attempts at species identification (Hu *et al.* 2008). Nonetheless, as different species of plants respond differently to light in the electromagnetic spectrum, the near infrared, middle infrared and thermal infrared bands are recommended for species discrimination. Other factors such as ground surface and understory components, canopy gaps, stand density and crown size, which contribute to spectral variation (Treitz *et al.* 1992; Eastwood *et al.* 1997), are unaccounted for adequately. Information on lower vegetation strata, such as herbs or shrubs is lost when optical sensors are utilised due to their inability to penetrate through the top canopy of vegetation.

Other challenges to the use of remote sensing in studying tropical forests as noted by Jusoff and Ibrahim (2009) include sensor design and accuracy, algorithm development and availability of baseline ecological and taxonomical data. Jusoff and Ibrahim (2009) also pointed out that the data supplied by remote sensing imagery are very complex and hence require complex and sophisticated procedures to extract the relevant information. The

availability of such skills in developing nations is a significant constraint in effective natural resource management. A further obstacle as noted by Lucas *et al.* (2015) is the absence of a standardised, systematic approach to the classification of habitats from remotely sensed data that applies to all transects.

There are also limitations associated with sensor design. According to Carlson *et al.* (2007), land managers and scientists require a comprehensive understanding of species distribution on a scale commensurate with conservation, management and policy development programs to produce maps with less than 0.5km resolution. Such fine scaled biodiversity maps provide a baseline for temporal and spatial change assessment of landscape and evaluation of management decisions. They argue that these maps are defined better with high-resolution imagery as past efforts using Landsat data characterised by medium to coarse spatial resolution (>30m pixels), multispectral (<10 bands) data have failed to fully capture landscape, species and canopy-level diversity in monitored forests.

More recently, Mairota *et al.* (in press) identified several challenges associated with remote sensing application in biodiversity monitoring to include image processing, interpretation, integration with other data sources and timely application of results to management endeavours. Thenkabail *et al.* (2004) stated that the older generation of satellite sensors perform poorly in studies involving complex biophysical characteristics of plants and vegetation. They opined that higher spectral and spatial resolutions allow improved interpretation of remotely sensed data over and above that obtainable from lower resolutions. Their study comparing four different sensors namely- Hyperion (hyperspectral); IKONOS (hyper-spatial); ALI (multispectral), and ETM+ (Landsat) showed that the hyperspectral sensors had higher overall accuracies for individual vegetation types than the others did. Hu *et al.* (2008) agree that high-resolution remote sensing provides better details in species and spectral signature differentiation. For instance, hyperspectral data can provide near accurate information on particular characteristics of vegetation such as biochemical properties, biomass, leaf area index, stress, management impacts, and pigment contents. These factors are crucial for successful biodiversity monitoring and conservation strategies (Hu *et al.* 2008; Jusoff and Ibrahim, 2009; Thenkabail *et al.* 2013).

2.7 Essential Biodiversity Variables (EBVs)

An Essential Biodiversity Variable (EBV) is a measurement required for the study, reporting and management of biodiversity change (Pereira *et al.* 2013). They are standardised measurements and observations necessary to calculate indicator transformations necessary to derive biodiversity indicators. For instance, EBVs such as species population, abundance and distribution provide information for many indicators including: -

i.   Trends in extent of selected biomes, ecosystems and habitats
ii.   Trends in abundance and distribution of selected species
iii.   Coverage of protected areas
iv.   Change in status of threatened species
v.   Trends in genetic diversity

These, in turn, provide information on the status of the habitat. EBVs like biodiversity indicators provide information on the changes and the impact of these changes on ecosystems, species, genes and ecosystem services. EBVs are scalable (allowing for large-scale generalisations), measurable (using various techniques including remote sensing), feasible and are widely applicable across regions, sensitive to change over time and relevant to the CBD targets (Pereira *et al.* 2013).

The concept of EBVs recently evolved following the failure of the CBD parties to meet the 2010 targets. Compounding this was the lack of a global, harmonised system for biodiversity monitoring and data acquisition. The Group on Earth Observations- Biodiversity Observation Network (GEO BON) spearheaded the exercise to develop these variables to form the basis of monitoring programmes worldwide. According to Pereira *et al.* (2013), the EBVs does for biodiversity what other observation initiatives such as the Global Observation System for Climate (GCOS) developed Essential Climate Variables (ECVs) and the Essential Ocean Variables (EOVs) developed by the Global Ocean Observing Systems (GOOS) does for global environment. Being a new concept and still in development, few studies exist on the application of EBVs in biodiversity monitoring schemes. The present research integrated the measurement of relevant EBVs to achieve its general aim. The

following EBVs measured through in-*situ* observations and remote sensing, were assessed to determine the impact of oil pollution on biodiversity in the study area

i. species abundance and distribution (vegetation inventory data)
ii. species traits (leaf chlorophyll data)
iii. community composition (polluted and control transects)
iv. ecosystem structure (differences between polluted and control transects)

2.8 Vegetation Indices (VIs)

Photosynthetic and protective processes involving pigments such as chlorophylls, carotenoids, and anthocyanins drive plant life cycles. These pigments generally absorb and convert solar radiation to the chemical energy needed for plant productivity through a process known as photosynthesis. According to Thenkabail *et al.* (2013), every plant species produces a unique spectral signature, which is dependent on the proportion of these pigments within the cell chloroplast. Additionally, the physiological status of the plant at the time of measurement also influences the plant spectral signature.

Vegetation indices are mathematical expressions derived from the spectral reflectance of plant materials on the earth's surface. They are functions of the reflectance in visible and near-infrared (NIR) spectral bands. Generally, leaf pigments including chlorophyll, carotenoids and anthocyanins absorb significant radiation at the visible light range (VIS, 400 nm -700 nm) while reflecting near-infrared light (NIR, 700 nm -1300 nm) (Huete, 2012). The abrupt transition between both spectral signatures is the red edge. Water, on the other hand, have moderate absorptions at the shortwave-infrared (SWIR, 1300 nm -2100 nm) bands (Huete, 2012). Many researchers use satellite-based vegetation indices to detect (Adamu, Tansey and Ogutu, 2015), explain (Bhandari, Kumar and Singh, 2012), estimate (Barati *et al.* 2011) various environmental phenomena.

Spectral reflectance signatures correlate well with biophysical and biochemical vegetation parameters (Arellano *et al.* 2015; Thenkabail and Lyon, 2016). Additionally, VIs are incorporated in models developed for estimating, monitoring, mapping and analysing ecosystem structures such as vegetation cover and species composition as well as functions

such as productivity and biomass (for instance, Pu, Bell and English, 2015; Bargain *et al.* 2013; Gong *et al.* 2003; Arellano *et al.* 2015). They are hence, essential tools in retrieving information about the state, biogeochemical composition and structure of an ecosystem (Huete, 1988; Jørgensen, Mortensen and Ohlsson, 2003; Alcantara, 2013).

Spectral VIs are designed to minimise the effect of external influences like solar irradiance, changes due to atmospheric effects or variations in soil background optical properties on vegetation reflectance (Gilabert *et al.* 2002). VIs derived from variations in spectral reflectance measured by hyperspectral and multispectral sensors contribute to biodiversity assressment at different spatial (Rocchini, Chiarucci and Loiselle, 2004) and temporal (Martinis *et al*, 2018) scales.

Several vegetation indices were analysed for their ability to detect oil pollution effects on biodiversity and these include the Normalised Difference Vegetation Index (NDVI); the Soil Adjusted Vegetation Index (SAVI); the Red Edge Position (REP); the Anthocyanin Reflectance Index (ARI) and the Carotenoid Reflectance Index (CRI). Detail descriptions of these indices and their formulae are provided in appendix 8.2; Description of vegetatiojn indices.

2.9 Plant Biophysical Parameters

These critical plant characteristics and processes interact with the environment and control ecological functions in various habitats. They are useful in ecological research and are important indicators of biodiversity assessment, monitoring and management (Pereira *et al.* 2013). They strongly influence the spectral signatures of plants and hence are measurable through remote sensing. Measurement of these parameters are either at individual plant levels or canopy levels. At canopy level, optical properties of leaves, leaf angle distribution, biomass and canopy structure influence reflectance whereas concentrations of pigments (chlorophyll, carotenoids, anthocyanins); moisture content, leaf area and so on determine leaf reflectance. Studies show that these parameters are affected by the presence of hydrocarbons in the soil (Rosso *et al.* 2005). The plant biophysical and biochemical parameters examined in the present study to determine the impact of oil pollution on plant biodiversity include.

2.9.1 Chlorophyll Content (CC)

Chlorophyll is a group of green pigments that capture light, which provides the energy for the process of photosynthesis in plants and other organisms. They are located in the chloroplast and directly proportional to the absorption of photosynthetic light. It is an essential indicator of the overall physiological state of a plant/vegetation (Gitelson, Gritz and Merzlyak, 2003; Wu *et al.* 2008). Chlorophyll plays a significant role in the process of photosynthesis through which plants manufacture their food and grow; hence, the total CC in healthy growing plants is expectedly higher than the content in dead or unhealthy plants (le Maire, François and Dufrêne, 2004; Wu *et al.* 2008). Investigations have evidenced a correlation between the presence of hydrocarbon compounds and the percentage content of chlorophyll in leaves (Baruah *et al.* 2014), making CC a good indicator of the physiological state of vegetation growing on hydrocarbon-polluted soil.

Other studies prove that chlorophylls strongly influence reflectance in the red and blue wavelength, with maximum absorption occurring in the 660 nm – 680 nm regions. However, empirical studies based on reflectance between 550 nm to 700 nm show higher accuracy in estimating CC in several species of leaves (Gitelson *et al.* 2002; Wu *et al.* 2008). CC estimation can be done at leaf-level using ratios of three or more bands (Gitelson, Gritz † and Merzlyak, 2003; le Maire, François and Dufrêne, 2004) or at canopy level using factor analysis, artificial neural networks and stepwise multiple regression. However, individual leaf measurements calibrate measurements at higher canopy or ecosystem levels (Mielke, Schaffer and Schilling, 2012). Although vegetation species have a similar spectral response, differences in leaf internal structure and presence of other pigments affect leaf reflectance of different species at similar wavelengths (Mielke, Schaffer and Schilling, 2012). For this study, chlorophyll content was determined using a hand-held chlorophyll meter and computed using chlorophyll related vegetation indices.

2.10 Research Questions and Objectives

The main aim of this research is to determine the impact of oil pollution on vascular plants species used as biodiversity proxies, by analysing remotely sensed hyperspectral and multispectral data and validated with field data To achieve this, the research sought answers to the following questions:-

2.10.1   Research Questions (RQ)

RQ1. Has oil pollution affected the vascular plants' species diversity index of the study area?

RQ2. Are vascular plants species susceptible to oil pollution and does this affect their biochemical parameters?

RQ3. Is there any relationship between spectral diversity metrics and vascular plant species diversity measured in the field?

RQ4. Can this relationship be modelled to estimate the diversity of vascular plants on oil-polluted transects?

2.10.2   Research Objectives (RO)

RO1. To determine the vascular plant species diversity index of the study area and investigate the effect of oil pollution on the biodiversity of the study area using vascular plants as indicators (RQ1*)*

RO2. To investigate the effect of oil pollution on plant biochemical parameters with focus on leaf chlorophyll content (RQ2)

RO3. To test the validity of the spectral variation hypothesis in estimating species diversity of the study area (RQ3)

RO4. To develop prediction models for vascular species diversity in oil-polluted areas (RQ4).

2.11 Thesis Structure

The arrangement of the chapters in this thesis may be visualised as an ice cream cone in the way the research questions listed in section 2.10.1 are tackled. Beginning with the

determination of oil pollution effect on soil and vegetation of the entire Rivers State, the thesis narrows in scope to investigating the spectral changes in vegetation characteristics detected by multispectral satellite sensor, and then focuses on determining the impact of oil pollution on vegetation biochemical parameters using hyperspectral data from a subset of the study area. Figure 2.1 portrays the relevant connections and the general direction of the research. The thesis commences in Chapter 1 with an introduction to the oil pollution problem in the study area and justification of the study. In Chapter 2, a general discussion on previous literature related to this research is presented with emphasis on remote sensing applications in biodiversity monitoring.

Chapter 3 provides a description of the methodology and datasets utilised in this research as well as the sources and characteristics of various satellite data. In this chapter, the geomorphological and ecological parameters of the study area are presented to provide the reader with a proper perspective of the connections between oil pollution and biodiversity loss. Finally, the various statistical tools employed in data analyses are explained.

Chapter 4 presents the answer to the first research question (RQ1) in section 2.10.1. The vascular plant species diversity in Rivers State is determined, and the impact of oil pollution on the soil and vegetation parameters is revealed from field data. Chapter 5 subjects the spectral variation hypothesis to test and evaluates its usefulness for detecting the impact of oil pollution on vascular plants species diversity. Chapter 5 marks the introduction of satellite data in answer to the second and third research questions (RQ2 and RQ3) and outlines the specific data and methods employed are outlined.

Chapter 6 provides a detailed evaluation of oil pollution impact on vegetation biochemical parameters, specifically chlorophyll and how this influences vegetation reflectance at various wavelengths. The higher spectral resolution of the Hyperion image proves suitable for this analysis; however, the scarcity of the dataset constrained its application to only a subset of the study area. Models derived from relationships among several variables are used to estimate species diversity on transects in answer to the fourth research question (RQ4).

Chapter 7 provides a general discussion, which ties together the results of the investigations completed in Chapters 4 to 6 in order to make valid conclusions. The challenges encountered

in this research, contributions to knowledge as well as recommendations for future work are also presented.

2.12 Summary

This chapter provided a review of related literature, with emphasis on the application of remote sensing in biodiversity monitoring, the research questions and objectives and the thesis structure. Chapter 3 will discuss the general methodology and data sets used in this research as well as descriptions of the study area.
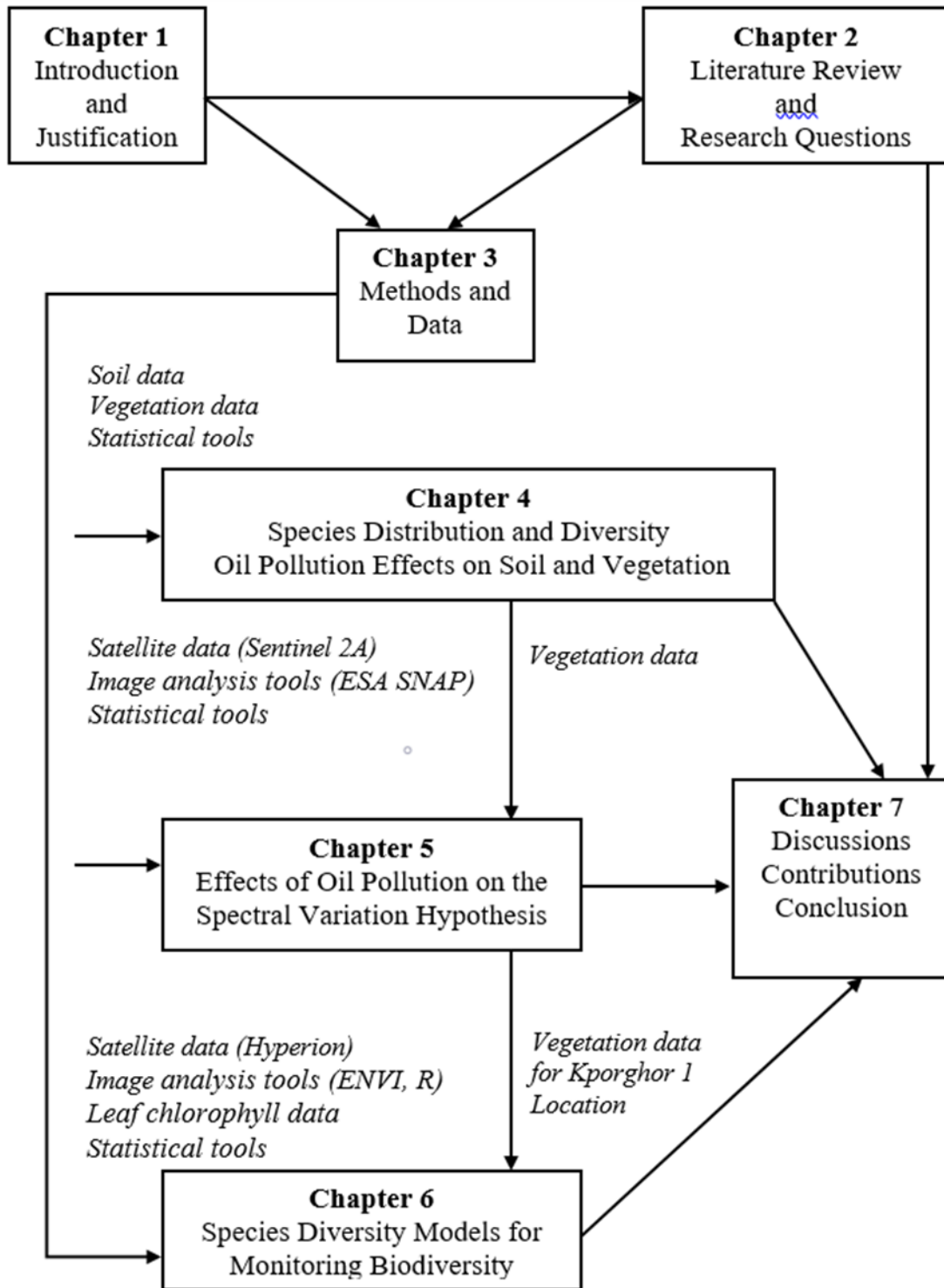
Figure 2.1: Thesis structure reveals interconnections among chapters, in line with research questions and objectives. Data and main procedures performed in each chapter shown in italics.

3 Methodology

This chapter aims to provide an overview of the methodology and datasets employed in this research. The chapter details the preliminary steps taken to access polluted locations and the difficulties encountered. A description of the study area, field sampling method and laboratory analysis follows. Furthermore, the chapter explains the attributes of the satellite data utilised and the various computational procedures applied. Although this chapter gives an overview of the general methodology of this research, specific methods applied to unique datasets are discussed in subsequent result chapters.

3.1 Description of the Study Area

Rivers State is located between latitude 4.75º North and longitude 6.83º East in the eastern part of the Niger Delta, on the oceanward extension of the Benue trough (Figure 3.1). It occupies an area approximately 11,077 km^2 of the delta described as constructive and fed mainly with sediments from the heavily-laden (about 330,000 cm^3/annum) River Niger originating from Guinea travelling through Mali, Niger, Benin Republic and Northern Nigeria (Netherlands Engineering Consultants, 1959). The Delta also receives sediments from the Benue River, albeit to a lesser degree. Rivers State is bounded on the South by the Atlantic Ocean, to the North by Imo, Abia and Anambra States, to the East by Akwa Ibom State and to the West by Bayelsa and Delta States. It receives some of the highest rainfall in the world of up to 3000mm annually (Omo-Irabor *et al.* 2011). The temperature ranges from 20^0 to 30^0 C during the day. The Intertropical Front wind originates from the meeting point of humid air masses of the Gulf of Guinea and dry air masses from the north continuously blow over the delta, resulting in high levels of humidity of up to 75% (Elenwo and Akankali, 2014). The area is also characterised by high cloud cover, which invariably affects the quality of satellite data obtained at certain times of the year (Omo-Irabor *et al.* 2011).
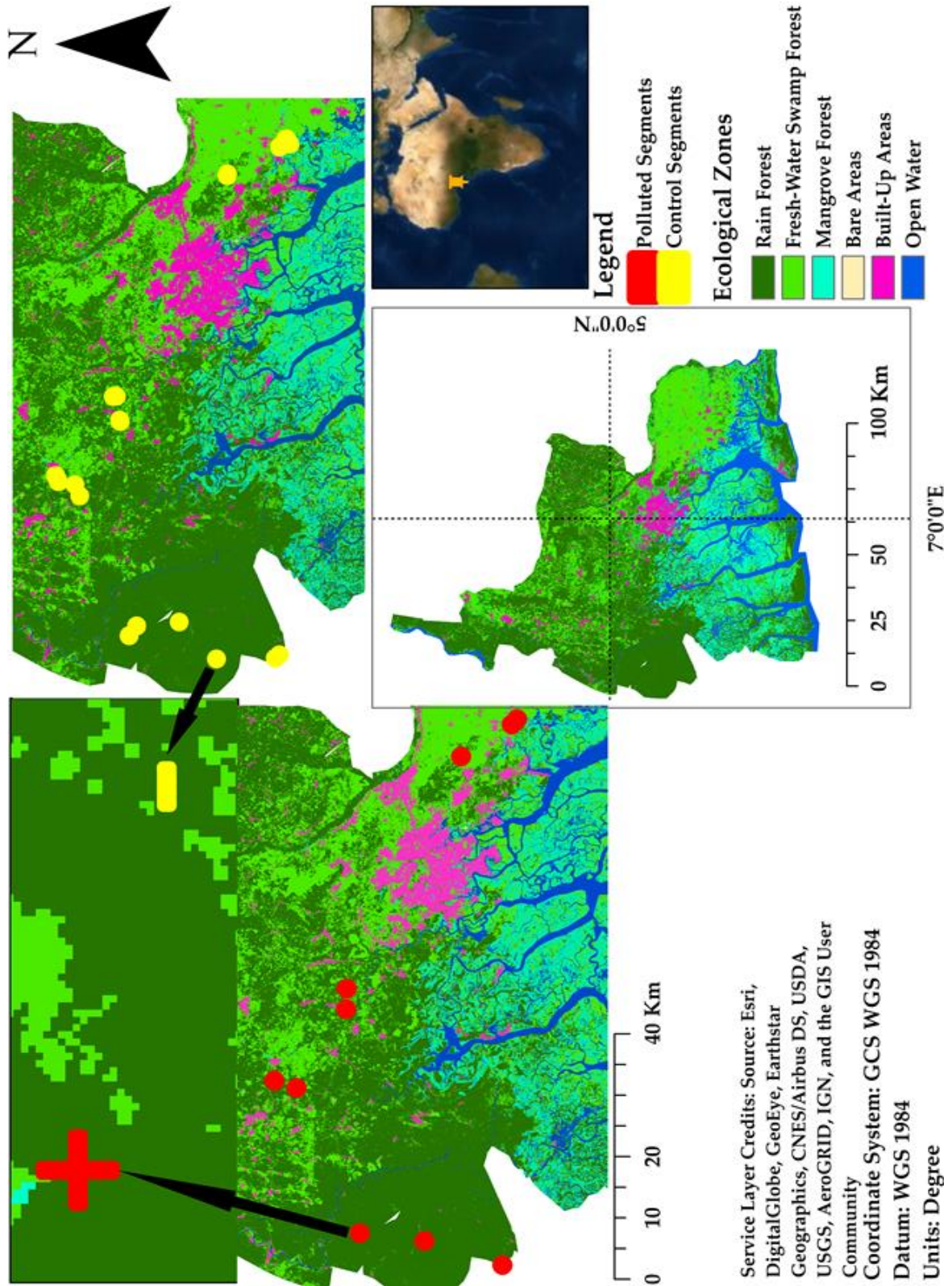
Figure 3.1 Map of Rivers State showing the location of investigated spill transects (Polluted and non-polluted i.e. control), ecological zones and waterbodies (rivers and creeks).

54

In line with the rest of the delta geomorphology, Rivers State consists of alluvial deposits of sands, silts and clays deposited during the late Miocene-Pliocene times. Coarse sands and gravels underlie parts of the area while fine sands and clays underlie other areas (United Nations Environmental Programme, 2011). The landscape of the area is generally flat with altitude ranging between 6 to 14m above sea level. Investigated transects located in various local government areas fall in the coastal plain and freshwater ecological zone populated by forest tree species, mangrove, palms, shrubs, ferns, lianas and so on, however, the rainforest is degraded with fewer trees as observed during the field work. Vegetation around spill transects is variable with evidence of fire occurrence within 30 m radius of the spill epicentre at one of the polluted locations in Kporghor. Other features include untarred roads which is part of the oil companies right of way (ROW), vegetated land (natural and farmed) and bare soil.

Records from the Nigerian Oil Spill Monitor website (NOSDRA, 2015)(https://oilspillmonitor.ng) indicate that the spills occurred between July to December 2015 with sabotage being the leading cause. Sabotage of oil pipelines is the typical method by which crude oil is illegally extracted or diverted. It involves exploding dynamites near pipelines, loosening valves, cutting the pipes, drilling holes in the pipes to fit taps, applying corrosive substances all in the bid to access the crude oil (Adishi *et al.* 2017). The extracted crude is either sold in the black market or locally refined for personal use. Estimated spill volumes reported range from 46 barrels to over 5000 barrels (at Egbalor and Kporghor2, there was no data on the volume of spill). Consequently, between July and December, 2015 (about six months) over 10,641 barrels of crude oil was spilt into the vulnerable ecosystem of Rivers State in the Niger Delta region of Nigeria.

Figure 3.2 Field photo showing the extent of fire damage on the vegetation of the study transect. Cause of the fire is unknown and was not reported in the initial impact assessment conducted by the joint investigation team.

3.2 Ecology of the Study Area

Rivers State is characterised by four biodiversity important vegetation zones, namely, the lowland rainforests, freshwater swamp forests, mangrove forests, and barrier island forests. Ebeku (2006) reported that these zones form a critical component of the ecosystem on which the economy and livelihood of the inhabitants depend. According to the World Bank (1995) classification, the vegetation zones include

1. The lowland rainforests (LRF) which represents the coastal plains. The World Bank (1995) reported that the study area was predominantly vegetated by these forests. The rain forest is characterized by up to four strata of trees growing up to 50 m tall (Izah, 2018). However, as pointed out by Ugochukwu and Ertel (2008), large chunks of this forest has been taken over by agricultural lands. The vegetation found in this ecological zone are mostly used for timber, tannins, fuelwood, fences, furniture, saw wood, particle board, poles and traditional medicine (Nuga and Offodile 2010).

2. The freshwater swamp forests (FSF) occurs between the lowland and mangrove forests. It can be subdivided into two ecosystems

    a. The rarely flooded riverbank levees most of which is converted to farmlands supporting trees, palms and shrub species.

b. The flooded back swamps, which support very diverse plants species.

This ecological zone represents an important biodiversity area, providing habitat for endangered and rare wildlife (Igu and Marchant, 2017). It is also a source of freshwater supply for inhabitants as well fuel, food, medicine, construction and textile materials (Izah, 2018; Igu and Marchant, 2017).

3. The mangrove forest (MGF) is characterised by a dense network of inundated creeks and supports the growth of a variety of mangrove and other tree species. The ecological zone comprises of estuarine and marine ecosystems which are separated by barrier islands. Both habitats are predominantly populated by mangrove tree species.

4. The barrier island forest (BIF) which gradually demarcates the coastal zones and the estuarine mangroves. The forest is vegetated by a range of diverse flora and fauna species. The zone is bounded by the mangrove swamps inland and beach strand on the seaside. It is also characterised by four ecozones namely ridge-top rainforest with similar characteristics as the LRF, freshwater swamp forest between the ridges, brackish-water swamp forest and the beach strand.

Each of these zones harbours distinct variations in flora and fauna essentially in response to the hydrological variations (Abam, 2001). The dominant species, their habits and ecological zone(s) in which they occur are shown in Table 3.1.

Table 3.1: List of dominant species occurring in the different ecological zones of Rivers State of Nigeria. LRF = Lowland Rainforest; FSF = Freshwater Swamp Forest; MGF = Mangrove Forest and BIF = Barrier Island Forest

Species name	Family name	Life form	Ecological Zone
Agelea oblique	Connaraceae	Tree	LRF, FSF
Albizia adianthifolia	Fabaceae	Tree	LRF, FSF, BIF
Alchornea cordifolia	Euphorbiaceae	Shrub	FSF
Alstonia boonei	Apocyanaceae	Tree	FSF
Anthocliesta vogelii	Gentianaceae	Tree	FSF
Antidesma vogelianum	Euphorbiaceae	Tree	LRF
Avicennia africana	Acanthaceae	Tree	MGF
Berlinia spp	Caesalpiniaceae	Tree	LRF, FSF, BIF
Bligha sapida	Sapindaceae	Tree	LRF
Bombax buonopozense	Malvaceae	Tree	LRF, FSF, BIF
Borassus aethiopum	Arecaceae	Tree	LRF, FSF, BIF
Ceiba pentandra	Bombacaceae	Tree	LRF, FSF, BIF
Chassalia spp	Rubiaceae	Shrub	FSF,MGF,BIF
Cleispholis patens	Annonaceae	Tree	LRF
Cynometra megalophylla	Fabaceae	Tree	MGF, BIF
Dacryodes edulis	Burseraceae	Tree	LRF, FSF
Dalbergia ecastaphyllum	Papilionoideae	Shrub	MGF, BIF
Dichrostachys cinerea	Fabaceae	Shrub	LRF
Dryopteris spp	Dryopteridaceae	Fern	LRF, FSF, BIF
Eichornia crassipies	Pontederiaceae	Creeper	FSF
Elaeis guineensis	Arecaceae	Tree	FSF, MGF,
Entandrophragma cylindricum	Meliaceae	Tree	LRF
Entradrophragma angolensis	Meliaceae	Tree	LRF
Funtumia elastica	Apocynaceae	Tree	LRF
Harungana madagascariensis	Clusiaceae	Tree	FSF
Irvingia gabonensis	Irvingiaceae	Tree	FSF
Languncularia racemosa	Combretaceae	Tree	MGF
Lophira alata	Ochnaceae	Tree	LRF, FSF, BIF
Lovoa trichilioides	Meliaceae	Tree	LRF
Macaranga bacteri	Euphorbiaceae	Tree	FSF, BIF
Machaerium lunatum	Fabaceae	Tree	MGF, BIF
Milicia excelsa	Moraceae	Tree	LRF, BIF
Millettia griffoniana	Leguminosae	Tree	LRF, FSF
Musanga cecropioides	Cecropiaceae	Tree	FSF
Nypa fruticans	Arecaceae	Tree	MSF
Pandanus spp	Pandanaceae	Tree	FSF, MGF, BIF
Paullinia pinnata	Sapindaceae	Climber	LRF
Pentaclethra macrophylla	Fabaceae	Tree	LRF
Piptadeniastrum africanum	Leguminosae	Tree	LRF
Psychotria manii	Rubiaceae	Shrub	LRF
Pycnanthus angolensis	Myristicaceae	Tree	FSF
Raphia spp	Arecaceae	Tree	FSF, MGF
Rhizophora spp	Rhizophoraceae	Tree	MGF
Sterculia tragacantha	Malvaceae	Tree	LRF, FSF, MGF
Symphonia globulifera	Clusiaceae	Tree	LRF, FSF
Terminalia ivorensis	Combretaceae	Tree	LRF
Terminalia superba	Combretaceae	Tree	LRF
Treculia Africana	Moraceae	Tree	LRF, FSF
Triplochiton scleroxylon	Malvaceae	Tree	LRF
Uapaca heudelotii	Euphorbiaceae	Tree	FSF, BIF

The well-endowed ecosystem is abundantly rich in biodiversity with very high densities of flora and fauna (Emoyan, Akpoborie and Akporhonor, 2008). The mangrove and freshwater swamp forests of the Niger Delta are the largest in Africa and the third largest in the world spanning about 70,000 km^2. However, large chunks of the forests are lost to extensive logging, fragmentation for oil exploration and agriculture. This ecosystem is under threat from unsustainable farming systems such as slash-and-burn practices, shifting cultivation and bush burning, indiscriminate hunting and poaching as well as over-exploitation of fisheries resources (Zabbey, 2004; United Nations Development Programme, 2006). Pollutants generated by a multiplicity of oil and gas related activities have exacerbated these threats, including seismic operations, drilling operations and production operations (United Nations Environmental Programme, 2011; Emoyan, Akpoborie and Akporhonor, 2008). Several other studies (United Nations Development Programme, 2006; Emoyan, Akpoborie and Akporhonor, 2008; Ugochukwu and Ertel, 2008; Lindén and Pålsson, 2013) documented the negative impact of oil exploration and exploitation on the Niger Delta environment. In the 2011 report on the environment of Ogoniland in Rivers State, the UNEP disclosed that oil pollution has destroyed the mangrove ecosystem, which had served as spawning areas for fish, thereby affecting the fish yield (United Nations Environmental Programme, 2011). The report also highlighted the effect of oil pollution on the productivity of valuable cash and food crops, vegetation and the introduction of invasive alien species. Despite the critical role biodiversity plays in maintaining and sustaining the livelihood of the present and future generations in the region, the rate of biodiversity loss remains very high.

Contrary to the United Nations Environmental Programme Convention on Biodiversity (UNEP-CBD) demands in Articles 6 and 7; there is continued absence of a standardised environmental monitoring and surveillance systems to capture these occurrences and provide data for effective management decisions (Emoyan, Akpoborie and Akporhonor, 2008). Also, where these data exist, it is fragmented, incomplete, outdated, off-line and often inaccessible (United Nations Development Programme, 2010). This study evaluates the suitability of remote sensing and GIS applications in biodiversity monitoring in oil-polluted locations.

3.3 Sampling Methods

3.3.1 Access to Oil Spill Transect

Oral and written communication with stakeholders in the community, the Nigeria Department for Petroleum Resources (DPR) and Shell Petroleum Development Company (SPDC) Nigeria Limited was initiated to obtain the needed permission to access the spill transects. The DPR authorised the project instructing the oil companies to render assistance and access to available data where necessary. Community leaders particularly the members of the youth forum offered both the guides and access to polluted and control locations for sample collection and vegetation survey.

Arrangements with the Michael Okpara University of Agriculture, Umudike department of Environmental Toxicology and the Forestry Research Institute of Nigeria (FRIN), Umuahia provided facilities and literature for species identification.

3.3.2 Field Observations (FO)

3.3.2.1 Global Positioning System (GPS)

Numerous sites were marked for sampling, however, only few were accessible. Global Positioning System (GPS) devices Oregon 550T were used to identify the spill epicentres and sample points at both polluted and control transects in various locations. Sampled transects were predetermined from the Nigeria Oil Spill Monitor website and were located to within 3 m using the GPS. Accessing some selected locations was constrained by the difficult terrain, vegetation and insecurity. However, the support of the local community was invaluable in facilitating the field work.   Once the polluted and control transects were identified, the GPS coordinates were recorded and was utilised in identifying the corresponding pixels in the satellite image for correlation and validation with field data.

3.3.2.2 Transect Establishment (TE)

Vegetation sampling involved the line-intercept method discussed in Cummings and Smith (2000). Due to the unique circumstances prevailing at the study area during this campaign, the line intercept method offered the most potential at capturing adequate field data to

determine species composition and abundance (Kercher, Frieswyk and Zedler, 2003). Cummings and Smith (2000) and Buckland *et al.* (2007) agree that vegetation sampling based on the line intercept method although less intensive than quadrant based sampling methods, provide sufficient data to determine relative estimates of vegetation frequency, coverage, abundance and other relevant vegetation characteristics. Furthermore, according to Cummings and Smith (2000) and Kercher *et al.* (2003), the line intercept method offers a handy tool for detecting community transition (such as ecotones) or ecological gradients in habitats. It adapts well for investigating the relationships between changes in floristic compositions and environmental variables with little room for errors.

The investigation occurred at ten oil spill locations in the Rivers State of Nigeria. Most of the spills emanated from damaged pipelines that criss-cross the landscape of the Niger Delta; however, a few occurred at oil well locations and wellhead sites. Accessibility to oil wells and wellheads was unavailable; hence, the field survey occured on the more easily accessible pipeline spill locations. Table 3.1 shows the location of polluted and control transects investigated. Spill epicentres were identified from the Nigerian oil spill monitor website and located using GPS devices. Unhindered access to spill locations determined its selection for sampling whereas certain attributes of polluted transects such as proximity to roads and company right of ways were considered in locating control transects in an attempt to minimize the between sample errors. Additionally, control transects were selected based on distance from the spill locations.

Transects were 100 m long and transverse the polluted locations in order to study the effect of crude oil on vegetation composition. Polluted transects labelled A, B, C and D originated from epicentres of spill locations (SS0) and proceeded in the four cardinal directions respectively. Location of the control transects was random in unpolluted areas but within the same locations as the oil spills. The randomisation of control transects was to minimise error from bias. In addition to the spill epicentre, SS0, each transect was subdivided into five segments of 20 m length labelled SS1 to SS5. These segments numbering SS1 to SS5 corresponded with increasing distance from the spill epicentre (SEC). For instance, SS1 started from the SEC (SS0) and ended at 20m from the SEC. SS2 was from 20m to 40m; SS3 was from 40m to 60m; SS4 was from 60m to 80m and SS5 was from 80m to 100m. For each

segment, species richness and diversity (alpha) values, vegetation abundance, leaf chlorophyll content and the total petroleum hydrocarbon (TPH) concentration in the soil were recorded. However, to correct for spatial autocorrelation effects, analysis of data involved alternate segments on each transect including the SS0s.

Table 3.2 Locations of the investigated polluted and control transects in the Rivers State of Nigeria. Also shown are the type of facility, date of spill and volume of the spill in barrels. Oil spill data source https://oilspillmonitor.ng

NOSDRA ID	Location	LGA	Date	Latitude	Longitude	Volume (cbm)	Facility
49636	Alimini	Emokua	04/07/2016	5.056672	6.703269	42	Pipeline
	Control 1			5.050888	6.718027		
	Control 2			5.0519	6.716672		
41981	Amuruto	Abua-Odual	17/12/2015	4.731917	6.432667	803.586	Pipeline
	Control 1			4.718925	6.44518		
	Control 2			4.725071	6.439931		
52553	Anyu	Abua-Odual	17/11/2016	4.842944	6.468194	20.1	Pipeline
	Control 1			4.812299	6.43763		
	Control 2			4.86774	6.493655		
45420	Egbalor	Eleme	12/08/2015	4.7906111	7.178528	Unknown	Pipeline
	Control 1			4.79906	7.173313		
	Control 2			4.798188	7.175265		
41405	Kporghor	Tai	12/09/2015	4.718553	7.225111	137.4	Pipeline
	Control 1			4.711046	7.227604		
	Control 2			4.710883	7.22987		
52014	Kporghor 2	Tai	16/10/2016	4.7148611	7.225333	Unknown	Pipeline
	Control 1			4.705858	7.221231		
	Control 2			4.720984	7.217364		
37708	Obua	Abua-Odaul	22/08/2015	4.934889	6.479278	7.31	Pipeline
	Control 1			4.941858	6.473319		
	Control 2			4.930635	6.487469		
37791	Omoigwor	Emuohua	31/08/2015	4.95364	6.837996	150.4	Pipeline
	Control 1			4.962524	6.837512		
	Control 2			4.96662	6.83611		
41640	Umukpobu	Emuohua	11/09/2015	4.954519	6.808028	101.3	Pipeline
	Control 1			4.956759	6.798752		
	Control 2			4.95705	6.801251		
37378	Rumuekpe	Emuohua	16/08/2015	5.025361	6.692444	190.8	Pipeline
	Control 1			5.023084	6.701912		
	Control 2			5.015748	6.68483		

Figures 3.3 and 3.4 are illustrations of the transect establishment in the study area.

Figure 3.3 Pre-spill digital globe image of investigated polluted locations in the study area. A1. Alimini, B1. Amuruto, C1. Egbalor spill points in Rivers State, Nigeria. Bold red lines illustrate transects transversing the spill epicenter. Image downloaded from Google Earth, A2, B2 and C2 were images acquired few days after the oil spill during the post-impact assessment. Images downloaded from the www.oilspillmonitor.ng; A3, B3 and C3 are field photos of same locations acquired during the field campaign.
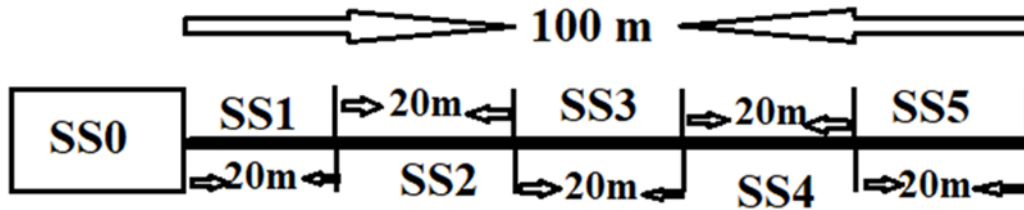
Figure 3.4: A sketch of transects and investigated segments. Each transect measured 100 m from the spill epicentre, and each segment was 20 m in length. Although sampling was on all the segments shown, statistical analysis included data from only segments SS1, SS3 and SS5 as well as the segment overlaying the spill epicentre (SS0).

The nature of the polluted transects varied widely. At a few locations like Kporghor and Anyu, there is clear evidence of fire incidence following the discharge of crude oil on the surface. At other locations, such as Egbalor, Omoigwor and Amuruto, vegetation on polluted transects consist mainly of mixed annuals and perennials with few tree species. At others, there was a visible ring of vegetation demarcating the epicentre from the surrounding areas. Other landscape features include mostly untarred roads, which form part of individual oil companies right of way (ROW) for oil pipelines, abandoned farmlands and excavated gutters about four meters wide usually installed as containment measures after the spill.

Based on preliminary reports by a joint team of investigators, and available on the Nigerian Oil Spill Monitor website (https://oilspillmonitor.ng) most of the spills were because of pipeline vandalism by oil thieves. The spills occurred between August 2015 to November 2016 with up to 5054 barrels of crude oil discharged into the environment in Amuruto, Abua-Odual LGA (see Table 3.1 for estimated spill volume for other sites). The area impacted by the spill varied from 0.001 km^2 at Alimini to 2.22 km^2 at Omoigwor. Initial containment measures implemented by the host companies involved the use of booms, dykes, pits, trenches and natural depressions. This study investigated spills on lands, even though spills occurred on different habitats, to maintain optimum similarity of transects.

3.3.2.3 Soil Sample Collection (SC)

Soil sample collection was carried out in two phases. The first set from transects in Kporghor 1and second set from the other locations during the second phase of the field study. A total of 210 samples were analysed in the laboratory for various physicochemical properties.

Samples were obtained at 30 cm depths from the spill epicentre and 20 m intervals along each transect. At each segment including the spill epicentre, three samples were obtained and mixed, and a composite sample scooped into sterilised and labelled brown air-tight glass bottles to control further chemical reactions. These were stored in a plastic box filled with ice packs for transportation to the laboratory for chemical analysis.

3.3.2.4 Vegetation Survey (VS)

A comprehensive vegetation survey was carried out at the polluted and control transects. Inventory of all vascular plant species present on transects was done with the aid of prepared tally sheets and local experts. Tally sheets listing indigenous species and photographs were taken to the field to help in species identification with consideration given to the type and shape of leaf, margin, apex and base of each species Also considered were the arrangement of leaves and leaflets on the petioles. Previous reports of common species in the Niger Delta area such as Ubom (2010); Agbagwa and Ekeke (2011) provided material for tally sheets. Photographs of unknown plants were taken to the Herbariums of the Forestry Research Institute of Nigeria, Umuahia and the Michael Okpara University of Agriculture Umudike both in Abia State, Nigeria for identification.

Occurrence and number of individuals for each species was recorded per segment of transects starting from the spill epicentre. Plants that occurred within 500cm on both sides of the transect lines were included in the count (Figure 3.5). The data was used to determine several phytosociological characteristics such as abundance, density and importance value index of species; and vascular plants species indices including the similarity, richness, evenness and diversity.

Psychotria nigerica plant inventoried during sampling

Manihot esculenta also inventoried

Fibre tape used for measuring transects and segments
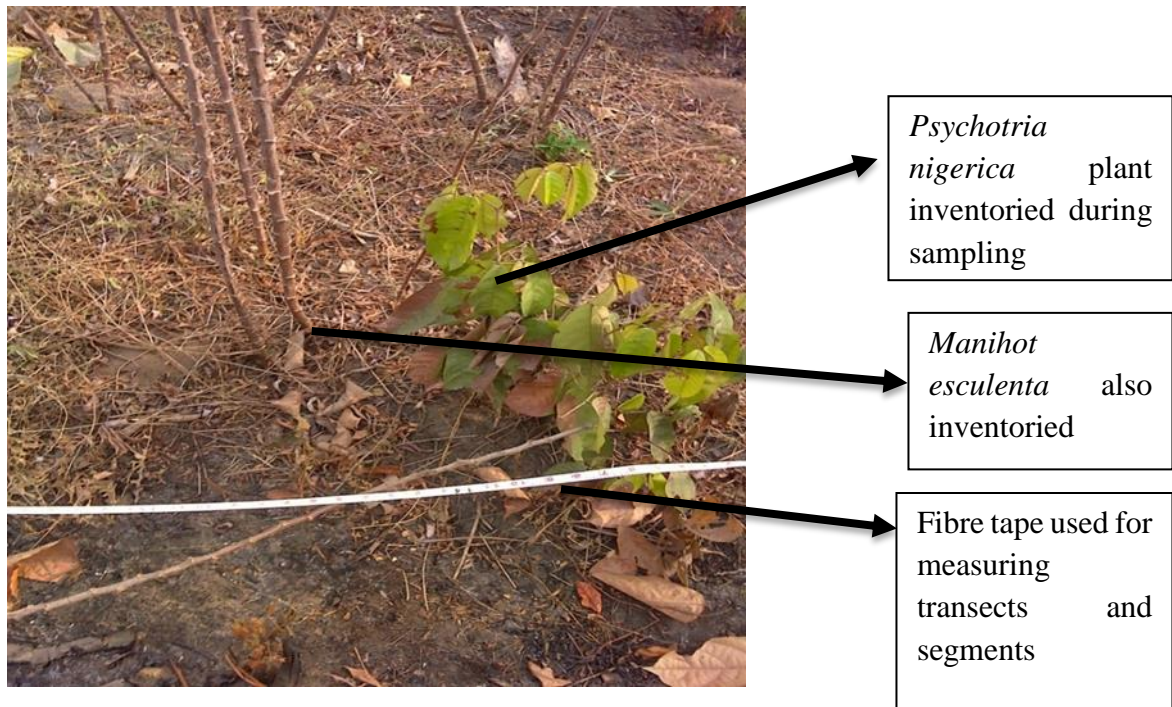
Figure 3.5: An example of a counted individual plant species occurring along a transect.

3.3.2.5 Insitu Chlorophyll Data using SPAD-502 Chlorophyll Meter (ICM)

The proportion of chlorophyll in leaves is a good indicator of the physiological status of vegetation. Laboratory determination of chlorophyll is often, expensive, time-consuming and destructive, the Soil Plant Analysis Development (SPAD-502) chlorophyll meter offers an alternative which has been reported to provide relatively accurate values that are proportional to the chlorophyll content in leaves (Ling, Huang and Jarvis, 2011).

The SPAD-502 meter is a portable device that facilitates rapid and accurate measurement in the field without needing to detach the leaves from the plant. Previous researchers (Uddling, Gelang-Alfredsson and Piikki, 2007; Rodriguez and Miller, 2000) have successfully documented the conversion of SPAD-502 values to absolute chlorophyll measurements. However, the procedures appear to be sensitive to interspecies differences such as shape and size of leaves. In the light of this constraint and due to the number of species investigated in this research the SPAD-502 readings were used directly in all the statistical analysis.

Chlorophyll measurements occurred during the first phase of the fieldwork for only the Kporghor 1 location. Average readings were taken for all the plants present in segments along polluted transects, but on control transects with increased vegetation density, 20 plants were randomly sampled in each segment. Plants selected for sampling were those that

appeared unaffected by the presence of TPH in the soil. For each plant, four readings were obtained from the midpoint of fully developed healthy leaves located within reach, which is the best position to collect the chlorophyll readings from plant leaves (Hoel, 1998; Arellano *et al.* 2015). Leaves of tall trees were pulled down using elongated poles, but care was taken to cause only minimal damage during measurements. The device performs an automatic calculation for average measurements used in further data analysis.

3.3.3 Laboratory Analysis of Soil Samples (LAS)

Soil samples collected from the Kporghor 1 during the first phase of the fieldwork were stored and transported to the laboratory in appropriate media. The samples were analysed in an internationally accredited laboratory for soil physicochemical properties. These include total petroleum hydrocarbon (TPH), total organic carbon (TOC), heavy metals, nutrients, electrical conductivity, pH and temperature. Other parameters analysed include the total heterotrophic bacteria (THB) and total organic matter (TOM). Likewise, soil samples collected during the second phase of the fieldwork under similar conditions of storage and transportation were subjected to fewer tests, following preliminary results that showed no significant difference in some soil properties between polluted and control transects. Thus for these samples, only the TPH, TOM, Phosphates and Lead concentrations were tested.

The methods used followed international standards documented in the American Public Health Association (APHA, 2005) 20th Edition and the American Society for Testing and Material (ASTM, 2010). Details of the methodology employed in the soil analysis are provided in the appendix (Appendix 3.3). Figure 3.6 presents a flowchart of the overarching research methodology.
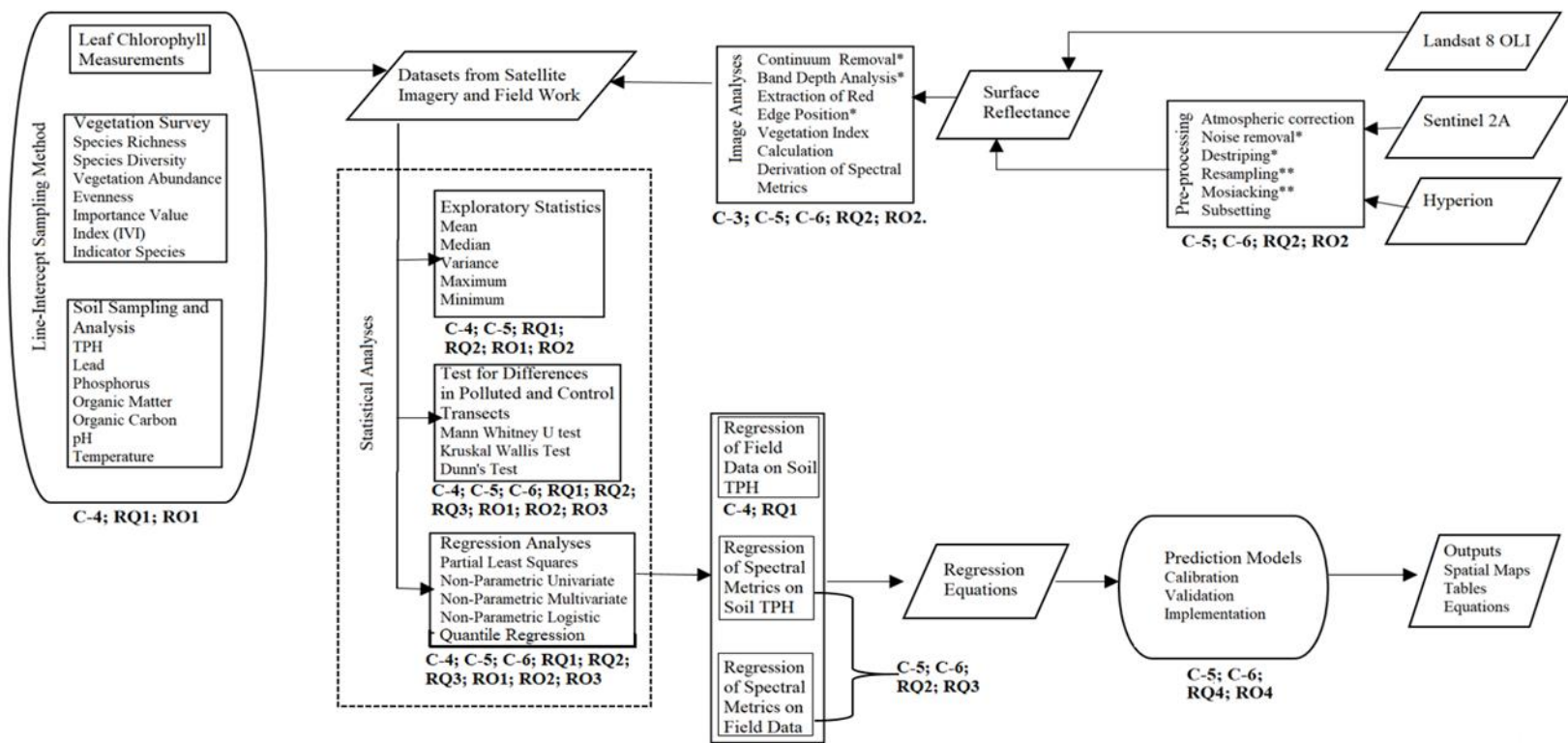
Figure 3.6: Flowchart of research methodology. Procedures and processes are enclosed in squares while inputs and outputs are enclosed in parallelograms. Methods enclosed in ovals indicate the start and end processes. The chapters (C), research questions (RQ) and objectives (RO) linked to each method are shown in bold. The single asterisk (*) denotes procedures carried out on Hyperion data using ENVI 5.3 while double asterisks (**) are procedures performed on Sentinel 2A dataset in ESA-SNAP

3.4 Satellite Data (SD)

A combination of multispectral (Sentinel-2 and Landsat 8) and hyperspectral (Hyperion EO1) data employed in this research are available and freely downloadable from the USGS data distribution tool, earth explorer. The Hyperion acquires 16 bits, 30 meters spatially resolved data in 220 discrete narrow-bands between the spectral range of 400 and 2500 nm. Although the Hyperion captures about 75 times more data than the Landsat from a similar area (Kuenzer *et al.* 2014), Landsat offers a vast database of the earth's surface over several years which facilitates the identification and mapping of temporal changes in the study area (Roy *et al.* 2014). The images were subjected to pre-processing algorithms using available software such as QGIS. R, ArcGIS and ENVI. Various broadband and narrowband indices were extracted and statistically correlated with the field data to identify any relationships in line with the objectives of the study.

3.4.1 Sentinel-2A Image Acquisition and Processing (S2AD)

The Multi-Spectral Imager (MSI) sensor on board the Sentinel 2A satellite acquired the images used in this analysis. The Sentinel-2A satellite launched on the 23rd of June 2015 is one of the fleets of satellites owned by the European Commission (EC), in partnership with the European Space Agency (ESA). It is designed to provide imagery that supports environmental monitoring under the EC/ESA's Copernicus programme. An optical sensor named multi-spectral imager (MSI) on-board the satellite acquires images in 13 spectral bands with wavelengths ranging from 443-2190nm. The spectral bands include three visible (Red, Green and Blue), one near infrared (NIR), and three short-wave infrared (SWIR) bands. As an added advantage, the MSI also has three red-edge bands, which are useful for differentiating crop types and detecting vegetation stress and one coastal aerosol band useful for atmospheric correction (http://www.esa.int//Copernicus/Sentinel-2). For the present study, however, only eight bands relevant for vegetation analysis were used. These were the visible (bands 2, 3 and 4), NIR (band 8) and red-edge bands (bands 5, 6, 7 and 8A). The bands, bandwidths, central wavelengths and spatial resolution of the Sentinel 2A image relevant to this study are shown in Table 3.2.

Table 3.2: Spectral and spatial resolution of Sentinel-2A image

Sentinel-2A bands	Band Number	Bandwidth (nm)	Central Wavelength (nm)	Resolution (m)
Blue	2	65	490	10
Green	3	35	560	10
Red	4	30	665	10
Vegetation Red Edge	5	15	705	20
Vegetation Red Edge	6	15	740	20
Vegetation Red Edge	7	20	783	20
NIR	8	115	842	10
Vegetation Red Edge	8A	20	865	20

Spatially, the Sentinel-2A images have a swath width of 290km and a resolution of 10 m (VNIR), 20 m (Red-edge and SWIR) and 60 m (atmospheric correction bands). These are some of the best spatial resolutions for freely available satellite data. Six level 1C processed images (geometric and radiometrically corrected) were downloaded from the Copernicus Services Data Hub (https://cophub.copernicus.eu/) to cover the study area. These images acquired between 29th December 2016 and 5th January 2017 and downloaded as 100 by 100 km^2 granules were selected based on cloudy pixel percentage.

The identity of downloaded and processed images are as follows:-

COPERNICUS/S2/20161229T095402_20161229T100805_T31NHF
COPERNICUS/S2/20161229T095402_20161229T100805_T32NKK
COPERNICUS/S2/20161229T095402_20161229T100805_T32NKM
COPERNICUS/S2/20170105T094401_20170105T095718_T32NKL
COPERNICUS/S2/20170105T094401_20170105T095718_T32NLK
COPERNICUS/S2/20170105T094401_20170105T095718_T32NLL

Each image was atmospherically corrected and subjected to image analysis (band analysis, vegetation index computation and derivation of spectral metrics) before performing further geo-processing procedures including resampling, mosaicking and clipping, in order to retain as much original information in the pixel texture as possible. Rocchini *et al.*(2016) observed that the image analysis that involves smoothing processes could cause a loss of vital information. Resampling was done to downscale the pixel resolution of the various bands to 10 m. Resampling is a geometric process that transforms an original image to a suitable

image. This procedure was necessary in order to perform further image processing on the ESA SNAP platform as well as to achieve uniformity in the results. Upsampling performed in SNAP used the bilinear interpolation method which is highly recommended for satellite data. Mosaicking was performed to combine the different granules that cover the extent of the study area, and clipping was performed to extract the exact extent image of the study area from the mosaic. The clipped images for the various sentinel 2A bands are shown in Figure 3.7
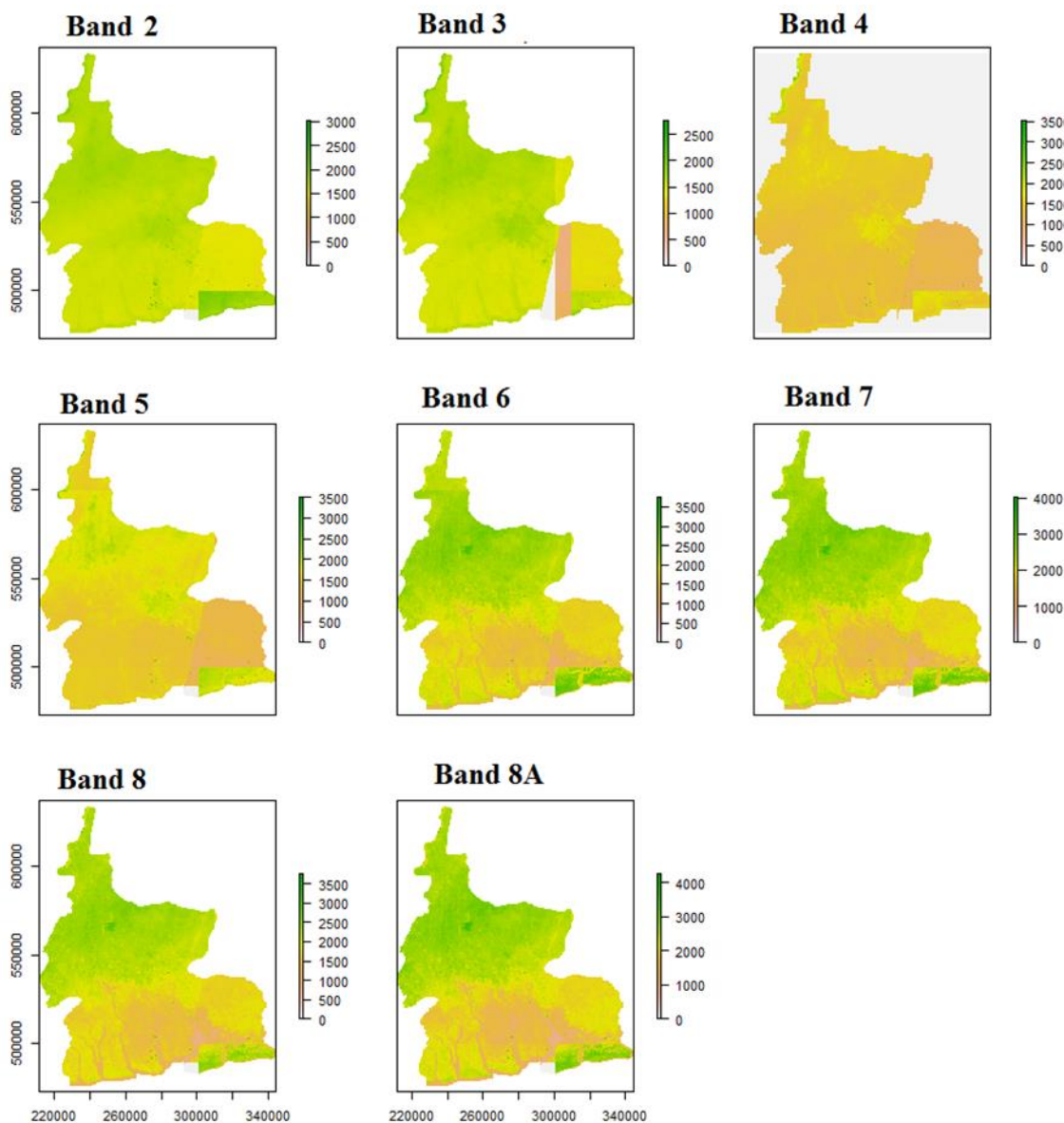
Figure 3.7: raster image of the mosaicked and clipped bands of Sentinel 2A data. Pixel reflectance values range from 0 to 4000

All the analyses were performed in the ESA image-processing platform for sentinel data (ESA SNAP) including the atmospheric correction using the Sen2cor plugin tool in ESA SNAP software for image processing. The Sen2cor plugin tool is a level 2A processor used to remove atmospheric effects from sentinel 2A level 1C images. The processor computes surface reflectance from the top of the atmosphere reflectance values in the level 1C images. Details of the procedure are documented and available at the ESA SNAP website (http//www.step.esa.int/main/third-party-plugins-2/sen2cor).

3.4.2 Hyperion EO-1 Image Acquisition and Processing (HSD)

Following the observed shortcoming of broadband sensors in capturing discrete scene information, hyperspectral imagery was a welcome development in the field of remote sensing of vegetation. It has the added advantage of differentiating spectrally similar materials. Several researchers have investigated its application in identifying plant species and communities, as well as detecting the biophysical and biochemical characteristics of vegetation with more accuracy (Thenkabail *et al.* 2004a; Blackburn and Ferwerda, 2008; Houborg and Boegh, 2008).

3.4.2.1 Description of the Hyperion EO-1 Dataset

The Hyperion sensor was on board the Earth Orbiter 1 (EO-1) spacecraft of NASA's New Millennium Program (NMP) launched on 21 November 2000. The sensor provides radiometrically calibrated spectral data acquired by a push broom system in single frames measuring 7.65 km (cross track) by 185 km long (along-track). The Hyperion image acquisition was from a NADIR position and altitude of 705 km. The image consists of pixels, which approximate 30 m by 30 m regions on the ground. For each pixel location, the sensor acquired data in 242 spectral channels ranging from 400 nm to 2500 nm and a resolution of 10 nm. There are, however, only 196 useful and calibrated bands (Thenkabail *et al.* 2013; Datt *et al.* 2003) while the others due to the effect of bad detectors (also known as bad pixels) are set to zero during the level 1 processing. The calibrated bands include VNIR bands 8-57 (427.55 nm to 925.85 nm); SWIR bands 79 to 224 (932.72 nm – 2395.53 nm). Furthermore, due to the strong absorption of water vapour and oxygen at wavelengths ranging from 1356 nm - 1417 nm, 1820 nm - 1932 nm and >2395 nm, as well as the overlap of wavelengths in

the VNIR (band 56 and 57) and SWIR (77 and 78) regions, the list of useful bands was limited to 176 (Datt *et al.* 2003).

On acquisition, the Hyperion image passes two levels of pre-processing, namely level 0 and level 1. The Hyperion data are downlinked to a ground station and then sent to the Goddard Space Flight Centre (GSFC) for the initial processing. Level 1 processing involves the removal of image artefacts, which occur in the SWIR namely SWIR echo and SWIR smear, bad pixel replacements, dark pixel subtraction, radiometric calibration and image quality assessment (Barry, 2001; Pal and Porwal, 2015). The fully processed level 1 product is written in a16-bit signed integer with units of radiance ($W/m^2/um/sr$) times a factor of 40 for the VNIR bands (1-70) and a factor of 80 for the SWIR bands (71-242).

The Hyperion image used for this study was a Level 1T (in GeoTIFF format) downloaded from the USGS website (https://earthexplorer.usgs.gov). The image was acquired on the 23rd of November 2015 by the Hyperion sensor on board the Earth Observation (EO1) satellite following the submission of a data acquisition request (DAR) form. Due to its narrow swath width (7.65 km), only one investigated polluted location in Kporghor fell within the image.

3.4.2.2 Pre-processing of Hyperion Image

Despite the level 1 processing of the Hyperion image, noise and other artefacts remain and these arise from several factors which include atmospheric disturbances and internal sensor defects (Scheffler and Karrasch, Oct 17, 2013; Adler-Golden *et al.* 2013). Various entities in the atmosphere such as water vapour, aerosols and clouds interfere with the electromagnetic radiation reflected from the surface and measured by the sensor in space. Equipment defects occur due to the failure of one or more components during image acquisition. Previous studies have investigated several ways of correcting these defects in order to produce an image with a very high signal-to-noise ratio (SNR). Some of these methods have resulted in modified data with amplified noise; however, the general aim of pre-processing the Hyperion image is to generate high-quality bands that provide meaningful information to the user. In this study the following pre-processing steps were performed on the raw Hyperion image:

1. Original Hyperion image sub-setting to the Kporghor spill site. The resulting image had 68 columns and 66 lines, a total of 4,488 pixels and approximately 134 km^2 in area.
2. Removal of smile effect
3. Radiometric Calibration and Atmospheric Correction
4. Noise reduction; minimum noise fraction transformation applied.
5. Destriping to remove scan lines
6. Masking of non-vegetated areas in the image

There procedures where undertaken using different versions of the environment for visualising images (ENVI) image analysis software package from Exelis Inc., (now Harris Geospatial Solutions).

3.4.2.3 Hyperion Image Subset

The region of interest tool (ROI) in ENVI 5.3 was used to select the Kporghor spill epicentre (SEC) and the surrounding areas as well as the location of the control transects. Recorded coordinates of the SEC from the fieldwork in February 2016 identified the relevant points in the image.

A new region labelled KporghorSA in Figure 3.8 B was used to extract corresponding data from the raw Hyperion image EO1H1880562015327110PR_MTL_L1T.TXT to reduce data volume and processing time. Designated bad bands (121–126; 167-180; 222-224) known to correspond with strong water vapour absorption were removed following suggestions from Datt *et al.* (2003) before the subset routine. Figure 3.8 B shows the subset area (red dot in map B) and examples of a useful Hyperion band (D) and others with different artefacts (C. stripes also known as scan lines; E. Noise).
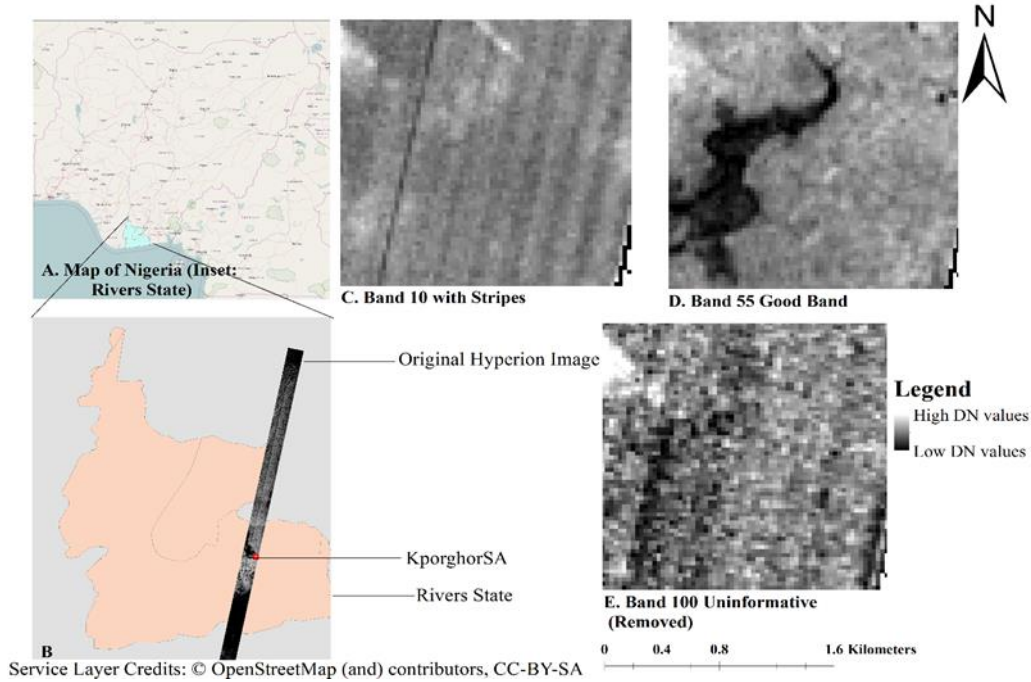
Figure 3.8: Examples of useful and uninformative bands of the Hyperion image. The noisy data was eliminated through the Minimum Noise Fraction Transformation (MNFT) while the scan lines (stripes) were removed following the method of Datt *et al.* (2003).

3.4.2.4 Atmospheric Correction

The image subset was radiometrically and atmospherically corrected using the Fast Line-of-sight Atmospheric Analysis of Hypercubes (FLAASH) module in ENVI 4.4. The FLAASH module incorporates the MODTRAN radiation transfer code developed by Spectral Sciences Inc. (Burlington, MA, USA). The algorithm involves the accurate derivation of atmospheric properties such as surface pressure, water vapour column, oxygen, carbon dioxide, aerosol and cloud overburdens which are incorporated into a correction matrix to convert sensor detected radiance measurements into surface reflectance values (Felde *et al.* 2003). The technique develops from a standard equation that incorporates at-sensor spectral radiance for each pixel, from the mid-infrared (IR) through the ultra-violet (UV) wavelengths with thermal emission omitted; and flat, Lambertian materials or their equivalents (López-Serrano *et al.* 2016). The equation is as follows:

$$L = \left(\frac{Ap}{1 - p_e S}\right) + \left(\frac{Bp_e}{1 - p_e S}\right) + L_a \qquad (3)$$

Where:

p is the pixel surface reflectance

p_e is an average surface reflectance for the pixel and the surrounding region

S is the spherical albedo of the atmosphere

L_a is the radiance backscattered by the atmosphere

A and B are surface independent coefficients that vary with atmospheric and geometric conditions.

The first term in equation (13) corresponds to the radiance reaching the surface while the second term measures the radiance backscattered by the atmosphere into the sensor. The difference between these radiances is attributed to the adjacency effect (radiance contributions from neighbouring pixels) caused by atmospheric scattering. The values for A, B, S and L_a are derived from MODTRAN calculations that incorporate user-supplied parameters such as data type, sensor, sensor altitude, solar and viewing geometry. This information was extracted from the metadata file supplied with the Hyperion image. FLAASH generates other results that are not relevant in the present study such as a water vapour look-up-table (LUT), a cloud mask for identifying cloud-containing pixels in a scene and aerosol scale height. They are, however, employed in the correction matrix to solve for the pixel surface reflectance (*p*) in all the sensor channels.

Following the atmospheric correction, the number of good Hyperion bands reduced from 175 to 164. Eleven (11) bands displayed only missing data: bands 120, 127-133 and 165, 166 and 181. It appears that these bands were affected by strong water vapour absorption. Figure 3.9 shows the spectral profile of sampled polluted and control pixels.

A. Spectral Profile of Raw Hyperion Image

B. Spectral Profile of FLAASH Corrected Hyperion Image
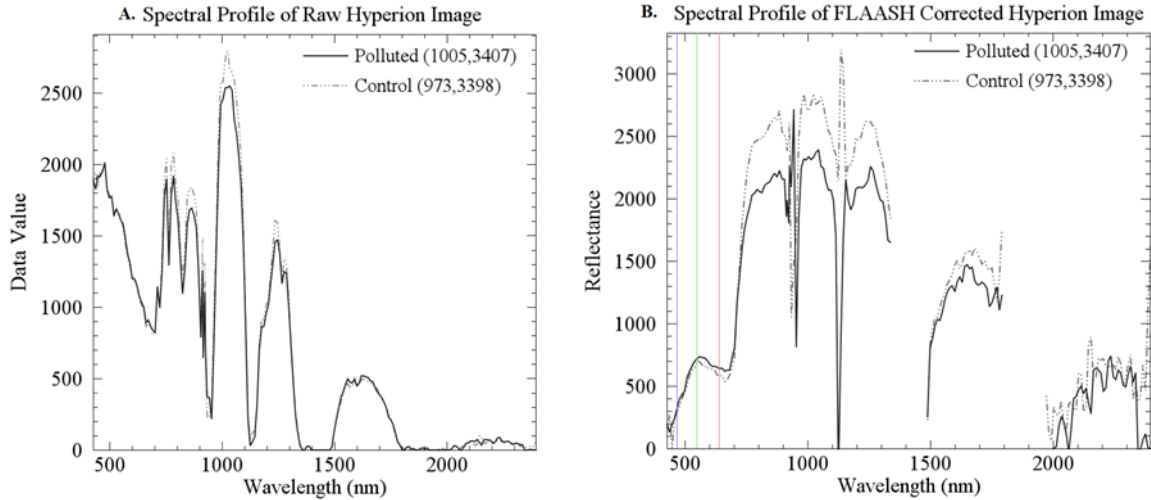
Figure 3.9: The spectral profile of sampled pixels from polluted and control transects illustrated the influence of FLAASH atmospheric correction module on surface reflectance. Atmospheric interference elimination significantly reduced the at-sensor radiance values in the VNIR region while also portraying the robust absorption features in the SWIR region (3.9 B).

3.4.2.5 Removal of Smile Effect

Images acquired by pushbroom instruments such as the Hyperion EO-1 suffer from a line curvature artefact known as the smile or frown effect (Dadon, Ben-Dor and Karnieli, 2010). This effect is attributed to the spatial misalignment of wavelength and bandwidth that occur during the dispersion of the slit-acquired image over straight rows of detector grid in the wavelength dimension (Dadon, Ben-Dor and Karnieli, 2010). An across-track shift from a centre wavelength characterises the spatial misalignment (Gersman *et al.* 2008). Arellano *et al.* (2015) reported that these centre wavelength shifts vary across the VNIR and SWIR regions. In the VNIR bands, the shifts range from 2.6 to 3.5 nm, while in the SWIR bands, they are less than 1 nm. The smile artefact affects the proper retrieval of surface reflectance due to the presence of strong atmospheric absorption features in the spectrum. Gersman *et al.* (2008) pointed out that ignoring this effect alters pixel spectral values and cause an error in subsequent applications.

The smile effect in the Hyperion image was not apparent in any of the individual bands; it was however detected using the first component of a minimum noise fraction transformation (MNFT). The first eigenimage (MNF-1) portrayed a brightness gradient only visible in the

78

VNIR bands and not detected in the SWIR region. Several studies (including (Goodenough *et al.* 2003; Datt *et al.* 2003; Dadon, Ben-Dor and Karnieli, 2010) have used the MNF-1 as an indicator of smile effect in Hyperion image. Correction of the smile effect in the image was performed by the cross-track illumination correction (CTIC) package provided in ENVI. The CTIC approach was selected firstly for simplicity and because of the limited Hyperion data available for analysis. Dadon *et al.* (2010) evaluated the performance of CTIC in removing smile and reported that it compared favourably with their proposed method across varying scenes. A spectral subset of the radiance image (containing only the calibrated VNIR bands) was subjected to the CTIC and to the MNF transformation to check for the presence of the smile effect in the first eigenimage (MNF-1). The CTI corrected MNF-1, as well as the pre-CTIC image, are shown in Figure 3.10; the smile effect in A, MNF-1 of VNIR bands; B: MNF-1 of CTI-corrected VNIR bands and C: the spectral profile of corrected and uncorrected pixels from the polluted and control transects.
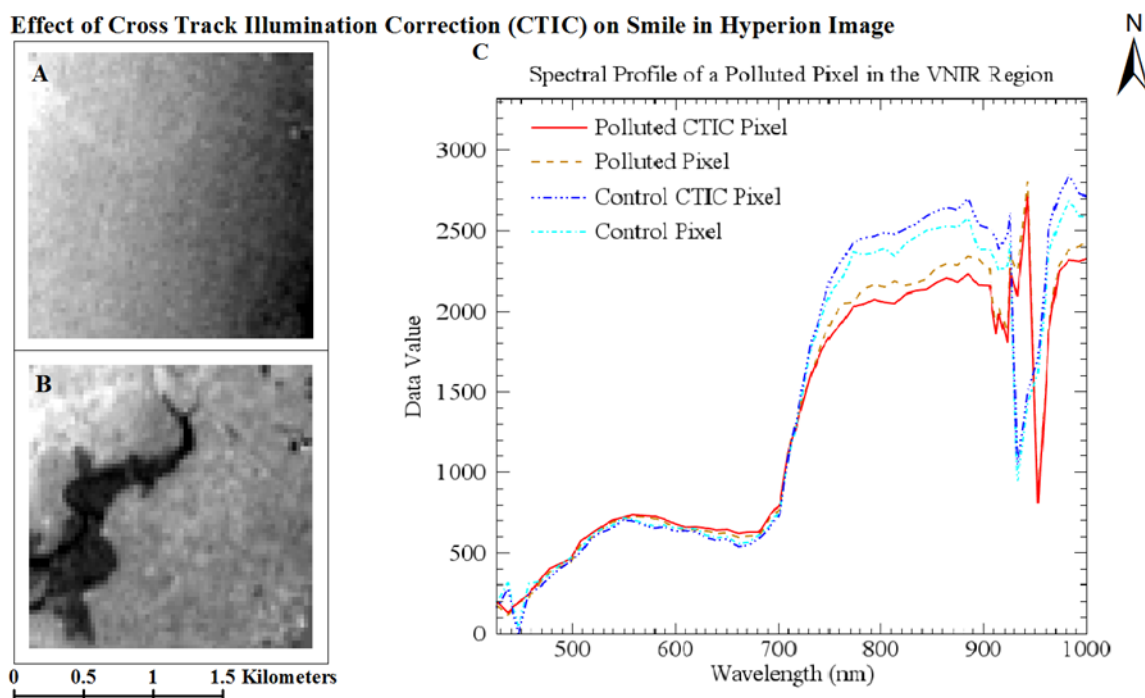
Figure 3.10: The effect of the CTIC performed in ENVI 5.3 shows that the smile effect evident in the MNF-1 of transformed VNIR bands (3.10 A) was successfully removed (3.10 B). The spectra of sampled pixels from the polluted (x, y: 1005.46, 3407.50) and control transects (x, y: 973.25, 3398.3) as illustrated in figure 3.10 C show minor differences in the basic spectral features of the image, thus satisfying the requirement for maintaining spectral fidelity of the image after the removal of the smile effect (Goodenough *et al.* 2003).

3.4.2.6 Noise Reduction

Noise reduction was performed on the image using the Minimum Noise Fraction Transformation (MNFT). This procedure aimed to select the components that maximised the signal to noise ratio and eliminate noisy components. Green *et al.* (1988) and Buddhiraju and Porwal (2015) reported that MNFT was more effective at noise and dimensionality reduction because it produces a set of images arranged in order of decreasing information content and increasing noise fraction. The MNF is a linear transformation involving two distinct principal components analysis (PCA) rotations and a noise-whitening step. The covariance matrix of estimated noise is used to decorrelate and rescale noise in the data, a procedure known as noise whitening. The transformed data with unit noise variance and uncorrelated bands is further subjected to a standard principal component analysis (Buddhiraju and Porwal, 2015). The first few MNF components have large eigenvalues and coherent eigenimages, while the last few components have near unity eigenvalues and noise dominated images (Galidaki and Gitas, 2015). Selection of viable components involved visual inspection of all 164 MNF components in conjunction with eigenvalues and scree plot. Pal and Porwal (2015) suggested that a visual inspection of the MNF images was necessary to ensure the retention of relevant information during noise removal.

In total, 7 MNF components with eigenvalues ranging from 7.03 (MNF7) to 100.4 (MNF1) were selected. These 7 MNF components make up 67% of the variability in the data. Although it would have been reasonable to select more components to explain up to 90% of data variability, this was not done as the rest of the components (MNF8 to MNF 164) did not present any discernible information and hence were discarded. The selected components were inversely transformed through the same MNF procedure to its original spectral space. This procedure also available in ENVI 5.3 was performed using the statistics obtained from the forward MNF procedure. Figure 3.11 shows the spectra of both reflectance images with minimal difference in the spectral information.
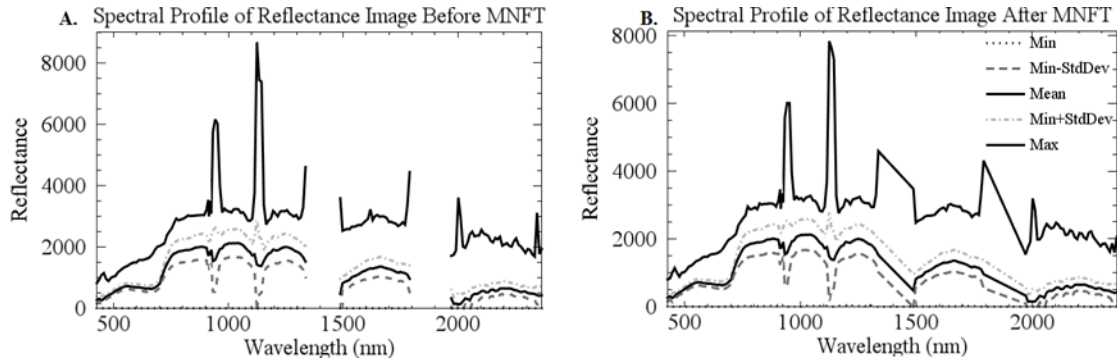
Figure 3.11: Spectral profile of MNF transformed image shows that the process did not significantly affect the reflectance values of the original image except for the non-zero minimum values and the removal of some strong water absorption bands in the SWIR region (1396nm-1487nm).

The MNFT appeared to have effectively removed both noise and scan lines from the Hyperion Image. Figure 3.12 illustrates the difference between pre-MNFT and post-MNFT images. There is a remarkable increase in the signal-to-noise ratio (SNR) of the highlighted bands following the MNFT procedure.
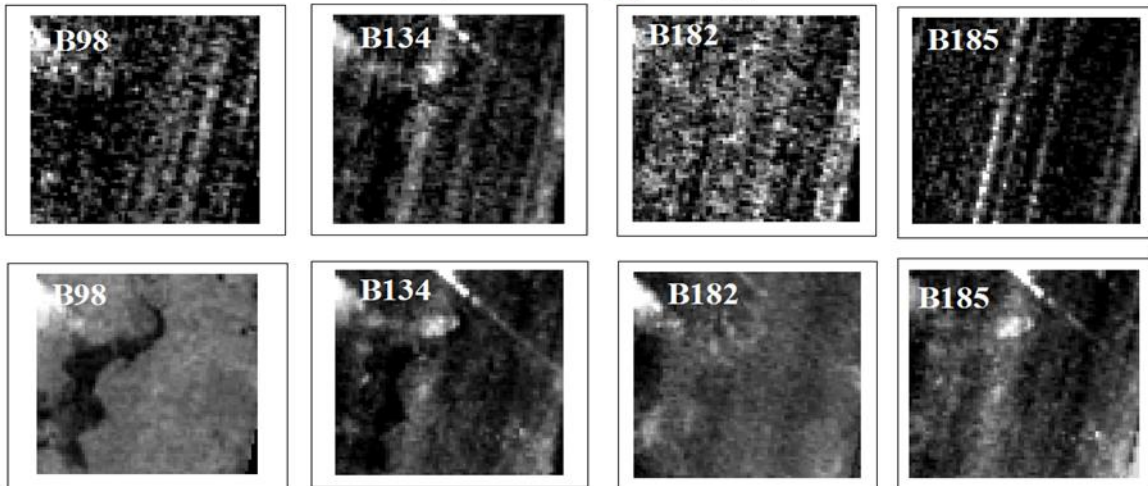
Figure 3.12: Various effects of the minimum noise fraction transformation (MNFT) on the Hyperion bands. The images on the top row are pre-MNFT showing the presence of noise and stripes in the bands listed. The bottom row shows post-MNFT images with most of the noise and stripes removed. The post-MNFT images clearly show increase SNR in the bands listed following the MNFT procedure.

81

3.4.2.7 Band Selection

A total of 164 bands were selected for analysis. As stated earlier, the Hyperion image has 242 channels; however, only 196 bands are calibrated and useful. Further pre-processing reduced the number of valid bands to 164. Table 3.3 below shows the summary of the unused bands and reasons as well as those selected for analysis.

Table 3.3: List of discarded and selected Hyperion bands used in the study. In total, 164 bands were utilised to derive the statistical model

Hyperon Bands	Wavelength Range (nm)	Reason
A. Unused Bands		
1-7	355.95-416.64	Uncalibrated and values set to zero during L1 processing and subsequently removed
225-242	2405.6-2577.08	
71-76	851.92-902.26	Uncalibrated SWIR due to overlap with VNIR bands, values set to zero
58-70	935.58-1057.68	Uncalibrated VNIR due to overlap with SWIR bands, values set to zero
77-79	912.45-932.64	Removed during pre-processing due to overlap with VNIR bands 56-58
120-126	1346.25-1406.84	Strong water vapour absorption
167-180	1820.48-1951.57	Strong water vapour absorption
222-224	2375.3-2395.5	Strong water vapour absorption
B. Used Bands		
8-57	426.8-925.41	
80-119	942.73- 1336.15	
134-164	1487-1790	
182-224	1971-2395	
Total used bands	164	

The selected bands were subjected to minimum noise fraction transformation procedure, and from the results, the first 7 MNF components were selected and used for the inverse transformation back to the original spectral space.

3.4.3 Landsat Data (LSD)

The Landsat-series was launched by the USGS in March 1984 and remain in operation for over 30 years. Landsat data offer a record of the earth's terrestrial surface and changes over time at local, regional and global scales (Roy *et al.* 2014). The Landsat series offer a massive

database of systematic remotely sensed images for use in determining the spatial and temporal changes that have occurred in the study area during this period. The Landsat based sensor acquires imagery at 30m spatial resolution from 6 to 8 spectral bands including a thermal band. Many researchers have applied Landsat data to investigate the status and dynamics of ecosystems at local, regional and global scales. Biodiversity evaluation in forests (Dymond, Mladenoff and Radeloff, 2002; Thenkabail *et al.* 2004a), agricultural lands (Kuenzer and Knauer, 2013) and several other ecosystems has been carried out. In general, Landsat data is highly recommended for mapping and monitoring vegetation and land cover changes (Roy *et al.* 2014).

A Landsat 8 OLI surface reflectance image downloaded from the USGS data download website (earth explorer) was utilised in this study. The image acquired by the OLI sensor onboard the Landsat 8 satellite provides information over nine bands ranging from 435 nm to 1384 nm in 16 bits. The Landsat Surface Reflectance image downloaded was already processed to a Level 2 product, hence needed only a spatial subset to the study area before computation of broadband indices in ENVI 5.3. The Level 2 product measured the fraction of incoming solar radiation reflected from the earth's surface to the Landsat sensor (United States Geological Survey, USGS, 2016) hence; atmospheric interferences are removed at level 2 pre-processing. The index computed from the Landsat data was NDVI.

3.5 Data Analysis

3.5.1 Statistical Analysis (STA)

Analysis of field and satellite data required several statistical packages. These packages include Statistical Package for the Social Sciences, (SPSS), R-Packages vegan, LabDSV, Betapart and np, Paleontological Statistics Software Package, (PAST) and Microsoft Excel (Excel). Excel and SPSS were used for preliminary exploratory analyses and determine the characteristics of the data (mean, median, variance, standard deviation and so on). Furthermore, relationships among the environmental variables (for instance the relationship between total petroleum hydrocarbon and phosphorus in the soil) and between soil properties and floristic data were examined through correlation and regression analysis. Analysis of non-parametric data was by the R package (np) whereas the PAST software supported the

computation of species diversity and other multivariate analysis including principal component and correspondence analyses.

The general null hypothesis tested in this study was that there was no difference in TPH, vegetation characteristics (taxa, frequency, abundance, and density), species diversity and vegetation reflectance of polluted and control transects.

Three datasets analysed in this study were the species inventory data, the soil parameters data obtained from the laboratory analysis of soil samples and the spectral data derived from various remotely sensed images. For each ecosystem component (polluted or control), these datasets were grouped by segments of corresponding transects. Exploratory analysis of the soil dataset identified the centre and spread of the variables on polluted and control transects, as well as the relationship among soil parameters, which helped determine the effect of oil pollution on other soil parameters such as phosphorus, electric conductivity, pH and so on. The analysis performed with the floristic data determined firstly, the similarity and diversity status of polluted and control transects, identified the relationship between soil parameters and floristic characteristics such as taxa (species number), abundance, richness, and diversity and evaluate relationships between these characteristics and spectral metrics derived from satellite imagery.

The Anderson-Darling test for normality performed on the datasets revealed a non-normal distribution of the datasets. The Anderson-Darling test compares the empirical cumulative distribution function of the sample data with the expected normal equivalent. Due to the non-normal distribution of both datasets, and failure to obtain appropriate transformation that met the assumptions of parametric multivariate analysis (such as the Levene's test for homogeneity), non-parametric statistical procedures including Mann-Whitney, Kruskal-Wallis one-way analysis of variance (K-W) and non-parametric regressions were employed in the statistical analysis.

Further multivariate analytical procedures including ordination were used to infer the presence of and then subsequently identify the environmental variables that significantly affect floristic composition on transects. This was achieved by investigating the strength of

84

association among species and their habitats (polluted or unpolluted) using the canonical correspondence analysis.

After confirming the similarity of the polluted and control transects across all 20 locations (ten polluted and ten control) using the Sorenson's Similarity Index, the dissection of the field data was carried out for the two eco-systems components encountered in the study area. These are the polluted and unpolluted (control) transects. Attributes investigated for each component included: -

  i. Soil parameters: Mean and median values, standard deviation, test for differences (Mann-Whitney, Kruskal-Wallis, Dunn's test with Bonferroni correction) between polluted and control transects and regression with vegetation data.

  ii. Vegetation data:

- ➢ Species number (taxa), number of individual plants, frequency, abundance, density;
- ➢ Relative frequency, relative abundance, relative density and important value index;
- ➢ Species occurrences, accumulation and abundance distribution curves
- ➢ Species richness, evenness, dominance, diversity indices and beta diversity;
- ➢ Regression with soil parameters.
- ➢ Test for differences between polluted and control vegetation using Mann-Whitney, Kruskal-Wallis, Dunn's test with Bonferroni correction.

  iii. Leaf chlorophyll data: Mean and median values, test for differences in means, correlation and regression with soil parameters. Test for differences between polluted and control vegetation using Mann-Whitney, Kruskal-Wallis, Dunn's test with Bonferroni correction.

3.5.1.1 Mann-Whitney U Test (M-W Test)

The M-W test is a non-parametric statistical model, which test for differences in the medians of two groups (Das, 2009). The null hypothesis is that it is equally likely that a randomly selected value from polluted samples will be less than or greater than a randomly selected value from the control transects. For all tests, the type I error (the probability of rejecting the null hypothesis when it is true) was controlled at $\alpha = 0.05$. All tests evaluated the impact of

oil pollution on various parameters including field-measured data and spectral metrics derived from satellite images by comparing between polluted and control transects.

3.5.1.2 Kruskal-Wallis Test (K-W Test)

The Kruskal-Wallis one-way analysis of variance by ranks was employed to test the null hypothesis of no difference in median values of more than two independent samples (Wallis and Kruskal, 1952). It compared samples from segments of polluted and control transects, and significant result from the omnibus test was subjected to pairwise multiple-comparisons of mean rank sums using the Dunn's test. Dunn's test identified which samples differed significantly. The Bonferroni correction procedure adjusted the p values, which controlled family-wise error that may lead to false discoveries. The Bonferroni adjustment divides the overall alpha (0.05) by the total number of multiple tests (Dunn, 1964).

3.5.1.3 Regression Methods (RM)

The potential of independent variables (soil properties and spectral metrics) to estimate the species richness and diversity of the study area was assessed using non-parametric statistics. Vegetation indices such as the normalised difference vegetation index (NDVI) are commonly used to predict species richness and diversity (Gould, 2000; Peng *et al.* 2018b; Kamaljit Bawa *et al.* 2002; Mohammadi and Shataee, 2010; Mapfumo *et al.* 2016; Heumann, Hackett and Monfils, 2015). Each diversity index was modelled as a function of the independent variables (for instance spectral metrics and vegetation indices derived from the satellite images). Partial least square regression (PLS) and non-parametric multivariate regression (NPM) procedures were employed to model the relationship between independent variables and the response (for instance, Shannon's, Simpson's, Menhinick's and Chao-1indices). These regression models were selected because they are not limited by assumptions of data distribution common with parametric regression procedures. Model performance was evaluated based on the coefficient of determination, residual errors and graphical residual analysis. In all the models, the null hypothesis was that there was no relationship between the independent and response variables.

A. Partial Least Squares Regression (PLS)

PLS technique performs multivariate regression without the restrictions associated with the standard regression methods. It is particularly useful when predictor variables outnumber response variables and when there is high multicollinearity between the predictor variables. The procedure transforms the predictor data into a smaller set of uncorrelated components and performs least square regression on these components instead of the original data. PLS is adequate for the analysis of hyperspectral data (Asner and Martin, 2011; Heumann, Hackett and Monfils, 2015) due to high multicollinearity of the wavelengths. Selection of the optimum number of components depends on the coefficient of determination (R^2) which refers to how much of the variance in the predictors and between the predictors and response is explained by each component. For highly correlated predictors, it is normal for fewer components to appear in the model.

B. Non-Parametric Regression (NPM)

NPM regression analysis was performed to account for any violations of the assumptions about the distribution of the data. Non-parametric methods allow the modelling of densities and local polynomial regression on both continuous and categorical data which do not necessarily follow any pre-defined distribution (Albek, 2003). Hayfield and Racine (2008) (Hayfield and Racine, 2008) developed the np package in R used for this analysis. The procedure commences with the selection of optimum bandwidths estimated from second-order Gaussian kernel densities. The bandwidth objects are then assigned to an appropriate regression function, which determines the fitting of the curve and calculates the fitted, predicted and error values. The np package has a multi-start function, which helps to avoid errors that occur in the presence of local minima. Since the NPM relies on kernel density estimation, choosing the smoothing parameter (bandwidth) is very crucial. In this study, optimum bandwidths were selected using the Akaike information criterion (AIC), which provides an unbiased estimation that minimises the expected Kullback-Leibler divergence (Hurvich, Simonoff and Tsai, 1998). Three NPM procedures employed in the statistical analysis in this study were Multivariate Regression (NPMR) which models the relationship among one or more response variables and multiple predictor variables; Univariate Regression (NPUR) which models the relationship between one response variable and one

predictor variable and Logistic Regression (NPLR) which models the relationship between the predicted probability of a binary response variable (usually categorical) and one or more predictor variables. All three procedures are extensively discussed in Hayfield and Racine (2008). For model validation purposes, original dataset was randomly sub-divided into training data and test data in the ratio of 6:4. The training data used to calibrate the models while the test data used for model validation. Evaluation of model performance was based on the type and the predictors used.

3.5.2 Vegetation Data Analysis (VDA)

3.5.2.1 Species Taxa

Taxa is a measure of the counts of species occurring in each segment along investigated transects. It provides an estimate of the species richness and diversity of the segments. Determined from species inventory tally sheets.

3.5.2.2 Sorenson's Similarity Index of Transects

Similarity index measures the degree of association or agreement of two entities or variables, in this case, vegetation data from polluted and control transects (Warrens, 2008). In this study, segments of polluted and control transects across the entire study area were clustered into groups based on their similarity index which, quantifies their level of association concerning species composition. The formula for Sorenson's similarity index (IS) is:

$$IS = \frac{2MW}{MA+MB} * 100 \tag{4}$$

Where
MW = Sum of the smaller numbers of plant species common to the control and test transects
MA = the sum of all plant species in the transect A
MB = the sum of plant species in the transect B

3.5.2.3 Number of Individual Plants

This is a measure of the abundance of each species observed per segment. The number of individual plants per species was determined from tally sheets

3.5.2.4 Frequency

This is the probability of a plant species occurring in a given number of segments (Bonham, 2013a). Frequency of species occurrence was used to detect any changes in vegetation composition of polluted and control transects. Vegetation frequency was calculated from species inventory data as:-

$$\text{Frequency} \ = \ \frac{number\ of\ segments\ in\ which\ species\ occured}{number\ of\ segments\ investigated} \qquad (5)$$

3.5.2.5 Density

Also a measure of abundance defined as the number of individuals of a given species occurring in a given sample unit. Density estimate are relevant for monitoring plant responses to environmental disturbances (Bonham, 2013b). Density estimates for observed species in the study area were calculated to identify vegetation responses to oil pollution using the following formula:-

$$\text{Density} = \frac{number\ .of\ individuals\ of\ the\ species\ in\ all\ the\ segments}{Total\ number\ of\ segments\ studied} \qquad (6)$$

3.5.2.6 Importance Value Index

This is a measure of the ecological importance of a given species in an ecosystem. It is frequently used to prioritise species for conservation purposes (Zegeye, Teketay and Kelbessa, 2006), however, in this study, the IVI of species was used to determine the effect of oil pollution on vegetation structure by comparing the IVI of species on polluted and control transects. IVI was calculated by summing the relative values of frequency and density where

$$\text{Relative frequency} = \frac{frequency\ of\ a\ given\ species}{sum\ frequency\ of\ all\ species} * 100 \qquad (7)$$

And

$$\text{Relative density} = \frac{number\ of\ individuals\ of\ a\ species}{totalnumber\ of\ individuals} * 100 \qquad (8)$$

3.5.2.7 Indicator Species

Indicator species are organisms whose presence, absence or abundance provides an ecological indication of community or habitat types, environmental conditions or environmental changes (Cáceres *et al.* 2012). They can provide important information on the type and volume of environmental pollution and other stressors. A good indicator species is one that is both abundant in a specific type of habitat (specificity) and predominantly found in this type of habitat (fidelity).

Indicator values of a species (i) at a given site (j) is calculated as

$$\text{IndVal}_{ij} = \text{Specificity}_{ij} * \text{Fidelity}_{ij} * 100 \tag{9}$$

Where

IndVal_{ij} = indicator value of a given species (i) in relation to a (j) type of site
Specificity_{ij} = proportion of sites 'j' in which occurred species 'i'
Fidelity_{ij} = the proportion of the number of individuals (abundance) of species 'i' that occurred in site 'j'

In this study, indicator value of species was calculated in *R* using the *indicspecies* package developed by De Cáceres and Jansen (2016), to identify species whose presence or absence reveal the occurrence of oil pollution in the study area.

3.5.2.8 Species Occurrence Curve (SOC)

This is a measure of how individuals of a species are distributed among the sampling units (segments). Species occurrence curve was used to visualise the distribution of species in polluted and control segments and to determine the most frequently occuring species. The curve is derived by plotting the cumulative count of species on the x-axis and the number of plots on the y-axis.

3.5.2.9 Species Accumulation Curve (SAC)

Provide estimations of the number of species in a given habitat and is used to compare the richness of different communities at comparable levels of sampling efforts (Dorazio *et al.* 2006). In this study, the SAC was plotted to illustrate the differences in the species richness of polluted and control transects.

3.5.2.10   Beta-diversity of Transects

This was determined in *R* using the *betapart* package developed by Baselga and Orme (2012). Beta diversity is a measure of variation in species composition of two or more ecological units. Beta diversity is usually partitioned into two components namely species turnover and species nestedness. The species turnover component measures the degree at which species observed in one site are replaced by different species at another site (Baselga *et al.* 2018). On the other hand, species nestedness describes the absence of species in one, but not another site. Both components of beta diversity were analysed in this study to evaluate the changes on species composition of polluted transects. The presence-absence data was used for this analysis as recommended by Baselga and Orme (2012). Beta diversity analysis was performed to compare vegetation on polluted and control transects across the entire study area and for each location. A multivariate analysis of group dispersion was performed using the betadisper function in the r package, vegan developed by Oksanen *et al.* (2018). The analysis which test for the homogeneity of variances of both groups (polluted and control) was aimed at isolating the effect of soil TPH on species composition of polluted transects by evaluating the differences in distances of group members to the group centroid. According to Anderson, Ellingsen and McArdle, (2006), betadisper function is important for comparing betadiversity among classes or factors.

3.5.2.11   Canonical Correspondence Analysis

Species occurrence and distribution are a function of environmental variables. To evaluate the impact of the environmental variables particularly the TPH concentrations on the species composition and distribution, canonical correspondence analysis was performed. Canonical correspondence analysis (CCA) is a multivariate ordination method used to detect the influence of environmental variables on biological assemblages of species (Braak and Verdonschot, 1995). CCA reveals synthetic environmental gradients from ecological data sets that determine habitat preferences of species. Hejcmanovā-Nežerková and Hejcman (2006) applied CCA to reveal the environmental variable most affecting the structure of woody vegetation. In this study, the procedure was carried out to determine the environmental variable that most influences species occurrence and abundance. The soil

parameters that exhibited strong relationship (0.5 < r <-0.5) with taxa and number of individuals were selected as environmental variables.

3.6 Summary

This chapter presented the datasets and methods applied in this research. Attributes of the satellite datasets including the spatial and spectral resolutions, sensors, acquisition dates and pre-processing steps were outlined. The statistical and computational procedures performed were also discussed. Chapter 4 presents the results obtained from answering the first research question.

4 Species Distribution and Diversity in Rivers State and the Effects of Oil Pollution

This chapter addresses the first and second research questions (RQ1 and RQ2 in Section 2.10.1,). Therefore, the objective is to determine the vascular plant species diversity index of the study area and to investigate the impact of oil pollution on the characteristics, diversity and biophysical parameters of vascular plant species as surrogates for biodiversity. To achieve this objective, a hierarchy of hypotheses were tested in the following order

H_O: Observed differences in TPH concentration and vegetation of polluted and control transects are random and not significant

H_1: Observed differences in the TPH concentration and vegetation of polluted and control transects are not random and are significant

Sub-hypotheses:

H_{1a}: The difference in the TPH concentration of polluted and control transects is significant;

H_{1b}: The difference in characteristics of vegetation on polluted and control transects is significant;

H_{1c}: The difference in the vascular plant species diversity of polluted and control transects is significant.

H_{1d}: The difference in the biophysical parameter of vegetation on polluted and control transects is significant.

4.1 Methodology

The methodology for this chapter is elaborated in Chapter 3 and includes field observation (FO, section 3.3.2), analysis of soil samples (LAS, section 3.3.3), and data analysis (STA and VDA, section 3.4).Results

4.1.1 Soil Analysis

4.1.1.1 The Physicochemical Properties of Soil Samples

Results of laboratory analysis to determine the physicochemical properties of samples collected from investigated transects for comparison between polluted and control are illustrated in Figure 4.1 From the chart, soil samples from transects in Amuruto appear to

have the highest TPH concentrations of nearly 100,000 mg/kg of soil. This may be due to the estimated volume of the spill (5054 barrels) reported at the Nigerian oil spill monitor website (https://oilspillmonitor.ng/#/41981.2015/LAR/183/492) of which only 332 barrels were recovered.
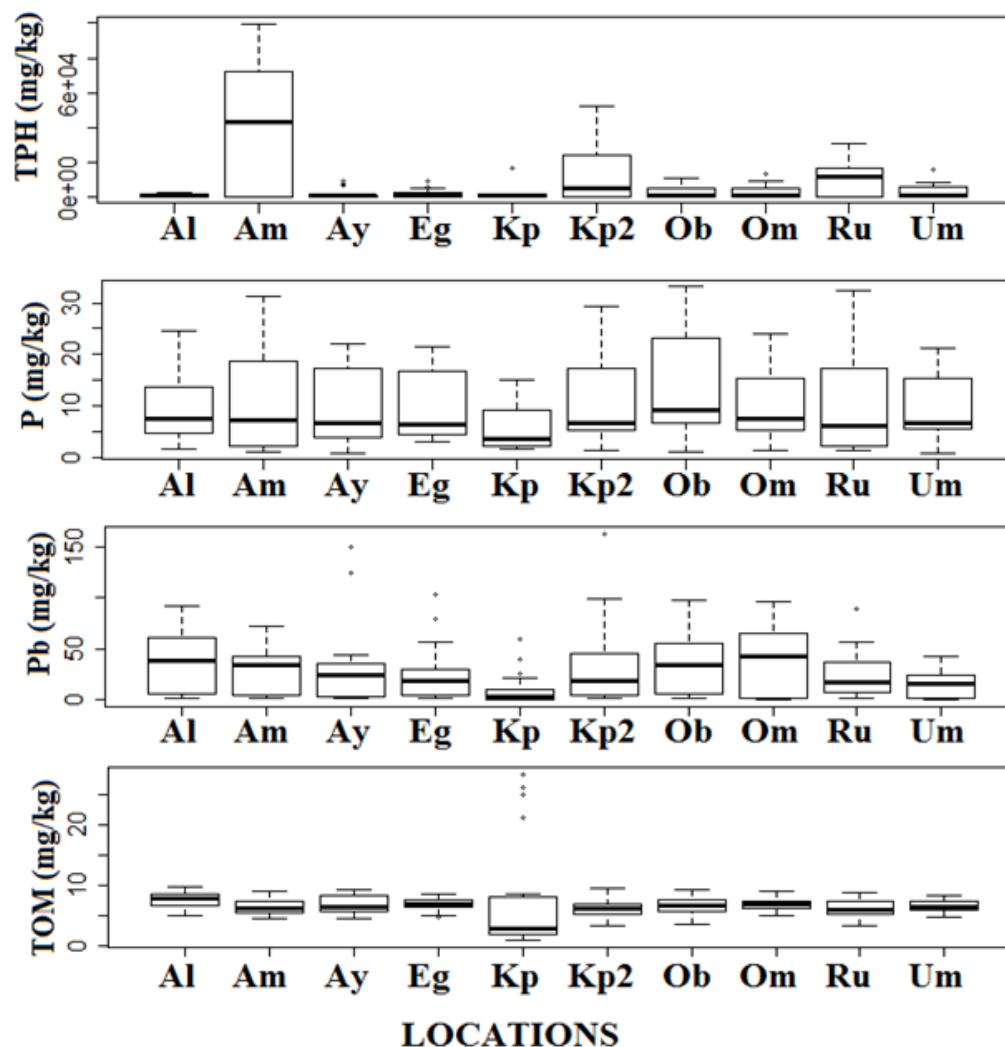
Figure 4.1: Box plots showing the differences in the concentrations of total petroleum hydrocarbons (TPH), phosphorus (P), lead (Pb) and total organic matter (TOM) in samples collected from various locations in the study area. The locations are Al (Alimini), Am (Amuruto), Ay (Anyu), Eg (Egbalor), Kp and Kp2 (Kporghor 1 and 2 respectively), Ob (Obua), Om (Omoigwor) and Ru (Rumuekpe).

Other highly polluted transects appeared located in Kporghor 2 and Rumuekpe. Although there was no estimated crude oil volume for Kporghor 2; about 1200 barrels was reportedly spilt at the Rumuekpe location. Locations with the least soil TPH concentrations were Alimini, Anyu and Kporghor.

The relationship among the soil properties was investigated to determine their independence or correlation with one another. The scatterplots in Figure 4.2 confirm the presence of correlation between the concentrations of TPH, Phosphorus and Lead. While Lead increased with TPH ($r = 0.71$), Phosphorus exhibited an inverse relationship with TPH as seen in the negative correlation coefficient result ($r = -0.69$).
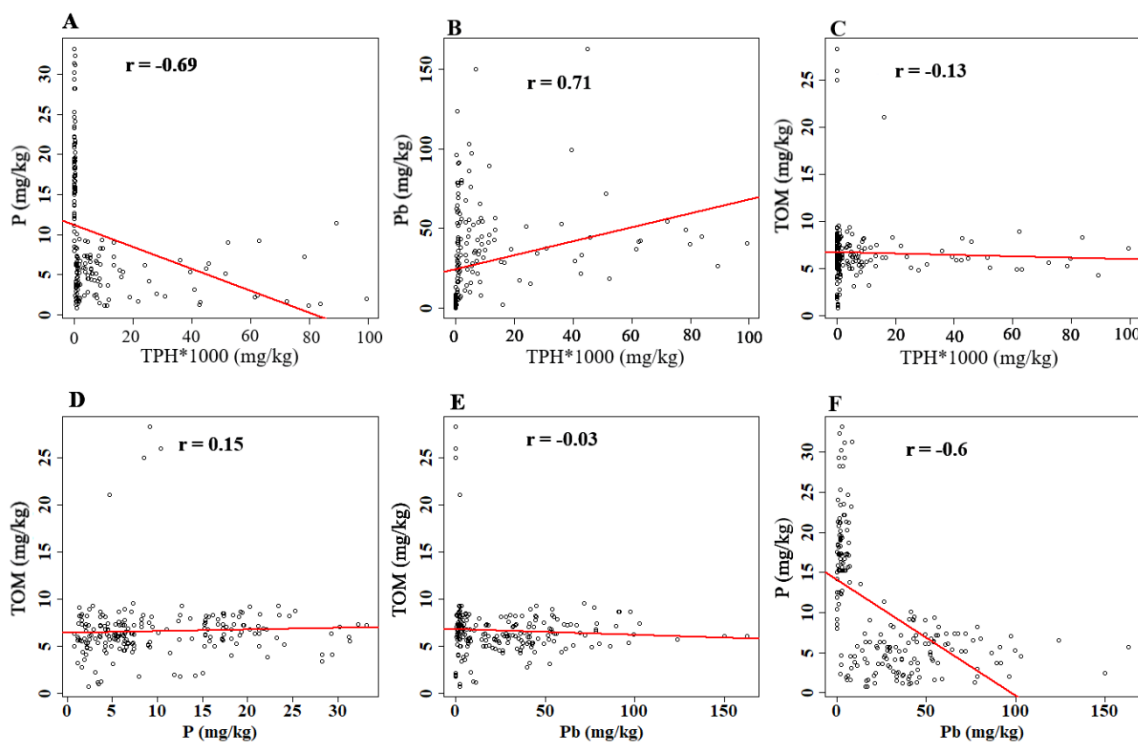
Figure 4.2: Joint distribution of soil parameters showing a strong positive correlation between Pb (a heavy metal) and TPH, and a strong negative relationship between phosphorus (a soil nutrient) and TPH. Conversely, TOM has a weak correlation with TPH, P and Pb

The strong relationship between these variables signifies the critical effect of crude oil pollution in the environment. Considering that phosphorus, for example, is an essential soil nutrient that promotes vegetation growth, this result suggests that floristic differences between polluted and control transects may be attributable to the presence of TPH in the soil.

Preliminary analysis of soil properties from the polluted and control soil samples in Kporghor 1 location (Appendix 4.1) showed there was little variation in the soil acidity and soil temperature. While pH values ranged from 4 to 4.9; the mean soil temperature was 29.1 on polluted transects and 29 on the control transects. There were, however, significant differences ($p<0.05$) in the total petroleum hydrocarbons (TPH) concentration, electrical

95

conductivity (EC), soil nutrients (Phosphorus, P) and heavy metals (Lead, Pb) content in polluted and control transects from Kporghor. The heavy metals tested for and detected in the soil samples include lead (Pb), cadmium (Cd) and arsenic (As). Both Cd (Mean = 2.35 mg/kg) and As (<0.001 mg/kg) levels were negligible and very much below the Environmental Guidelines and Standards for the Petroleum Industry in Nigeria (EGASPIN) intervention values. The EGASPIN intervention values for Cd = 100 mg/kg and As = 200 mg/kg.

Similarly, the total organic carbon (TOC), total organic matter (TOM) and total heterotrophic bacteria (THB) content were also significantly different for the polluted and control transects. Across the entire study area comprising ten spill locations and ten control locations, four soil properties were tested. These were TPH, Phosphorus, Lead and TOM. Median Pb values varied significantly (H = 139.02, N = 210, DF = 19, p<0.05) for the polluted (39.15 mg/kg) and control (2.14 mg/kg) transects. Levels of Pb in soil samples from several segments of polluted transects were above the EGASPIN intervention values whereas this was not the case in control transects. Mean and median Pb values are 27.76 mg/kg (S.E. = 2.04) and 19.7 mg/kg of soil respectively across investigated transects.

Soil nutrients availability represented by the phosphorus (P) content in the soil also varied among polluted and control transects in all investigated locations. The mean and median values for P was 10.09 mg/kg (S.E =0.54) and 6.94 mg/kg respectively. On polluted transects, median P was 4.69mg/kg while on control transects it was 17.49 mg/kg. Kruskal-Wallis analysis of variance (K-W) results (H = 146.17, N = 210, DF =19, p < 0.05) show that these values were significantly different. The result is similar to that of the total organic matter (TOM) content in the soil which showed significant differences among polluted and control transects (H = 5.66, N = 210, Df = 19, p<0.05). Following the significant results of the omnibus K-W tests of these properties and rejection of the null hypothesis of no difference in the mean ranks, a non-parametric post-hoc analysis using the Dunn's test with Bonferroni adjustment was performed to determine which transects differed significantly. The results are tabulated in Table 4.1 with significant p-values shown as red asterisks.

Table 4.1: Results of Dunn's pairwise multiple comparison tests with Bonferroni adjustment. The results indicate that at six out of ten locations, the phosphorus content was significantly different

between polluted and control transects. Conversely, the lead content of soil samples differed significantly between polluted and control transects at only four locations. Although the omnibus test for TOM was significant, the observed difference is between groups (locations). Significant values ($p < 0.05$) are shown as red asterisks (*). Titles are derived from the first two letters of location names and P or C representing polluted or control transect respectively. For instance, AlC is Alimini control transects.

P	AlC	AmC	AyC	EgC	Kp2C	KpC	ObC	OmC	RuC	UmC
AlP	0.27	-	-	-	-	-	-	-	-	-
AmP	*	*	-	-	-	-	-	-	-	-
AyP	0.10	*	*	-	-	-	-	-	-	-
EgP	0.25	*	*	*	-	-	-	-	-	-
Kp2P	0.52	*	0.07	0.10	0.09	-	-	-	-	-
KpP	*	*	*	*	*	*	-	-	-	-
ObP	1.00	0.10	0.26	0.38	0.32	1.00	*	-	-	-
OmP	0.36	*	*	0.07	0.06	1.00	*	0.28	-	-
RuP	*	*	*	*	*	0.35	*	*	*	-
UmP	0.31	*	*	0.06	*	1.00	*	0.24	*	0.11
Pb	AlC	AmC	AyC	EgC	Kp2C	KpC	ObC	OmC	RuC	UmC
AlP	*	-	-	-	-	-	-	-	-	-
AmP	0.26	0.06	-	-	-	-	-	-	-	-
AyP	1.00	0.33	0.09	-	-	-	-	-	-	-
EgP	1.00	0.77	0.22	0.49	-	-	-	-	-	-
Kp2P	0.34	0.08	*	*	*	-	-	-	-	-
KpP	1.00	1.00	1.00	1.00	1.00	0.28	-	-	-	-
ObP	0.06	*	*	*	*	*	*	-	-	-
OmP	*	*	*	*	*	*	*	*	-	-
RuP	1.00	0.31	0.08	0.19	0.09	*	0.43	*	0.46	-
UmP	1.00	1.00	1.00	1.00	1.00	*	1.00	0.07	1.00	0.08

4.1.1.2 Total Petroleum Hydrocarbon (TPH) in Polluted and Control Transects

The average concentration of TPH in polluted and control transects across investigated areas are shown in Figure 4.3. The boxplots depict the minimum, [first] quartile, median, [third] quartile and maximum values of TPH at the different locations as well as the 95% confidence intervals of the median values and outliers. The highest concentration of TPH (>99000 mg/kg) occurred in samples from the Amuruto spill epicentre. In Figure 4.3A raw TPH values used in plotting the bars demonstrate a considerable difference in TPH concentrations in polluted and control transects. Overall mean and median TPH values for polluted transects were 12,692 and 3933 mg/kg respectively, while for the control, the values were 40.53 and 36.50 mg/kg respectively. In Figure 4.3B, the raw TPH data was transformed to its common logarithm and plotted to highlight the reference line, which signifies the average

recommended Environmental Guidelines and Standards for the Petroleum Industry in Nigeria (EGASPIN) intervention value of different components of petroleum hydrocarbon in the soil. EGASPIN intervention values (mg/kg of soil) documented for different aromatic hydrocarbons that make up crude oil range from 1 for Benzene to 130 for Toluene (Department of Petroleum Resources, (DPR), 2002). Figure 4.3B reveals that TPH concentration in polluted transects is well above EGASPIN intervention values. Although lower TPH values were observed in control transects, these values were just within the borderline of intervention values and also above the target values of 0.05 mg/kg for the various petroleum hydrocarbon components.

TPH concentrations in polluted and control transects were compared for significant differences using the Kruskal-Wallis test. The omnibus test was significant; hence the null hypothesis of 'no difference in samples' was rejected. A post-hoc analysis was then performed to determine which locations were affected. Interesting, significant differences between polluted and control transects only occurred at three out of ten locations. this suggests that the observed differences were not statistically significant, however, when segments of polluted and control transects were compared, the results reflected significant differences in soil TPH concentrations particularly between spill epicentres (SS0s) and control segments.
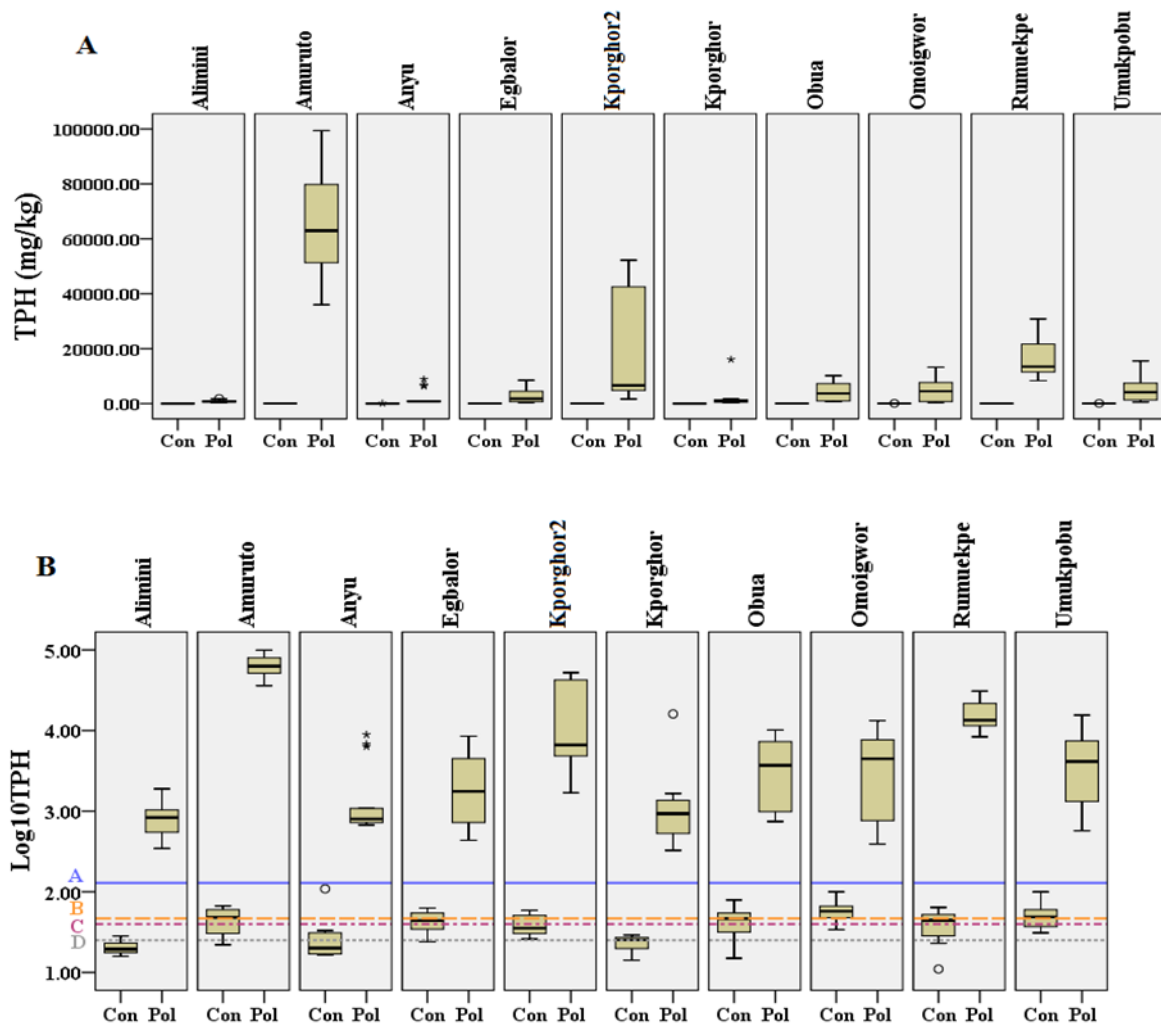
Figure 4.3: Total petroleum hydrocarbons levels in soil samples from polluted and control transects (N=210). Bar charts were plotted using **A**: raw TPH values and **B:** transformed (common log) values. The coloured reference lines on chart **B** illustrates the average EGASPIN intervention value for A: Ethylbenzene = 50mg/kg (1.669 on the log scale); B. Phenol = 40 mg/kg (1.6); C. Toluene = 130 mg/kg (2.11) and D. Xylene = 25 mg/kg (1.4). TPH levels in polluted transects were well over the recommended intervention value, whereas levels in control 1 transects were borderline.

4.1.1.3 Total Petroleum Hydrocarbon (TPH) in Segments Along Polluted Transects.

There appears to be a trend of decreasing TPH concentration as the distance from the spill epicentre (SS0) increased along polluted transects (Figure 4.4). For instance, the average TPH level at SS1 (0-20m from SS0) was 7659 mg/kg; SS3 (40-60m from SS0): 3375 mg/kg; and at SS5 (80-100m from SS0): 2571 mg/kg. Performing Kruskal-Wallis analysis of variance for TPH in segments of polluted transects revealed significant differences in the

values. (N = 130, H = 170.9, $p < 0.05$). The result was further subjected to multiple comparisons using Dunn's test to identify the segments significantly different.
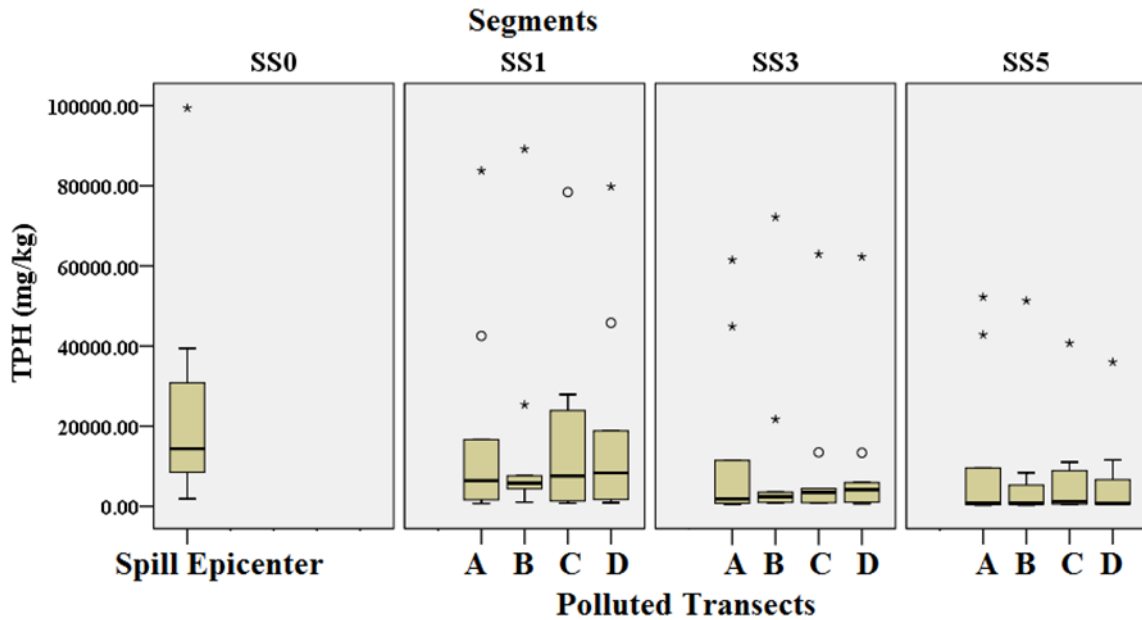
Figure 4.4: A comparison of average TPH levels at the spill centre and segments SS1, SS3 and SS5 along polluted transects A, B, C and D (N = 130). Lines on the box show the 1st, median and ^{third} quartiles. The coloured box is the confidence interval at 95% for the median value.

The results in Table 4.2 showed that the TPH concentration in SS5 as determined by the distance from SS0 along polluted transects was significantly different from SS0 and SS1 but not with SS3. There were no significant differences among SS0, SS1 and SS3 suggesting that regardless of TPH concentration, the detrimental effects of oil pollution remains significant in areas up to 60 m from the spill epicentre.

Table 4.2: A Dunn's multiple comparison tests to determine the significance of the rank mean differences in soil TPH along polluted transects (SS0, SS1, SS3 and SS5). P values were adjusted using the Bonferroni method

H₀ (Null Hypothesis)	Dunn's Test Statistic	P-value (Adjusted)	Decision
SS0 = SS1	1.16	1	Accept
SS0 = SS3	2.37	0.18	Accept
SS0 = SS5	3.71	<0.05	Reject
SS1 = SS3	1.92	0.55	Accept
SS1 = SS5	4.04	<0.05	Reject
SS3 = SS5	2.12	0.34	Accept

4.1.1.4 Other Soil Parameters along Polluted Transects in Kporghor

Data from Kporghor 1spill location show certain soil properties like temperature and pH were nearly constant along polluted transects. Nevertheless, the soil phosphorus (P) appears to increase with increasing distance from the spill epicentre (SEC), whereas the heavy metals (Lead and Cadmium) appear to decrease with distance from the SEC. Similarly, the Total Organic Matter (TOM), Total Organic Carbon (TOC) and Total Heterotrophic Bacteria (THB) where higher in the segments closer to the SEC (SS1 and 3) than the segment further away from the SEC (SS5). The result generally confirms the relationship between soil TPH and other parameters as previously shown in the joint distribution chart in Figure 4.2.

Although there is no apparent correlation between TPH and soil properties such as pH, temperature and nitrates, there was a clear negative correlation between TPH and P (r = -0.69) TOC and P (r = -0.423). TPH also positively correlated with TOC (r = 0.878); THB (r = 0.941); TOM (r = 0.496) and EC (r = 0.368), but correlated negatively with Cd (r = -0.333).

4.1.2 Vegetation Analysis

The Anderson-Darling test for normality of the floristic dataset was 1.619 for the polluted transects and 1.526 for the control transects. The p-value for both results was less than 0.05; hence the null hypothesis of population normality was rejected. Furthermore, due to the excessive skewness of the data (skewness = 6.01) as well as the occurrence of non-positive values (0), exponential, lognormal, Weibull, gamma, log-logistic distributions could not be fitted to the data. Moreover, the box-cox transformation procedures (lambda values ranged from -2 to 2) performed produced distributions which failed the goodness of fit test. Consequently, non-parametric procedures were applied to the data set.

In total, 163 plant species belonging to 52 families were recorded on investigated transects. There were 37 families on polluted, and 52 on control (non-polluted) transects. In all the locations, Poaceae was the most abundant family with 19 species. *Cyperaceae* followed with 13 species, then *Euphorbiaceae* and *Leguminoceae* with ten species each. Other families with over five members were *Asteraceae*, eight; *Arecaceae* and *Fabaceae,* seven each; *Malvaceae* and *Rubiaceae*, six each and *Sterculiaceae*, five. Species-wise, polluted transects

had fewer species than control transects. The number of species on polluted transects was 93 and was substantially lower than the 154 observed on control transects.

Annual herbs dominated on polluted transects with 48 species, followed by shrubs (11), trees (18), climbers (4) and trailers (2). Similarly, herbs dominated on control transects with 73 species but was followed by trees with 42 species. Other lifeforms present were shrubs (17), climbers (7), and trailers (4). The tree species were at various stages of secondary growth on polluted transects while on the control, they were mostly fully matured. The sum of counts of individual plants across the entire study area was 4245 (1264 individual plants at the polluted transects and 2657 individual plants at the control transects).

Table 4.3 lists the 52 families comprising trees, shrubs, herbs, climbers and trailers inventoried in the study area. The dominant family based on individual count was *Poaceae, which* had 627 plants and formed 16.89% of the total population. *Euphorbiaceae* with 410 (11.04%) followed closely. Other dominating families by numbers were *Cyperaceae*, 346; *Leguminosae*, 246; *Asteraceae*, 226; *Arecaceae*, 222*; Rubiaceae,* 193; and so on (see Table 4.3).

On the other hand, the rarest family encountered at the field was *Anthyriaceae*, which had only one individual observed in Kporghor polluted transect B. Other rare families included *Cecropiaceae*, 3; *Rutaceae*, 3; *Dracaenaceae*, 4; and *Lamiaceae*, 5 (Table 4.3). These five families together made up less than 0.5% of the total population of plants observed across the entire state.

Table 4.3: List of plant families observed in the field with their life forms, taxa and abundance

Family	Life Form	Species	Individuals	% of Total population
Acanthaceae	Herb	2	12	0.32
Amaranthaceae	Herb	4	126	3.39
Amaryllidaceae	Herb	1	8	0.22
Anacardiaceae	Tree	2	22	0.57
Apocynaceae	Herb	3	40	1.08
Araceae	Tree	7	97	2.61
Arecaceae	Climber	1	222	5.98
Asclepiadaceae	Herb	8	15	0.40
Asteraceae	Tree	2	226	6.09
Bignoniaceae	Tree	1	31	0.84
Bombacaceae	Herb	1	10	0.27
Boraginaceae	Tree	2	55	1.48
Burseraceae	Tree	1	25	0.67
Caricaceae	Tree	1	47	1.27
Cecropiaceae	Shrub	1	3	0.08
Chrysobalanaceae	Tree	2	7	0.19
Combretaceae	Herb	1	17	0.46
Commelinaceae	Trailer	4	5	0.13
Convolvulaceae	Herb	3	89	2.40
Costaceae	Climber	2	103	2.77
Cucurbitaceae	Herb	13	15	0.40
Cyperaceae	Climber	2	346	9.32
Dioscoreaceae	Tree	1	40	1.08
Dracaenaceae	Tree(Threatened)	1	4	0.11
Ebenaceae	Shrub	10	17	0.46
Euphorbiaceae	Tree	7	410	11.05
Fabaceae	Tree	2	99	2.67
Gentianaceae	Herb	1	26	0.70
Lamiaceae	Herb	10	5	0.13
Leguminosae	Herb	6	246	6.63
Malvaceae	Tree	1	115	3.10
Meliaceae	Tree	2	6	0.16
Moraceae	Tree	1	26	0.70
Moringaceae	Herb	1	12	0.32
Orchidaceae	Herb	1	49	1.32
Passifloraceae	Tree	1	8	0.22
Phyllanthaceae	Herb	18	9	0.24
Poaceae	Herb	1	627	16.89
Pteridaceae	Herb	6	72	1.94
Rubiaceae	Tree	1	193	5.20
Rutaceae	Tree	2	3	0.08
Sapindaceae	Herb	1	135	3.64
Solanaceae	Herb	1	5	0.13
Sterculiaceae	Herb	5	50	1.35
Verbenaceae	Herb	1	28	0.75
Zingerberaceae	Herb	1	6	0.16

4.1.2.1 Similarity Index of Polluted and Control Transects

The Sorenson similarity index results computed for the investigated transects are shown in Table 4.4 All the values are over 0.6 except at Kporghor 2, Amuruto and Rumuekpe, which had index values of 0.42, 0.45 and 0.48 respectively. The results confirm the similarity of polluted and control transects in terms of floristic composition hence validating the comparison of both sites for effects of oil pollution

Table 4.4: Sorenson's similarity index values for polluted and control transects across the study area. Titles are derived from the first two letters of location names and P or C representing polluted or control transect respectively. For instance, AlC is Alimini control transect.

	AlC	AmC	AyC	EgC	Kp2C	KpC	ObC	OmC	RuC	UmC
AlP	0.71	0.27	0.43	0.48	0.37	0.23	0.48	0.31	0.44	0.38
AmP	0.35	0.45	0.29	0.43	0.47	0.17	0.52	0.31	0.3	0.27
AyP	0.35	0.41	0.86	0.52	0.47	0.27	0.71	0.54	0.48	0.54
EgP	0.35	0.32	0.29	0.7	0.42	0.23	0.38	0.62	0.41	0.38
Kp2P	0.29	0.32	0.36	0.43	0.42	0.13	0.38	0.38	0.3	0.35
KpP	0.12	0.14	0.25	0.26	0.16	0.93	0.19	0.15	0.11	0.12
ObP	0.29	0.41	0.43	0.39	0.42	0.13	0.67	0.46	0.37	0.46
OmP	0.53	0.5	0.32	0.48	0.68	0.17	0.33	0.77	0.48	0.42
RuP	0.41	0.41	0.43	0.48	0.42	0.27	0.43	0.38	0.48	0.27
UmP	0.41	0.5	0.39	0.43	0.53	0.2	0.43	0.62	0.33	0.92

4.1.2.2 Characteristics of Vegetation in the Study Area

The *LabDSV* package in *R* language was used to examine the characteristics of the vegetation dataset. Firstly, Figure 4.5 shows the box plots of species number (taxa), frequency, abundance and density of vegetation for different locations investigated. The [first] and [third] quartiles, the medium as well as the minimum and maximum values of these characteristics are illustrated in the plots. The notches on the boxes approximate 95% confidence interval (CI) for the median value of each characteristic. According to Chambers and Brown (1983), non-overlap of box notches indicate significantly different median values that are likely from different populations. The reverse is the case for overlapping notches.
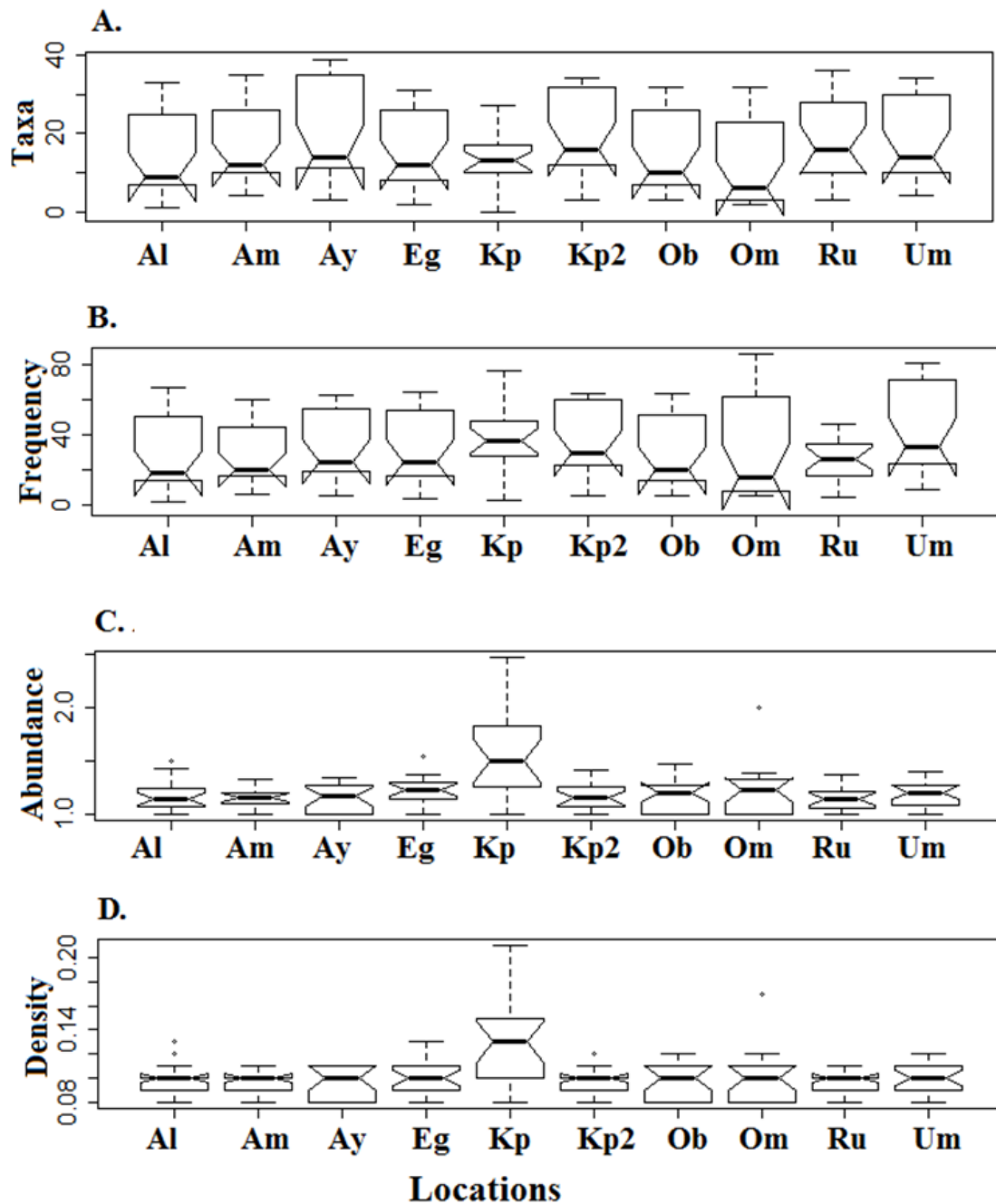
Figure 4.5: Boxplots of vegetation characteristics for various locations in the study area. Both taxa and frequency do not appear significantly different across the locations; however, the least number of species (taxa) was recorded for Kporghor. Surprisingly, Kporghor had the most species abundance and density among all investigated locations.

As the boxes illustrate, taxa and frequency of vegetation on locations overlap at the notches, suggesting that there are no significant differences in these characteristics among the different locations. Likewise, abundance and density overlap at the notches for almost all the locations except for Kporghor 1 providing further evidence of the similarity of the investigated locations in terms of floristic composition.

The cumulative empirical density function (CEDF) of species occurrences was plotted using the vegetation dataset (Figure 4.6).
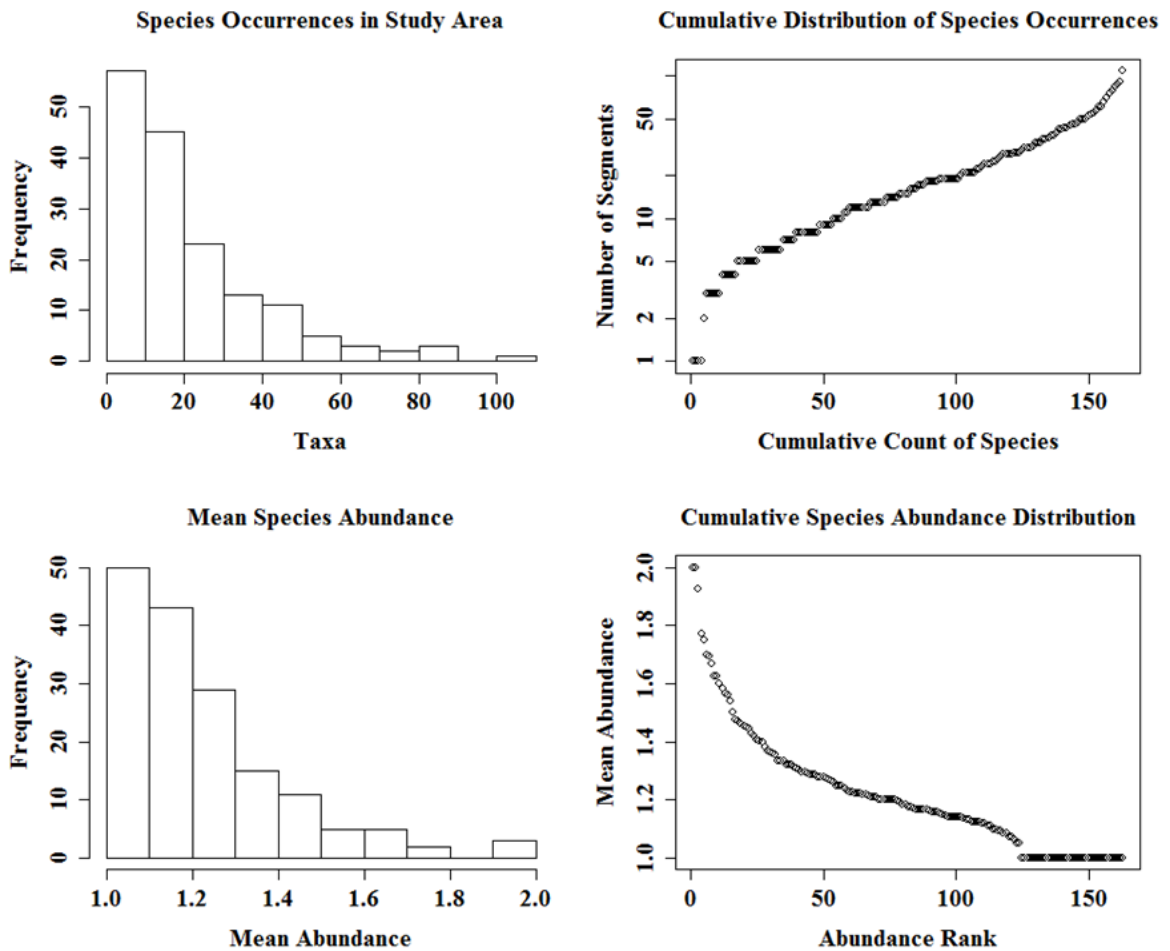
Figure 4.6: Plots of the histograms and cumulative empirical density functions (CEDF) of species occurrences and mean abundance. The curves reveal that most of the 163 species occurred in only about 50 segments out of the 210 segments surveyed and where they occurred, the abundance was also very low.

The graph shows that about 54 species occurred in less than ten plots while about 91% of the total species (149) occurred in 50 plots or less. Only three species (*Adianthum vogelli* (Adivogt), *Gomphrena celosioides (*Gomcelh*) and Chloris pilosa* (Chlpilh) out of 163 occurred in over half of the 210 plots. The rarest species were those that occurred in fewer than five plots. These include the tree species *Albizia adiantifolia* (Albadit) and *Capsicum frutescens* (Capfrut) as well as the herbaceous species *Aframonum melagueta* (Afrmelh) and *Solenostemo monstachyus* (Solmonh). This result suggests that most of the species were rare or infrequent in occurrence and underscores the need for effective monitoring of biodiversity in the Niger Delta. Besides, the abundance distribution curve offers a

visual expression of the species richness and species evenness of the study area. The steepness of the slope portrays a large margin between high and low abundant species.

The number of species per plot ranged from 1 to 35, with mean and median taxa of 17 and 13 species respectively. The larger mean value portrays the positive skew of the dataset suggesting that a significant number of plots had fewer species occurrences (Figure 4.7). On the other hand, the total number of individuals per species per plot ranged from 1 to 47. The mean and median values are 21 and 16 respectively, also indicating a positive skew in the dataset. Mean abundance plot of each species reveals that the most abundant species were herbaceous and occurred an average of two times per plot although there were only a few of such species (*Acacia kamerunensis* (Acakams) *and Millettia macrophylla* (Milmacs). Generally, 148 species out of 163 had an average abundance of 1.5 individuals or less per plot.
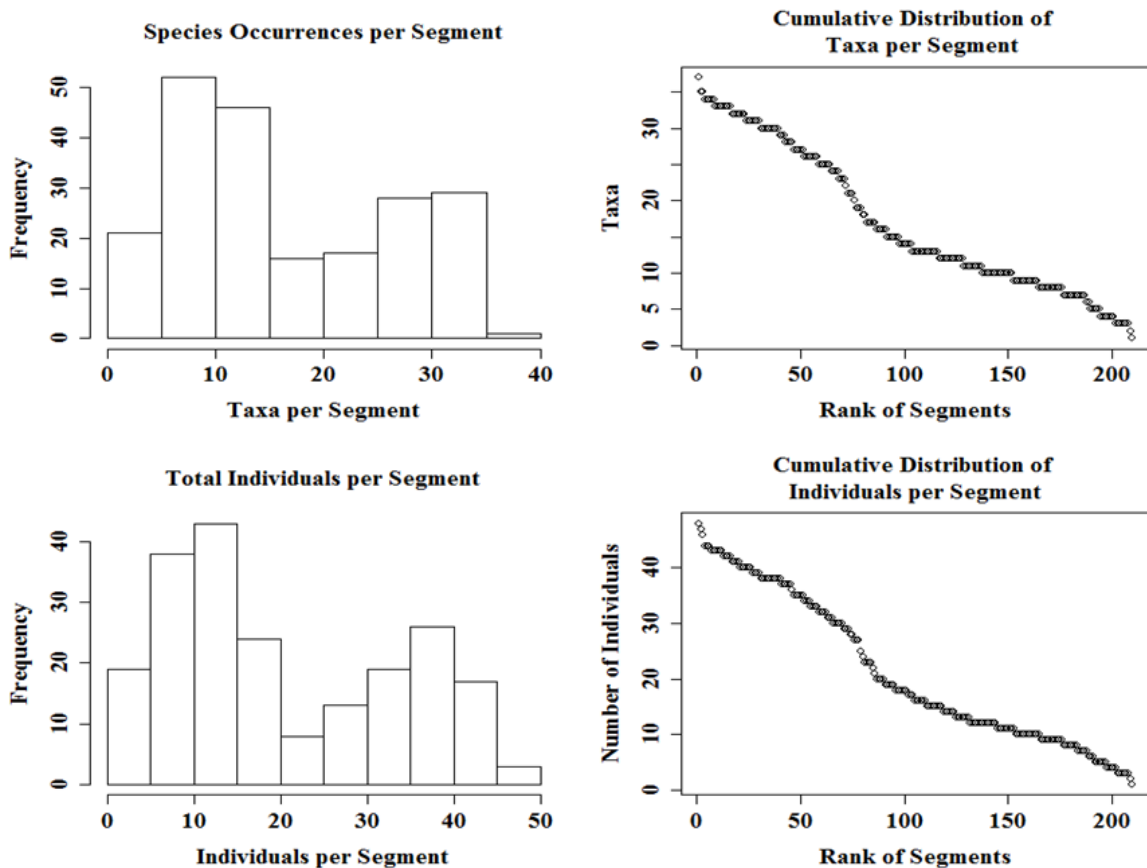
Figure 4.7: Histograms and Cumulative Empirical Density Functions (CEDF) of species and the total number of individuals per segment. The steepness of curves for taxa and number of individuals reveal sharp differences among the segments. It appears that in segments with over 20 species, there was a gradual decrease in evenness whereas, in segments with less than 20 species, the decrease in evenness is more pronounced.

Further analysis proved that the frequency of species occurrence did not necessarily correlate with species abundance. A low Spearman's correlation coefficient of 0.3 was computed for these characteristics. The abundance versus occurrence plot in Figure 4.8A reveals that the most abundant species such as Milmacs was among the least frequent species while the more frequent species such as *Costus afer* (Cosafes) was among the least abundant in the study area. On the other hand, only one species *Manihot esculenta* (Manescs) showed both high abundance and frequency values.

In contrast, there was a strong positive correlation between total abundance and number of species per segment. The correlation coefficient of 0.97 confirms the strength of this relationship as illustrated in Figure 4.8B.
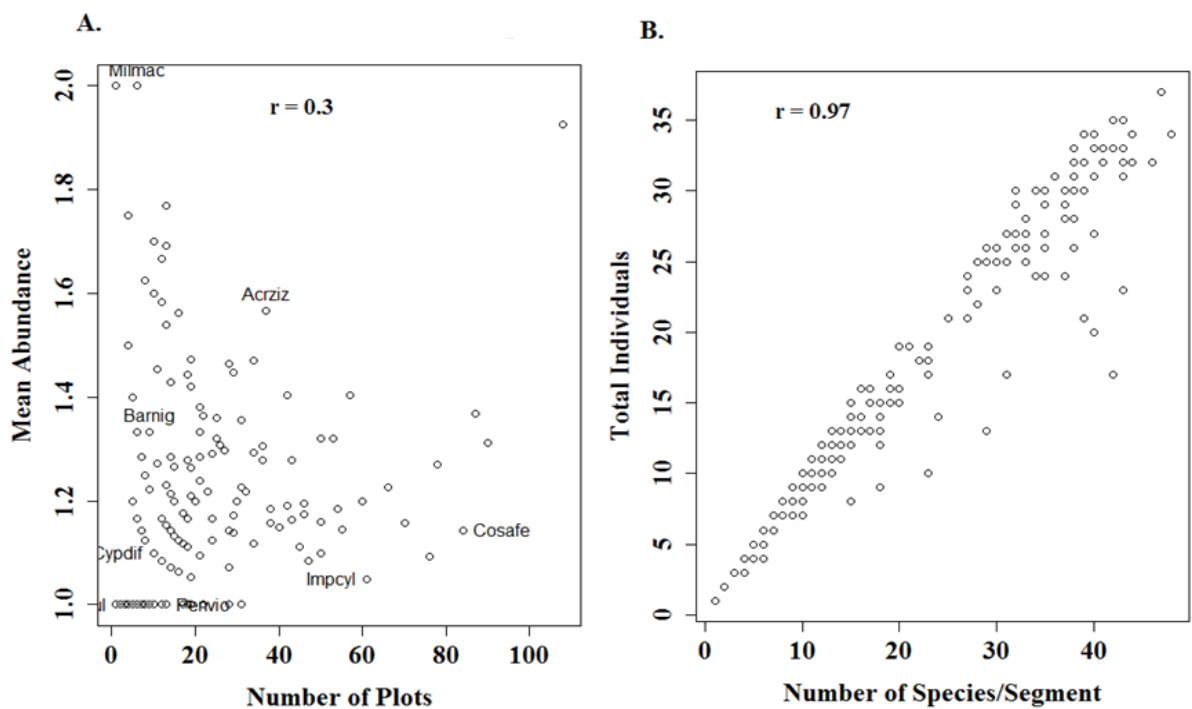
Figure 4.8: Scatterplots of A. abundance versus occurrence of species in the study area, and B. total individuals versus the number of species per segments. There is an apparent correlation among the variables; however, the relationship becomes much stronger within segments. Hence, it indicates the presence of a determining factor in the segments that affect both the number and abundance of species of individual segments.

4.1.2.3 Comparison of Vegetation Characteristics on Polluted and Control Transects.

Generally, 11 species on the polluted transect occurred in at least 30 segments out of 130 while on control transects, 15 species occurred in 30 segments out of 80. The most common species on polluted transects was *Ageratum conyzoides* (Ageconh), and on control transects, it was *Manihot esculenta* (Manescs). At soil TPH levels greater than 50,000mg/kg; only two species, namely *Costus afer* (Cosafes) and *Chloris pilosa* (Chlpilh), both annual plants occurred up to six times.

Significant differences were apparent in vegetation characteristics measured from polluted and control transects. The bar charts in figures 4.9A show that median taxa and frequency of vegetation on polluted transects are considerably lower than those of control transects at all the locations. However, this is not the case with abundance and density (Figure 4.9B) as the median values are only slightly different, although, they were higher in control transects.

The species number (taxa) indicates the total number of unique species occurring on transects at the time of the investigation. Anyu had the highest taxa of 28 and 52 on polluted and control transects respectively. The median taxa value for polluted and control segments were 9 (n=130) and 28 (n=80) respectively.

As mentioned previously, the floristic data did not meet with the assumptions of parametric statistics, hence a non-parametric procedure that is, the Kruskal-Wallis one-way analysis of variance by ranks procedure (K-W) was performed to test the significance of the differences in species composition of transects. The results of the analysis showed that these differences were significant ($H = 170.03$, $DF = 19$, p-value < 0.05) for taxa; ($H = 169.49$, $DF = 19$, $p = <0.05$) for frequency; ($H = 76.05$, $DF = 19$, p-value $= <0.05$) for abundance and ($H = 81$, $DF = 19$, p-value $= <0.05$) for density. This procedure was followed by a post-hoc analysis using Dunn's-test for multiple comparisons of independent samples. The results are shown in Table 4.5 for taxa and abundance. The differences observed for taxa (and frequency) are not significant at all the studied locations. For instance, there was no significant difference between polluted and control transects in Egbalor, Kporghor2, Kporghor and Rumuekpe locations.
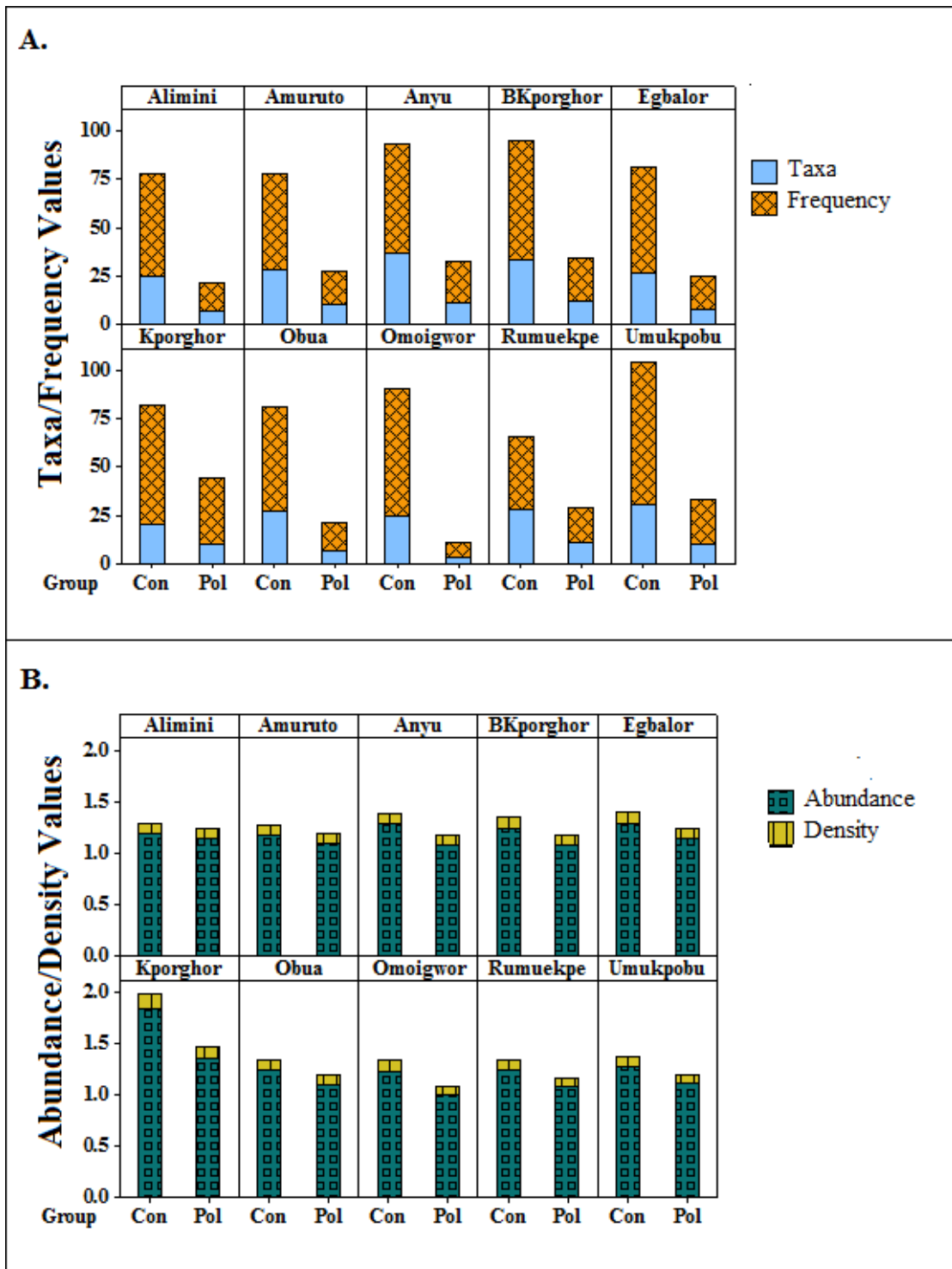
Figure 4.9: Bar charts of median values of A. taxa (number of species), frequency, and B. abundance and density of vegetation on polluted and control transect at each location. Taxa and frequency of vegetation on polluted and control show considerable difference while abundance and density do not.

For abundance, the post-hoc results revealed that the differences observed was between locations and not within. In other words, the abundance (and density values) were not significantly different between polluted and control transects across the study location.

Table 4.5: Dunn's test to compare the mean rank of taxa and abundance on polluted and control transects. The p-values show significant differences in the taxa of polluted and control transects at six locations. However, there is no significant difference for abundance values from polluted and control transects within locations. Significant values ($p < 0.05$) are shown as red asterisks (*).Titles are derived from the first two letters of location names and P or C representing polluted or control transect respectively. For instance, AlC is Alimini control transect.

Taxa	AlC	AmC	AyC	EgC	Kp2C	KpC	ObC	OmC	RuC
AlC	*	-	-	-	-	-	-	-	-
AmC	0.39	*	-	-	-	-	-	-	-
AyC	0.39	*	*	-	-	-	-	-	-
EgC	0.12	*	*	0.09	-	-	-	-	-
Kp2C	1.00	0.60	*	1.00	0.08	-	-	-	-
KpC	0.21	*	*	0.16	*	1.00	-	-	-
ObC	*	*	*	*	*	0.18	*	-	-
OmC	*	*	*	*	*	*	*	*	-
RuC	1.00	0.23	*	1.00	*	1.00	0.81	1.00	0.17
UmC	0.94	0.14	*	0.74	*	1.00	0.51	1.00	0.10
Abun	**AlC**	**AmC**	**AyC**	**EgC**	**Kp2C**	**KpC**	**ObC**	**OmC**	**RuC**
AlC	1.00	-	-	-	-	-	-	-	-
AmC	1.00	1.00	-	-	-	-	-	-	-
AyC	1.00	1.00	0.48	-	-	-	-	-	-
EgC	1.00	1.00	1.00	1.00	-	-	-	-	-
Kp2C	1.00	1.00	0.38	0.08	1.00	-	-	-	-
KpC	1.00	1.00	1.00	1.00	1.00	1.00	-	-	-
ObC	1.00	1.00	1.00	0.55	1.00	*	1.00	-	-
OmC	1.00	1.00	1.00	1.00	1.00	*	1.00	1.00	-
RuC	1.00	1.00	0.20	*	0.90	*	0.44	1.00	1.00
UmC	1.00	1.00	1.00	0.44	1.00	*	1.00	1.00	1.00

Species frequency data reflects the number of segments each species occurred in. The frequency of species occurrence was highest at control transects across the entire study area. Highest frequency values for control transects were recorded at Kporghor2 with 34 species occurring 259 times and a total frequency of 7.34%. Conversely, lowest frequency values were recorded for polluted transects at Alimini (17 species occurring 81 times, total frequency =2.47%). While for control transects, lowest frequency values were observed at Kporghor (33 species occurred 163 times with total frequency = 4.62%). Median frequency value for polluted transects was 18.35%, while on control transects, it was 58%. Average species frequency per segment in control transects was 0.15, while for

polluted it was a mere 0.05. The results show that species frequency values as taxa were higher on control transects than on polluted transects. Further analysis using the Kruskal-Wallis test to compare these values was performed, and the results were similar to that obtained for taxa (Table 4.5) which showed significant differences between polluted and control transects at most of the locations.

Vegetation abundance on polluted transects appeared lower than on control transects. Median values were 1.27 plants per occurrence on control transects and 1.19 on polluted transects. The difference is not significant when subjected to Kruskal-Wallis test. Likewise, the median density of plants on polluted transects was 0.09 plants/m^2 while at the control transects it was 0.21 plants/m^2. These values were not significantly different.

4.1.2.4 Characteristics of Vegetation in Segments along Polluted Transects

In addition to the inter-transect differences between the polluted and control transects, there were also observable differences along transects that corresponded to decreasing levels of soil TPH. Firstly, the species number (taxa) appear to increase with a decrease in soil TPH. For instance, median taxa at spill epicentres with median TPH concentration of 10490 mg/kg of soil is 3, while at SS1 (20m from spill point) with median TPH concentration of 6028 mg/kg, median taxa = 7. Furthermore, at SS3, (60 m from spill point) median TPH concentration decrease to 1849 mg/kg and median taxa increase slightly to 10, while at SS5 (100 m from spill point), median TPH concentration = 721 mg/kg, median taxa = 13. Contrastingly, median taxa on control segments = 28 and median TPH concentration in soil = 36.5 mg/kg. A similar pattern is observed in vegetation frequency, abundance and density. The occurrence of species along polluted transects became more frequent, abundant and dense as soil TPH concentration decrease. These results clearly show the effect of varying levels of soil TPH on vegetation characteristics. As the boxplots of taxa, frequency, abundance and density values for segments on polluted transects in Figure 4.10 illustrate, median values for each characteristic increased with a decrease in soil TPH concentration.
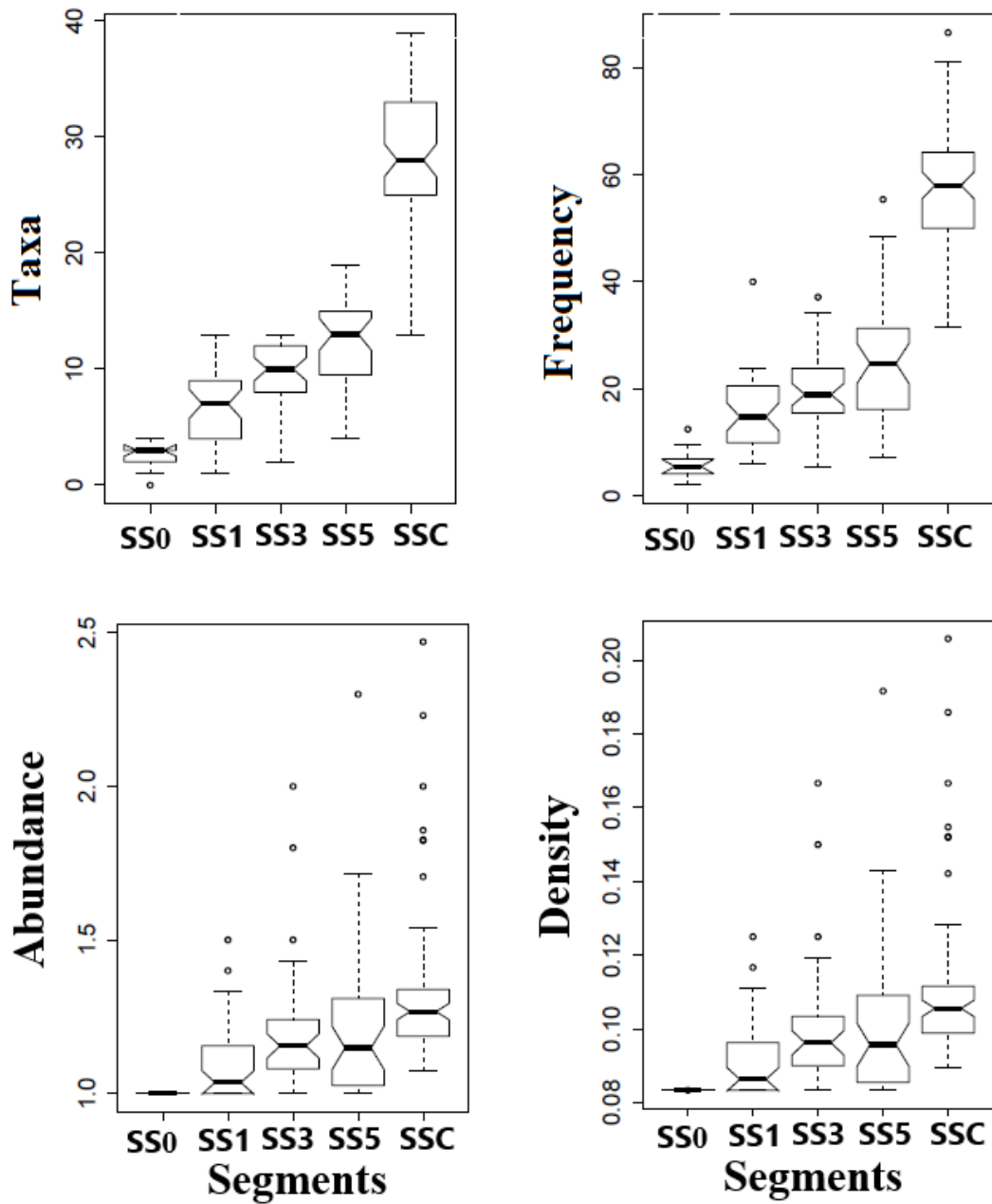
Figure 4.10: Boxplots of taxa, frequency, abundance and density values for segments on polluted transects and control segments (SSC) for comparison. For each characteristic, the median values increase with a decrease in soil TPH concentration. The occurrence of species along polluted transects increased in frequency, abundance and density with decreasing TPH. The notched boxes illustrate the confidence interval of the values and the absence of overlap between SS0 values and other segments suggest significant differences.

To determine the actual effect of TPH on these characteristics, an omnibus Kruskal-Wallis test was performed on the data with a significant result suggesting that at least one of the medians was from a different sample. Table 4.6 highlights the result of the Kruskal-

Wallis test for taxa, frequency, abundance and density of segments along polluted transects.

Table 4.6: Kruskal-Wallis omnibus test results for differences in the mean rank of taxa, frequency, abundance and density of vegetation along polluted transects. The results show significant differences in all the characteristics leading to a post-hoc analysis using Dunn's test.

Variable	H	DF	P	Decision
Taxa	169.11	4	<0.05	Reject
Frequency	167.36	4	<0.05	Reject
Abundance	62.55	4	<0.05	Reject
Density	69.31	4	<0.05	Reject

Rejection of the null hypothesis led to a post-hoc Dunn's test to determine the relationship between concentrations of TPH and vegetation characteristics. The results reveal that SS0 (with the highest median TPH concentration on polluted transects differed significantly with SS3 and SS5 in all the characteristics, but not with SS1. An earlier result from section 4.3.1.3 which revealed a significant difference in TPH concentration of segments SS0 and SS5. However, it appears that taxa and frequency were more affected by increasing TPH along transects than abundance and density. This effect is evident in the absence of significant differences in vegetation abundance and density among segments except between SS0 and SS5.

4.1.2.5 Importance Value Index of Species

Importance value index (IVI) of naturally occurring species across the study transects was calculated to determine the species that contributed most to the ecosystem structure and function. IVI further provided insight into the tolerance level of various species to the presence of petroleum hydrocarbon and heavy metals in the soil. For this analysis, the importance function in R package Labdsv was used to determine the importance value of the various species in the study area. The weighted average (WA) value of soil TPH weighted by species abundance on segments was initially computed to reveal the most tolerant and most vulnerable species. Table 4.7 lists the most tolerant and most susceptible species along with the WA scores. Interestingly, the most tolerant species were herbs, mainly *Perotis indica* (Perindh) which can tolerate over 67,000 mg/kg of TPH in the soil. The last letter in species code name indicates the life form of the species, s = shrub, h = herb, c = climber/creeper, t = tree). Other tolerant species include *Albizia adiantifolia* (Albadit), *Kyllinga erecta* (Kylereh), *Sida cordifolia* (Sidcorh) and

Andropogon tectorum (Andtech). The most susceptible species was *Terminalia catappa* (Tercatt), *Synedrella nodiflora* (Synnodh), *Oldenlandia corymbosa* (Oldcorh), *Albizia zygia* (Albzygt) and *Psychotria nigerica* (Psynigs).

Table 4.7: Weighted average scores of soil TPH concentration in investigated transects showing species most susceptible and most tolerant to oil pollution. The last letter in species code name indicates the life form of the species, s = shrub, h = herb, c = climber/creeper, t = tree).

Most Susceptible		Most Tolerant	
Species Code	WA scores of TPH (mg/kg)	Species Code	WA scores of TPH (mg/kg)
Tercatt	16.5	Perindh	67940.25
Synnodh	19.2	Albadit	61232.8
Oldcorh	25.9	Kylereh	22048.08
Albzygt	26.25882	Sidcorh	16728.76
Psynigs	26.53333	Andtech	14470.86

Similarly, the species with the highest importance value indices on both polluted and control transects were mostly shrubs, herbs and climbers and his contrasted clearly with tree species, which exhibited low importance index values. The ten most important species in the study area are *Manihot esculenta* (Manescs), IVI = 33.21; *Paullinia pinnata* (Paupinc), IVI = 23.95; *Elaeis guineensis* (Elaguit), IVI = 19.86; *Cocos nucifera* (Cocnuct), IVI = 18.49; *Chloris pilosa* (Chlpilh), IVI = 15.94; *Ageratum conyzoides* (Ageconh), IVI = 15.82; *Alchornea cordifolia* (Alccors), IVI = 14.46; *Carica papaya* (Carpapt), IVI = 13.79 and *Gomphrena celosioides* (Gomcelh), IVI = 13.67. IVI values showed susceptibility to soil TPH as certain species with high IVI values on control transects appear to decline on polluted transects. These species include *Phyllanthus amarus* (Phyamah), IVI = 4.2 and 8.04 respectively on polluted and control transects; *Axonopus compressus* (Axocomph), IVI = 3.66 and 7.73; *Adianthum vogelli* (Adivogh), IVI = 3.71 and 7.53; *Spermacoce verticillata* (Speverh), IVI = 2.66 and 7.4; *Blighia sapida* (Blisapht), IVI = 1 and 7.21; *Calopogonium mucunoides* (Calmuc), IVI = 2.17 and 7.12; *Cyperus haspan* (Cyphash), IVI = 0 and 6.92; *Cyperus esculentus* (Cypesch), IVI = 0 and 6.62; *Millettia macrophylla* (Milmacs), IVI = 1.5 and 2.25.

Conversely, the most critical species on polluted transects were equally important on control transects. However, a few species were more abundant on polluted transects. These were *Ageratum conyzoides* (Ageconh), *Carica papaya* (Carpapt), *Bulbophyllum*

barbigerum (Bulbarh), *Ipomoea involucrata* (Ipoinvc), *Scleria verrucosa* (Sclverh), *Oplismenus burmanii* (Oplburh) and *Desmodium triflorum* (Destrih).

Figure 4.11 is a scatterplot of IVI of species on polluted and control transects. The plots show that fewer species on polluted than on control transects scored IVI > 5. Additionally, several species with IVI values > 5 on control transects declined in value on polluted transects.
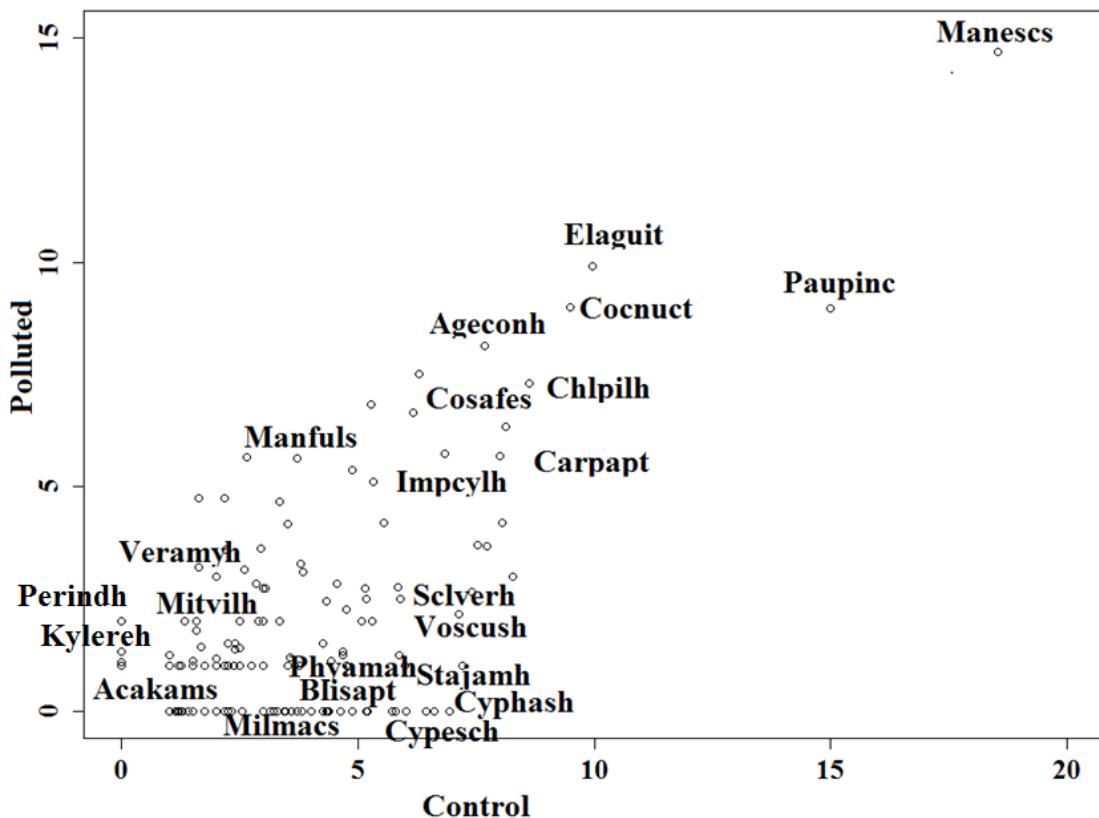
Figure 4.11 Scatterplot of IVI values for species on polluted and control transects. Highest IVI values were obtained for most shrubs, followed by herbs on both transects, whereas, lowest IVI values were obtained for trees. The last letter in species code name indicates the life form of the species, s = shrub, h = herb, c = climber/creeper, t = tree).

Indicator species was determined for each location, and the result plotted in Figure 4.12. Interestingly, no two sites had the same indicator species contrary to expectations considering that all the sites were located within the same ecological zone. The indicator species were not necessarily dominant in their habitats; however, they showed a preference for particular environments based on their importance values. For instance,
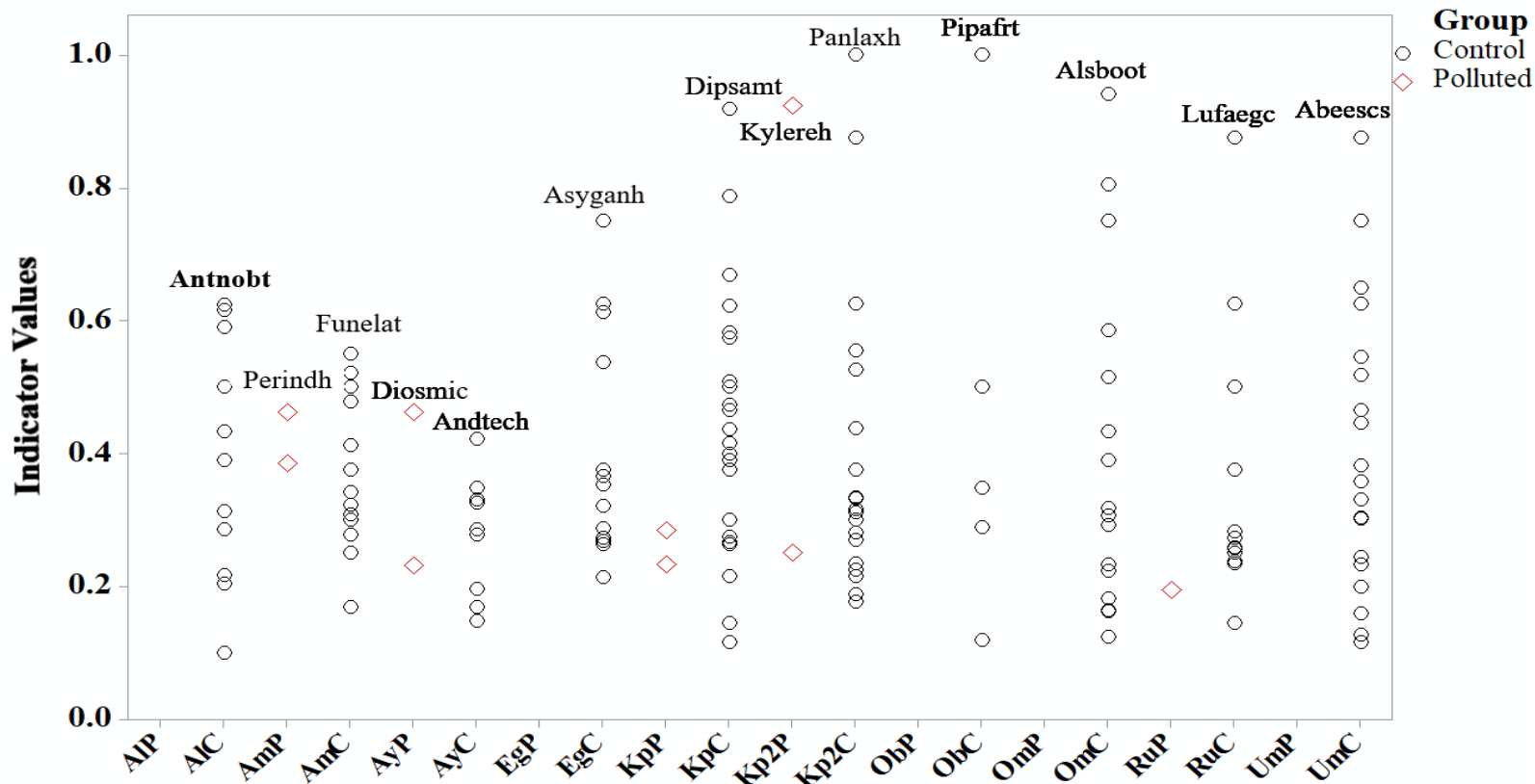
Figure 4.12 Indicator species at different locations investigated. The species with highest indicator values on polluted transects include Kylereh (*Kyllinga erecta)* at Kporghor 2; and Perindh (*Perotis indica*) at Amuruto. On control tranestc, indicator values were much higher with Pipafrt (*Piptadeniastrum africanum*) and Panlaxh (*Panicum laxum*) dominating in Obua and Kporghor 2 respectively. All the locations had different indicator species, which is a pointer to the species diversity and high turnover (beta-diversity) of the study area.

Carluts, *(Carpolobia lutea,)* a shrub with high indicator value in Kporghor exhibited a preference for non-polluted transects whereas Lepowac (*Lepistemon owariense*), a creeping plant with moderate indicator value at Egbalor showed a preference for polluted transects.

4.1.3 Species Diversity Analysis

4.1.3.1 Species Richness and Diversity on Investigated Transects

Many indices were used to calculate the diversity of both the polluted and control transects across the entire study area. These included those for estimating species diversity such as Shannon's (H) and Simpson's (D), those for estimating species richness such as Menhinick's index (M) and Chao-1 (CH) indices; and for estimating the evenness of species (EV) distribution and species dominance (DM). The analysis was performed using PAST software using the abundance data of all inventoried species. Table 4.8 summarises the results of the diversity analysis, shows the median value for each index, and transect at different locations. From the table, it is clear that there are differences in the diversity values for vegetation on polluted transects and control transects.

Table 4.8 Summary of diversity analysis using PAST for polluted and control transects

Location	Transect	Shannon's	Simpson's	Chao-1	Menhinick's	Evenness
Alimini	Polluted	1.89	0.84	10.33	2.33	0.96
	Control	3.18	0.96	72.25	4.63	0.95
Amuruto	Polluted	2.3	0.9	31.33	3.05	0.97
	Control	3.31	0.96	82.13	4.93	0.96
Anyu	Polluted	2.4	0.91	28	3.32	0.97
	Control	3.53	0.97	78.94	5.42	0.94
Egbalor	Polluted	2.08	0.88	19.33	2.83	0.96
	Control	3.2	0.96	67.22	4.53	0.91
Kporghor	Polluted	2.2	0.88	17	2.83	0.92
	Control	2.82	0.92	28.31	3.26	0.82
Kporghor2	Polluted	2.49	0.91	42	3.33	0.98
	Control	3.43	0.96	87.8	5.08	0.94
Obua	Polluted	1.95	0.86	19.5	2.65	0.97
	Control	3.23	0.96	70.6	4.76	0.92
Omoigwor	Polluted	2.51	0.91	31.5	3.18	0.95
	Control	3.38	0.96	88.8	5.08	0.93
Rumuekpe	Polluted	2.4	0.91	46	3.32	0.98
	Control	3.29	0.96	128.3	4.93	0.94
Umukpok u	Polluted	2.25	0.89	24.25	3	0.97
	Control	3.36	0.96	77.22	5.03	0.94

Generally, for all the indices computed, control transects exhibited higher richness and diversity values than polluted transects at all locations. Among polluted transects, Menhinick's richness index ranged from 2.33 to 3.33 while Shannon diversity values ranged from 0 to 2.93 computed for Rumuekpe. Among control transects, species richness (Menhinick's Index) ranged from 3.26 to 5.42, and Shannon's index ranged from 1.87 to 3.6. Zero index values were mostly obtained on spill epicentres in Kporghor and Alimini, where fire incidence wholly removed the vegetation.

Species accumulation curve (Figure 4.13) showed that species richness for polluted transects was lower than for polluted transects and that species accumulated more rapidly in control segments than in polluted segments. Although the sample sizes varied for polluted (n = 130) and control (n = 80) segments, the curves show that at a comparable sample size of 50, the species richness for polluted segments was 87 (SD = 3.72) while that of control segments was 154 (SD = 1.99)
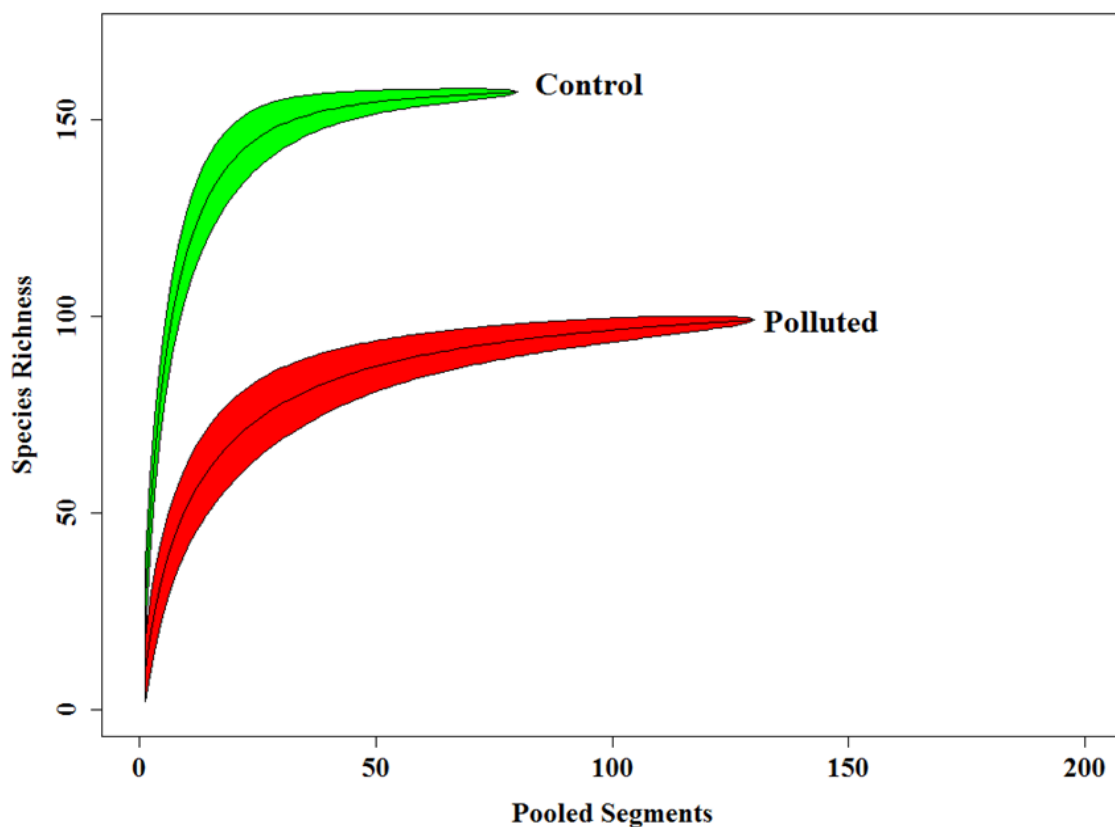
Figure 4.13 Species accumulation curves comparing the species richness on polluted and control transects in the study area. Curves show that species richness and the rate of accumulation (the rate at which new species were observed in segments) was higher on control transects than on polluted transects.

The Anyu control transects had the highest Shannon index of 3.6. Similar patterns were observed for other diversity indices, Simpson's and Chao-1 as evident in Figure 4.14. Both indices were higher for control transects than for polluted transects.
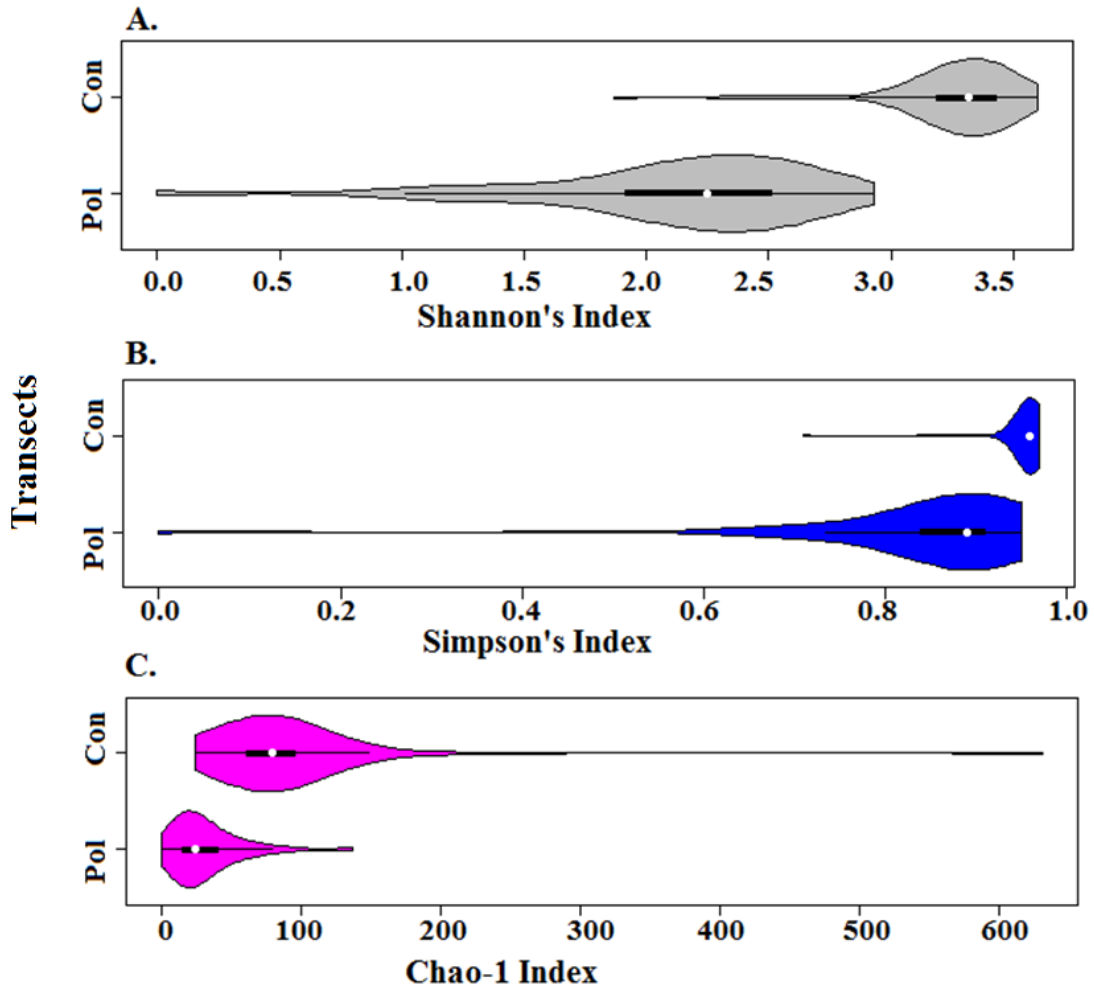
Figure 4.14 Violin plots of A. Shannon's, B. Simpson's and C. Chao-1 diversity indices on polluted and control transect. The density plots with long tails show the non-normal distribution of variables, further justifying the use of non-parametric statistics for data analysis. For all indices, median values are higher on control transects than on polluted transect. Index values on polluted transects exhibited more variability than control transects except in Chao-1 which showed a reverse with more variability in values obtained from control transects.

Species dominance was not strongly exhibited on investigated transects though it appeared to be slightly more present on polluted transect than on control transects. This difference was significant between transects at only four sites namely Alimini, Amuruto, Anyu and Obua. By far, the most dominant species encountered across the entire study area was *Manihot esculenta* (DM = 0.99). Four other species which dominated investigated transects include *Paullinia pinnata* (DM = 0.57), *Chloris pilosa* (DM = 0.56), *Ageratum conyzoides* (DM = 0.47) and *Costus afer* (DM, 0.46) which were all

herbs and shrubs. Species dominance also varied by location as different species exhibited dominance at different locations. Figure 4.15 displays the dominant species at each location.
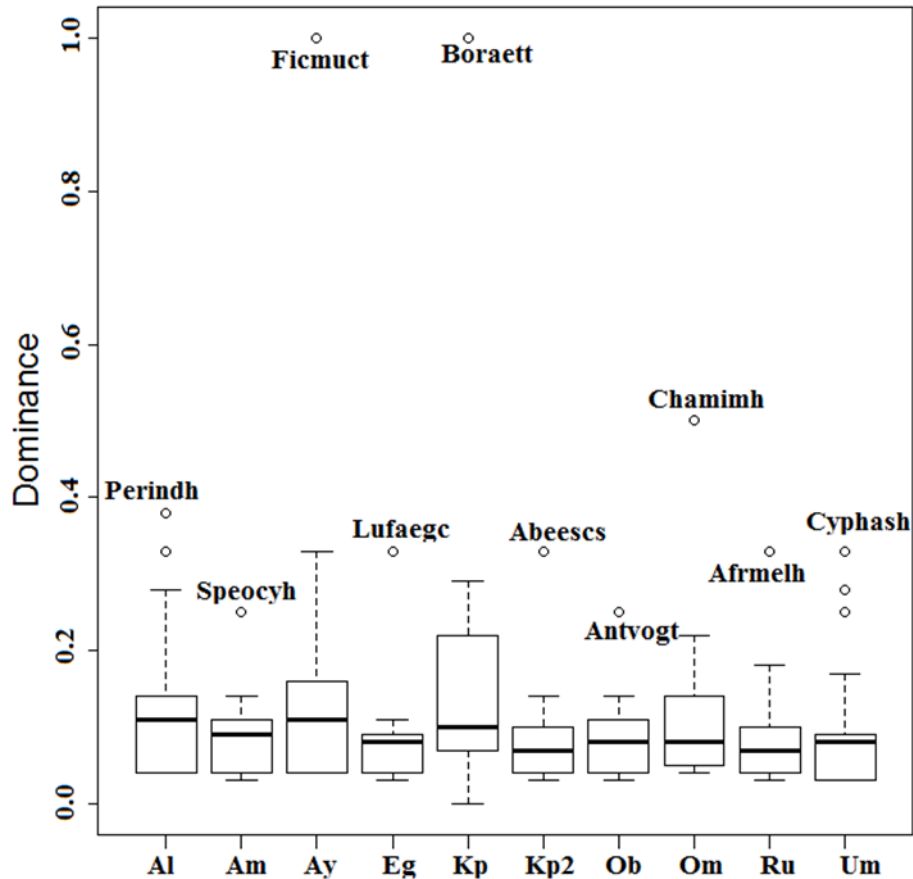
Figure 4.15 Boxplot of vascular plant species dominance at investigated polluted locations in the study area.

While the dominance of species was very low across the study area, evenness was high and slightly higher on polluted transects. Median evenness on polluted transects was 0.97 while on control transects, it was 0.94, and the difference appeared significant when subjected to a Kruskal-Wallis test (H = 95.54, DF=19, P-value < 0.05). However, a post-hoc analysis revealed that the significant difference was between rather than within locations.

Apart from evenness, other evaluated diversity and richness indices showed a considerable difference between polluted and control transects at various locations and are illustrated in Figure 4.16.
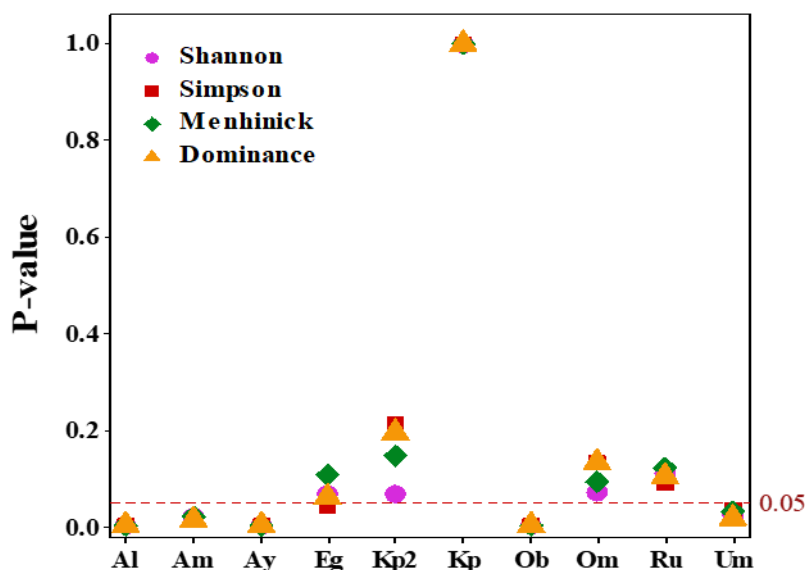
Figure 4.16 Results of post-hoc analysis using Dunn's test plotted against locations to illustrate the significance level of differences in diversity indices between polluted and control transects. All indices were significantly different at Alimini (Al), Amuruto (Am), Anyu (Ay) and Obua (Ob). At Umukpoku, only Shannon's and Menhinick's indices were significantly different between polluted and control transects.

4.1.3.2 Species Richness and Diversity on Segments of Polluted Transects

The average index value of segments from polluted transects (A, B, C and D) from the diversity analysis performed in the PAST package is shown in Table 4.9. There is an observed pattern of increase in index values as the distance from spill epicentre (SEC) increased. Vascular plant species diversity indices (Shannon's, Simpson's, Chao-1, and Menhinick's) appeared to respond to varying TPH concentrations.

Table 4.99 Summary of diversity analysis using PAST for segments along polluted transects with control segments for comparison.

Index	Segments (SS) on Polluted Transects				Segments on Control Transects
	SS0	SS1	SS3	SS5	SSC
Shannon's	1.1	2.04	2.27	2.57	3.32
Simpson's	0.67	0.86	0.89	0.92	0.96
Chao-1	6	18.5	23.63	38.35	78.47
Menhinick's	1.73	2.67	3.01	3.47	4.87
Evenness	1	0.97	0.96	0.96	0.94
Dominance	0.33	0.14	0.11	0.08	0.04

Box plot of results (Figure 4.17) for vascular plant species diversity indices further highlight the general pattern of increasing values along polluted transects as TPH levels declined. However, a reverse trend is observed for evenness and dominance as these indices appeared to decrease with increasing TPH concentration in soil.
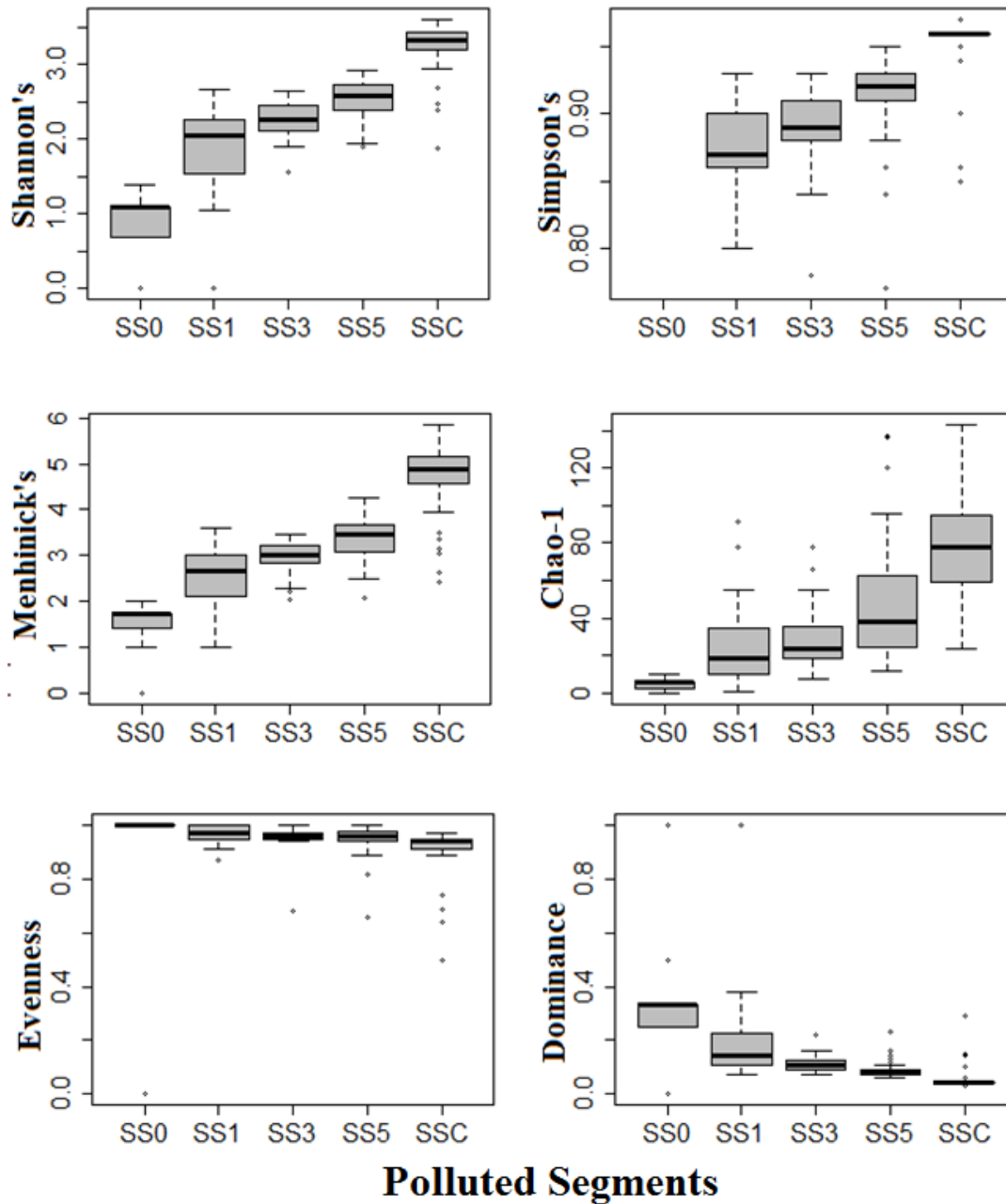
Figure 4.17 Boxplot of diversity indices along segments (SS) of polluted transects. There is a clear pattern of increasing diversity index values as the distance from the spill epicentre (SEC) increases. The increasing distance also corresponds with declining TPH concentration in the soil. On the other hand, both dominance and evenness decreased as TPH concentration in the soil decreased.

4.1.3.3 Beta Diversity of Investigated Transects

The beta diversity polluted and control transects across the entire study area and for each location was calculated, and the results are summarised in Table 4.10. Beta diversity of polluted transects across the entire study area was quite high, (0.59) suggesting that transects were somewhat dissimilar in species composition. Similarly, on control transects, beta diversity values were also high (0.53) though slightly lower than polluted transects confirming the high biodiversity of the Niger Delta.or.

Table 4.10 Beta diversity of investigated transects calculated using Sorensen's dissimilarity index

	Beta diversity		Turnover		Nestedness	
	Polluted	**Control**	**Polluted**	**Control**	**Polluted**	**Control**
Study Area	0.59	0.53	0.56	0.51	0.06	0.02
Alimini	0.4	0.23	0.36	0.22	0.14	0.04
Amuruto	0.38	0.2	0.33	0.15	0.07	0.05
Anyu	0.44	0.22	0.36	0.2	0.1	0.02
Egbalor	0.41	0.2	0.37	0.17	0.15	0.03
Kporghor	0.36	0.18	0.3	0.12	0.1	0.09
Kporghor2	0.25	0.13	0.23	0.11	0.12	0.02
Obua	0.4	0.22	0.31	0.19	0.1	0.03
Omoigwor	0.33	0.12	0.23	0.11	0.11	0.03
Rumuekpe	0.47	0.39	0.34	0.27	0.11	0.05
Umukpoku	0.39	0.14	0.32	0.12	0.09	0.02

Furthermore, results show that species turnover was consistent in determining the beta diversity of transects. Nestedness of species was higher in polluted transects than in control transects implying that oil pollution may have caused the disappearance of some vascular plant species from segments along polluted transects. Beta dispersion analysis to determine the effect of pollution on species composition showed significant differences in the species composition of polluted and control transects. The results of the analysis are shown in Figure 4.18.
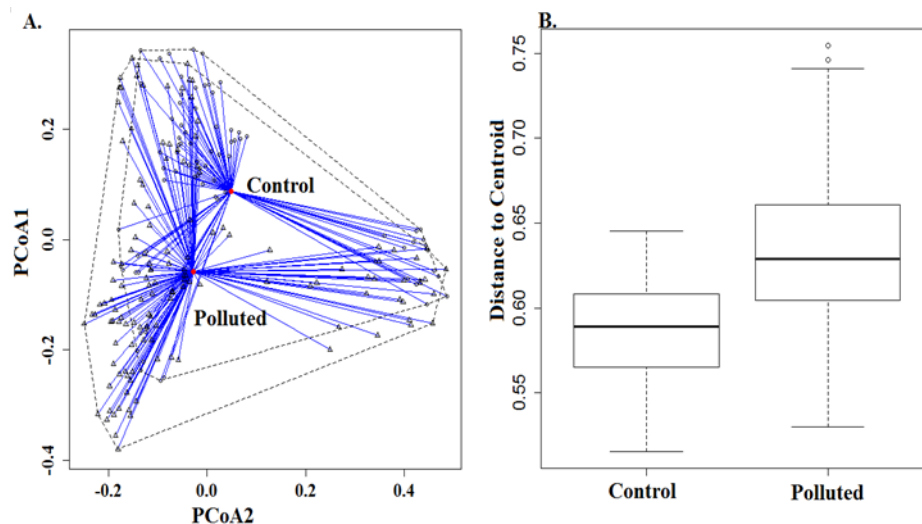
Figure 4.18 Plots of distances of polluted and control segments from centroids. The non-metric dimensional scale plot in A. shows that the vegetation composition of polluted and control transects differ. In B, the box plots show that polluted transects vary significantly in their species composition across the entire study area.

Both plots show that polluted transects differed in species composition with control transects, although, there appeared to be other underlying factors in addition to soil TPH that may have caused this. However, the boxplot of the distance of segments to the centroids (Figure 4.18B) showed that polluted transects were more dissimilar in species composition than control transects. An analysis of variance (ANOVA) test performed on the distances (N = 210, DF= 1 and 208, F = 57.73, $p < 0.05$) showed significant differences.

Within locations, comparison of pairs of segments using Sorenson's index revealed that species composition on oil spill epicentres (SS0s) completely differed from other segments with larger dissimilarity values obtained on polluted transects. Average beta diversity values among segments on polluted transects were 0.64 (SS0); 0.6 (SS1 and SS3); and 0.56 (SS5) while on control transects it was 0.56. An omnibus test comparing the differences in beta diversity among segments was significant; hence a post-hoc analysis using Dunn's test was performed. Although the result showed that beta diversity differences were only significant at $p < 0.05$ between SS0 and SS5 as well as SSC; it suggests a linear relationship between TPH in soils and beta diversity. The presence and strength of any relationship between beta diversity components and soil TPH was tested using a linear regression model in R. The results of the procedure confirms that soil TPH positively influenced both the species turnover component of beta diversity and the nestedness as summarised in Table 4.11

125

Table 4.11 Summary of the linear regression analysis to determine the relationship between beta diversity components and soil TPH. For each variable, N = 210, DF = 1 and 208, p-value < 0.05

Variable	F	R-squared	RSE	Equation
Beta diversity	106.6	0.34	0.13	Beta diversity = 0.06 + 0.09 (LogTPH)
Turnover	90.88	0.3	0.12	Turnover = 0.05 + 0.08(LogTPH)
Nestedness	48.39	0.2	0.07	Nestedness = 0.02 + 0.04(LogTPH)

4.1.4 In-Situ Leaf Chlorophyll Data Analysis

Data measured using the SPAD (Soil Plant Analysis Development)-502 chlorophyll meter are summarised in Table 4.12 below. The results show that estimated chlorophyll contents of vegetation on the control transects were higher than chlorophyll estimates of vegetation on polluted transects. The mean SPAD values for the control transects were over 55 while the means from polluted transects were less than 40.

Table 4.12 Summarised chlorophyll data measured using a SPAD-502 chlorophyll meter taken from Kporghor spill location. The means of the data obtained from the control transects are higher than those obtained from the polluted transects. Similarly, the maximum values are also higher in control transects than in the polluted transects.

	Transect A	Transect B	Transect C	Transect D	Control 1	Control 2
Minimum	21.1	26.5	25.4	26.3	39.9	42.1
1st Quartile	33.49	33.8	34	32.8	46.6	48.9
Median	38.5	41.49	35.4	38.2	49.8	52.7
Mean	39.33	40.52	36.98	39.22	55.32	55.06
3rd Quartile	46.7	45.6	39.8	44	58.1	57.5
Maximum	65.7	56.5	58.2	66.3	111	96.4

4.1.4.1 Leaf Chlorophyll Data from Polluted and Control Transects in Kporghor

The SPAD measured chlorophyll content of vegetation on investigated transects reveals the variation in the data readings from both the control and polluted transects. For instance, the SPAD chlorophyll measured in vegetation on polluted transects ranged from 21 to 68, with a median value of 36.06; while on control transects, values ranged from 39.9 to 111 with median = 50.33 The wider range of data readings from vegetation on the control transects connotes a wider species variation as previously noted in the species number (taxa). A Mann-Whitney test performed on the data showed a significant difference between chlorophyll content in vegetation from polluted and control transects.

The one-tailed test showed that SPAD chlorophyll estimates on polluted transects were significantly less than control transects (N = 31, W = 214, p < 0.05).

4.1.4.2 Leaf Chlorophyll Data from Segments along Polluted Transects

SPAD-502 chlorophyll meter reading also showed significant variations in segments along polluted transects as is evident in the boxplot in Figure 4.19 It appears that the values were increasing as the distance from the spill epicentre increased; further proof that the TPH levels in the soil affected the chlorophyll content of vegetation growing on the segments. The median values for the segments were SS1 = 32.45; SS3 = 35.17; and SS5 = 42.95. An omnibus Kruskal-Wallis test showed significant differences among the segments (H = 13.05, DF = 4, p< 0.05), however, following a multiple comparison Dunn's test, the significant difference was between SS1 and SS5. The spill epicentre at Kporghor was excluded from the analysis due to the absence of vegetation within the segment (SS0). There were differences in the SPAD chlorophyll values estimated for SS1 and SS3, but these differences were not significant (p < 0.05). Likewise, between SS3 and SS5, there was no significant difference in the SPAD chlorophyll estimates.
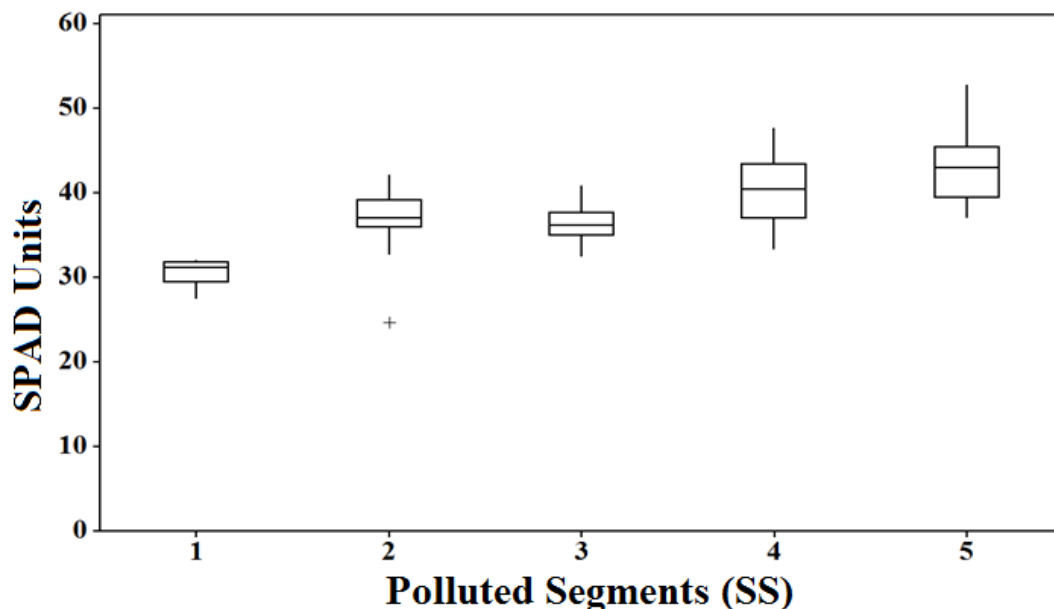
Figure 4.19 Boxplot of SPAD-502 chlorophyll meter readings from segments along polluted transects. Higher readings suggesting higher chlorophyll content were obtained from vegetation growing on segments further away from the spill epicentre (not shown in the graph).

127

4.1.4.3 Effect of Oil Pollution on Leaf Chlorophyll Data

Estimated chlorophyll content in vegetation strongly correlated with soil parameters. The relationship was inverse with soil TPH, Lead and TOC but positive with Phosphorus. The corrgram plot in Figure 4.20 illustrates the nature of relationships.
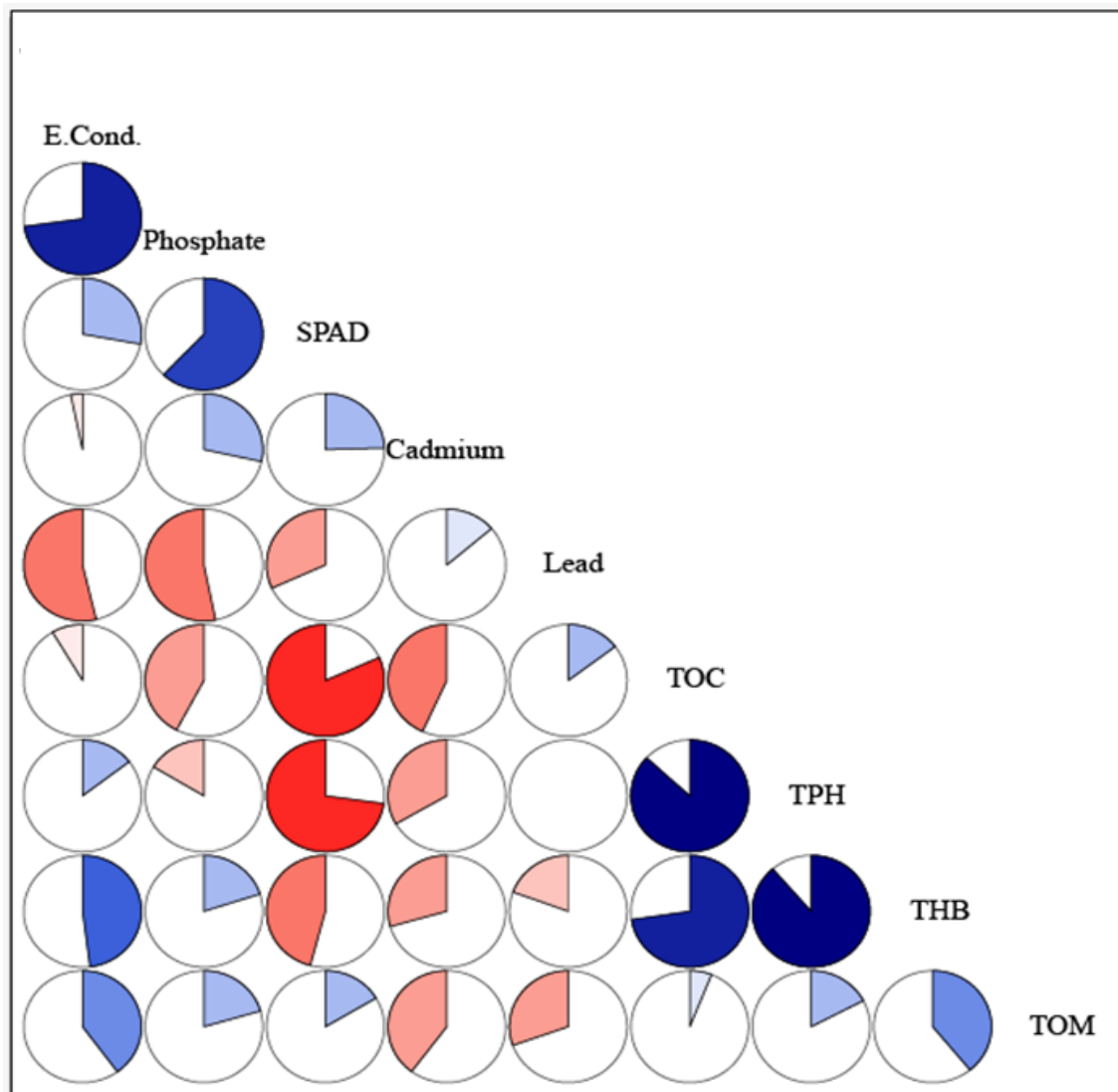
Figure 4.20: A corrgram illustrating the correlation ratios of various soil parameters and the SPAD-502 chlorophyll data obtained from the study transects. The colour and intensity of shading define the pattern and magnitude of the relationship between the variables. The red pies represent the negative correlation while the blue coloured pies illustrate positive correlations. Carbon-related parameters (TPH, TOC and THB) and the heavy metal (Lead) correlated negatively while TOM and Cadmium had weak positive correlations with the leaf chlorophyll data. Conversely, Phosphorus (soil nutrient) had strong positive correlations with the leaf chlorophyll data.

Additionally, a comparison of the average chlorophyll concentration of selected plant species namely *Manihot esculenta*, *Vossia cuspidata* and *Ficus mucuso* on polluted and control transects using the Kruskal-Wallis test (H = 126.23, DF = 17, p-value < 0.05) showed that differences were significant. Post-hoc analysis revealed that interspecific differences in chlorophyll content were not significant, however intraspecific differences between polluted and control transects were significant for all species. This may be attributed to the effect of oil pollution. Results of the post hoc analysis are shown in Table 4.13.

Table 4.13: Dunn's test to compare the mean rank of SPAD chlorophyll in selected species on polluted and control transects. The p-values show significant differences in the estimated chlorophyll content of *Ficus mucuso* (*Fm*) and *Vossia cuspidata* (*Vc*) on polluted transects A (TA), B (TB), C (TC) and D (TD) and control transects C1 and C2. However, there is no significant difference in chloropyll content of *Manihot esculentus* (*Me*) on polluted and control transects. Significant values (p < 0.05) are shown as red asterisks (*). Variable names are a combination of transects label and first letters of plants genus and species names eg C1*Me* refers to *Manihot esculentus* on control 1 transect.

	C1*Me*	C1*Fm*	C1*Vc*	C2*Me*	C2*Fm*	C2*Vc*
TA*Me*	0.851	*	*	0.1	*	*
TA*Fm*	1	*	*	0.361	*	*
TA*Vc*	*	*	*	*	*	*
TB*Me*	0.824	*	*	0.096	*	*
TB*Fm*	1	*	0.263	1	*	0.162
TB*Vc*	1	0.868	1	1	0.425	1
TC*Me*	1	*	*	0.818	*	*
TC*Fm*	1	0.172	1	1	0.076	1
TC*Vc*	1	*	*	0.488	*	*
TD*Me*	1	*	0.103	1	*	0.061
TD*Fm*	1	*	0.202	1	*	0.123
TD*Vc*	0.857	*	*	0.1	*	*

4.1.5 Effects of Environmental Variables on Species Occurrence

Species occurrence and distribution are a function of environmental variables. To evaluate the impact of the environmental variables particularly the TPH concentrations on the species composition and distribution, the canonical correspondence analytical (CCA) procedure was employed. The CCA was performed using species abundance data from all transects investigated. The procedure was carried out to determine the

environmental variable that most influences species occurrence and abundance. The soil parameters that exhibited strong relationship ($0.5 < r < -0.5$) with taxa and number of individuals were selected as environmental variables and these were total petroleum hydrocarbon (TPH, $r = -0.74$ and -0.76), phosphorus (P, $r = 0.7$ and 0.72) and lead (Pb, $r = -0.74$ and -0.78).

Results from the canonical correspondence analysis produced strong associations among the vegetation data and the environmental variables. While the first CCA axis represented 39.2% of the total variance in the data and associated with increasing TPH and Lead and decreasing phosphorus, the second CCA axis accounts for 24.89% of the total variance in the data and associates with decreasing TPH. The plot of the two axes shown in Figure 4.21 A and B successfully partitioned the study area into polluted microhabitat (characterised by high levels of TPH and lead and low levels of phosphorus and TOM) and unpolluted microhabitats. The distribution of vegetation in these microhabitats showed that the nutrient-rich unpolluted portion supported over 60% of the species while 40% occurred on the polluted/contaminated portion. The ordination of species on these axes revealed the optimal conditions and the effect of changes in these conditions for species occurrence and abundance. For instance, the most common life forms of species populating the polluted microhabitat are herbs and shrubs while trees preferred unpolluted fertile microhabitats.

Moreover, the plot revealed that certain species thrived in polluted transects scoring high IVI values and WAScores but absent in control transects. These species were labelled as TPH-tolerant species as they thrived in polluted soils. 65 species that populated the unpolluted microhabitat and were absent in the polluted microhabitat were labelled as TPH-sensitive species due to their low WA scores (less than 60 mg/kg) and the requirement of good soil conditions to thrive. However, due to their absence or minimal presence on polluted transects, their IVI values ranged from 1 to 1.75.
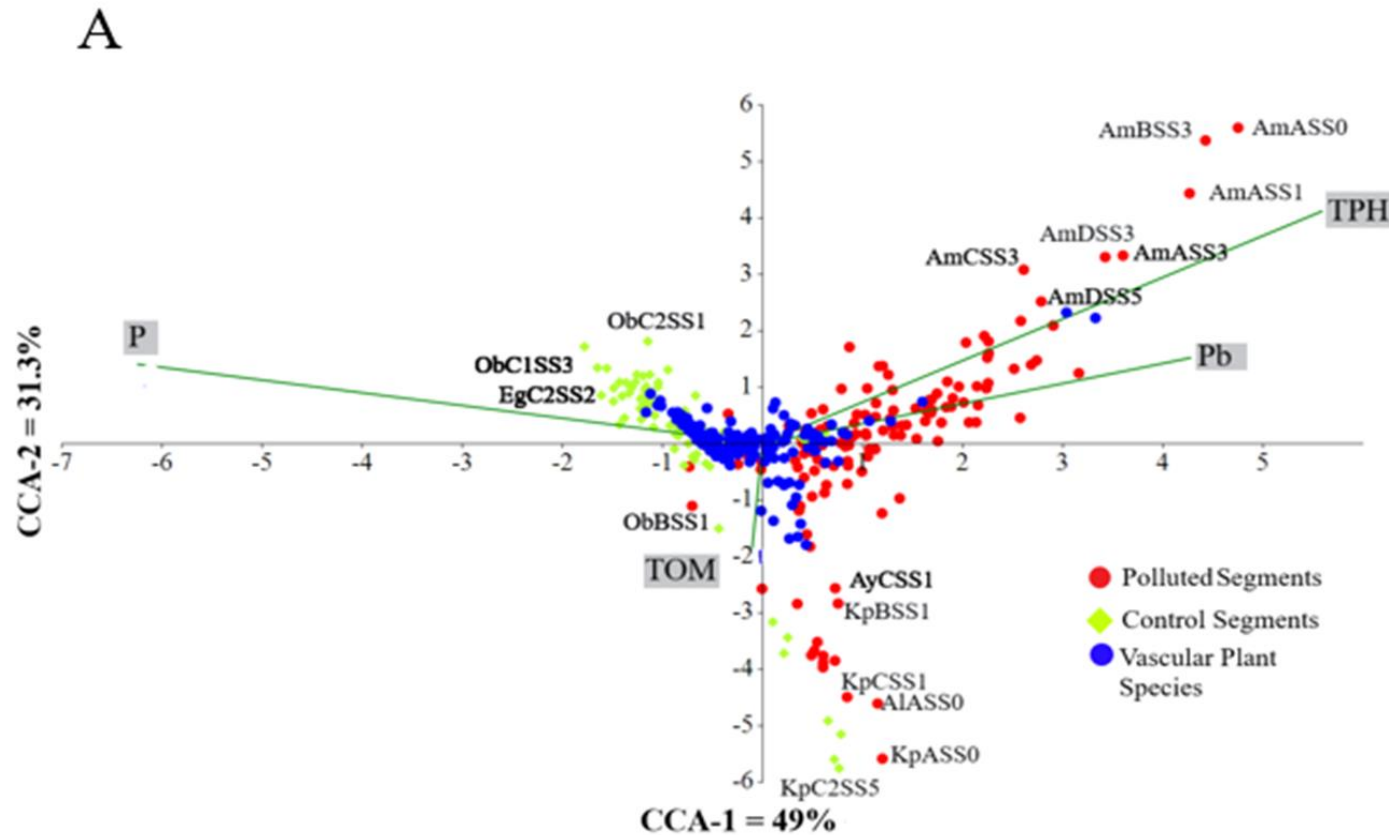
Figure 4.21A Plot of the first two axes of the CCA result scaled to display segments. The first CCA axis associates with increasing TPH and the second CCA axis associates with increasing TOM. The length of the tri-plots shows that both soil TPH and P were dominant gradients affecting species distribution. The plot successfully apportioned the ordinated space into polluted and unpolluted microhabitats which also correspond with particular species populating each microhabitat
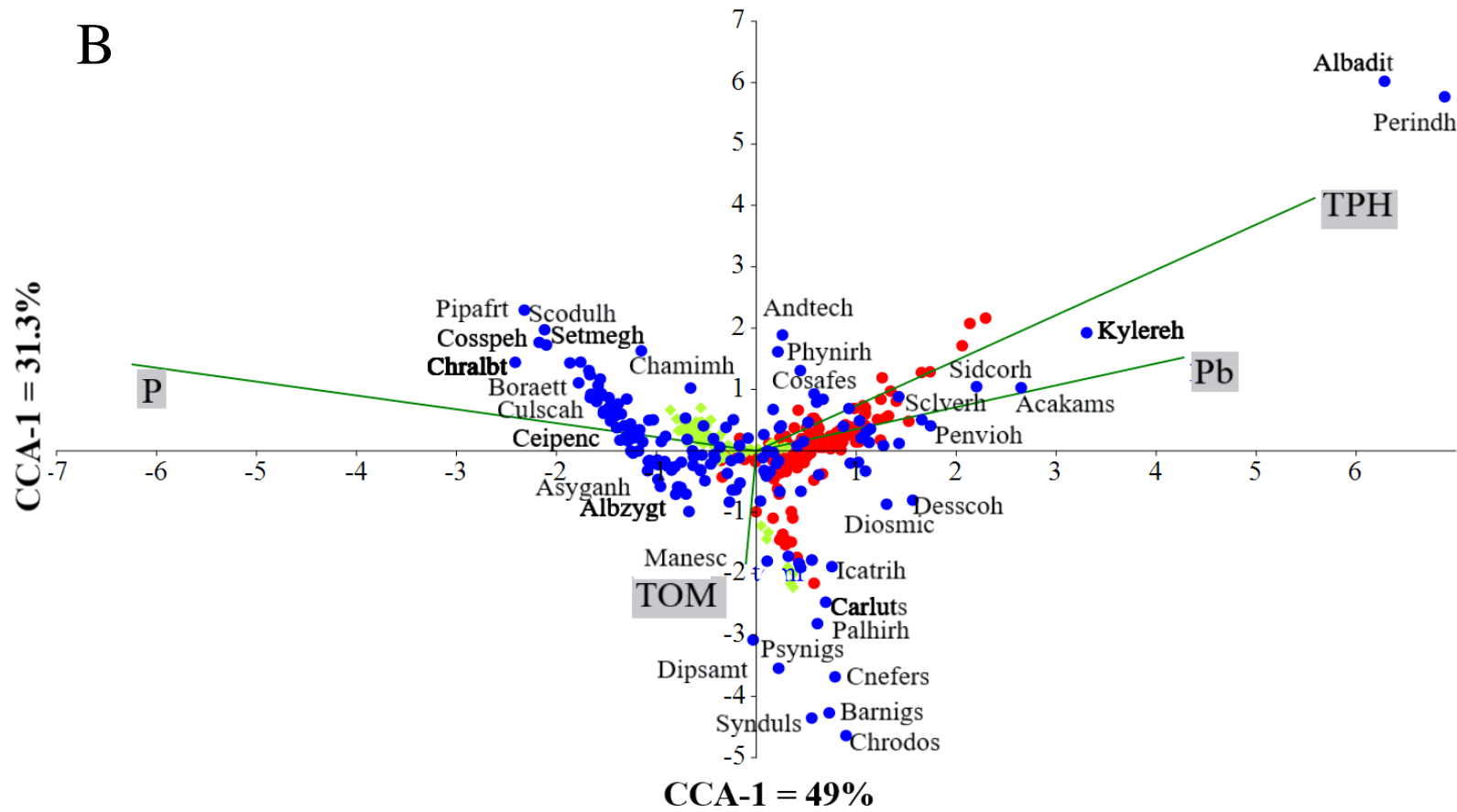
Figure 4.22B Plot of the first two axes of the CCA result scaled to displaysSpecies. The first CCA axis associates with increasing TPH and the second CCA axis associates with increasing TOM. The length of the tri-plots shows that both soil TPH and P were dominant gradients affecting species distribution. The plot successfully apportioned the ordinated space into polluted and unpolluted microhabitats which also correspond with particular species populating each microhabitat

Species populating the centre of the plot are those present in both polluted and unpolluted microhabitats and were labelled 'adaptable species'. Table 4.14 shows examples of each group of species.

Table 4.14: Examples of Most TPH tolerant species, most TPH-sensitive species and most adaptable species that thrived at the center of the plot.

Code-name	Species name	Lifeform	IVI	WAScore
TPH-Tolerant Species				
Acakams	*Acacia kamerunensis*	Shrub	2	4480
Albadit	*Albizia adiantifolia*	Tree	1	61232.8
Desscoh	*Desmodium scorpiurus*	Herb	2	1440.7
Diosmic	*Dioscorea smilacifolia*	Creeper	1	1679.5
Kylereh	*Kyllinga erecta*	Herb	2.42	22048.8
Perindh	*Perotic indica*	Herb	1.33	67940.25
TPH-Sensitive Species				
Chralbt	*Chrysophyllum albidum*	Tree	1	55.5
Dramant	*Dracaena mannii*	Tree	1	42.8
Pipafrt	*Piptadeniastrum africanum*	Tree	1.25	45.4
Funelat	*Funtimia elastic*	Tree	4.38	47
Spomont	*Spondias mombin*	Tree	5.2	35.8
Colhiss	*Cola hispida*	Shrub	2.25	38.5
Scodulh	*Scoparia dulcis*	Herb	1	59
Solmonh	*Solenostemo monstachyus*	Herb	1	46.3
Boraett	*Borassus aethiopum*	Tree	1	54.7
Tettet	*Tetrapleura tetraptera*	Tree	2.25	52.8
Dalecas	*Dalbergia ecastaphyllum*	Shrub	4.87	34.1
Asyganh	*Asystasia gangetica*	Herb	1.17	48.6
Malcorh	*Malvastrum coromandelianum*	Herb	1.4	48.6
Setmegh	*Setaria megaphylla*	Herb	1.75	27.2
Albzygt	*Albizia zygia*	Tree	4.36	26.3
Cyphash	*Cyperus haspan*	Herb	6.92	41
Cosspeh	*Costus spectabilis*	Herb	1.50	40
Ancdifh	*Anchomanes difformis*	Herb	5.79	45.4
Adaptable Species				
Voscus	*Vossia cuspidata*	Shrub	6.56	1301.1
Chlpilh	*Chloris pilosa*	Herb	15.94	8564.9
Alccors	*Alchornea cordifolia*	Shrub	14.46	2009.5
Sidcorh	*Sida cordifolia*	Herb	6.36	16728.8
Ageconh	*Ageratum conyzoides*	Herb	15.82	7566.8
Andtech	*Andropogon tectorum*	Herb	4.75	14470.9
Phyamah	*Phyllanthus amarus*	Herb	12.24	1196.9
Eleindh	*Eleiss indica*	Herb	4.89	9797.8
Tricorh	*Triumfetta cordifolia*	Herb	7.3	548
Phynirh	*Phyllanthus niruri*	Herb	5.79	11673.3

These species appear to have been affected by the presence of TPH in the soil as IVI values decreased on polluted transects. The low abundance of the species mentioned above (abundance class 2 and 3) may be attributed to their decreased population on polluted transects. This decimation is also evident in the vast difference between corresponding IVI values on polluted and control transects.

The correlation coefficient of the first two CCA axes 2 (associated with increasing TPH and elevation respectively), and vegetation characteristics show that both TPH and elevation influenced the distribution and composition of species in the study area. Table 4.13 how that taxa, frequency of species occurrence and diversity decreased with increasing TPH as well as elevation.

Table 4.15 Rank correlation coefficient (r) between relevant variables and CCA axes 1-3. TPH = total petroleum hydrocarbon, Pb = lead, P = phosphorus, TOM =total organic matter, taxa, the frequency of species occurrence, number of individuals and Shannon's diversity.

Variable	CCA-1	CCA-2	CCA-3
TPH	0.61	0.22	-0.06
TOM	-0.23	0.12	0.34
Taxa	-0.42	-0.13	0.04
Frequency	-0.36	-0.26	-0.06
Individuals	-0.39	-0.18	0.03
Shannon's	-0.36	-0.1	0.02

4.2 Discussion

4.2.1 Oil Pollution at Spill Locations in Rivers State

The high levels of petroleum hydrocarbon (TPH) recorded in soil samples collected from identified spill points and along polluted transects confirm that oil spill incidents polluted the land surrounding the area. The levels of TPH extracted from soil samples were in varying amounts and higher than the EGASPIN intervention values for different components of hydrocarbons. The high average TPH concentration from polluted transects (12692 mg/kg) clearly distinguishes them from the control transects which had an average TPH of 40.53 mg/kg. These results are comparable to those previously reported for soil samples extracted from polluted sites across the Niger Delta. For instance, Alinnor, Ogukwe and Nwagbo, (2014) obtained mean TPH concentration of up to 5199.52mg/kg from polluted soil in five communities in the Rivers State of Nigeria. Also, Ibezue (2013) reported high concentrations of TPH (up to 13949.42mg/kg) for soil

samples from spillage sites in Gokana Local Government Area of Rivers State similar to the TPH content of 16063mg/kg measured from the spill epicentre in Kporghor location.

The significant difference between observed TPH concentration in polluted and control transects a noted in earlier investigations. Osuji and Nwoye (2007) reported as low as 0.6mg/kg of TPH in the control sample and between 3400-6800mg/kg from polluted soil samples. Tanee and Albert (2015) also reported TPH levels of about 27.90mg/kg in soil samples collected from their control site and about 542mg/kg measured at the polluted site. Other environmental factors may have contributed to the high TPH concentrations observed in polluted transects. For instance, the topography of investigated locations may have enhanced the retention of crude oil at the spill points and the almost steady migration of oil along polluted transects. Elevation of polluted transects did not vary at each location except at Rumuekpe where it ranged from 16 to 17 m. Previous studies such as Seibert, Stendahl and Sørensen (2007); Zhang *et al.* (2012b) and Bockheim *et al.* (2014) have reported topographical influences on soil properties for different biomes. The observed high levels of petroleum hydrocarbon in samples from polluted transects in Kporghor location gives an insight on the quantity absorbed into the soil as well as the effectiveness of the containment measure implemented by the company despite over 60% of the total spilt amount recovered.

4.2.2 Effect of Oil Pollution on Soil Parameters

Increased concentration of petroleum hydrocarbon increased soil acidic (pH) and temperature values. Whereas some researchers report that oil pollution leads to increased soil pH (Obire and Nwaubeta, 2002; Udeh, Nwaogazie and Momoh, 2013; Wang *et al.* 2013); others showed that oil pollution in soil tends to increase soil acidity (lower pH values). For instance, Osuji and Nwoye (2007) and Akubugwo, Elebe and Osuocha (2016) reported a significant decrease in the pH of polluted soils. Similarly, Baruah *et al.* (2011) analysed crude oil contaminated soil in North East India and found that the contaminated soils were slightly more acidic (pH = 5.8±0.3) than the uncontaminated soils (pH = 6.4±0.2), although, they did not clarify if the difference in pH values was significant. The increased acidity of polluted soils was attributed on the one hand to the formation of organic acids by microorganisms responsible for the biodegradation of hydrocarbons, and on the other hand to the non-removal of leachates from the crude oil polluted substrate (Das and Chandra, 2011). Furthermore, while Wang *et al.* (2013)

135

reported a significant decrease in the temperature values of polluted soil samples collected from the Momoge Wetland in China. Akubugwo, Elebe and Osuocha (2016) reported the reverse for polluted soil in Khana area of Rivers State Nigeria.

Soil samples collected from Kporghor spill location, however, did not show this trend. Although there was a slight increase in the pH and temperature of soil samples obtained from the polluted transects, the increase was not statistically significant. The mean pH and temperature values of polluted samples were 4.33 and 29.1^0C while that of control samples were 4.2 and 29^0C respectively. This result compared favourably with those posited by Okonokhua et $al.$ (2007), Tanee and Albert (2015). TPH concentration in soil influenced soil fertility status. Soil electrical conductivity (EC) used as to indicate soil fertility (determines the cation exchange capacity, organic matter level, drainage conditions and other subsoil characteristics of the soil) showed a significant difference in polluted and control transects at the Kporghor spill location. Mean EC values were 10.36 µS/cm and 29.85 µS/cm respectively. The values were comparable to those reported by Benka-Coker and Ekundayo (1995); Okonokhua et $al.$ (2007); Tanee and Albert (2015) for studies conducted on polluted soils in the Niger Delta region. Benka-Coker and Ekundayo (1995) reported EC range of 35-54 µS/cm from the soil sample collected at a depth of 15-30 cm within the heavily impacted zone and range of 27-68 µS/cm at similar depth for the unimpacted zone. Tanee and Albert (2015) likewise reported lower values of 6.33 µS/cm and 10.33 µS/cm for polluted and unpolluted soil respectively. Osuji and Nwoye (2007) in their appraisal of the impact of petroleum hydrocarbons on soil fertility in Owaza reported very high EC values (688 µS/cm for polluted and >1890 µS/cm for control soil samples). The extremely high EC value reported by Osuji and Nwoye may have been due to the agricultural use of the land. Other factors that affect soil EC not analysed in the current research are soil texture and particle size, cation exchange capacity of the soil and depth of topsoil. However, Ayotamuno et $al.$ (2006) and Akubugwo et $al.$ (2016) reported significantly higher EC values for polluted soils ($p < 0.05$); Although evidence from previous reports as well as the current research suggest a negative relationship between soil TPH and EC; a correlation analysis of the soil parameters data showed that EC had a weak positive correlation ($r = 0.146$; $p = 0.434$) with TPH concentration in soil.

The increased TPH in the soil also influenced soil nutrients. The nitrate content of soil samples analysed in the current research was negligible (< 0.02 mg/kg) for both polluted and control transects in Kporghor spill location. In contrast, Tanee and Albert (2015) reported very high nitrate values (132.36 mg/kg and 95.57 mg/kg for polluted and unpolluted soils respectively) and Udeh, Nwaogazie and Momoh (2013) posited high nitrate values of 22.06 mg/100g for uncontaminated soil. However, Benka -Coker and Ekundayo (1995) reported lower nitrate values of 0.3 mg/kg and 0.9 mg/kg for impacted and unimpacted sites respectively. Obire and Nwaubeta (2002) and Osuji and Nwoye (2007) also reported lower figures for nitrate in polluted than in control soil samples. The reported decrease in nitrate contents of polluted soils indicates inhibition of nitrification in polluted soils due to the effect of competition from petroleum compounds (Rasche, Hyman and Arp, 1990; John, Ntino and Essien, 2016).

Phosphorus values of polluted and control transects showed significant differences. Caravaca and Roldán (2003) reported available P values of 32 mg/kg for control and 28 mg/kg for contaminated soils obtained from semiarid Mediterranean conditions. Similarly, Wang *et al.* (2013) in their analysis found that crude oil reduced the available phosphorus concentrations in impacted soils (P = 30 mg/kg at control and 13.9 ± 2.8 mg/kg at polluted sites). They also observed significant differences in phosphorus concentrations at different seasons for the polluted soils. Ugboma (2014) and Akubugwo *et al.* (2016) in their various studies reported that available phosphorus in polluted soil samples was significantly lower than that in samples obtained from the control site. These results were consistent with those obtained in the present study, which showed lower concentrations of phosphorus in polluted transects than in the control transects. The median phosphorus content in soil samples from polluted transects was 4.69 mg/kg while from the control transects it was 17.59 mg/kg. These values were very low compared to the mean P value of 75.62 mg/kg, and 103.12 mg/kg reported by Tanee and Albert (2015) for polluted and control soils respectively. The higher P values reported by Tanee and Albert (2015) for soil collected from a similar ecological area may be due to the lower TPH levels of the polluted soil as well as the season of collection. Wang *et al.* (2013) reported that seasonal variation significantly affected phosphorus availability in the soil in Momoge, China.

Decreasing phosphorus levels in polluted soils may be linked to the presence of hydrocarbons stimulating the growth of oil-degrading micro-organisms and hence increasing the utilisation of available phosphorus (Atlas, 1981; Eneje, Nwagbara and Uwumarongie-Ilori, 2012; Wang *et al.* 2013). The negative correlation (r = -0.423, p < 0.05) between phosphorus and total organic carbon (TOC) levels in Kporghor investigated transects supports this assertion. Nevertheless, some studies have shown available phosphorus to be higher in polluted soil than in the unpolluted soil (Essien and John, 2011).

Low total organic carbon (TOC) values obtained from control transects contrasted with Osuji and Nwoye (2007); Atuma and Ojeh (2013) whom both observed higher levels of TOC in control samples than in polluted samples. The values are, however, consistent with other studies including Obire and Nwaubeta (2002); Essein and John (2011); Marinescu *et al.* (2010); Wang *et al.* (2013); Udoh and Chukwu (2014) who reported a significant increase in TOC content of polluted soil which they attributed to the presence of carbonaceous substances in the soil.

Values for total organic matter (TOM) content of soil samples varied considerably across the entire study area and between polluted and control transects. The difference between polluted and control transects was also significant. Higher levels of TOM in soil samples from control transects may be attributed to the increased presence of vegetation since most soil organic matter originate from living and decomposing plant tissues (Bot and Benites, 2005).

Total heterotrophic bacteria (THB) counts differed significantly between the polluted and control transects with the highest levels (5.63*106 CFU/ml) recorded at the spill epicentre in Kporghor spill location. The mean THB count on polluted transects was 106 CFU/ml and 14.3*106 CFU/ml on control transects. These values agreed with those reported by Obire and Nwaubeta (2002); Okoye and Okunrobo (2014) for spill sites in the Niger Delta region of Nigeria. The reduced THB counts observed in the polluted transects may be connected to the inhibition of microbial and enzymatic activities in the (Okoye and Okunrobo, 2014; Alrumman, Standing and Paton, 2015). Conversely, the natural conditions of the unpolluted control transects may have supported normal microbial growth and activities.

The heavy metals investigated and detected in the soil samples collected from the study area were lead and cadmium. The values for lead ranged from 2.16 to 163 mg/kg in the polluted transects while in control transects lead values were less than 13.2 mg/kg. Although these amounts were higher than those documented by Benka-Coker and Ekundayo (1995) in their study of a heavily impacted spill site in the Niger Delta, they are consistent with results obtained by Udoh and Chukwu (2014); Fatoba *et al.* (2016) for similar sites. Other investigations such as Kisic *et al.* (2009) for contaminated soil in Croatia and Fu, Cui and Zang, (2014) for oil-polluted soil in Shengli Oilfield, China also yielded comparable results. Heavy metal contamination in the polluted transects may have been due to the oil spill as crude oil have been identified to contain heavy metals such as lead, cadmium, zinc, nickel and so on (Kisic *et al.* 2009; Dickson and Udoessien, 2012; Fu, Cui and Zang, 2014), however, it may also have been from other sources. For instance, the high values recorded for polluted transect (C) in Kporghor spill location may have been because of the application of pesticide and bio-solids on the cassava farm intersected by transect. Wuana and Okieimen (2011) reported that about 10% of approved chemicals utilised in the production of pesticides contained lead and other metals.

In summary, crude oil pollution in Rivers State exerted deleterious effects on the physical, chemical and biological properties of the soil. The presence of petroleum hydrocarbon in the soil led to reduced levels of beneficial parameters such as electrical conductivity, phosphorus, organic matter and microbial population. This effect contributed to the stripping of nutrients from polluted transects and might have also accounted for the reduced vegetation growth and abundance on these transects as evidenced in the present research. Chong *et al*, (2017) asserted that the efficiency of soil nutrient absorption by plants is controlled by soil properties, hence, nutrient deficiency invariably leads to reduced vegetation productivity. However, other factors which were not explored in this research may have also contributed to the depletion of soil nutrients, for instance the disturbance history of polluted transects.

4.2.3 Effect of Oil Pollution on Vegetation

Osam, Wegwu and Uwakwe (2011), UNEP (2011), Lindén and Pålsson (2013); Tanee and Albert (2015) previously reported the devastating effect of oil pollution on the ecosystem flora and fauna. The vegetation on and around polluted transects responded to the presence of TPH in the soil by the thinning out of plants and outright disappearance

of some species. Oil pollution in soil impedes the growth of plants (Ogbo, Zibigha and Odogu, 2009; Chima and Vure, 2014). This effect is attributed to the unavailability of essential soil nutrients such as nitrogen and oxygen to the plants (Njoku, Akinola and Oboh, 2008; Ogbo, Zibigha and Odogu, 2009). Furthermore, oil constituents block stomata and intercellular spaces (Baker, 1970) thereby reducing transpiration rates and consequently plant uptake of nutrients (Novák and Vidovič, 2003).

Statistical analysis of the floristic data showed significant differences between polluted and control transects in the study area. The taxa, frequency, abundance and density results were all higher in control transects than in the polluted transects, though, a few species were observed only on polluted transects and not on the control transects. A total of 163 plant species belonging to 52 families were inventoried across investigated transects. The ratio of species to families corresponds with those obtained from several studies on species composition and diversity in the Niger Delta region such as Tanee and Albert (2015); Daniel, Jacob and Udeagha, (2015); Ubom, (2010) and Agbagwa and Ekeke (2011). For instance, Ubom (2010) recorded 339 plant species belonging to 88 families in the forests and homestead gardens in the Niger Delta. Agbagwa and Ekeke (2011) reported that 90 plant species belonging to 40 families for Bonny Local government area in Rivers State, Nigeria. Furthermore, Daniel, Jacob and Udeagha, (2015) documented 38 species belonging to 22 families for trees in the Abam Itak sacred forest in the Cross River State of Nigeria.

The taxonomical distribution of vegetation in the current study is consistent with those submitted in previous studies. For instance, Onyekwelu, Mosandl and Stimm (2013) reported that *Euphorbiaceae, Mimosoideae (Leguminosae), Sterculiaceae, Meliceae* and *Apocyanaceae* were the dominant families in the two natural forest they investigated. Similarly, Jacob *et al.* (2015) also identified *Fabaceae, Leguminosae* and *Sapotaceae* as the dominant families in their survey of sacred forest in South Eastern Nigeria.

Floristic data revealed that average species composition on polluted transects were about 34% while it was over 66% on the control transects suggesting a deficit of over 30% of species in oil-polluted transects. The results further indicate that shrubs, herbs and creepers suffered more losses than trees, which implies that not only do species differ in their sensitivity to oil pollution, but also the lifeforms of the plant species determine their susceptibility to the impact of oil pollution (El-Nemr, 2006). Similar observations were

made by Kinako (1981) who reported a species loss of at least 50% in oil-polluted habitats as well as Baruah and Sarma (1996) who following their study found that 80% of plant species were lost in crude oil spill sites in the Rudrasagar oil field. They also observed that annual plants were the most affected. The abundance and density of species on the investigated transects were different for the polluted and control transects. These results were consistent with those reported by Nkwocha and Duru (2010); Tanee and Albert (2015) who affirmed that oil spill impacted negatively on the abundance and density of vegetation in the Niger Delta region. Additionally, Lin and Mendelssohn (2012) also reported significantly lower levels of life above ground biomass (a measure of abundance) at oil-impacted sites than at reference sites in their study of the impacts of an oil spill on vegetation structure in coastal salt marshes of the northern part of the Gulf of Mexico.

Based on the IVI, the most valuable species in the study area are:-

i.   *Manihot esculenta* (Manescs),
ii.   *Paullinia pinnata* (Paupinc),
iii. *Elaeis guineensis* (Elaguit),
iv.   *Cocos nucifera* (Cocnuct),
v.   *Chloris pilosa* (Chlpilh),
vi.   *Ageratum conyzoides* (Ageconh),
vii. *Alchornea cordifolia* (Alccors),
viii. *Carica papaya* (Carpapt), and
ix.   *Gomphrena celosioides* (Gomcelh).

These species were equally present at both the polluted and control transects and appeared to have been more tolerant to oil spill impact than the other species. Interestingly, these highly tolerant species are all perennials. Burk (1977) and Cowell (1971) both observed that perennial species were less affected by an oil spill in a freshwater marsh and salt marsh respectively. The reason may be that some perennials such as *Manihot esculenta, Chloris pilosa,* have well-developed rhizomes which allow the plants to perennate during the crucial stages of oil inundation. Maslova (2014) studied the structure and metabolism of underground shoots in perennial rhizome-forming plants and reported that rhizomes in grassy perennials were extremely adept at self-restoration apparently through vegetative propagation. Additionally, some of these tolerant species were characterised by deep tap

roots (for instance *Elaeis guineensis, Cocos nucifera, Alchornea cordifolia*) with capacity for nutrient extraction from deeper soil layers (Don Santos and Wenzel, 2007).

As the results suggest, several species which declined in IVI values or absent on polluted transects were present on control transects, a phenomenon attributable to the secondary effects of an oil spill such as fire destroying vegetation or use of damaging oil recovery methods. However, since the most susceptible species (herbaceous annuals) were well represented on control transects but absent or significantly reduced on polluted transects, it is more likely that the presence of TPH adversely affected species diversity. This phenomenon is an indication of poor growth conditions expedited by oil pollution. These results compared favourably with Nwoko *et al.* (2007); Lin and Mendelssohn (2012) and Oyedeji *et al.* (2012) who found that plant population remarkably decreased in oil-contaminated soils. They asserted that this decrease is due to the intoxication of the soil microenvironment by crude oil, which interferes with the availability of essential nutrients as well as the plant uptake and utilisation of nutrients (Novák and Vidovič, 2003). In summary, therefore, oil pollution has adversely affected the vegetation of the area through outright loss of species as well as through reduced abundance of the surviving species on polluted transects.

4.2.4 Effect of Oil Pollution on Species Diversity

The Niger delta harbours a vast number of diverse living organisms and is a biodiversity hot spot (United Nations Development Programme, 2010; Nzeadibe *et al.* 2011). However, there continues to be an increasing threat to the rich biodiversity of this region due to ongoing oil production and related activities. Several reports show that oil pollution causes a decrease in species diversity of both long-lived woody species and shorter-lived herbaceous species through several processes, which include rendering soil nutrients unavailable for plant use (John, Ntino and Essien, 2016; Wang *et al.* 2013; Eneje, Nwagbara and Uwumarongie-Ilori, 2012; Atlas, 1981). The diversity of the study area reflected a similar pattern as observed for the tropical forest ecosystems. Vasilyevich (2009) reviewed several papers written on species diversity of plants in the tropical rainforest and reported species density of 0.03 to $0.25/m^2$ for the Peruvian Amazonia; $0.14 /m^2$ in Australia and $0.1/m^2$ in Southern Africa. These results compared favourably with the average species density of $0.1/m^2$ obtained from the current study area.

The diversity indices obtained for the entire study transects were similarly high (Simpson's = 0.95 and Shannon's = 3.22) but differed significantly between polluted and control transects. Although several studies have enunciated the inadequacy of species richness as an indicator of species diversity, results from the current research showed a strong positive correlation among the richness (Menhinick's) and diversity (Simpson's and Shannon's) indices evaluated. Despite the high diversity values, there were significant differences in the phytosociological characteristics of vegetation on the polluted and control transects due to the influence of hydrocarbon in the soil. However, other factors may have also induced these changes, for instance, Connell (2008) summarised in his paper on diversity in tropical rainforests and coral reefs that intermediate disturbances, equal chance and gradual change explain the differences in the diversity of tropical rainforests. Furthermore, Huston (1979) asserted that under non-equilibrium conditions, species diversity is altered by variations in the focus and intensity of competitive interaction among communities. He, therefore, opined that intense competition, particularly for nutrients and energy, would result in low diversity and vice versa.

The results from this study suggests that the presence of hydrocarbon in the soil induced nutrient loss and intensified competition among the surviving species of plants, induced species loss and consequently decreased the diversity of vascular plants on polluted transects. This interpretation is inferred from the recorded differences in the vascular plant species diversity of polluted and control transects. However, despite the conscientious effort to select locations with greater environmental similarity, the possibility that other extraneous factors may have contributed to the observed phenomena remains. Interestingly, the control transects showed higher richness indices (Menhinick's) whereas the polluted transects had higher evenness values. Evenness values for polluted transects ranged from zero to one, while on control it ranged from 0.5 to 0.97. Although these values were not significantly different, the higher evenness of polluted transects may be due to the general reduction in the population of individual plants occurring on those transects. The results of the current research show that species evenness negatively correlated with the number of individual plants in polluted transects ($r = -0.37$, $p < 0.05$). For polluted transects, this observation supports the hypothesis that plants community diversity stabilises functional properties such as equitability during ecological

disturbances such as fires, or nutrient perturbation caused by oil pollution (McNaughton, 1977).

The relationship between the two components of diversity and their suitability for measuring diversity has been a subject of interest among ecologists over the years. Some studies show a positive correlation between species evenness and species richness (Soininen, Passy and Hillebrand, 2012), thereby supporting the use of one or the other as a diversity measure, others show the reverse or no relationship between the two (Stirling and Wilsey, 2001; Gosselin, 2006; Jost, 2010; Zhang *et al.* 2012a). In the present research, the two indices weakly related across all investigated transects, however, the relationship between diversity, richness and evenness on the control transects was significantly positive ($r > 0.5$, $p < 0.05$; $n = 80$). Hence, either richness or evenness index could serve as a surrogate for diversity in unpolluted transects.

Among segments of polluted transects, evenness correlated negatively with species richness and may have contributed more to the diversity index of these transects. While evenness showed a consistent and directional response to a decreasing TPH gradient, the richness indices appeared stable after certain levels of TPH. Also, along the polluted transects, the pattern of species diversity seems to follow the TPH gradient in the soil. Results from the data showed that both the Simpson's and Shannon's indices increased significantly as the TPH levels in the soil decreased from one segment to another. Thus, it is inferred that the presence of TPH created a microenvironment, which caused changes in the diversity of vegetation along, transects. Cao and Zhang (1997) reported a similar phenomenon in their study of tree species diversity of tropical rainforest vegetation in Xishuangbanna, South-west China. They discovered that trees species diversity between different samples of the same forest types varied depending on the microenvironment of the forests.

Moreover, the scale of services derived from the ecosystem (which serves as the primary means of livelihood for the local people), is dependent on its functional diversity and productivity. In other words, the more functionally diverse an ecosystem is, the more productive it will be in providing essential ecosystem services for the maintenance of biogeochemical processes and human welfare. It then follows that changes in either variable will bring about losses in the productivity and services derived from the ecosystem. For instance, certain either economically important plant species that showed

higher importance value index (IVI) at control transects were seen to have disappeared or significantly reduced in IVI on polluted transects. These species include *Millettia macrophylla, Phyllanthus amarus, Albizia zygia, Blighia sapida, Ipomoea involucrata, Manihot esculenta, Carpolobia lutea, Setaria megaphylla, Newbouldia laevis* and so on. The IUCN has listed *Millettia macrophylla* in Red List of Threatened Species (IUCN, 2014) as vulnerable whereas Edu *et al.* (2015) reported *Phyllanthus amarus* as scarce in a hydrocarbon-impacted site in Rivers State, Nigeria following their investigation. Loss of these species, some of which are perennial plants in the rainforest ecological zone may instigate the loss of essential ecosystem services they support or provide. Previous studies have revealed a linear relationship between biodiversity and ecosystem service provisions such as nutrient cycles, biomass production and transfer (Cardinale *et al.* 2012; Flombaum and Sala, 2007; David U Hooper *et al.* 2012; Hector *et al.* 1999). A similar relationship was observed in the current research as there was a decrease in the chlorophyll estimates on polluted transects in comparison with control transects. The chlorophyll content in plants plays a crucial role in photosynthesis, which in turn determines primary productivity of biomass (McKendry, 2002; Beadle and Long, 1985).

Curiously and as reported in previous studies (Zak *et al.* 2003; Liu *et al.* 2008; Eisenhauer *et al.* 2010), all the diversity indices (Shannon's, Simpson's, richness and evenness) correlated positively with soil microbial population (in this case, total heterotrophic bacteria) on the control transects. However, the reverse was observed on polluted transects as results showed a strong negative correlation between the diversity indices and THB population in the soil. Although this discrepancy may be due to the limited scope of the microbial analysis performed in this study as most of the previous investigations analysed various microbes including fungal, bacterial and protozoan populations. Nevertheless, it is apparent that processes are occurring belowground which substantially affected by the presence of petroleum hydrocarbon in the soil. Under ideal conditions, soil microbial population will do well in a soil characterised by neutral pH, balanced moisture and aeration, temperatures below 400C and adequate nutrients (Nitrogen, Phosphorus, Potassium, Sulphur and so on) (Ng *et al.* 2012), but oil pollution in the study area has adversely affected these parameters. Since soil microorganisms largely control ecosystem functions (Eisenhauer *et al.* 2010; Steinauer *et al.* 2015), it follows then that any factor that adversely affects microbial population will also affect the services derivable from such ecosystems. The evidence from the present research

supports these previous results and shows how soil microbial communities respond to the anthropogenic activities that are changing the ecological landscape.

4.3 Summary

This chapter investigated the effect of oil pollution on the distribution and diversity of vascular plant species in the Rivers State of Nigeria. Comparison of soil and vegetation data from polluted and control (unpolluted) transects across 20 locations support the working hypothesis that oil pollution adversely abundance and diversity of vascular plant species. Specifically, evidence from the data suggests the rejection of the null hypothesis of no difference in the vegetation characteristics and diversity of polluted and control transects. The results revealed that soil and vegetation-related variables were significantly different between polluted and control transects.

Additionally, results showed that soil parameters beneficial to vegetation growth were also adversely affected by oil pollution in the study area. Results from the present investigation also insinuate that oil pollution impact negatively on nature and diversity of ecosystem services derived from the environment. The evidence of this effect is apparent in the reduced productivity (measured as chlorophyll content) and diversity of polluted transects.

Chapter 5 presents the results of incorporating satellite data in monitoring oil pollution effects on vegetation. The chapter assessed the validity of the spectral variation hypothesis by measuring changes in spectral metrics in response to soil TPH concentration.

5 Spectral Diversity Metrics for Detecting Effect of Oil Pollution on Biodiversity

An article from this chapter is has been accepted for publication by Elsevier as a chapter in a remote sensing book 'Hyperspectral Remote Sensing' and a second article was published in MDPI Remote Sensing journal

This chapter introduces the integration of remotely sensed data with field data for detecting oil pollution impact on biodiversity. The spectral variability hypothesis (SVH) was tested to determine the suitability of spectral diversity metrics derived from Sentinel 2A data for biodiversity monitoring in oil-polluted locations. In answering RQ3, which investigates the relationship between species diversity and spectral diversity, the following hypotheses are tested.

a) There is a significant difference between vegetation spectra from polluted and control transects.

b) There is a significant linear relationship between spectral diversity metrics and field measured variables (thereby validating the SVH).

Validation of the spectral variation hypothesis is tackled from two perspectives

i. The spectral variation associated with changes in soil properties due to oil pollution

ii. Spectral variation associated with changes in vegetation abundance, species richness and diversity

Additionally, the chapter presents an overview of the SVH as well as specific methods and datasets utilised in the analysis. A non-parametric multivariate regression analysis performed in R studio (please see Chapter 3 Section 3.5.1.3b) was used to determine the relationship between spectral diversity metrics and the listed variables (soil properties and species richness and diversity),

5.1 Overview of the Spectral Variability Hypothesis

The Spectral Variability Hypothesis (SVH) proposed by Palmer *et al.* (2002) asserts that the spatial heterogeneity of plant species positively correlates with spectral diversity of remotely sensed images. Spectral diversity, on the one hand, is determined by the extent of variation in reflectance values of corrected images. Plants, like other materials on the earth surface, reflect radiation from the sun uniquely for different species. The shape of the spectrum is dependent on the optical properties of the plants, which in turn are

controlled by biophysical and biochemical factors such as cellular structure, leaf anatomy, pigment concentrations and moisture content. According to Clevers *et al.* (2002), control of leaf reflectance is by pigments (chlorophyll a and b, β-carotene and so on) in the visible (VIS); the cellular structure in the near-infrared (NIR) and moisture content in the short-wave infrared (SWIR) regions of the electromagnetic spectrum. Variations in these properties induced by plant response to environmental stress, such as oil pollution manifest in the spectral signatures acquired by satellite sensors in orbit.

Plants response to environmental stress has been well-studied (Sewelam *et al.* 2014) as well as the adverse effect of such stressors to plant productivity (Anjum, 2015). Environmental stresses that affect plants are biotic and abiotic. Abiotic factors include natural and human-made conditions such as air pollution, heavy metal contamination of soil, oil spills, fire incidents and so on. All these variables also result in biodiversity loss globally (Arellano *et al.* 2015; Pysek and Pysek, 1989).

Oil spills release hydrocarbons in the soil which displace oxygen and nutrients and adversely affect plant growth and productivity (Scholten and Leendertse, 1991; Beaubien *et al.* 2008; Noomen *et al.* 2012). Zhang *et al.* (2007) investigated the effect of lubricating oil pollution on mangrove species in Hong Kong and reported that the hydrocarbons induced the formation of excessive free radicals in plant cells. These radicals caused oxidative stress by impairing biological processes that enhance growth and productivity in plant seedlings. In their work at a leakage site in Central Bohemia, Czechoslovakia (present-day Czech Republic) Pyšek and Pyšek (1989) noted a decrease in the growth and number of individual plants present on contaminated sites.

Species diversity on the other hand is recognised as an ecosystem status indicator by global organisations such as Group on Earth Observation (GEO BON), the World Climate Research Programme (WRCP), the International Geosphere-Biosphere Program (IGBP) and the |Committee on Earth Observation systems (CEOS) (Rocchini *et al.* 2016). Past studies show links between species diversity and ecosystem productivity such that loss of the former threatens the goods and services derived from the latter (Vihervaara *et al.* 2014; Mace, Norris and Fitter, 2012; Norris, 2012; Chapin *et al.* 2000; Waide *et al.* 1999). Similarly, Pereira and Cooper (2006) observed that species diversity determines ecosystem functioning and type of ecosystem services provided at the local, regional or global scale. Remote sensing is used in biodiversity monitoring to estimate plant species

diversity using very high spectral and spatial resolution images that are analysed for spectral diversity and habitat heterogeneity (Block *et al.* 2016; Heumann *et al.* 2014; Hall *et al.* 2011; Saatchi *et al.* 2008 and so on). Hence, the SVH represents a valuable resource that integrates spectral and field data for detecting various effects of oil pollution on the ecosystem.

5.2 Sentinel 2A Data Analysis

This section presents the specific tools, procedures and dataset employed in investigating the research questions addressed in this chapter.

5.2.1 Scale Matching Satellite Image and Study Area

Sentinel 2A image was spatially scaled to match the sampling units of the field survey. Rocchini *et al.* (2010) suggested that appropriately scaling imagery resolution with species data was essential for implementing the SVH. Similarly, Small (2004) and Rocchini (2007) noted that matching the field sampling units with the spatial resolution of an image will enhance the detection of sub-pixel variability and strengthen the relationship between species diversity and spectral variability. Also, Turner *et al.* (2003) and Chen and Henebry (2009) suggested that the calculation of spectral variability is enhanced when several pixels cover the spatial dimension of sampling units.

The region of interest tool in ENVI 5.3 was used to create vector polygons of each segment on investigated transects. Each segment of 20 m corresponded to 2 x 10 m pixels of the Sentinel 2A image; however, a 2 x 2-pixel window was used in this analysis to incorporate information from the surrounding area. Although the total area of the pixel window was more than the sampling units (segments), this was not considered a limitation since incorporating spectral information of landscape surrounding sampling units improve the performance of models linking species to spectral diversity (Parviainen, Luoto and Heikkinen, 2009; Rocchini *et al.* 2010). In total, 210 x 4 pixels (equivalent to an area of 84,000 square meters) were used to test the spectral variability hypothesis in this study.

5.2.2 Spectral Diversity Metrics from Bands

The study utilised only eight bands out of the original 13 bands of the Sentinel-2A imagery, these were bands 2 = blue; 3 = green; 4 = red; 5 - 7, 8A = red edge and 8 = near infrared (NIR). A vector layer of polygons representing segments of investigated transects as overlaid on the pre-processed satellite imagery. For each segment measuring 20m in length, four pixels were identified to encompass it. The reflectance of individual Sentinel-2A bands was then extracted from these four pixels.

Evaluating the reliability of the spectral variability hypothesis required each pixel considered a distinct species; thus perceiving spectral diversity as the diversity of the pixels in each spectral band computed from procedures involving the centre and spread of the band reflectance values. Other metrics computed to reflect the spectral heterogeneity of the Sentinel 2A data included the Simpson's and Shannon's diversity indices. Spectral diversity computation adopted different approaches from literature, and the performance of various metrics for validating the SVH was compared.

Metrics computed from the mean, standard deviation, Shannon and Simpson's indices of the pixels followed the method outlined in Warren *et al.* (2014). Two additional metrics defined as spectral heterogeneity (SH) and quartile-based coefficient of variation (QCV) derived from the methods of Hall *et al.* (2012) and Heumann, Hackett and Monfils (2015) respectively, emerged from the Sentinel 2A bands. SH is the mean difference between the mean of each 2 x 2-pixel window overlaying a segment and the mean of all 2 x 2-pixel windows on each transect (overlaying five segments in total). QCV is a non-parametric approach that measures the dispersion of data around a centre (median value) by taking the ratio of the interquartile range to the median of the data set (IQR/Median).

Further spectral metrics computed from the original 8 Sentinel-2A bands include those obtained by principal component analysis (PCA) which is a mathematical algorithm that transforms high dimensional and correlated data to lower dimension and uncorrelated components. Data reduction involves identifying the direction (eigenvectors) of the most variance in the data (Ringnér, 2008). The Sorenson's similarity index (IS) of band was subtracted from one to determine spectral distances. These statistics were calculated using reflectance values of eight bands from the four pixels overlaying the investigated

segments. In total 56 band indices were derived from the eight Sentinel-2A bands utilised. Table 5.1 presents a list of derived metrics.

Table 5.1: Spectral indices derived from the Sentinel -2A bands used in the study. Band reflectance of four pixels overlaying each segment provided data for this analysis.

Band	Statistic	Index
2 (Blue)	Mean	M2
	Standard deviation	Sd2
	Spectral heterogeneity	Sh2
	Quartile coefficient of variation	QCV2
	Shannon's Index	H2
	Simpson's Index	D2
	Sorenson's Similarity Index	SI2
3 (Green)	Mean	M3
	Standard deviation	Sd3
	Spectral heterogeneity	Sh3
	Quartile coefficient of variation	QCV3
	Shannon's Index	H3
	Simpson's Index	D3
	Sorenson's Similarity Index	SI3
4 (Red)	Mean	M4
	Standard deviation	Sd4
	Spectral heterogeneity	Sh4
	Quartile coefficient of variation	QCV4
	Shannon's Index	H4
	Simpson's Index	D4
	Sorenson's Similarity Index	SI4
5 - 7, 8A(Red Edge)	Mean	M5 - M7, M8A
	Standard deviation	Sd5 - Sd7, Sd8A
	Spectral heterogeneity	Sh5 – Sh7, Sh8A
	Quartile coefficient of variation	QCV5 – QCV7, QCV8A
	Shannon's Index	H5 - H7, H8A
	Simpson's Index	D5 - D7, D8A
	Sorenson's Similarity Index	SI5-SI7, SI8A
8 (NIR)	Mean	M8
	Standard deviation	Sd8
	Spectral heterogeneity	Sh8
	Quartile coefficient of variation	QCV8
	Shannon's Index	H8
	Simpson's Index	D8
	Sorenson's Similarity Index	SI8
PC1	Scores	PC1
PC2	Scores	PC2
PC3	Scores	PC3

5.2.3 Spectral Diversity Metrics from Vegetation Indices (VIs)

Vegetation indices useful for detecting the chlorophyll content, primary productivity and vegetation stress in plants extracted from the original bands of the Sentinel-2A image are listed in Table 5.2. Metrics derived from VIs include the mean, standard deviation, Shannon's and Simpson's diversity indices, which were used in further analyses.

Table 5.2: Summary of selected vegetation indices used in evaluating the spectral variation hypothesis (SVH).

Parameter	Index	Formula	Reference
Chlorophyll Content	Canopy Chlorophyll Index (CCI)	$\dfrac{Band8 - Band5}{Band8 + Band4}$	(Pu, Gong and Yu, 2008)
	Normalised Difference Vegetation Index (NDVI)	$\dfrac{Band8 - Band4}{Band8 + band4}$	(Tucker, 1979; Rouse *et al.* 1974)
	Red Edge Position 2	$\dfrac{Band5 - Band4}{Band5 + Band4}$	(le Maire, François and Dufrêne, 2004)
Primary Productivity	Soil Adjusted Vegetation Index (SAVI)	$\dfrac{Band8 - Band4}{Band8 + Band4 + L}(1 + L)$	(Huete, 1988)
Leaf Pigments	Anthocyanin Reflectance Index (ARI)	$\dfrac{1}{Band3} - \dfrac{1}{Band5}$	(Gitelson, Gritz † and Merzlyak, 2003)
	Structure Insensitive Pigment Index (SIPI)	$\dfrac{Band\,8 - Band\,1}{Band\,8 - Band\,4}$	(Peñuelas and Filella, 1998)

5.2.4 Statistical Analysis

The correlation of each spectral metric with each species diversity measure identified the most sensitive metrics to oil pollution. Following the Spearman's Rank Correlation (SRC) of the data, metrics with large coefficient values ($r > \pm0.2$) were selected and further tested for significance at alpha = 0.05 using the Student T-test. A p-value less than 0.05 implies that there is sufficient evidence to conclude that there is a significant linear relationship between the spectral metric and the particular field-measured variable and that the relationship is replicable. Selected spectral metrics were grouped according to their sources (Sentinel 2A bands or vegetation indices) and regressed with field data to establish the strength of any relationships amongst the variables using a non-parametric regression model (NPM) described in section 3.5.1.3B.

The regression analysis was performed to investigate the possibility that the MSI detected changes in vegetation reflectance caused by oil pollution. Firstly, the spectral diversity of polluted transects should vary significantly with that of non-polluted transects. The

rationale for this presumption is the documented effects of oil pollution on vegetation, which includes the decrease in plant productivity and loss of vulnerable plant species, thereby reducing spectral diversity. Secondly, species diversity indices measured from the field were expected to regress linearly and positively with spectral diversity metrics (particularly on control transects) in line with the spectral variability hypothesis. Finally, selected spectral diversity metrics were predictors in models designed to test the SVH and estimate vascular plant species diversity in the study area. Metrics were selected based on the strength of their relationships with the diversity indices and the variance inflation factor (VIF). The VIF adopted to correct for collinearity in the explanatory variables was determined in R using the car package. Only metrics with VIF < 10 were selected for the models. Prediction modelling involved a non-parametric multivariate regression (NPMR) analysis using the np package in R. Two groups of spectral metrics namely, band-based (those derived from Sentinel 2A bands) and index-based (those derived from common vegetation indices) were used in models to estimate vascular plant species diversity. The dataset was randomly subdivided into training and test (validation data) using a ratio of 7:3 respectively. Thus, the training data contained 150 observations and the test data contained 60 observations. Regression coefficients derived from the calibration process were applied to the test data for validation. Assessment of model performance was by comparing the adjusted coefficient of determination values (Adj.R2), root mean square error (RMSE) and predicted square error (PSE) of both band-based and index-based models.

The presence of spatial autocorrelation among data points was acknowledged in this study and was minimized by the selection of alternate segments on investigated transects. However, the spatial structure of the field data aggregated over transects and locations may lead to model over fit. The models and parameters are listed in Table 5.3.

Table 5.3: Parameters of models used to estimate soil properties and other response variables from spectral diversity metrics computed using A. sentinel 2A bands 2 to 8A and B. common vegetation indices

Model ID	Predictors	Response Variables
1A. Band-Based Metrics	Selected spectral metrics from Sentinel 2A bands 2 to 8A with -0.3 < r > 0.3	1. Soil properties 2. Species diversity 3. Vegetation abundance
1B. Index-Based Metrics	Selected spectral metrics from vegetation indices with -0.3 < r > 0.3	1. Soil properties 2. Species diversity 3. Vegetation abundance

Spectral distance (Sorenson's) computed for pairwise segments using their reflectance values was plotted against species similarity to determine the presence of any relationship (distance-decay) and assess the validity of the SVH for estimating beta diversity of transects. Distance decay describes the inverse relationship between the similarity of a pair of observations and their geographical distance. According to Nekola and White (1999), distance decay of biological similarity is an essential element of ecological theory and biodiversity conservation. The pattern of this relationship and rates of change are indicators of the presence of a determinant factor such as an underlying environmental gradient or plant dispersal habits and so on. Steinbauer *et al.* (2012) pointed out that the rate at which species similarity decreases with geographical distance provides a measure of species turnover and beta-diversity. In line with this argument, both the pattern and rates of distance decay were expected to differ between polluted and control transects due to the impact of oil pollution, and segments along polluted transects as the concentration of TPH decreased from the spill epicentre.

Spectral distance decay rates were computed for each segment using Sentinel 2A bands (2 to 8 and 8A) reflectance values in a 2 by 2-pixel window. Due to the observed impact of oil pollution on vegetation, the distance decay rates should be higher on polluted transects than on control transects. This expectation followed Morlon *et al.* (2008) assertion that the distance decay relationship is sensitive to environmental variability, spatial distribution and autocorrelation. Hence, the difference in distance decay rates of polluted and control transects is an indication of oil pollution impact on species composition of transects. The distance decay relationship was estimated from quantile regression models as described by Rocchini (2010). In Rocchini and Cade (2008), they argued that quantile regression was a more competent tool for modelling distance decay relationships for ecological data characterised by a large number of zeros. As the quantiles (percentage points) are regressed, the coefficients (intercept and decay rate) are more representative of the variability in the dataset. Cade and Noon (2003) attributed the heteroscedasticity of ecological data to complex environmental interactions that influence ecosystem components. Furthermore, quantile regression models are non-parametric; thus, they are better suited to analyse the data set used for this study. Seven quantiles (also known as the tau) ranging from 0.3 to 0.9 were used to subset the data for the quantile regression analysis. The higher taus were selected because, at lower quantiles (0.1 and 0.2), the relationship between the variables was fragile due to the high number

of zero values. The distance and similarity computations were performed on a total (N) of 210 segments, whereas the quantile regression involved the two semi-matrices derived from the previous computation. Each semi-matrix of pair-wise distance (spectral bands) or similarity (species composition) values of all 210 segments comprised (N*(N-1)/2) = 21945 elements.

Similarly, the community variability hypothesis (CVH) suggested by Schmidtlein and Fassnacht (2017) was tested by correlating the fitted values from models predicting species diversity using spectral distances and the original species diversity data. R^2 values indicate the performance of spectral distance in estimating species diversity as suggested by the community variability hypothesis. Quantile regression procedure was performed in R using the *quantreg* package developed by Koenker *et al.* (2018).

5.3 Results

5.3.1 The Relationship between Spectral Diversity Metrics and Soil Properties

Results of the correlation analysis between spectral metrics and field data revealed the environmental gradient pervading in each microhabitat (polluted and control). On polluted transects, band-based metrics significantly correlated with TPH and negatively with Phosphorus, $(r > 0.2, p < 0.05)$. Conversely, Phosphorus concentrations strongly correlated with spectral diversity metrics on control transects, while TPH showed no discernible relationship with the metrics. This result supports the earlier results discussed in Chapter 4 Section 4.3.1.1 and illustrated in Figure 4.2 (joint distribution of soil parameters) which showed a strong negative relationship between soil TPH and Phosphorus. The inference here is that the debilitating effect of oil pollution such as increased patchiness following vegetation removal controls spectral diversity on polluted transects, whereas vegetation abundance and diversity enhanced by increased concentrations of soil nutrients (phosphorus) influence spectral diversity on control transects.

The regression analysis performed on the entire dataset was in answer to the second research question (RQ2) which investigates how spectral metrics respond to oil pollution. Since the preliminary results revealed strong relationships between spectral diversity metrics and field data from polluted transects, this pattern of association was expected to

be consistent across the entire study area not just on polluted transects, thus proving that the spectral diversity metrics were sensitive to oil pollution. Results of the regression analysis in Table 5.4 revealed that the most sensitive band metrics were those derived from the green, red and near infra-red channels (Sentinel 2A bands 3, 4, and 8 respectively) while sensitive index metrics are the chlorophyll-related indices (NDVI and SAVI) and SIPI which is a stress indicator. Table 5.4 summarises the results of the regression analysis of spectral diversity metrics and soil properties. The R^2 values ranged from 0.59 to 0.99 except for the blue and ARI2 metrics. Overall, band-metrics showed more sensitivity to soil TPH than index-metrics, which may be due to the strong influence of the visible light spectrum (Red, Green and Blue) on plant photosynthetic processes.

Table 5.4: Results summary of regression of spectral diversity metrics on soil properties showing the R^2 and RSE values. Explanatory variables were spectral metrics computed from individual Sentinel 2A bands (Table 5.1) and selected vegetation indices listed in Table 5.2.

Spectral metrics from	TPH		P		Pb		TOM	
	R^2	RSE	R^2	RSE	R^2	RSE	R^2	RSE
Blue	0.13	17318	0.16	7.19	0.08	28.15	0.31	2.62
Green	**0.99**	<0.01	0.12	7.32	0.07	28.45	0.42	2.45
Red	**0.99**	<0.01	0.23	6.88	0.15	27.14	0.3	4.01
Red Edge 1	0.66	10781	0.2	6.99	0.13	27.45	**0.88**	1.1
Red Edge 2	0.7	9915	0.11	7.38	0.08	28.34	0.18	2.82
Red Edge 3	0.77	8777	0.13	7.29	0.15	27.23	0.66	1.86
NIR	0.84	7408	0.19	7.08	0.12	27.7	0.52	2.22
Red Edge 4	0.59	11319	0.12	7.35	0.11	27.74	0.41	2,42
PC of bands	0.9	5886	**0.69**	4.43	**0.48**	21.54	0.34	2.54
CCI	0.65	11055	0.6	5	0.1	29.36	0.75	1.39
NDVI	0.75	9614	0.21	6.85	0.1	29.5	0.23	2.37
REP2	0.64	11109	0.18	6.98	0.1	29.35	0.78	1.27
SAVI	0.74	9598	0.21	6.85	0.1	29.47	0.79	1.24
ARI2	0.1	17613	0.25	6.69	0.32	25.67	0.8	1.2
SIPI	0.81	8119	0.38	6.09	0.43	23.43	0.83	1.11

5.3.2 The Relationship between Spectral Metrics and Species Diversity

Median values of band-based spectral metrics from polluted transects were higher than those of the control transects. The exception were SH metrics and all metrics computed from band 8 (NIR) reflectance with higher median values in control transects (Table5.5); however, the differences were not significant. Due to the increased RGB reflectance observed on polluted transects, the larger median values of polluted metrics were

156

expected. Similarly, the decreased NIR reflectance of polluted transects may have contributed to the reduced median values of polluted metrics in comparison to control metrics.

Table 5.5: Median values of some spectral metrics computed from Sentinel 2A bands showed higher values on polluted transects. The SH metrics and all metrics computed from band 8 (NIR) reflectance (in bold) showed higher median values in control than in polluted transects although the differences were not significant.

Bands	Mean		Spectral Heterogeneity		1st Principal Component	
	Control	Polluted	Control	Polluted	Control	Polluted
2	1662.5	1678.5	**0.03**	-0.78	-0.21	-0.04
3	1516	1529	**-0.17**	-0.54	0.37	0.42
4	1357.5	1402.5	**-0.11**	-1.52	-0.27	0.19
5	1543.5	1618	**-0.39**	-2.22	-0.13	0.28
6	2217.5	2229.5	**-0.32**	-2.11	0.33	0.36
7	2455.5	2462	**0.31**	-0.43	0.36	0.38
8	**2205**	2199	**-0.18**	-3.58	**0.38**	0.37
8A	2595	2598	**-1.58**	-2.76	443	445

Correlation analysis showed linear relationships between band-based spectral diversity metrics and field measured vascular plant species diversity on both polluted transects and non-polluted transects. However, while strong and negative relationship prevailed on polluted transects; on control transects, they were mostly positive. This contradicted the expected strong and positive relationship on control transects. The results of the Spearman's Rank Correlation analysis are illustrated in Figure 5.1. Plots were charted based on the metric derivation method so as to identify the best performing metric. Each dot represents the r-value of a band metric versus the indicated species index on the X-axis. Dots in green are from control transects and those in red are from polluted transects. Labels on X-axis are a combination of index (Sm = Simpson, Sh = Shannon, Me = Menhinick's and Ch = Chao-1) and transect group (Con = Control, Pol = Polluted). The plots show that most spectral metrics correlated positively with indices on control

transects and negatively with indices on polluted transects. The strongest positive relationships (r > 0.3) on control transects were from metrics based on the mean, median and PC1 of bands whereas the strongest inverse relationships (r < -0.4) observed on polluted transects were from metrics based on the spectral heterogeneity of bands. Furthermore, the plots reveal that the best metrics were those computed from M, SD, PC1 and SH.
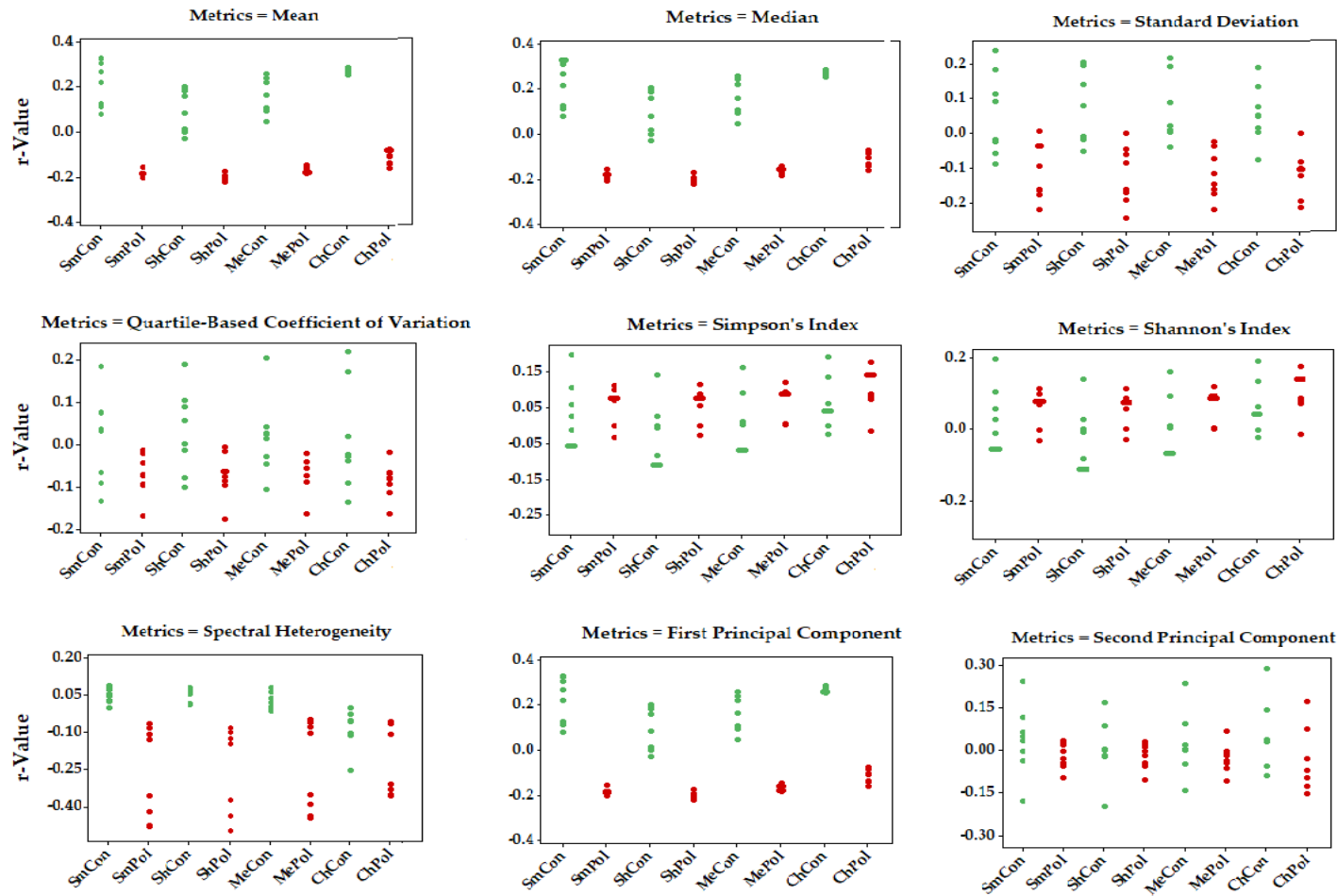
Figure 5.1: Dot plot of correlation coefficient (r) values of band-based spectral metrics and species diversity indices. The plot titles indicate the method of metric derivation. Each dot represents the r-value of a band metric versus the indicated species index on the X-axis. Dots in green are from control transects while those in red are from polluted transects. The plots show that most spectral metrics correlated positively with indices on control transects and negatively with indices on polluted transects. Labels on X-axis are a combination of index (Sm = Simpson, Sh = Shannon, Me = Menhinick's and Ch = Chao-1) and transect group (Con = Control, Pol = Polluted)

158

Results of the NPM regression analysis using derivatives of bands and indices reveal strong relationships with the field measured diversity indices (R2 values ranged from 0.19 to 0.98). The most robust relationships were found on control transects and involved metrics from both Sentinel 2A bands and vegetation indices. This strong relationship is however, seen to depreciate across the study area when analysed with data from polluted and control transects. This suggests the sensitivity of the spectral metrics to the presence of soil TPH. Overall, the Simpson's index was the most sensitive variable with R2 values greater than 0.5 for both metrics sets except those derived from SIPI (R2 = 0.3). The weakest relationships were between Chao-1 index and other spectral metrics (Figure 5.2).
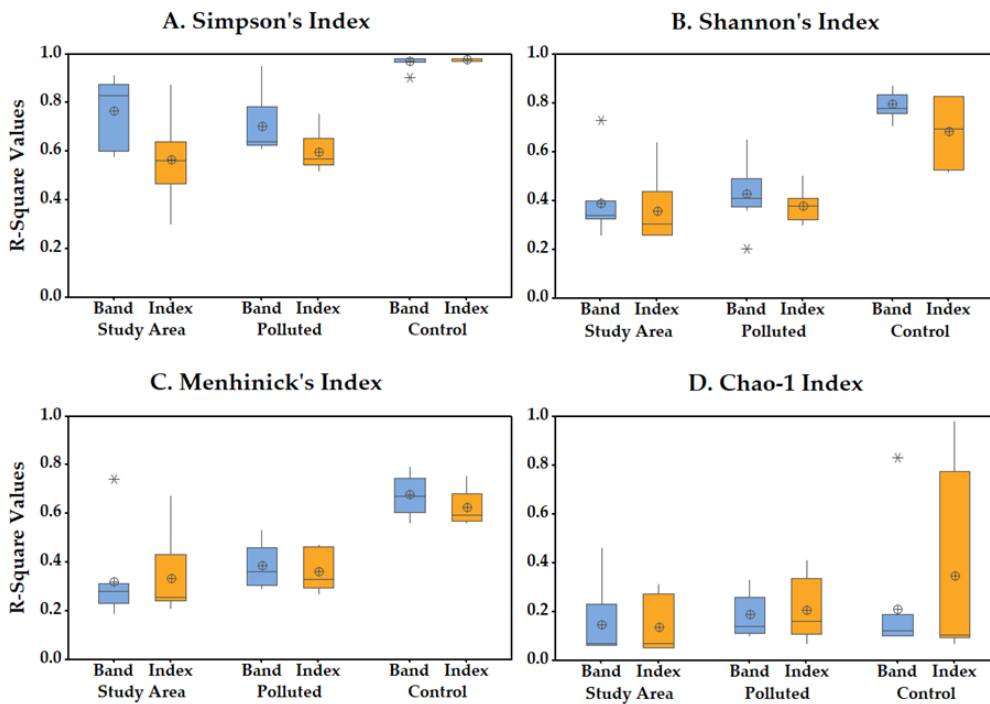
Figure 5.2: Boxplots of R-square values from regressing species diversity indices with spectral diversity metrics computed from Sentinel 2A bands and vegetation indices. Band-based metrics are coloured blue and Index-based metrics are in orange. R-square values are compared for band and index-based metrics as well as among the study area, polluted transects and control transects. The plots show that stronger relationships were present on control transects than on polluted transects which in turn influenced a general weakening of this relationship across the study area. Overall, the Simpson's index was the most sensitive variable with R-square values greater than 0.5 for both metrics sets except those derived from SIPI (R-square = 0.3).

The most robust relationships occurred between Simpson's diversity index and metrics derived from the PC of bands ($R^2 = 0.91$) across the study area, Blue band ($R^2 = 0.89$) on polluted transects and SIPI ($R^2 = 0.98$) on control transects. In contrast, the weakest relationships were observed between Chao-1 richness index and spectral metrics from NDVI ($R^2 = 0.05$) across the study area, REP2 ($R^2 = 0.07$) on polluted transects and CCI ($R^2 = 0.07$) on control transects. Spectral metrics derived from the PC of bands

consistently exhibited a strong relationship with all the field diversity indices with R^2 values well over 0.5 except for Chao-1 index. Both Shannon's and Menhinick's indices associated strongly with the transformed band metrics (PC of bands) and chlorophyll-based index (CCI) whereas Chao-1 richness index did not.

In terms of metrics performance, it appears that band-based metrics were more sensitive to diversity indices than the index-based metrics across the study area. However, when analysed separately, index-based metrics performed better on control transects whereas band-based metrics were better on polluted transects. The boxplots in Figure 5.3 shows
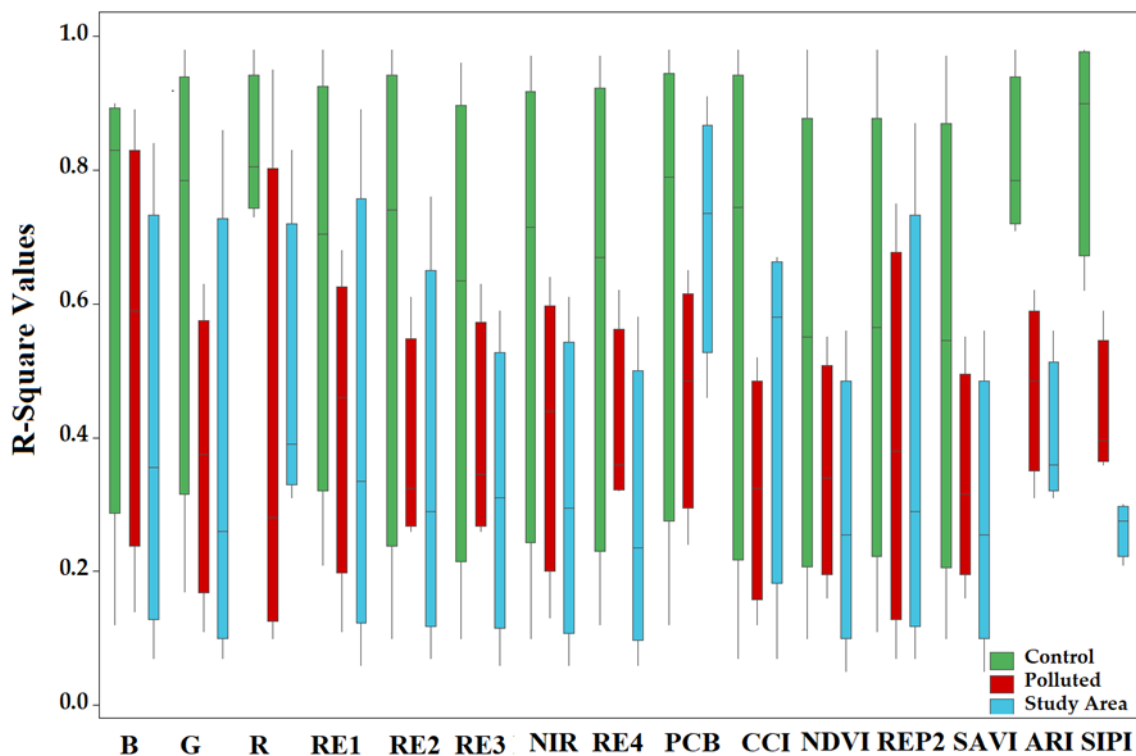
Figure 5.3: Boxplots of R^2 values illustrating the performance of metrics from individual bands and vegetation indices on polluted and control transects and across the entire study area. The plots show that the metrics were sensitive to the presence of TPH in the soil as strong relationships observed on control transects were weakened across the study area. The x-axis band labels are B = Blue, G = Green, R = Red, RE1 = Red Edge 1; RE2 = Red Edge 2; RE3 = Red Edge 3; NIR = Near Infrared; RE4 = Red Edge 4; PCB = Principal Components of Bands.

that that the various spectral metrics performed better on control transects than on polluted transects. It appears that the metrics derived from stress indicating VIs (ARI and SIPI) were most sensitive to the presence of soil TPH.

5.3.3 Distance Decay Relationship on Transects

The results of the distance decay modelling of the relationship between spectral distance and species similarity on transects are summarised in Table 5.6. The spectral distance was computed from Sorenson's index using the *vegdist* function of the R-package *vegan*.

Table 5.6: Quantile regression results of distance decay models of Sentinel 2A bands versus vascular plants species similarity values on polluted and control transects.

Transects	Quantiles (Taus τ)	Intercept	Intercept CI (95%) Lower	Intercept CI (95%) Upper	Decay Rate	Decay Rate CI (95%) Lower	Decay Rate CI (95%) Upper
Polluted	0.3	0.06	0.058	0.062	-0.08	-0.087	-0.073
N = 16900	0.4	0.08	0.077	0.083	-0.13	-0.141	-0.119
DF=16898	0.5	0.11	0.106	0.114	**-0.21**	-0.224	-0.196
	0.6	0.16	0.146	0.154	**-0.31**	-0.304	-0.276
	0.7	0.22	0.186	0.194	**-0.47**	-0.426	-0.394
	0.8	0.27	0.254	0.266	-0.61	-0.600	-0.560
	0.9	0.41	0.36	0.38	-0.99	-0.929	-0.851
Control	0.3	0.12	0.118	0.122	-0.1	-0.112	-0.088
N = 6400	0.4	0.14	0.137	0.143	-0.14	-0.152	-0.128
DF = 6398	0.5	0.16	0.157	0.163	-0.17	-0.183	-0.157
	0.6	0.18	0.175	0.185	-0.22	-0.236	-0.204
	0.7	0.22	0.210	0.230	-0.32	-0.349	-0.291
	0.8	0.37	0.345	0.395	**-0.77**	-0.846	-0.694
	0.9	0.58	0.560	0.600	**-1.3**	-1.378	-1.222

Species similarity inversely related to spectral distance on polluted and control transects; however, contrary to expectations, the rate of distance decay was generally higher on control transects than on polluted transects. At each tau (τ), the intercept (species similarity when distance = 0) was higher for control transects than for polluted transect while the rate of decay (decrease in species similarity by 1 unit increase in spectral distance) varied at different τ for each group of transects. For instance, at τ = 0.5, 0.6 and 0.7, distance decay rates were higher on polluted transects whereas they were higher on control transects at the rest of the quantiles (τ = 0.3, 0.4, 0.5, 0.8 and 0.9). An analysis of deviance results testing for differences in the regression estimates across quantiles revealed significant differences (F = 543.1 and 219.66 respectively for polluted and control transects, $p < 0.05$). Additionally, a test of the regression coefficients of transects using the two sample T-test showed that decay rates on both polluted and control transects were not significantly different (T-value = -0.31, DF = 10, p = 0.765). In like manner, intercept values (species similarity when distance = 0) were not significantly different for polluted and control transects (T-value = 1.04, DF = 10, p = 0.32).

Maximum similarity values predicted for polluted transects at the 0.9 quantile was 0.37 while on control transects it was 0.58. Furthermore, the 95% confidence intervals show that these values were significantly different. The quantile regression plots in Figure 5.4 reveal the pattern of the relationship between spectral distance and species similarity. The scatterplots (Figure 5.4 A1 and B1) clearly show that on polluted transects, several segments had much lower compositional similarity than control transects
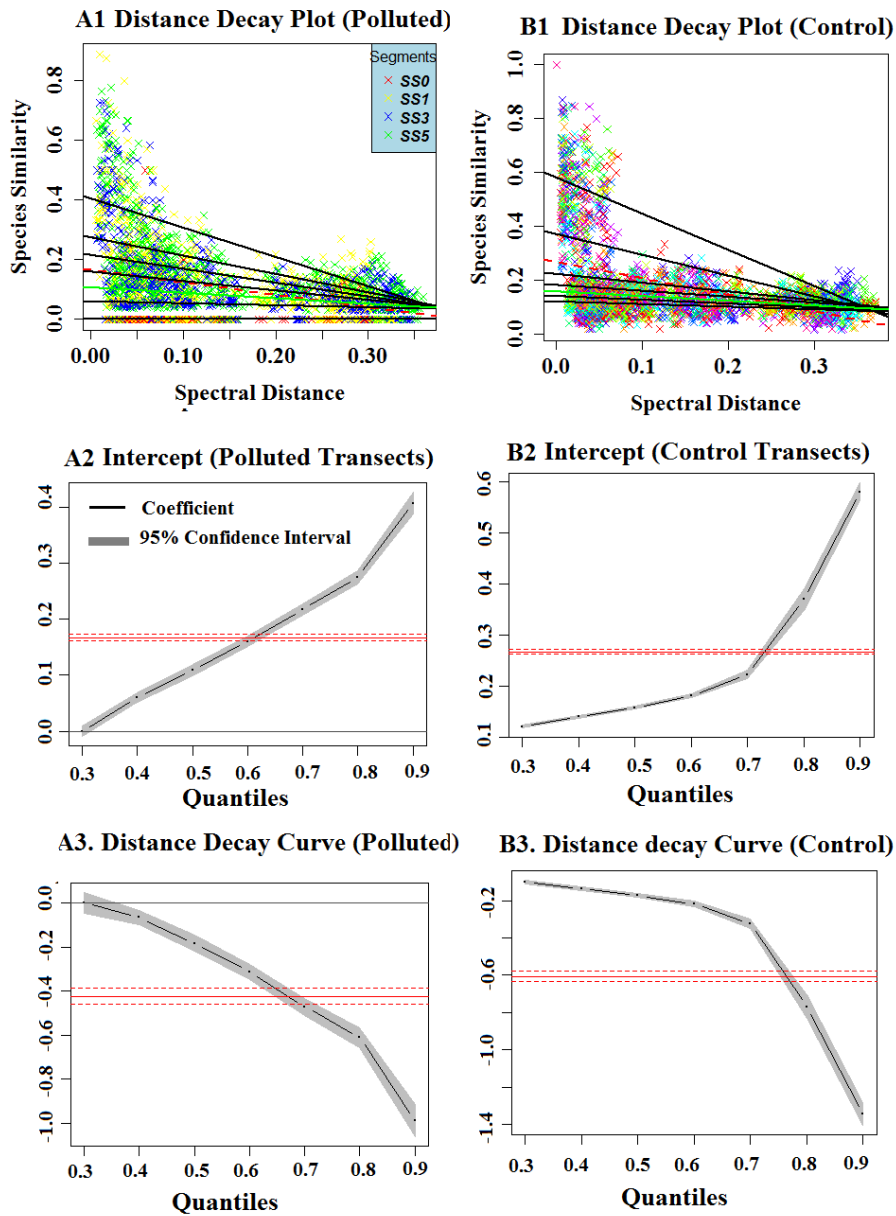
Figure 5.4: Quantile regression plots of A: polluted and B: control transects. A1 and B1 are scatterplots of spectral distance versus species similarity using different regression models. Red dashed line is computed from ordinary least square regression, solid green line from quantile regression at tau = 0.5 (median) while the solid black lines are quantile regression at six different taus (τ = 0.3, 0.4, 0.6, 0.7, 0.8, 0.9). The points within the scatterplot represent pair-wise spectral

distances and species similarity distances between 210 segments. Figures A2 and B2 are the intercepts while A3 and B3 are the distance decay curves.

At spectral distance = 0 (intercept, Figures 5.4 A2 and B2), species similarity values were much higher at all quantiles on control transects than on polluted transects, however, as spectral distance increased, similarity values decreased. From the distance decay curves (Figures 5.4 A3 and B3), it appears the rate of decay on polluted transects was relatively constant for all quantiles, however on control transects, the rate of decay initially lower than polluted transect suddenly increases after $\tau = 0.7$ (the steepness of the curve increases significantly after $\tau = 0.7$). Low R^2 values obtained from correlating species distance and predicted values from the spectral distance model did not agree with the community variability hypothesis. However, the models appeared to perform better on control transects ($R^2 = 0.17$) than on polluted transects ($R^2 = 0.12$).

5.3.4 Estimating Soil Properties using Spectral Metrics

Soil properties including TPH, P, Pb and TOM were estimated from the spectral metrics using non-parametric models. Two model types (Table 5.3) based on band metrics and index metrics as predictors were used and compared for their accuracy. The selected metrics regressed linearly with soil properties in both models; however, the index-based metrics outperformed the band-based metrics in estimating soil properties. Furthermore, TPH and phosphorus were better estimated than Lead and TOM. The R^2 values for the test data were 0.35 and 0.31 respectively for TPH and phosphorus estimated using band metrics whereas, R^2 values were 0.45 and 0.62 respectively for TPH and phosphorus estimated using index metrics. Result of the regression analysis are summarised in table 5.7.

Table 5.7: : Performance summary of models estimating soil properties using spectral diversity metrics computed from Sentinel 2A bands and vegetation indices. The combined dataset from polluted and control transects (N = 210) were employed in this analysis. The dataset was subdivided into training (n = 150) and test (n = 60) data. Explanatory variables (EV) for each model was a combination of all band-based or index-based metrics which showed a strong correlation (r > ±0.2) with the response variables.

Response Variable	Parameter	Band Metrics	Index Metrics
$Log_{10}TPH$	No. of EV	13	22
	R^2 (Train)	0.5	0.8
	R^2 (Test)	0.35	**0.45**
	F	30.76*	47.09*
	RMSE	0.79	0.72
	PSE	0.62	0.51
Phosphorus	No. of EV	9	22
	R^2 (Train)	0.49	0.702
	R^2 (Test)	0.31	**0.62**
	F	26.18*	93.99*
	RMSE	6.92	5.04
	PSE	47.86	25.4
Lead	No. of EV	8	21
	R^2 (Train)	0.36	0.54
	R^2 (Test)	0.1	**0.11**
	F	2.35ns	7.19*
	RMSE	24.95	29.24
	PSE	622.57	855.2
TOM	No. of EV	5	25
	R^2 (Train)	0.26	0.82
	R^2 (Test)	0.06	**0.07**
	F	3.74ns	4.79*
	RMSE	3.83	3.79
	PSE	14.63	14.38

The residual graphs in figure 5.5 demonstrate that the models for estimating Lead and TOM were not good fits for the dataset despite the high R^2 values obtained from calibrating the model with training data.
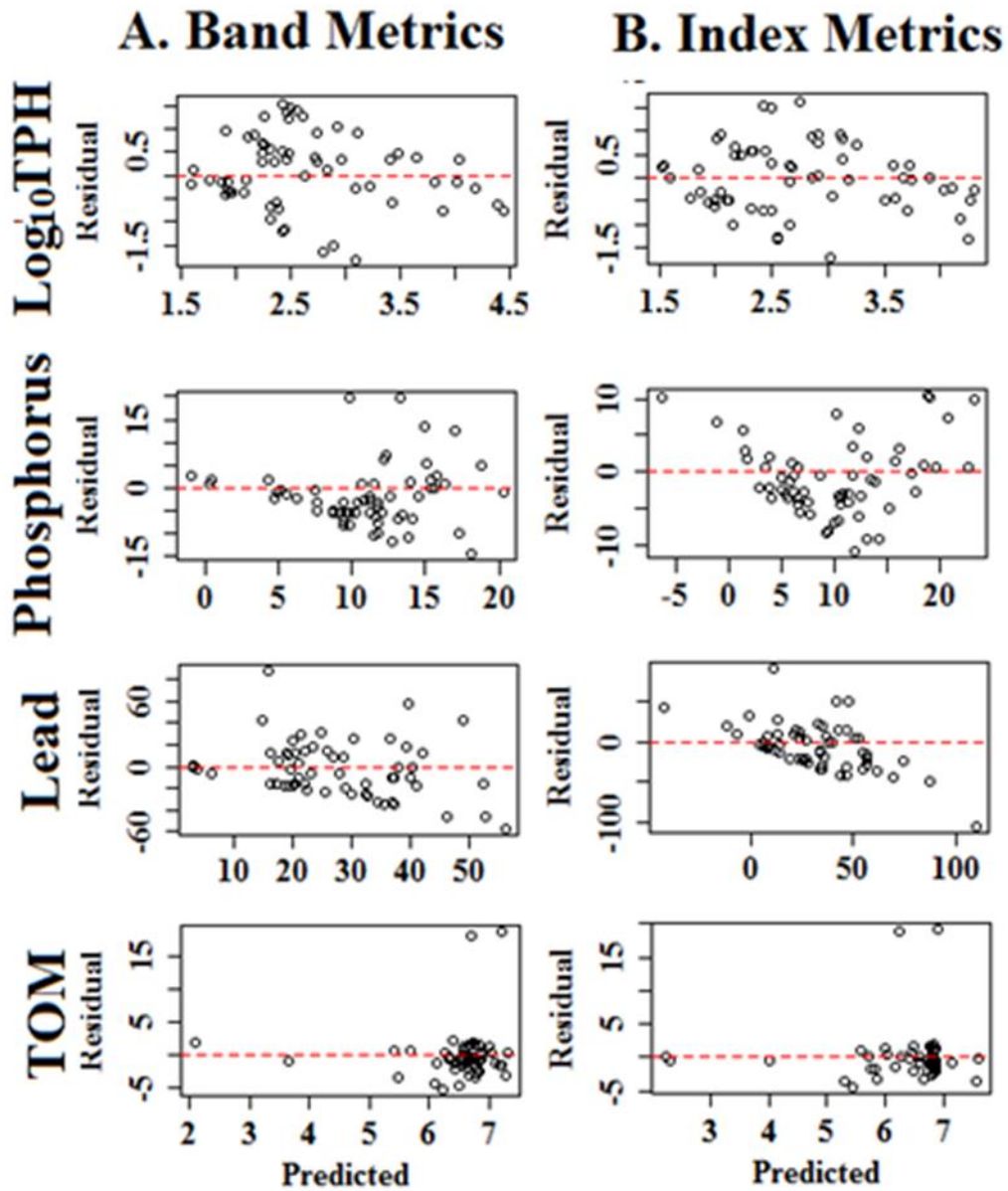
Figure 5.5: Graphical plots of residuals from model validation using test data. Model parameters are from the regression of spectral diversity metrics (A = band metrics and B = index metrics) on soil properties using test data (n = 60). The residual plots from band-based models estimating TPH, phosphorus and Lead meet the goodness-of-fit assumptions of linearity, randomness and homoscedasticity. For the index-based models, only the TPH residual plot met the assumptions.

5.3.5 Estimating Species Diversity Using Spectral Metrics

The SVH was tested using the spectral metrics that strongly correlated with the diversity measures ($r > \pm 0.2$) and a VIF < 10. The results in Table 5.8 show the R^2 values of training data and adjusted R^2 values test data, RMSE and PSE of validation data sets for both models.

Table 5.8: Performance summary of models estimating species richness and diversity using spectral diversity metrics computed from Sentinel 2A bands and vegetation indices. The combined dataset from polluted and control transects (N = 210) were employed in this analysis. The dataset was subdivided into training (n = 150) and test (n = 60) data. Explanatory variables (EV) for each model was a combination of all band-based or index-based metrics which showed a strong correlation ($r > \pm 0.2$) with the response variables.

Response variable	Parameter	Band Metrics	Index Metrics
Simpson's	No of EV	9	11
	R^2 (Train)	0.82	0.63
	Adj. R^2 (Test)	**0.49**	0.32
	F	54.84*	28.35*
	RMSE	0.05	0.25
	PSE	0.002	0.06
Shannon's	No of EV	8	6
	R^2 (Train)	0.36	0.41
	R^2 (Test)	0.18	**0.29**
	F	12.81*	22.82*
	RMSE	0.68	0.63
	PSE	0.47	0.4
Menhinick's	No of EV	7	6
	R^2 (Train)	0.29	0.57
	R^2 (Test)	0.19	**0.31**
	F	14.26*	27.12*
	RMSE	1.11	1.03
	PSE	1.23	1.07
Log$_{10}$Chao-1	No of EV	5	10
	R^2 (Train)	0.41	0.32
	R^2 (Test)	0.02	0.07
	F	1.04ns	4.13*
	RMSE	0.45	0.42
	PSE	0.2	0.18

The results demonstrate that both sets of metrics performed well during model calibration with training data, but underperformed at model validation. For instance, among diversity indices, Simpson's index is the most predictable with higher R^2 values (0.82) obtained from calibrating models with band-based metrics and $R^2 = 0.63$ obtained from model calibration with index metrics. However, at validation, the adjusted R-square values were less than 0.5 for both sets of metrics, band-based metrics (Adj.$R^2 = 0.49$) and index-based

metrics (Adj.R^2 = 0.32). For this index, band-based metrics were better estimators. Similar patterns were observed for Shannon's and Menhinick's indices with reduced Adj.R^2 values, although, index-based metrics outperformed band-based metrics as estimators of these indices. The least performing models were those that estimated the Chao-1 index. Despite high R^2 values at calibration, the models did not perform well at validation (results show no relationship among the variables). Graphical plots of residuals from model validation using test data are shown in Figure 7. Model parameters are from regression of spectral diversity metrics (A = band metrics and B = index metrics) on species diversity indices using test data (n = 60).
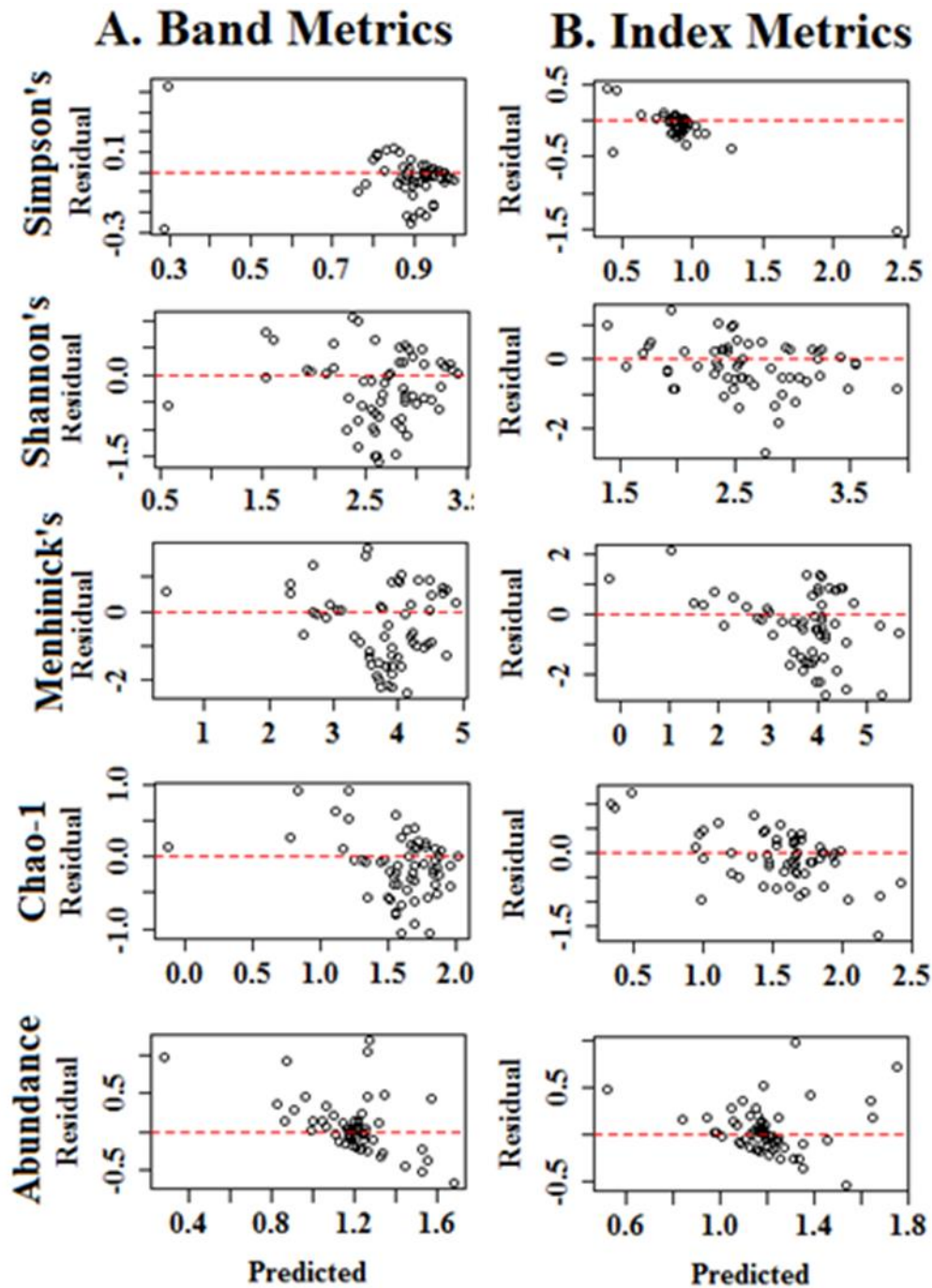
Figure 5.6: Graphical plots of residuals from model validation using test data. Model parameters are from the regression of spectral diversity metrics (A = band metrics and B = index metrics) on species diversity indices using test data (n = 60). The residual plots from both band and index-based metrics meet the goodness-of-fit assumptions of linearity, randomness and homoscedasticity except for abundance.

5.4 Discussion

The concept of the spectral variability hypothesis as proposed by Palmer (2002) provides ecologists with an essential tool for biodiversity monitoring and conservation in the Niger Delta region, without the need for labour intensive and time-consuming field work (Heumann, Hackett and Monfils, 2015). Understanding and modelling the relationship between spectral diversity metrics and local species richness or diversity measures provide decision makers with preliminary information on conservation priorities, particularly in cases were indicator species co-occur with rare or threatened species (cross-taxon surrogacy, (Rocchini, Hernández-Stefanoni and He, 2015). Spectral variation hypothesis has been used severally to estimate species diversity and distribution in different landscapes and ecosystems. Hall *et al.* (2012) reported that the area of the site might influence spectral variation of large sites; however, this phenomenon is not expected to occur within similar sized sample sites, as is the case in this study. The relationship between spectral variables and species diversity are usually weak with R^2 values ranging from 0.2 to 0.6 (Hall *et al.* 2012), however the present study reveals that a combination of various derivatives of spectral bands strongly associate with field data. Rocchini, Hernández-Stefanoni and He (2015) stated that R^2 values of up to 0.5 could be considered valid to estimate species diversity from spectral variation, thus, providing an integrated and efficient method for monitoring vascular plant species diversity at a regional and global scale.

5.4.1 Spectral Diversity Metrics for Estimating TPH in the Soil

Environmental transformations have a significant effect on species diversity at both local and large scales. In the Niger Delta, oil exploration activities including forest fragmentation for pipelines, fire occurrence and flooding that occur following oil pollution have a bearing on the diversity of vascular plant species of the region. Newbold *et al.* (2015) and Paz-Kagan *et al.* (2017) reported that land use changes affected both alpha and beta diversity at the regional scale because they alter the environment and induce loss of biodiversity and ecosystem services.

The combination of the metrics to estimate soil properties was successful for TPH and phosphorus. A clear pattern of decreasing spectral diversity with increasing TPH concentrations signifies that oil pollution reduced species diversity, which in turn

decreased the spectral diversity of the location. This pattern was most evident for metrics derived from the green and red bands as well as from chlorophyll related indices. The sensitivity of these metrics to the presence of soil TPH is attributable to the known deleterious effects of oil pollution on vegetation. Studies investigating this phenomenon (Ogbo, Zibigha and Odogu, 2009; Chima and Vure, 2014; Njoku, Akinola and Oboh, 2008; Wang, Zhu and Tam, 2014a; Naidoo and Naidoo, 2018) reported that hydrocarbons in the soil hinder uptake of plant nutrients, damage plant cellular structures, inhibit photosynthesis and transpiration as well as cause plant mortality (please see Chapter 4 Section 4.4.3 for discussion on the effects of oil pollution on vegetation).

Furthermore, Zhu *et al.* (2013); Noomen *et al.* (2009); Li, Ustin and Lay (2005) documented that oil pollution induced stress in vegetation and changes in leaf pigments and structure. Vegetation stress is characterised by decreased absorption of solar radiation at chlorophyll absorption maxima (around 600 nm) and increased absorption of anthocyanins (AnC) and carotenoids (CaR). Leaf chlorophyll content measured in the field using the SPAD-502 chlorophyll meter showed significant differences between polluted and control vegetation. Mean chlorophyll concentration was 39.01 and 55.19 respectively on polluted and control transects. Merzlyak *et al.* (2008) reported increased AnC occurrence in vegetation subjected to stress. These changes affect plant growth and health; quality and quantity of photosynthetic pigments, mainly chlorophyll; thickness of leaves and overall plant productivity, thereby increasing the variability of reflectance in the green channel (Warren *et al.* 2014), as well as in the red channel since maximum chlorophyll absorption occurs at the red band (Noomen, Van der Meer and Skidmore, 2005). Spectral diversity metrics from chlorophyll related indices were also seen to associate strongly with soil TPH concentration. Adamu, Tansey and Ogutu (2018) affirmed that these indices were sensitive to changes in leaf chlorophyll content and internal structures and were able to discriminate polluted sites from non-polluted sites. The superior predictive performance of index-based metrics may be attributed to the enhanced spectral information vegetation indices provide. Vegetation indices are designed to maximise information from green vegetation while suppressing reflectance from other sources such soil and water, unlike band reflectance that consist of optical properties of vegetation and surrounding material (Zhu *et al.* 2013). The results of the present study imply that TPH presence in the soil can be detected and the approximate

concentration estimated from spectral metrics without incurring additional costs of soil sample collection and chemical analysis.

The relationship observed between the spectral distance, and species similarity provides evidence of the impact of oil pollution on vegetation in the Niger Delta region of Nigeria. Species similarity was much lower on polluted transects than on control transects, thus fulfilling the competitive exclusion principle of niche theory which states that two species with identical niches cannot coexist in the same habitat (Abrams, 1983). This phenomenon is particularly apparent at spill epicentres (SS0) of different locations where very few species remained; hence, most of the pair-wise similarity values were zero for this segment. The implication is that even for species resilient to the direct effects of oil pollution such as *Perotis indica* (Perindh), which can tolerate TPH concentrations of up to 60,000 mg/kg of soil (please see Chapter 4 Section 4.3.2.5), increased competition for diminished resources presents a threat to their existence. The increased TPH concentration on polluted transects appeared to have triggered some form of resource partitioning among extant species as their importance value index (IVI, a measure of species frequency and abundance) on polluted and control transects were not significantly different. The scatterplot of IVI values (Figure 4.11) revealed that the most valuable species were almost equally important on both transects. Resource partitioning is an ecological concept that refers to the differential use of limited resources by similar species (Griffin and Silliman, 2011). Vascular plant species growing on polluted transects may have differed in their nutrient uptake, rooting depth or light use, for instance, Kahmen *et al.* (2006) reported that plants could differ in the forms of nitrogen they prefer.

Regression of species similarity at upper quantiles of spectral distances demonstrates the presence of an environmental factor that influenced species composition and richness on different segments. Unlike at lower quantiles where the regression line is nearly flat, suggesting a lack of relationship, the gradient of the regression line at upper quantiles (0.7 to 0.9) was steeper (Figure 5.4 A1) and depicted the expected inverse relationship between spectral distance and species similarity (distance decay). Although it is difficult to identify the environment variables influencing species composition in the study area from spectral distances, the input of field data of soil TPH concentrations support the conclusion that oil pollution is one of the most influencing environmental factors. This conclusion is supported by higher decay rates of species similarity observed on polluted

transects compared to control transects. Tovo and Favretti (2018) recently suggested that steeper curves symbolise the presence of rare species in sampled sites

5.4.2 Spectral Diversity Metrics for Estimating Species Richness and Diversity

Spectral diversity metrics correlated inversely with field measured vascular plant species diversity on polluted transects and positively on control transects. The coefficient of variation (CV) for metrics of polluted transects were larger than CV of metrics of control transects, and suggest that polluted pixels were more diverse than control pixels, but it is also a reflection of the higher beta diversity of polluted transects as observed earlier in Chapter 4, Section 4.3.3.3. In this case, the spectral metrics do not depict vascular plant species diversity but rather the heterogeneity of investigated transects. The reason for this is not far-fetched since oil pollution accentuated habitat heterogeneity by creating patches where TPH susceptible species used to grow. Additionally, the weak positive correlation between the individual spectral metrics and species diversity indices of control transects is ascribable to the homogeneity of segments of control transects in terms of species composition and distribution patterns. Since the SVH relies on habitat heterogeneity, it follows that its application is limited in densely vegetated forests with little or no disturbance.

Despite the observed aberrations, a combination of spectral diversity metrics successfully estimated the species richness and diversity of investigated locations with high R^2 values obtained between the observed and predicted index values. The result was consistent with previous studies testing the SVH such as Warren *et al.* (2014); Hall *et al.* (2012); Rocchini, Hernández-Stefanoni and He (2015); Schmidtlein and Fassnacht (2017). As observed with soil TPH estimation, index-based metrics outperformed band-based metrics in estimating species richness and diversity indices of investigated transects. The stronger association between spectral metrics and species diversity indices was more apparent on polluted transects than on control transects. Perhaps, the above emanates from the increased heterogeneity of polluted transects induced by oil pollution and evident in the higher beta diversity values obtained for polluted locations. However, variability in the species composition of the different locations (beta diversity) did not provide a better association with spectral diversity than the alpha diversity measures of segments. Hence, the community variability hypothesis (CVH) suggested by Schmidtlein

and Fassnacht (2017) involving the use of beta diversity values instead of species count did not improve the performance of the SVH.

The use of spectral distance as a metric to determine beta-diversity of transects yielded exciting results. Several studies reviewed in Rocchini, Hernández-Stefanoni and He (2015) demonstrated that spectral distances are more reliable for summarising the beta-diversity of sites as it takes into account the habitat heterogeneity. Despite the low R^2 values between the two variables (spectral distance and beta-diversity), the results revealed that the spectral distance better explained species composition on control transects than on polluted transects. The reason may be ascribable to the issue of scale, as noted by Palmer *et al.* (2002), the relationship between spectral variation and species richness is scale dependent. Regardless of spatial scale, distance decay plots of species dissimilarity versus spectral distance showed that beta-diversity increased with increasing spectral distance at all scales (control, polluted and study area). This result is consistent with other studies reported in Rocchini, Hernández-Stefanoni and He (2015).

5.5 Summary

This chapter investigated the spectral variation hypothesis t's potential for detecting oil pollution effects on vegetation characteristics species diversity using spectral diversity metrics derived satellite data. Metrics computed using Sentinel 2A bands and vegetation indices proved sensitive to changes in soil properties and vegetation characteristics following oil pollution. The strength of the relationship resulted in successfully estimating species richness and diversity values of investigated transects. Also, spectral metrics displayed high potential for estimating the concentration of total petroleum hydrocarbon (TPH) in the soil. Chapter 6 will focus the investigation on a subset of the study area and utilises a hyperspectral data set to develop models for predicting species diversity on polluted transects.

6 Species Diversity Models for Monitoring Biodiversity

(*Two articles from Chapter 6 were published in a remote sensing journal 'Remote Sensing Special Issue' and presented at a remote sensing conference in 'IGARSS 2018'.*)

The third research questions (RQ3) addressed in chapter 5 identified the nature of relationships among oil pollution, species diversity and vegetation reflectance. Having established in Chapter 4 the effect of oil pollution on vegetation abundance and diversity, this chapter investigates how strongly and in which wavelengths the changes in vegetation parameters and species composition influenced reflectance from the polluted transects. Accomplishing this task required spectral metrics created from Hyperion wavelengths, which were used to answer research questions RQ3 and RQ4, (section 2.10.1)

The Hyperion image analysed in this chapter helped to determine the impact of oil pollution on vegetation, species richness and diversity. Spectral signatures of vegetation from polluted and control transects revealed the Hyperion wavelengths that responded to the presence of TPH in the soil. These sensitive wavelengths produced indices that measured vegetation vigour of polluted and control transects. Moreover, the application of the continuum removal procedure on spectra of polluted and control vegetation generated the band depths of chlorophyll absorption features. Background soil effect on vegetation reflectance was removed by computing the red edge position using different methods and extracting the REP values for each segment on polluted and control transects. Regression models determined the capability of derived spectral metrics to discriminate polluted from unpolluted sites and to predict various diversity indices of vegetation on investigated transects. The statistical procedures performed on datasets are discussed in Chapter 3 Section 3.5.1.

6.1 Hyperspectral Remote Sensing of Biodiversity

The application of remote sensing technology in biodiversity monitoring has been an area of considerable research in the recent past, for instance (Johnson, Hay and Rogers, 1998; Nagendra, 2001; Carlson *et al.* 2007). Several studies have combined remote sensing and field data to determine the spatial and temporal distributions of biodiversity (Wilfong, Gorchov and Henry, 2009; Foody and Cutler, 2003). Motivated by the need to devise a

standardised methodology for monitoring biodiversity at regional and global scales and to overcome some limitations of conventional monitoring methods such as *in situ* field surveys; researchers have developed integrated methods using remote sensing and field data (Yoccoz, Nichols and Boulinier, 2001; Kerr and Ostrovsky, 2003; Muchoney, 2008; Lindenmayer and Likens, 2010; Han *et al.* 2014). The Group on Earth Observations Biodiversity Observation Network (GEO BON) have spearheaded these efforts leading to the development of the essential biodiversity variables (EBVs).

Although there are inherent challenges associated with integrated schemes, studies (Clevers *et al.* 2002; Andrew, Wulder and Nelson, 2014; Guyon *et al.* 2011), confirm that they provide useful information on the response of biodiversity to natural and anthropogenic changes. While some studies investigated the link between spectral diversity and species diversity through the biochemical diversity of vegetation (Asner *et al.* 2008), others used land cover classifications derived from multispectral sensors such as Landsat to estimate the species diversity of the area of interest (Gould, 2000). Critics of the land cover approach describe it as inadequate for collecting fine-scale detail of vegetation structure and chemistry due to the coarse spectral and spatial resolution (Carlson *et al.* 2007; Gould, 2000) of multispectral sensors.

Generally, mapping of species diversity estimates are empirically supported by defining the relationship between variation in spectral signal and variation in species or habitat diversity (Rocchini, Hernández-Stefanoni and He, 2015; Aneece, Epstein and Lerdau, 2017; Foody and Ajay Mathur, 2004; Wilfong, Gorchov and Henry, 2009) and in some cases, variations in pigment concentrations (Féret and Asner, 2014; Asner and Martin, 2011; Asner *et al.* 2009). However, this procedure may not be enough if the Aichi 2020 targets are achievable. There is a need to develop methodologies that estimate species diversity against the backdrop of environmental pressures such as oil pollution. Such methods will not only reveal the state of the ecosystem following impact (for instance, biodiversity change) but also reveal ecosystem resilience to particular external pressure.

Hyperspectral data not only measure vegetation biochemical and biophysical properties including water content, leaf pigments, nitrogen, cellulose and lignin concentrations (Guyon *et al.* 2011; Zhang, 2010; Curran, 1989; Jacquemoud *et al.* 1996), but also how these parameters vary across the ecosystem (Carlson *et al.* 2007; Asner *et al.* 2009). The Hyperion sensor onboard NASA's Earth Observation-1 satellite is an example of a

hyperspectral satellite mission (Ortenberg, 2012). It was the first satellite hyperspectral sensor launched onboard the Earth Orbiter-1 platform by the United States National Aeronautics and Space Administration (NASA) New Millennium Program (NMP).

The Hyperion acquire 16 bits, 30 meters spatially resolved data in 220 discrete narrow-bands between the spectral range of 400 and 2500 nm. The sensor capture about 75 times more data than multispectral sensors from a similar area, hence providing a large volume of data that need advanced analytical skills and techniques (Kuenzer *et al.* 2014). As oil pollution induces stress in vegetation, invokes changes in leaf pigments and structure (Wang, Zhu and Tam, 2014b; Noomen and Skidmore, 2009; Li, Ustin and Lay, 2005; Baker, 1970); these changes affect the spectral pattern of reflectance from different plant species. Hyperion data is reliable for detecting this subtle variation in reflectance. Arellano *et al.* (2015) used Hyperion data to map vegetation in the Amazon impacted by oil pollution. Other studies utilised Hyperion imagery for classification of vegetation/forests types and landscape (Yang *et al.* 2016; Deák *et al.* 2017; Friedel *et al.* 2018). Although the Hyperion sensor is decommissioned, other space-borne imaging spectrometers such as the Hyperspectral Environment and Resource Observer (HERO) and Environmental Mapping and Analysis Program (EnMAP) will provide needed data for similar applications.

Investigating the effect of oil pollution on vegetation using Hyperion data followed two strategies. The first strategy was the identification of wavelengths sensitive to TPH concentration in the soil and second was the comparison of reflectance at these wavelengths for significant differences between polluted and control transects. Sensitivity analysis differentiated between plant stress caused by TPH concentration in the soil and other factors while also correcting for irradiance, leaf orientation, irradiance angle and shading (Carter, 1993). Due to the strong association between polluted and control transects as shown in Chapter 4 section 4.2.2.1, and the congruity of geomorphological and ecological processes on both transects (Abam, 2001; Ugochukwu and Ertel, 2008; Adegbehin and Nwaigbo, 1990; Osuji, Adesiyan and Obute, 2004); any significant reflectance difference between the polluted and control transects is attributable to soil TPH.

6.2 Hyperion Data Analysis

This section presents the specific tools, procedures and dataset employed in investigating the research questions addressed in this chapter.

6.2.1 Narrowband Vegetation Indices (NBVIs)

Vegetation indices derived from the spectral reflectance of plants are discussed in Chapter 2 Section 2.8, but this chapter involved narrowband vegetation indices (NBVIs) derived from Hyperion data. Several studies applied NBVIs to determine the structure, biochemical, biophysical and physiological or stress status of vegetation in various habitats (Pu, Bell and English, 2015; Arellano *et al.* 2015; Galvao *et al.* 2009; Hestir *et al.* 2008; Vaiphasa *et al.* 2007). The main parameters measured by NBVIs include

   a. Chlorophyll Content: - used to monitor changes in green biomass, chlorophyll content and leaf structure. High values indicate increased chlorophyll content, green biomass and vegetation vigour and

   b. Primary Productivity: measure changes in the photosynthetic light use efficiency of plants. High values indicate reduced light use efficiency, hence reduced productivity.

NBVIs overcome the saturation problem associated with broadband vegetation indices such as NDVI (Mutanga and Skidmore, 2004). The NBVIs and NDVI evaluated in this paper are listed in Table 6.1. The indices were computed and index values extracted for each segment in polluted and control transects.

Table 6.1: Summary of selected vegetation indices used to investigate the impact of oil pollution on biodiversity.

Index	Formula	Reference
Red-Edge NDVI (RENDVI)	$(R_{750}-R_{705})/(R_{750}+R_{705})$	(Gitelson and Merzlyak, 1996)
Modified Red-Edge NDVI (MRENDVI)	$(R_{750}-R_{705})/(R_{750}+R_{705}-2*R_{445})$	(Datt, 1999)
Modified Red-Edge Simple Ratio Index (MRESRI)	$(R_{750}-R_{445})/(R_{705}+R_{445})$	(Sims and Gamon, 2002)
Vogelmann Red Edge Index 1 (VREI1)	R_{740}/R_{720}	(Vogelmann, Rock and Moss, 1993)
NDVI	NIR – Red/NIR + Red	(Pearson, R. L. and Miller, 1972)
Photochemical Reflectance Index (PRI)	$(R_{531}-R_{570})/(R_{531}+R_{570})$	(Gamon, Serrano and Surfus, 1997)
Structure Insensitive Pigment Index (SIPI)	$(R_{800}-R_{445})/(R_{800}+R_{445})$	(Peñuelas, Filella and Gamon, 1995)

6.2.2 Derivation of TPH-Induced Stress-Sensitive Wavelengths

Sensitivity analysis is a mathematical procedure, which determines how changes in levels of an independent variable affect changes in levels of a response variable (Alam *et al.* 2016). The particular wavelength of the response variable (vegetation reflectance, in this study) showing the most substantial relative change due to changes in levels of the independent variable (soil TPH) is considered the most sensitive wavelength (Cacuci, Ionescu-Bujor and Navon, 2005). According to Alam *et al.* (2016), this procedure is necessary to evaluate the influence of variables and rank their significance based on their influence. Sensitivity analysis for both polluted and control vegetation assumed that environmental and edaphic conditions are homogenous and that polluted vegetation would be more stressed than control vegetation due to the influence of TPH in the soil.

Vegetation response to soil TPH, expected to influence spectral reflectance formed the basis for identifying sensitive wavelengths (Jinru Xue and Baofeng Su, 2017). The sensitivity of vegetation reflectance spectrum to soil TPH was also necessary to differentiate between the plant stress caused by TPH concentration in the soil and other edaphic factors while also correcting for irradiance, leaf orientation, irradiance angle and shading (Carter, 1994).

Since vegetation reflectance at the visible and near infrared (VNIR) channels generally increases with plant stress (Li, Ustin and Lay, 2005; Mishra *et al.* 2012), sensitivity bands to TPH-induced stress in vegetation for VNIR Hyperion wavelengths was computed by firstly subtracting the reflectance of control vegetation (non-stressed) from that of polluted (stressed vegetation). The resulting difference was normalised by further dividing by the reflectance of the non-stressed vegetation to establish the sensitivity of each wavelength to soil TPH (Carter, 1994). The formulae for computing the reflectance difference and sensitivity are as follows:

$$R_\Delta = Ru - Rn, \tag{10}$$

$$Rs = (Ru - Rn)/Rn, \tag{11}$$

Where

Rn is reflectance of non-stressed vegetation
Ru is reflectance of stressed vegetation
R_Δ is reflectance difference
Rs is reflectance sensitivity.

Following the sensitivity analysis, the VNIR Hyperion wavelengths were ranked based on their sensitivity to soil TPH. The most sensitive wavelengths ranked at the top of the order were those with the highest sensitivity values and high reflectance difference values, while the least sensitive bands with sensitivity values closer to zero ranked at the bottom. The five most sensitive and five least sensitive wavelengths were selected and used in creating the normalised difference vegetation vigour index (NDVVI). These wavelengths were selected and combined to create an index with maximum sensitivity to vegetation response to soil TPH because an index performance is improved when it is created from created sensitive and insensitive wavelengths (Eigemeier *et al.* 2012). Besides, vegetation sensitivity to soil TPH appeared to be limited to specific wavelengths in the blue, red and NIR channels; hence, the NDVVI variants created from these channels investigated the full range of oil pollution impact on vegetation.

6.2.3 The Normalised Difference Vegetation Vigour Index (NDVVI)

Vegetation vigour defined as active, healthy, well-balanced and robust growth of plants (Merriam-Webster Dictionary, 2017) is an essential environmental quality index (Melillo *et al.* 1993). Enhanced growth, extent as well as increased productivity characterise vigorous vegetation (Reynolds *et al.* 2016). Several studies on vegetation link the index to climate change (Melillo *et al.* 1993); soil erosion (Vrieling, 2006); and biological conservation (Lindenmayer, Margules and Botkin, 2000). Some organisations such as (the United States Environment Protection Agency, (USEPA), 2012; OECD, 2006) recommend the use of vegetation vigour index in tests to evaluate the effect of chemical substances such as pesticides on the growth of various plant species.

In this study, vegetation vigour is a touchstone of vegetation productivity and biomass production in line with previous publications such as (Cardinale *et al.* 2012; David U Hooper *et al.* 2012; Cardinale *et al.* 2011; Vihervaara *et al.* 2014; Mace, Norris and Fitter, 2012; Norris, 2012; Waide *et al.* 1999; Chapin *et al.* 2000; Xu *et al.* 2012; Pearlman *et al.* 2001; Cadotte, Cardinale and Oakley, 2008; Balvanera *et al.* 2006; Tilman, 1996; Naeem *et al.* 1994; Hector *et al.* 1999), which revealed strong relationship between these parameters and vascular plant species diversity. Tillman *et al.* (1996) as well as (Naeem *et al.* 1994; Hector *et al.* 1999; Hooper *et al.* 2005), found a positive relationship between

plant species diversity and plant productivity (measured as above ground biomass) which they attributed to several factors including the complementarity of resource use.

More recently, determination of vegetation vigour has been from remotely sensed images using proxy vegetation indices such as the normalised difference vegetation index (NDVI) and net primary productivity (NPP) (Xu *et al.* 2012; Hector, 1998; Maselli, 2004; Salinas-Zavala, Douglas and Diaz, 2002). Other studies have used vegetation cover as an indicator of vegetation vigour and established a positive linear relationship between both variables (Karthikeyan, Shashikkumar and Ramanamurthy, 2010; Munyati and Ratshibvumo, 2011; Wiesmair, Otte and Waldhardt, 2017). With advancement in earth observation technology in the way of increasing spectral and spatial resolutions, researchers have exploited these relationships with concerted effort to identify individual species and estimate species diversity of a given area using spectral metrics derived from satellite imagery(Nagendra, 2001; Wulder, 1998; Rocchini *et al.* 2016; Boyd and Danson, 2005; Warren *et al.* 2014; Galidaki and Gitas, 2015; Lucas *et al.* 2015).

In this section, a new vegetation vigour index was created to measure precisely the response of vegetation to the presence of TPH in the soil, and compare how the response differs on polluted and control transects. The index referred to as the normalised difference vegetation vigour index (NDVVI) computed for each segment by normalising reflectance difference at the least and most sensitive Hyperion wavelengths used the formula

$$NDVVI = (R_i - R_j) / (R_i + R_j), \tag{12}$$

Where
R_i = reflectance at the least sensitive wavelength
R_j = reflectance at the most sensitive wavelength

The most sensitive wavelengths were those that exhibited a large difference in reflectance between polluted and control transects while the least sensitive wavelengths were those whose reflectance values hardly changed in the presence of TPH. Wavelengths of the NIR channel showed the least sensitivity to TPH consistent with previous studies, which revealed that average NIR reflectance, did not vary much between healthy leaves and stressed leaves. (Carter and Miller, 1994; Lichtenthaler, 1996). Figure 6.2A shows smaller difference between NIR reflectance of polluted and control transects compared

to the reflectance at the visible range. With near constant reflectance at these NIR wavelengths, the index relies on reflectance at the most sensitive wavelengths, which occurred in the blue and red channels. Thus, NDVVI value is zero when reflectance at either the red or the blue channel is high and 1 when reflectance at these channels is low. The inclusion of the least sensitive wavelengths in creating the NDVVI corrects for reflectance from non-vegetated areas (such as bare soils and buildings, which show high reflectance at the NIR region). Eigemeier (2012) stated that maximising the performance of a vegetation index requires the inclusion in the algorithm, sensitive and insensitive bands to the monitored variable. Six NDVVI variants were created combining the five most sensitive and least sensitive Hyperion wavelengths. These were $NDVVI_{814,437}$, $NDVVI_{824,427}$, $NDVVI_{844,447}$, $NDVVI_{752,630}$, $NDVVI_{773,641}$, and $NDVVI_{844,630}$.

6.2.4 Continuum Removal and Band Depth Analysis

The depth of the wavelengths where radiance absorption by chlorophyll is maximal was using the continuum removal procedure. Continuum removal involves the normalisation of spectra by applying a convex hull made up of line segments over the top of the spectrum, which connect the local maxima in the spectrum portion of interest (Kokaly and Clark, 1999; Mutanga, Skidmore and Prins, 2004). The reflectance at wavelengths of selected absorption features was divided by the reflectance value of the convex hull at that wavelength to give a unit-less absorption value for chlorophyll ranging from 0 (complete absorption) to 1 (no absorption) (Clark and Roush, 1984; Mutanga, Skidmore and Prins, 2004). Removing the continuum from original spectra enhances the detection of subtle spectral shifts, eliminate soil background and sloping effects (topography), minimises the influence of atmospheric and water absorptions, and provide more precise information on the spectral intensity and band depth (Mutanga and Skidmore, 2004; Yan *et al.* 2010). Several authors have used these absorption features to retrieve plant biochemical and biophysical parameters including chlorophyll, lignin, nitrogen content (Curran, Dungan and Peterson, 2001; Kokaly *et al.* 2003; Mutanga, Skidmore and Prins, 2004).

Continuum removal was used in this study primarily to determine the changes that occurred in the chlorophyll absorption features of vegetation on investigated transects. Since oil pollution induces stress in vegetation (Wang, Zhu and Tam, 2014b; Noomen and Skidmore, 2009; Li, Ustin and Lay, 2005; Baker, 1970), it is expected that changes

in reflectance will occur in vegetation growing on impacted sites. Carter (1993) and Lichtenhaler (1996) reported increased reflectance in chlorophyll and water absorption regions of the spectrum in stressed vegetation. Therefore, an in-depth analysis of the spectra at these absorption wavelengths is necessary to highlight the impact of oil pollution. Although several parameters such as band depth, band position, the full width of the absorption at half the band depth (FWHM) are derivable from the continuum removal process, only the band depth was considered relevant in the present study.

Chlorophyll absorption is known to occur mainly at 430 nm and 460 nm in the blue region as well as 640 nm and 660 nm in the red region of visible spectrum. Selection of the edges of these absorption features for the continuum removal procedure captured the range of spectral characteristics of the vegetation reflectance. Hence, all the Hyperion wavelengths between 400 nm to 550 nm and between 550 nm to 750 nm were subjected to the procedure performed in ENVI 5.3 and transferred to MS Excel for further computations. The band depth of the absorption features was firstly calculated by subtracting the continuum removed reflectance (R′) value from 1 and then normalised following the methods of Kokaly and Clark (1999). Normalising the band depths was used to minimise the influence of non-foliar factors such as atmospheric absorption on the reflectance. The formula for calculating the band depth (D) and normalised band depth (D_{norm}) are as follows

$$D = 1 - R'$$ (13)

$$D_{norm} = D/D_{max}$$ (14)

Where:
R′ is the continuum removed reflectance value
D_{max} is the maximum band depth for the absorption feature.
D_{norm} is normalised reflectance.

6.2.5 The Red Edge Position (REP) of Reflectance Spectra

Red-edge position (REP) index derived from the reflectance spectra of each segment on both the polluted and control transects was developed to overcome the challenges associated with the normalised difference vegetation index (NDVI) which saturates easily in dense vegetation (Gitelson *et al.* 2002; Clevers *et al.* 2002). The red edge is a slope of the abrupt transition between the red and near infrared (NIR) wavelengths of a vegetation spectrum. The slope which occupies a range of wavelengths usually between 670 nm and

780nm (Kanke *et al.* 2012) is subjected to some mathematical manipulations to derive the red edge position (REP). Several methods are used to determine REP, however, in this study, the linear interpolation method as defined by (Clevers *et al.* 2002; Clevers and Büker, 1991) and the maximum first derivative procedure (Savitzky and Golay, 1964) were utilised. Previous researchers successfully detected REP in vegetation spectra (For instance, Chen, Elvidge and Jansen, 1993; Jong and Meer, 2006; Shafr, Salleh and Ghiyamat, 2006), by applying these procedures. However, Gholizadeh et al. (2016) assessed various REP extraction techniques for estimating chlorophyll and LAI (leaf area index) using data from different sensors. Their results confirmed the superiority of REP derived from the linear interpolation method also known as the four point linear interpolation method over the other methods tested.

There are numerous studies employing REP index in investigating plant biochemistry, health, and stress (Kanke *et al.* 2012; Adamczyk and Osberger, 2015; Tian *et al.* 2011; Jong and Meer, 2006; Peñuelas and Filella, 1998). These studies mostly controlled in experimental fields or laboratories may have limited success in field applications. The present study utilises field data integrated with remote sensing information to evaluate changes in the red edge position of oil-polluted vegetation. Peñuelas, Filella and Gamon (1995) and Tian *et al.* (2011) both found the REP strongly correlated with the chlorophyll content of vegetation canopy. Jong and Meer (2006) reported that chlorophyll content; leaf structure and leaf area index influenced the REP, which exhibited greater sensitivity at increased chlorophyll content.

Earlier studies established a linear relationship between ecosystem productivity and species diversity (Vihervaara *et al.* 2014; Mace, Norris and Fitter, 2012; Norris, 2012; Waide *et al.* 1999; Chapin *et al.* 2000). Some researchers ascribe this relationship to the presence of complementary species, which maximise available resources, particularly the photosynthetic active radiation (PAR) (Hooper *et al.* 2005; Sapijanskas *et al.* 2014). Perring *et al.* (2015) observed that the productivity of a restored woodland in southwestern Australia increased with greater species number. Kanke *et al.* (2012) reported that REP correlated highly with SPAD meter readings.

The following methods derived REP index

1. **The maximum slope of the first derivative (REPder)**

$$REP = \max\left(\frac{\partial y}{\partial x}\right) \qquad (15)$$

$$\frac{\partial y}{\partial x} = \frac{R_{a+1} - R_a}{\lambda_{a+1} - \lambda_a} \qquad (16)$$

Where

R_a is reflectance at λ_a
R_{a+1} is reflectance at λ_{a+1}
λ_a is wavelength at the start of the slope segment
λ_{a+1} is wavelength at the end of the slope segment

2. **Linear interpolation method:- (REPlnr)**

$$R_{red\ edge} = R_{670} + R_{780}/2 \qquad (17)$$

$$REP = 700 + 400\left[\frac{R_{red\ edge} - R_{700}}{R_{740} - R_{700}}\right] \qquad (18)$$

Reflectance at the REP derived from the two techniques mentioned above were extracted for each segment on polluted and control transects and compared for significant differences and to determine their response to TPH concentration in the soil. Furthermore, the indices were regressed with field data (soil TPH, chlorophyll readings taken from the SPAD meter as well as with vegetation abundance) to determine the pattern and strength of any relationships among the variables. For each model, the dependent variable was either REPder or REPlnr while the independent variables were soil TPH concentrations, SPAD chlorophyll data, vegetation frequency and abundance. The regression coefficients were used to determine the nature of the relationship between the dependent and independent variables, while the coefficient of determination (R^2) was used to determine the strength of the relationship. Furthermore, REP indices were tested for their ability to correctly classify transects as polluted or control using non-parametric logistic regression analysis in R. This was done to assess the potential of REP indices to detect oil pollution when it occurs. For this analysis, the dependent variable soil TPH concentration was categorised into polluted (pol) and control (con), while the independent variables were the spectral indices REPder and REPlnr

6.2.6 Statistical Analysis

The answer to the main research questions RQ2, RQ3 and RQ4 mentioned earlier involved testing the three hypotheses which follow

1. That there is a difference between the reflectance of vegetation growing on polluted and control transects;
2. There is a strong linear relationship between spectral metrics derived from Hyperion data and field measured diversity indices;
3. That the relationship can be modelled to predict richness and diversity of vascular plant species in the Niger Delta region of Nigeria.

Hyperspectral metrics derived from Hyperion data were subjected to statistical analysis discussed in Chapter 3 including Mann-Whitney Test (Section 3.4.1.1) and Non-Parametric Regression (NPM, Section 3.5.1.3). the 8 different models developed from these metrics and shown in Table 6.2 were tested.

Table 6.2: Characteristics of the models predicting of diversity indices, chlorophyll content and vegetation abundance using spectral metrics computed from Hyperion data.

Model ID	Regression Method	Predictors	Response Variables
1A	Partial Least Squares (PLS)	NDVVIs	Simpson's
1B	,,	NBVIs	Shannon's
2A	Non-Parametric Multivariate Regression (NPMR)	NDVVIs	Menhinick's
2B	,,	NBVIs	Chao-1
3A	Non Parametric Univariate Regression (NPUR)	REPder	Chlorophyll
3B	,,	REPlnr	Content
3C	Non-Parametric Logistic Regression (NPLR)	REPder	Abundance
3D	,,	REPlnr	

The Spearman's rank correlation coefficients (r), coefficients of determination (R-squared), residuals, biases and error values from all models were compared to identify the set or subset of spectral metrics best suited for species diversity estimation in a polluted field.

The implementation of the best performing NDVVI-based model featured the extraction of spectral values of random pixels termed 'predsites' from the NDVVI images ($NDVVI_{752,630}$, $NDVVI_{814,437}$, $NDVVI_{824,427}$, $NDVVI_{773,641}$, $NDVVI_{844,447}$, $NDVVI_{844,630}$), using the Raster and GISTools packages in R (Figure 6.1). Thirty pixels selected to encompass all the visible land cover types (waterbody, swamp, farmland, mixed vegetation and forested) within the location made up in the dataset (preddata). The

decision to select pixels from within this location (Kporghor) is because of its polluted nature according to several reports of oil spills at sites across the area in the past (UNEP, 2011). However, soil TPH concentrations are expected to be lower in the predsites than at polluted transects; consequently, higher species diversity values were anticipated from implementing the selected model.
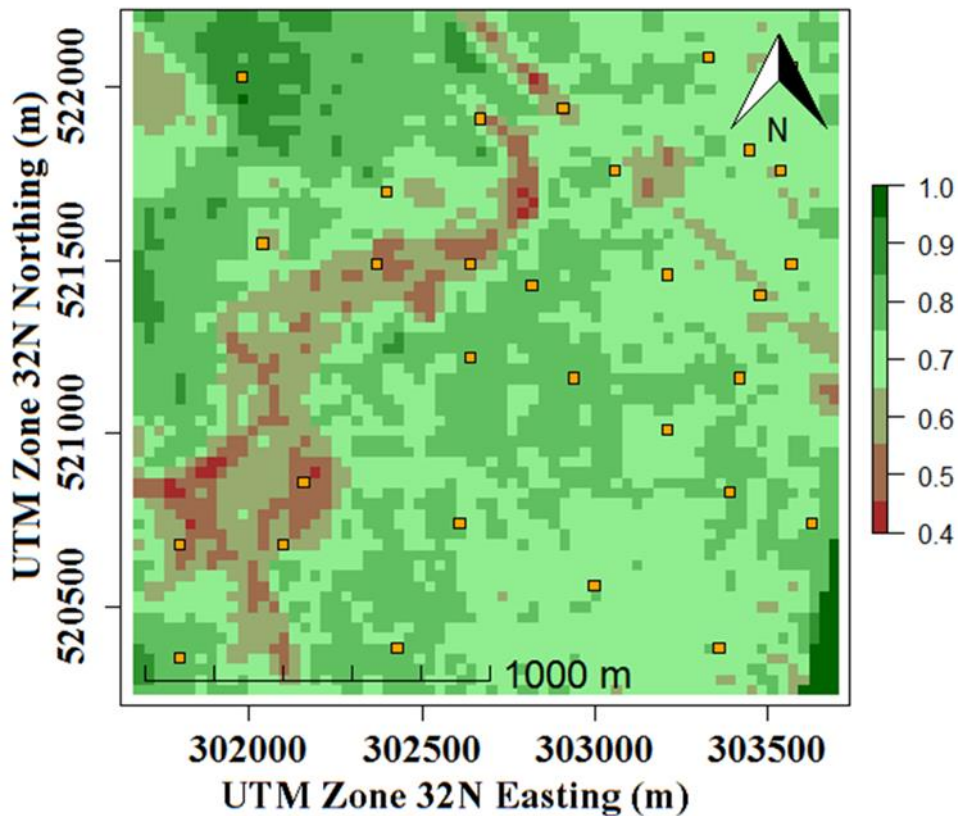
Figure 6.1: Map of NDVVI$_{814,437}$ for Kporghor displaying the locations of the randomly selected pixels (predsites) used for evaluating the regression model. Shannon's, Simpson's, Menhinick's and Chao-1 diversity indices were estimated for the predsites using the NDVVI variants.

Each diversity index (Shannon's, Simpson's, Menhinick's and Chao1 index) was estimated separately for the predsites. Due to the absence of field data for the predsites, estimation accuracy was determined by correlating fitted values with corresponding NDVI values computed from a Landsat 8 and Sentinel-2A images of the study area. NDVI was selected because it is a well-known index commonly used to quantify vegetation performance in terms of growth and biomass (Huete, 1994; Gamon et al, 1995). The index has been applied in several studies as a surrogate for measuring species diversity (Gould, 2000; de Bello *et al*, 2010; Parviainen, Luoto and Heikkinen, 2010). Since vegetation productivity increases with species diversity (Cardinale *et al.* 2012; Hooper *et al.* 2012; Cardinale *et al.* 2011; Vihervaara *et al.* 2014; Mace, Norris and Fitter, 2012; Norris, 2012; Waide *et al.* 1999; Chapin *et al.* 2000; Xu *et al.* 2012), it is presumed

that the NDVI values will strongly correlate with the diversity estimates of the 'predsites'. The choice of a different sensor to calculate the NDVI was to minimise bias from using an NDVI image calculated from Hyperion data. Both the Landsat 8 and Sentinel 2A images were downloaded from the USGS earth explorer tool, and the vegetation index computed using ENVI 5.3. Please see sections 3.4.1 and 3.4.3 for the description of Sentinel 2A and Landsat multispectral images respectively). Additionally, the accuracy of predictions was visually evaluated using very high-resolution imagery from digital globe freely available in Google Earth (GE, hereafter). Some researchers utilised the GE images as a visualisation tool for land use and land cover maps (Hu *et al.* 2013; Yu and Gong, 2012; Kaimaris *et al.* 2011).

6.3 Results

6.3.1 Correlation of Hyperion Bands with Soil TPH

Because of the non-normality of the spectral metrics dataset, Spearman's rank correlation analysis was performed to determine the relationship between the Hyperion bands and the levels of total petroleum hydrocarbon (TPH) in the soil. The results of this analysis are presented in Table 6.3. Generally, the VNIR bands (426.82 nm - 721.9 nm) positively correlated with soil-TPH contrary to the negative relationship observed between the SWIR bands (1971.76 nm -2052.45 nm) and soil TPH. This result agrees with previous investigations which revealed that petroleum hydrocarbon in the soil increases stress in vegetation and this stress is evident in increased reflectance in the VNIR and shift of the red-edge towards the shorter wavelengths. A few of the highly correlating wavelengths also showed high sensitivity to soil-TPH levels and were utilised in developing the new vegetation index suggested for monitoring biodiversity in the Niger Delta region.

Table 6.3: Results of the correlation analysis to determine Hyperion bands that strongly correlated with soil TPH. All values are significant at $p < 0.05$

Wavelength (nm)	Hyperion Band Number	Spearman's Rank Correlation Coefficient
426.82	8	0.683
518.39	17	0.645
620.15	27	0.537
711.72	36	0.584
813.48	46	0.427
912.45	77	0.458
983.08	84	0.355
1537.92	139	0.397
1638.81	149	0.427
1749.79	160	0.345
1971.76	182	-0.474

6.3.2 Analysis of TPH-induced Stress-Sensitive Wavelengths

The maximum, mean and minimum reflectance of the polluted and control transects is shown in Figure 6.2. Reflectance in the visible and NIR regions was high and low respectively on polluted transects while the reverse was the case on control transects. The greatest reflectance difference between the control and polluted transects occurred at the wavelength range 420 nm - 470 nm (blue channels) and 620 nm - 670 nm (red channels, Table 6.4). Reflectance at these wavelengths increased significantly ($p < 0.05$) on the polluted transects which due to the TPH in the soil. As chlorophyll absorption is highest at the wavelengths of 430 nm, 460 nm, 640 nm, and 660 nm (Noomen and Skidmore, 2009), the spectral absorption from chlorophyll in plants was adversely affected by oil pollution.

Table 6.4: Wavelengths with maximum and minimum differences in reflectance and those least and most sensitive to TPH-induced stress.

Wavelength (nm) at Maximum Difference	436.99	447.17	630.32	426.8	650
Bands	9	10	28	8	30
Difference	195.96	170.87	123.1	122.48	102.25
Wavelength (nm) at Minimum Difference	844	813.48	752.43	823.65	732
Bands	49	46	40	47	38
Difference	1.79	3.49	3.67	4.11	6.22
Stress-Sensitive Wavelengths (nm)	447.17	436.99	426.8	630.32	640.5
Bands	10	9	8	28	29
Sensitivity	0.77	0.68	0.48	0.19	0.16
Stress-Insensitive Wavelength (nm)	844	813.48	823.65	752.43	772.78
Bands	49	46	47	40	42
Sensitivity	0.00087	0.0018	0.002	0.002	0.0034

Median reflectance in the visible wavelengths is shown in the boxplots in Figure 6.2 B. They differ significantly ($p < 0.05$) between the polluted and control transects according to the M-W test (Table 6.5).

Results of the sensitivity analysis indicate that reflectances at 440±10 nm (blue channels) and 640±10 nm (red channels) substantially increased ($p < 0.05$) in the presence of soil TPH. Conversely, at the wavelength range of 670 nm - 900 nm (NIR), the reflectance of the polluted transects decreased slightly but was not significantly different from the NIR reflectance of the control transects. Minimum reflectance difference (near zero difference) occurred at 730 nm – 830 nm (Figure 6.2 C). The highest reflectance sensitivity to soil TPH (Figure 6.2 D) was observed at wavelengths 440±10 nm (blue channels) and 640±10 nm (red channels). The least sensitive wavelengths are 730-790 nm (bands 38-44), 800-850 nm (bands 45-49) and 910-990 nm (bands 77 to 85).
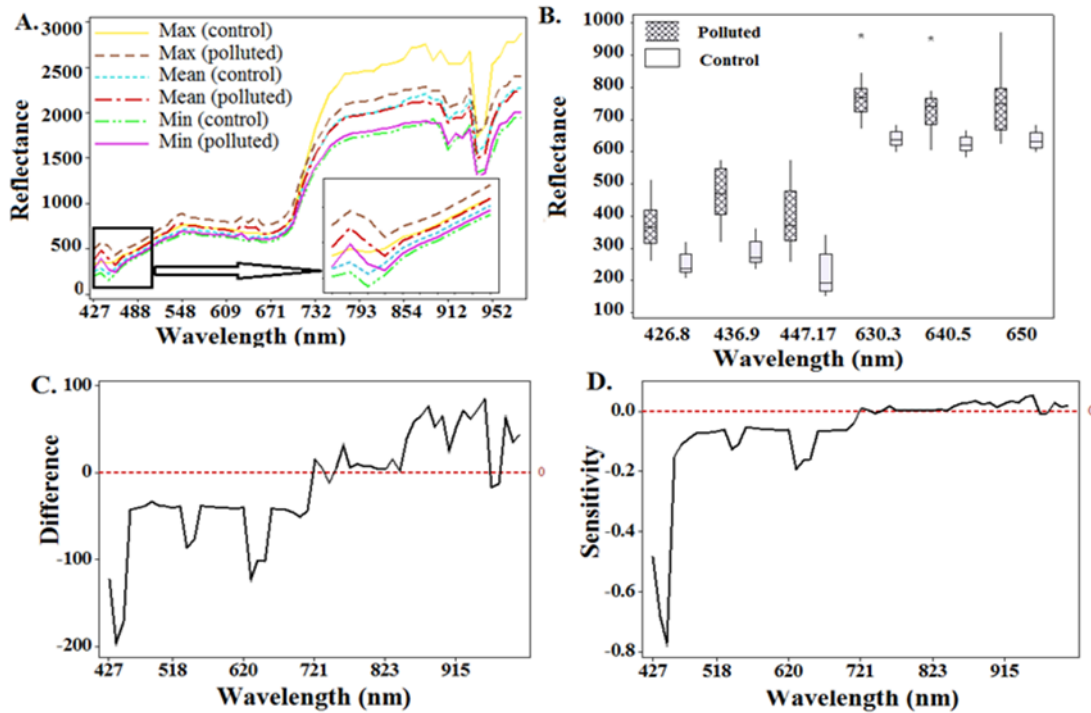
Figure 6.2 A: Reflectance of control (C) transects, (n=16) and polluted (P) transects (n=17) in Kporghor spill site measured in November 2015 by the Hyperion EO-1 sensor. The plots displayed are the maximum, mean and minimum reflectance of vegetation on transects at the VNIR region. B: Comparison of median reflectance of specific wavelengths that were observed to be sensitive to soil TPH concentration. Boxplots are for polluted and control transects. C: Reflectance difference of vegetation growing on polluted and control transects computed by subtracting the mean reflectance of vegetation on polluted transects (n=17) from that of control vegetation (n=16); D. Reflectance sensitivity to stress or relative change in reflectance computed by dividing the reflectance difference (Figure 2C) by the mean reflectance of the control transects. M-W test results show that the reflectance at the most sensitive wavelengths significantly differed between the polluted and control transects.

The M-W results in Table 6.5 reveal that blue and red reflectance from control vegetation is significantly lower than from polluted vegetation ($p < 0.05$). Vegetation reflectance at 426.8 nm (chlorophyll absorption feature in the blue range) is significantly lower ($p < 0.05$) for the control than for the polluted transects. Reflectance in the NIR wavelengths did not differ significantly between control and polluted transects and is attributable to the presence of TPH in polluted transects. Earlier studies reported that oil-contaminated substrates exhibit increased NIR reflectance attributed to the thickness of the crude oil (Clark *et al.* 2010; Kokaly *et al.* 2013). Although hydrocarbon absorption features occur in the 1730 - 2310 nm wavelengths in the SWIR region (Kühn, Oppermann and Hörig, 2004), in the NIR region the absorption from oil is decreased substantially leading to increased reflectance (Clark *et al.* 2010). With the increased NIR reflectance from both polluted and control vegetation, the characteristics of reflectance in the visible range differentiated between polluted and non-polluted vegetation.

190

Table 6.5: Summary of the Mann-Whitney U test results comparing the median reflectance of specified wavelengths from polluted and control transects. P < 0.05

Wavelength (nm)	Polluted (n1)	Control (n2)	Difference (n1-n2)	Confidence Interval (95%)		U
	N=17	N=16		Lower Limit	Upper Limit	
426.8	372.43	238.83	118.56	75.47	164.8	406
436.99	453.35	270.36	175.62	134.52	237.25	421
447.17	384.9	193.6	164.2	110.1	219.4	407
630.32	771.87	637.31	124.82	91.36	154.47	420
640.5	749.8	620.81	115.71	83.26	140.94	402
650	772.42	633.57	114.28	59.6	154.48	396

6.3.3 Analysis of the Normalised Difference Vegetation Vigour Index (NDVVI)

NDVVI was computed for all the segments in the polluted and control transects. Figure 6.3 shows the resulting images. The index values ranged from 0 to 1 with higher values shown in light grey and lower values in dark grey colours. High NDVVI values indicate increasing chlorophyll absorption at the blue or red wavelength which may be attributed to species composition, abundance and health on transects while low NDVVI values indicate the reverse.
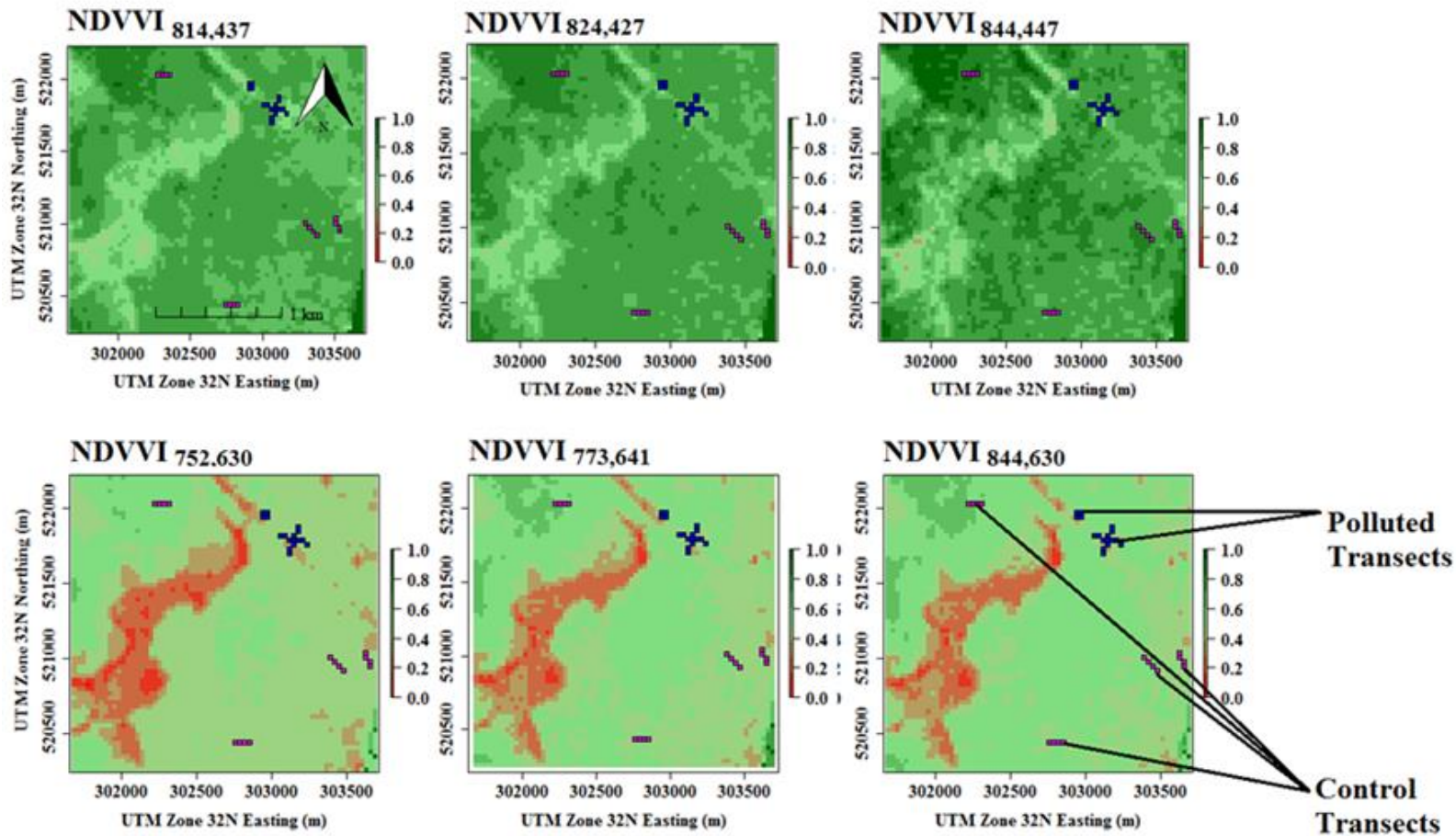
Figure 6.3: Images of reflectance ratios of vegetation at Kporghor spill site. The general formula applied was Bi (least sensitive band) - Bj (most sensitive band) / (Bi+Bj). High values (dark green) represent increased chlorophyll absorption at the blue and red wavelengths while low values (red) indicate increased reflectance at those wavelengths. The increased reflectance at these wavelengths signifies TPH-induced stress. Thus, the index is a measure of vegetation vigour and health.

The M-W test was applied to NDVVI values extracted from segments of polluted and control transects to test for differences between them. Results revealed significant differences between the median NDVVI for the polluted and control transects ($p < 0.05$). The NDVVI variants exhibited a strong correlation with field diversity measurements including Shannon's and Menhinick's as well as soil TPH (albeit inversely, Table 6.6). The variants also compared significantly better than traditional narrowband vegetation indices (NBVIs, Table 6.1). $NDVVI_{773,641}$ had the most robust relationship with the diversity indices but the weakest inverse relationship with soil TPH.

Table 6.6: Spearman's Rank Correlation Coefficients of NDVVI values extracted from polluted and control transects and field measured diversity indices in Kporghor location. $P < 0.05$.

Index	Shannon's	Menhinick's	Simpson's	Chao-1	TPH
$NDVVI_{752,630}$	0.65*	0.62*	0.65*	0.66*	-0.54*
$NDVVI_{773,641}$	**0.73***	**0.7***	**0.72***	**0.79***	-0.53*
$NDVVI_{814,437}$	0.72*	0.69*	0.67*	0.67*	**-0.69***
$NDVVI_{824,427}$	0.66*	0.64*	0.62*	0.59*	-0.63*
$NDVVI_{844,447}$	0.64*	0.64*	0.6*	0.58*	-0.68*
$NDVVI_{844,630}$	0.65*	0.61*	0.65*	0.66*	-0.53*
RENDVI	0.26 ns	0.3 ns	0.33 ns	0.32 ns	-0.11 ns
MRENDVI	0.17 ns	0.22 ns	0.21 ns	0.15 ns	-0.44**
MRESRI	0.17 ns	0.22 ns	0.21 ns	0.15 ns	-0.44**
VREI1	0.34 ns	0.34 ns	0.39*	0.36*	-0.15 ns
REPI	0.36*	0.36*	0.36*	0.36*	-0.19 ns
PRI	0.08 ns	-0.05 ns	-0.07 ns	-0.08 ns	-0.16 ns
SIPI	-0.26 ns	-0.24 ns	-0.26 ns	-0.19 ns	0.47*
RGRI	-0.35*	-0.36*	-0.36*	-0.4*	0.27 ns
ARI2	-0.37*	-0.48*	-0.45*	-0.36*	0.48*
CRI2	0.23 ns	0.22 ns	0.23 ns	0.25 ns	0.01 ns

*Is significant
 ns is non-significant

6.3.4 Analysis of Continuum Removed Reflectance and Band Depth

6.3.4.1 Continuum Removed Reflectance

Continuum removed reflectance (CRR) of vegetation from polluted and control transects showed considerable variation in the concentration of the pigment of primary interest, chlorophyll. Additionally, the spectra also distinguished the concentration of carotenoids (CaR) and anthocyanins (AnC) in polluted and controlled vegetation. Both CaR and AnC are stress indicators in vegetation (Hatier and Gould, 2008; Gitelson, Chivkunova and Merzlyak, 2009). Although there are diverse opinions on the location of maximum CaR absorption in the spectrum, previous studies established that this occurs between 470 nm to 500 nm (Chappelle, Kim and McMurtrey, 1992; Blackburn, 1998; Merzlyak *et al.* 2008). Conversely, there appears to be some consensus on the absorption peak of AnC in the leaf spectrum. Merzlyak *et al.* (2008) and Gitelson *et al.* (2001) reported this peak as being around 540 nm to 550 nm.

The CRR plots in Figures 6.4 and 6.5 clearly shows vegetation reflectance on polluted transects increased at the chlorophyll absorption features (around 445 nm and between 650-700 nm) and decreased at the CaR (around 460 nm) and AnC (around 560 nm) absorption features. Hence, implying that oil pollution altered the pigment concentration in vegetation growing on impacted transects.
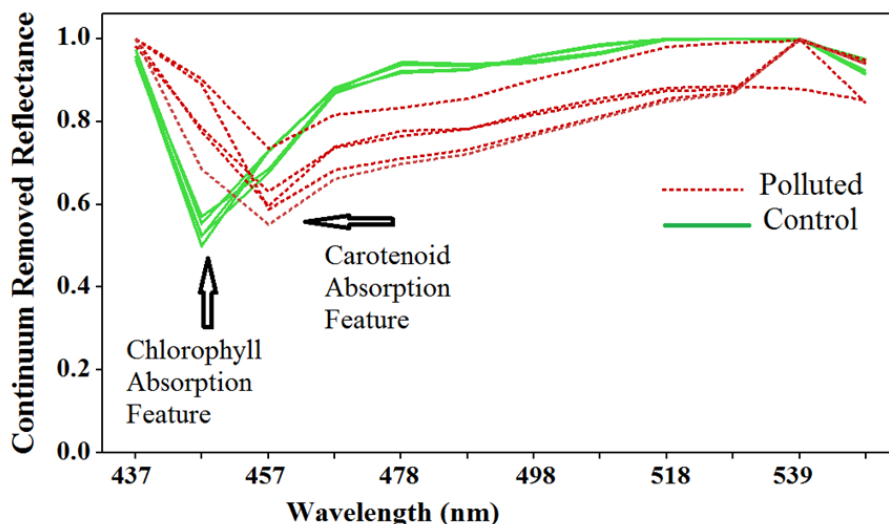
Figure 6.4: Continuum removed reflectance (CRR) of randomly selected segments of polluted and control transects plotted for the chlorophyll b (Chl-b) and carotenoid (CaR) absorption features in the blue channel of visible spectra (400-550nm). The curves distinguished reflectance of vegetation on polluted and control transects. The CRR values were lower for Chl-b absorption and higher for CaR on control transects, and the reverse on the polluted transects
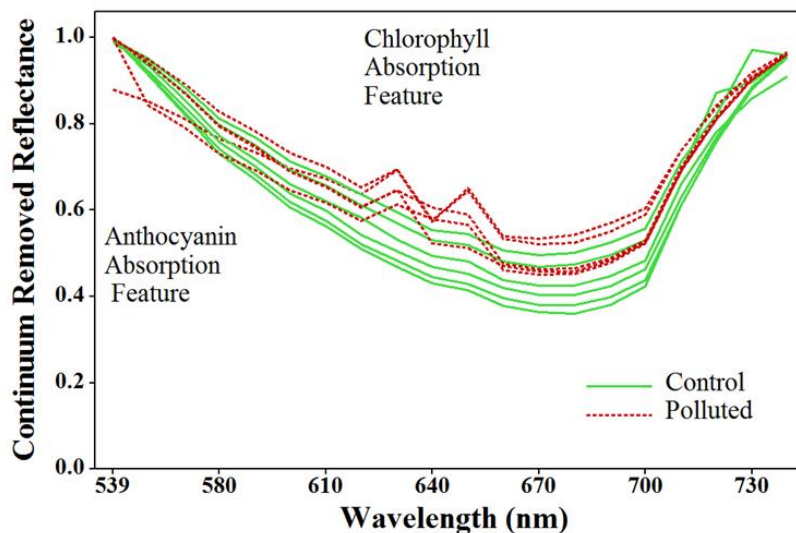
Figure 6.5: CRR of polluted and control segments showing the chlorophyll and AnC absorption in the red range (550-750nm). CRR values were lower for chlorophyll absorption, and higher for AnC on control transects, and the reverse on the polluted transects

6.3.4.2 Band Depth Analysis and Comparison

Spectral band depth (D) of the relevant wavelengths was derived by subtracting the CRR values from 1, and normalised band depth (D_{norm}) was computed by dividing each band depth by the band depth at the wavelength centre. The band depth at the wavelength centre is the maximum band depth, hence this procedure was performed to identify any changes in vegetation reflectance within each absorption feature. Both datasets were subjected to the Mann-Whitney U to test the null hypothesis that there was no difference in the medians of the band depths (D) and normalised band depth (D_{norm}) of absorption features in vegetation growing on polluted and control transects. The M-W test was performed separately for chlorophyll absorption features with an alternative hypothesis (H_{A1}) that the median D and D_{norm} of control transects are significantly higher than those of polluted transects. Conversely, the H_{A2} for testing the stress-indicating pigments (CaR and AnC) was that the D and D_{norm} of the control transects were less than those of the polluted transects. The results of these tests are displayed in Table 6.7 for chlorophyll absorption features and Table 6.8 for CaR and AnC.

Chlorophyll absorption in the blue (CHB) channel was significantly higher in vegetation growing on control than on polluted transects as evident in the result of the M-W test (U = 352 for CHB1 and U = 337 for CHB2, $p < 0.05$). It appears that there was higher chlorophyll absorption in the red channel (CHR) than in the blue channel (Figure 6.14 A and C) in both polluted and control transects and these differed significantly (Table 6.7)

195

for the first three absorption channels namely CHR1 (630.32 nm); CHR2 (640.5 nm); and CHR3 (650.67 nm). However, chlorophyll absorption at the longer wavelengths (CHR4-CHR7) of the feature was not significantly different between the polluted and control transects despite the maximal band depth (wavelength centre) located at 671.02 nm (CHR5).

Table 6.7: Results of Mann-Whitney U test of differences in the band depths and normalised band depths of chlorophyll absorption features for the control and polluted transects. Band depths computed from subtracting the continuum removed reflectance value from 1.

Absorption Features		Chlorophyll in blue channels		Chlorophyll in red channels				
		CHB1	CHB2	CHR1	CHR2	CHR3	CHR4	CHR5
Wavelength (nm)		437	447	630	641	651	661	671
N	Polluted (n1)	17	17	17	17	17	17	17
	Control (n2)	16	16	16	16	16	16	16
		Band Depth (D)						
Median	Polluted	0.00	0.22	0.36	0.42	0.44	0.52	0.53
	Control	0.028	0.37	0.43	0.47	0.48	0.52	0.53
Difference	(n2-n1)	0.028	0.15	0.07	0.05	0.04	0	0
CI (95%)	Lower	0.003	0.02	0.036	0.02	0.02	-0.01	-0.01
	Upper	0.04	0.22	0.11	0.09	0.1	0.05	0.06
U		352	337	369	357.5	342.5	299	296
$P < 0.05$		*	*	*	*	*	ns	ns
		Normalised Band Depth (D_{norm})						
Median	Polluted	0.00	1	0.69	0.85	0.87	0.97	1
	Control	0.09	1	0.81	0.88	0.90	0.97	1
Difference	(n2-n1)	0.5	0	0.12	0.03	0.03	0	0
CI (95%)	Lower	0.00	-0	0.02	-0.00	-0.00	-0.00	-0
	Upper	0.09	0	0.15	0.14	0.134	0.00	0
U		361	284	354	326	333	238	288
$P < 0.05$		*	ns	*	ns	*	ns	ns

* = median differences are significant
ns = not significant
\# = null hypothesis of 'no difference in median' accepted

Both the band depth (D) and normalised band depth (D_{norm}) analyses suggest that chlorophyll absorption along polluted transects differed slightly and correlated with soil TPH. CHB2 had the highest coefficient of -0.77, followed by CHR3, r = -0.46. Chlorophyll absorption in the red range did not vary greatly along polluted transects despite the large differences in TPH concentration in the soil. The coefficient of variation (CV) ranged between 9-11%, whereas in the blue range, the CV=329.9 for CHB1 and

CV=58.3 for CHB2. Nevertheless, there was a strong positive relationship between the chlorophyll absorption features and the species diversity indices along polluted transects.

Table 6.8: Results of Mann-Whitney U test of differences in the band depths and normalised band depths of carotenoid and anthocyanin absorption features for control and polluted transects. Band depths computed by subtracting the continuum removed reflectance value from 1.

Absorption Features		Carotenoids			Anthocyanins	
		CAR1	CAR2	CAR3	ANT1	ANT2
Wavelength (nm)		**457**	**468**	**478**	**539**	**559**
N	Polluted (n1)	17	17	17	17	17
	Control (n2)	16	16	16	16	16
Band Depth (D)						
Median	Polluted	0.37	0.12	0.08	0.00	0.06
	Control	0.27	0.26	0.23	0.003	0.05
Difference	(n2-n1)	-0.1	-0.14	-0.15	0.003	-0.01
CI (95%)	Lower	-0.19	-0.21	-0.2	-0.00	-0.00
	Upper	-0.03	-0.06	-0.08	0.004	0.004
U		214	192	179	279	226
$P < 0.05$		*	*	*	#	*
Normalised Band Depth (D_{norm})						
Median	Polluted	1	0.71	0.28	0.00	1
	Control	1	0.45	0.63	0.07	1
Difference	(n2-n1)	0	-0.26	-0.35	0.07	0
CI (95%)	Lower	-0	-0.30	-0.39	-0.07	-0
	Upper	0	-0.11	-0.14	0.08	0
U		272	145	164	302	273
$P < 0.05$		ns	*	*	#	ns

* = median differences are significant
ns = not significant
# = null hypothesis of 'no difference in reflectance median' accepted

The central wavelength for the CaR absorption feature was at 457.34 nm while that of AnC was at 559.09 nm. Radiance absorption at these wavelengths was significantly different between polluted and control transects. Results of the Mann-Whitney U test agreed with the alternative hypothesis that the D and D_{norm} of the CaR and AnC absorption features were lower in the control vegetation than in the polluted vegetation. Thus, providing further proof of oil pollution induced stress in vegetation. The boxplots

in figure 6.6 D consistently show substantial differences in pigment absorption at relevant wavelengths between polluted and control vegetation.
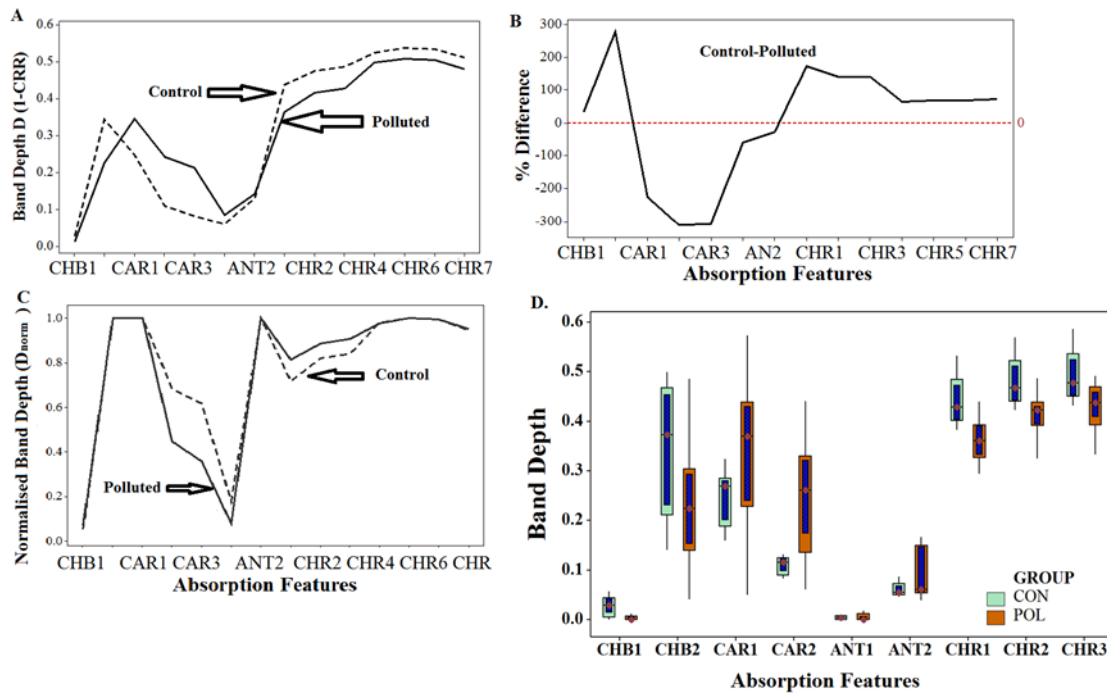
Figure 6.6: Illustrates the A - average band depth values (D = 1 - CRR) for control and polluted transects; B - the difference curve calculated by subtracting the D (polluted) from the D (control) and multiplied by 100 showed the difference in pigment absorption between polluted and control transects. Chlorophyll absorption in control vegetation was up to 300%, while that of CaR was down to -300% and AnC, down to -90%. Positive differences indicate greater band depth or increased absorption of radiance at that wavelength; C: Average D_{norm} values showing the magnitude of the difference in absorption between the polluted and control transects; and D: box plots of band depths of chlorophyll, carotenoids and anthocyanins absorption in polluted and control transects.

6.3.5 Oil Pollution Effects on Red Edge Position (REP) of Transects

6.3.5.1 Effects of Soil TPH on REPder and REPlnr

The presence of TPH in the soil seemed to affect vegetation reflectance, and this effect is apparent in the first derivative spectra of the red edge. Original spectra of polluted vegetation with low diversity indices (red dashes in Figure 6.7A) showed increased reflectance in the red and reduced reflectance in the NIR region. The original curve displays a slight shift to the shorter wavelengths (also known as 'blueshift') in vegetation spectra from the polluted transects, whereas reflectance from control transects shifted slightly to the longer wavelengths (also known as 'redshift'). Clear differences are also apparent in the shape of the red edge slope of polluted and control vegetation. Figure 6.7

A reveals flatter slopes for polluted spectra and steeper slopes for control spectra. Additionally, the TPH-induced stress in vegetation which may have initiated the blueshift also led to a general increase in visible reflectance and particularly in the chlorophyll absorption features around 680 nm (Figure 6.7A).
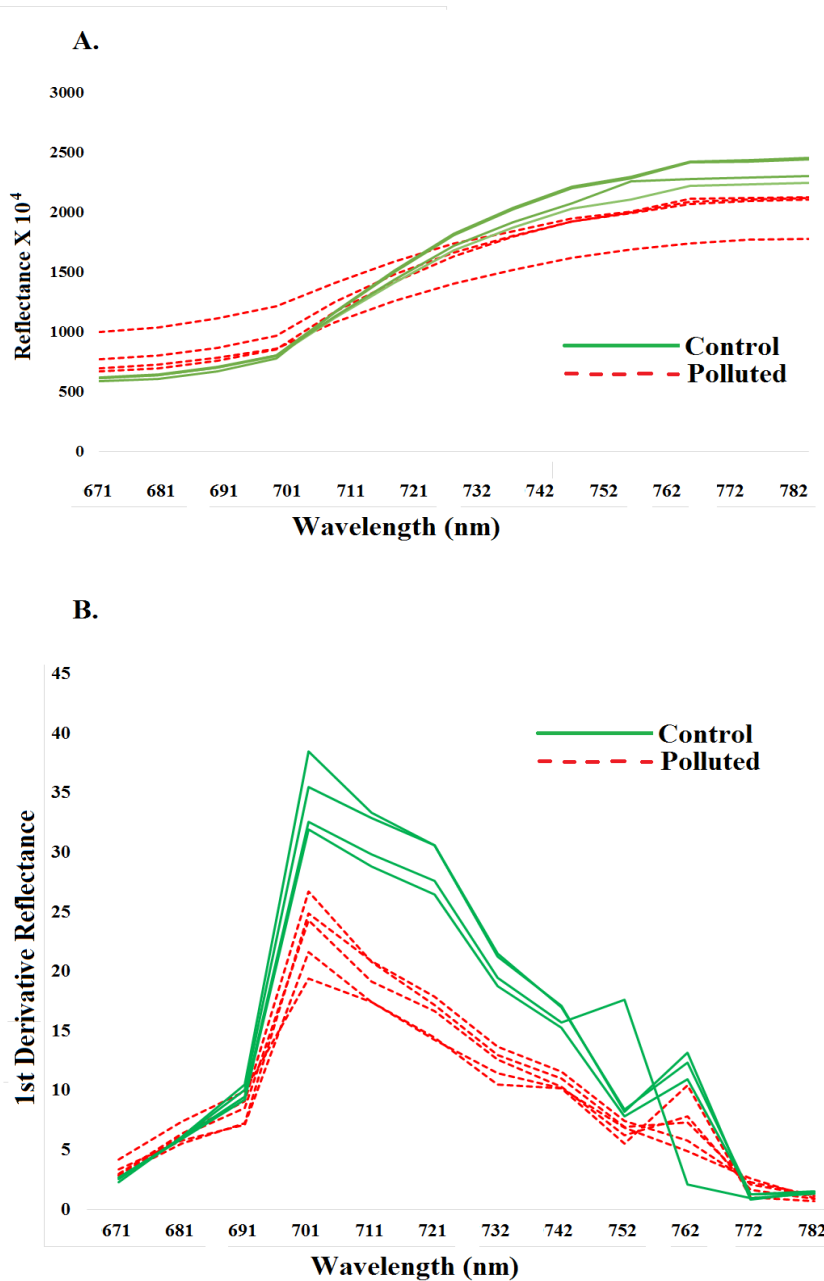
Figure 6.7: A. Original and **B**. first derivative reflectance curves of randomly selected segments from polluted and control transects. The reflectance of polluted vegetation is slightly shifted to shorter wavelengths while reflectance from control vegetation slightly shifts towards longer wavelengths. Comparison of reflectance from polluted and control transects using the Mann-whitney test shows significant differences ($p < 0.05$).

First derivative reflectance maxima occur at 701.6 nm for both polluted and control vegetation. Reflectance at this wavelength is selected as the red edge position and denoted as REPder. Distinctively, while derivatives curves from polluted vegetation have single peaks, the control curves have additional peaks at 742.25 nm, 752.43 nm and 762.6 nm. Since each curve represents the combined reflectance of all materials on the ground surface covered by the 30 m X 30 m pixel, the presence of multiple peaks in control curve may be attributed to increased intra-specific differences in vegetation.

The average REPlnr reflectance is 893.14 on the polluted transects, and 893.49 on the control transects with standard deviations of 0.15 and 0.51 respectively. Based on this method, REP occurred at different wavelengths for each segment however, the REP reflectance upheld the earlier interpretation from REPder that there's significant difference between polluted and control transects.

Reflectance at the identified REPs for all segments was subjected to the non-parametrics two-tailed Mann-Whitney U test for two independent samples. The null hypothesis tested was that REP reflectance from polluted and control transects were not significantly different while the alternative hypothesis was that they were significantly different. Results of the test are summarised in table 6.9.

Table 6.9: Summary of the Mann-Whitney U test analysis comparing reflectance at REP from polluted and control transects. The REP index is derived from two different methods using Hyperion data.

Index	U-Value	z-Value	p-Value	Decision
REPder	54	-2.936	0.03*	Reject
REPlnr	63	-2.612	0.01*	Reject

From the table, it is clear that soil TPH impacted on reflectance at the REP of polluted vegetation significantly regardless of the REP derivation method. For both indices, the U-values supports the alternative hypothesis of difference between polluted and control REP reflectance, hence, the null hypothesis of no difference is rejected.

6.3.5.2 The Relationship between REP and Selected Field Measurements

Results of the non-parametric multivariate regression (NPMR) analysis of REP (REPder and REPlnr) with field data (soil TPH, SPAD chlorophyll data, abundance and frequency) are presented in Table 6.9

Table 6.10. Regression statistics of REP on field measured data. REPder computed from the first derivative method whereas REPlnr computer from linear interpolation method. Both indices derived from Hyperion data acquired over Kporghor spill location were extracted from segments of polluted and control transects in the location.

	REPder			REPlnr		
Parameter	R^2	RSE	MSE	R^2	RSE	MSE
Soil TPH	0.61	2.27	5.14	0.16	0.47	0.22
Chlorophyll	0.48	2.63	6.92	0.32	0.42	0.18
Abundance	0.32	2.99	8.94	0.01	0.51	0.26
TPH*Chlorophyll	0.57	2.37	5.63	0.16	0.47	0.22
TPH*Abundance	0.63	2.22	4.93	0.15	0.47	0.22

REP indices derived from both the maximum first derivative method (REPder) and the linear interpolation method (REPlnr) showed a significant relationship with field data. Generally, the indices inversely related to soil TPH concentrations and positively related to the vegetation variables. It is deducible from the results that the presence of TPH in the soil interfered with the biochemical parameters in vegetation and the interference exhibited in the changing shape of the red edge curve and position in spectra of polluted vegetation. Between the two indices, the REPder with an R^2 of 0.61 and 0.48 had stronger relationships with the soil TPH concentrations and SPAD chlorophyll readings respectively than REPlnr.

Scatterplots in Figure 6.9 show that both REPder and REPlnr decreased in reflectance as soil TPH increased. The R^2 values were significant at $p < 0.05$. Field measured vegetation characteristics (abundance and SPAD chlorophyll estimates), showed a significant positive relationship with both indices. The regression coefficient of REPder and REPlnr versus chlorophyll estimates were 0.48 and 0.32 respectively, $p < 0.05$, although only REPder significantly related with abundance ($R^2 = 0.32$, $p < 0.05$). However, the introduction of soil TPH in the relationship caused a decrease in the REP reflectance values as shown in the scatterplots in Figure 6.8.
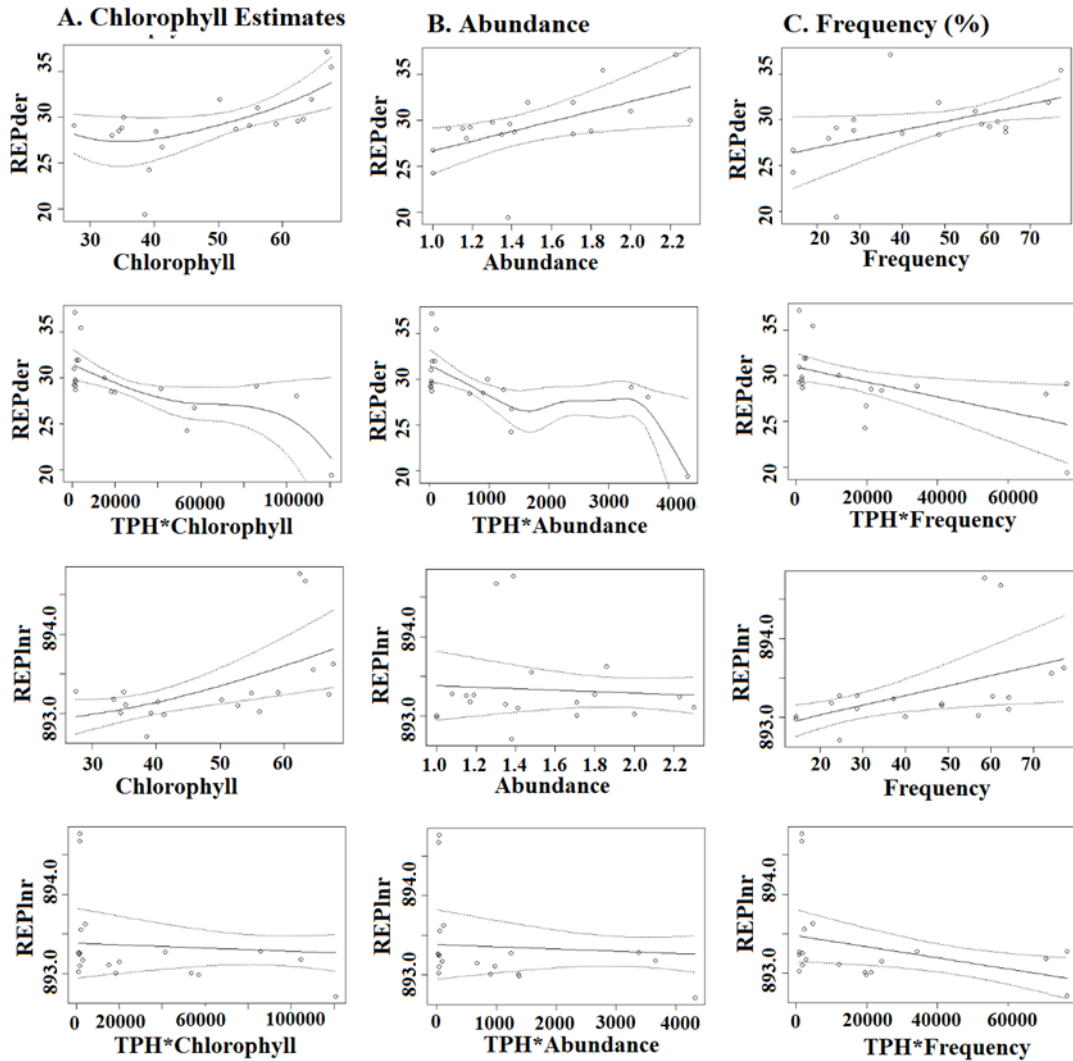
Figure 6.8: Scatter plot, regression line and 95% confidence intervals of REP versus SPAD chlorophyll estimate, vegetation abundance and frequency as well as their interactions with soil TPH. The plots show that both REPder and REPlnr decreased in the presence of soil TPH.

6.3.6 Modelling Species Diversity Using Hyperspectral Indices

Predictors in models estimating the species diversity index of polluted and control transects included two sets of indices namely the NDVVIs and the traditional NBVIs. This analysis aimed to determine the performance of the new indices in estimating the diversity of plant species in areas impacted by oil pollution in comparison with traditional NBVIs. The dataset comprising measurements from polluted and control transects was subdivided into training and testing data using a ratio of approximately 6:4 for training and validation data respectively.

6.3.6.1 Model Calibration Using Training Data

Partial Least Square (PLS) regression (please see Chapter 3 Section 3.5.1.3 A for discussion on this procedure) commenced with an initial transformation of the predictor datasets (6 NDVVI variants and 6 NBVIs listed in Table 6.1) into a smaller set of uncorrelated components with the optimum number selected from R^2 value associated with each component. A maximum of 5 components was chosen to run the procedure; however, the optimum number of components varied for different response variables as shown in Table 6.10. For the NDVVI dataset, selection resulted in only 1 to 2 components which best explained the variation in the dataset, for the regression analysis. For the NBVIs, 1 to 4 components were used in the models. A leave-two-out procedure cross-validated the components before selecting the optimal number. The NDVVI-based PLS model had larger R-squared (R^2) values than the NBVI-based PLS model. Additionally, prediction error sum of squares (PRESS) was smaller for the NDVVI predictors than for the NBVIs. Thus confirming that the PLS model of NDVVI variants has greater predictive ability than that of traditional NBVIs. The results from model calibration are summarised in Table 6.11.

Table 6.11: Calibration parameters of NDVVI and NBVI-based models used in the PLS and NPM regression methods. NDVVI values were computed from Hyperion wavelengths sensitive to oil pollution and extracted from segments of polluted and control transects while NBVIs were computed from Hyperion data.

Response	Number of Components	R^2	PLS PRESS	F	P < 0.05	NPM R^2	RSE
			NDVVIs				
Shannon's	2	0.67	12.3	17.56	*	0.71	0.61
Simpson's	2	0.66	1.11	16.25	*	0.69	0.17
Menhinick's	1	0.54	44	20.82	*	0.61	1.23
Log(Chao-1)	2	0.6	8.69	12.75	*	0.69	0.49
Canopy Chlorophyll	2	0.56	2181	10.92	*	0.58	9.08
			NBVIs				
Shannon's	3	0.39	25.28	3.38	*	0.49	0.82
Simpson's	1	0.3	1.71	8.23	*	0.46	0.23
Menhinick's	4	0.48	67.78	3.54	*	0.58	1.31
Log(Chao-1)	3	0.50	11.74	5.35	*	0.55	0.58
Canopy Chlorophyll	1	0.11	4355	2.12	ns	0.59	8.89

*significant
ns - not significant.

203

The significance of the relationship between the predictors (NDVVI variants and NBVIs) and the response (diversity indices) was analysed using the F-statistic. The results show that each diversity index statistically related to the selected NDVVI components ($R^2 >$ 0.5, $p < 0.05$). Similarly, diversity indices also significantly regressed with the NBVI components; however as stated earlier, the R^2 values were much lower (≤ 0.5, $p < 0.05$) except for the Chao-1 index (Table 6.11). The significant relationship observed between satellite-based indices (NDVVIs and NBVIs) and field measured diversity indices is in line with previous results. These include (Levin *et al.* 2007) who reported R^2 as high as 0.87 between NDVI and plant richness; (Mapfumo *et al.* 2016) who reported R^2 values between 0.32 and 0.72 for NDVI and Shannon's diversity; and (Peng *et al.* 2018a) who reported R^2 values of 0.51 to 0.83 for first order hyperspectral indices and diversity indices including Shannon-Weiner, Pielou, Simpson, Margalef and Gleason. The scatterplots in Figure 6.9 show the observed versus predicted diversity values.
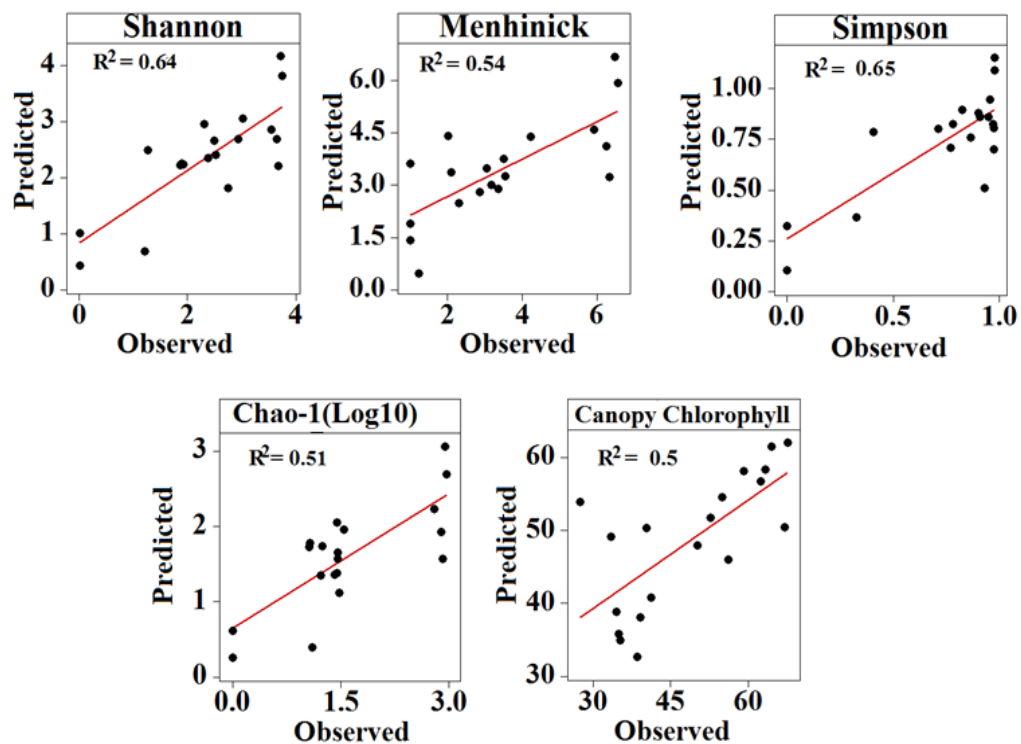
Figure 6.9: Observed versus predicted diversity indices using PLS NDVVI-based regression model. There appears to be a linear relationship between both sets of data leading to the high R^2 values. This result is consistent with results from previous studies predicting species diversity from vegetation indices.

From the scatterplots in Figure 6.10, it is apparent that the NDVVI variants performance in estimating species diversity is comparable to results reported in other studies. The mechanism explaining the relationship between satellite-derived indices and field measured diversity indices are not yet well understood; however, judging from the results of this study, we infer that vegetation biochemical parameters, mainly those strongly influenced by variations in pigment absorption at wavelengths sensitive to soil TPH are essential drivers of this relationship. The scatterplot of residuals versus predicted diversity index from the model calibration using the training data is shown in Figure 6.10. These plots suggest that the PLS model provided a good fit for the data and the residuals generally satisfy the goodness of fit requirements with randomness, homoscedasticity and linearity.

Similarly, the NDVVI-based NPM model has much smaller error values than the NBVI-based NPM model. The NDVVI-based model performed better during calibration with higher R^2 values (0.61–0.71 at the calibration stage) compared to NBVI-based models with $R^2 < 0.59$. Residual standard error (RSE) values from model calibration are smaller for the NDVVI NPM model and more substantial for the NBVI model
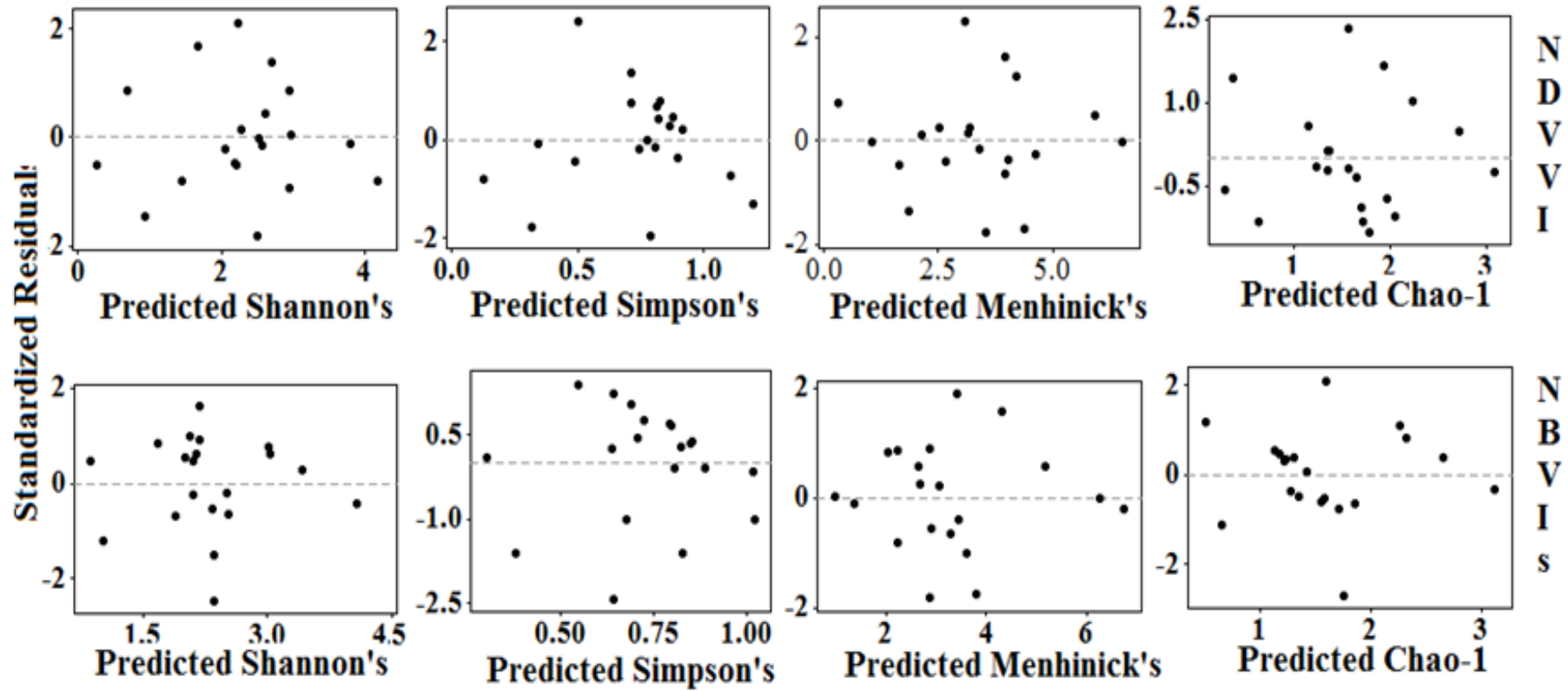
Figure 6.10: Scatterplot of residuals versus predicted values from NDVVI and NBVI PLS models. The residual plots from NDVVI models generally fulfil the goodness of fit requirements with randomness, homoscedastic and linearity except for Chao-1.

6.3.6.2 Model Validation Using Test Data

Validation of the trained models was performed using the test data ($n = 13$, polluted = 7, control = 6). The predictive capability of the spectral metrics inferred from predicted R^2, RSE, root mean square error (RMSE), bias and residual analysis of the different models revealed that the performance of the NDVVI-based models was uniform across both PLS and NPM model types. Analysis of residuals following model validation also affirms the superiority of NDVVI for estimating vascular plant species diversity over NBVI. The F-statistics, p, R^2, RMSE and Bias are summarised in Table 6.12 for all models.

Table 6.12: Results of the species diversity and canopy chlorophyll estimation of investigated transects using two different models for each set of predictors. Models 1 and 2 are the partial least square (PLS) and non-parametric (NPM) regression models respectively. Letters A and B indicate the set of predictors (spectral metrics) used in each model, A = NDVVIs and B = NBVIs, n = 13, df = 12); ns = not significant.

Response Variable	Model	F	P < 0.05	R^2	RSE	RMSE	Bias
Shannon's Diversity Index	1A	12.82	*	0.54	0.51	0.69	-11.4
	1B	1.77	ns	0.14	0.69	0.9	-16.2
	2A	13.08	*	0.54	0.5	0.5	-6.2
	2B	2.67	ns	0.2	0.67	0.94	-17.2
Simpson's Diversity Index	1A	6.66	*	0.38	0.05	0.24	-15.9
	1B	0.11	ns	0.01	0.07	0.22	-18.1
	2A	1.163	ns	0.1	0.07	0.14	-9.2
	2B	0.09	ns	0.01	0.07	0.21	-14.9
Menhinick's Richness Index	1A	14.32	*	0.57	1.15	1.13	-7.5
	1B	6.37	*	0.37	1.38	1.58	-21.6
	2A	5.35	*	0.33	1.42	1.32	1
	2B	7.4	*	0.4	1.34	1.31	-10.2
Log(Chao-1)	1A	8.55	*	0.44	0.24	0.57	3.3
	1B	2.12	ns	0.16	0.3	0.58	-1.1
	2A	10.16	*	0.48	0.23	0.56	2.1
	2B	1.93	ns	0.15	0.3	0.51	3.2
Canopy Chlorophyll Content	1A	7.89	*	0.42	7.85	7.87	6.7
	1B	1.14	ns	0.09	9.79	9.29	4.7
	2A	10.49	*	0.49	7.36	7.59	5.5
	2B	1.64	ns	0.13	9.6	13.49	9.9

*significant
ns - not significant

The NDVVI-based models (Models 1A and 2A) had the highest R^2 as well as lowest RSE values. Although non-parametric models are generally not as powerful as parametric ones, the spectral NDVVI metrics derived from TPH-sensitive Hyperion wavelengths consistently outperformed the traditional NBVIs as estimators of species diversity in all the

models. Poor estimates for Simpson's diversity index are obtained from NDVVI and NBVIs-based models, particularly using the NPM regression method, although the error values were low. From the results, the best index for estimating the Menhinick's Richness index is the NDVVI variants. The R^2 and RMSE values for NDVVI-based PLS model are 0.57 and 1.13 respectively, while for NBVIs-based PLS model, they are 0.37 and 1.58 respectively. Generally, all the models underestimated the response variables (Shannon's, Simpson's, Menhinick's, Chao-1, and Canopy Chlorophyll) as evident in the negative bias scores, although the biases were higher for the NBVI-based models. For monitoring biodiversity, this effect may be an advantage as it reduces the risk of overestimating the vascular plant species diversity of an oil affected location or a protected area. NDVVI-based model predictions were over 50% accurate for Shannon's and Menhinick's diversity indices, and less than 50% for Simpson's and Chao-1′s indices. The best predictions were for Menhinick's index as illustrated in the closeness of the fitted lines to the 1:1 line in all four models shown in Figure 6.11 for PLS models and Figure 6.12 for NPM models. In contrast, Simpson's index was the least accurate as the plots showed little or no relationship between the predicted and observed field measurements.
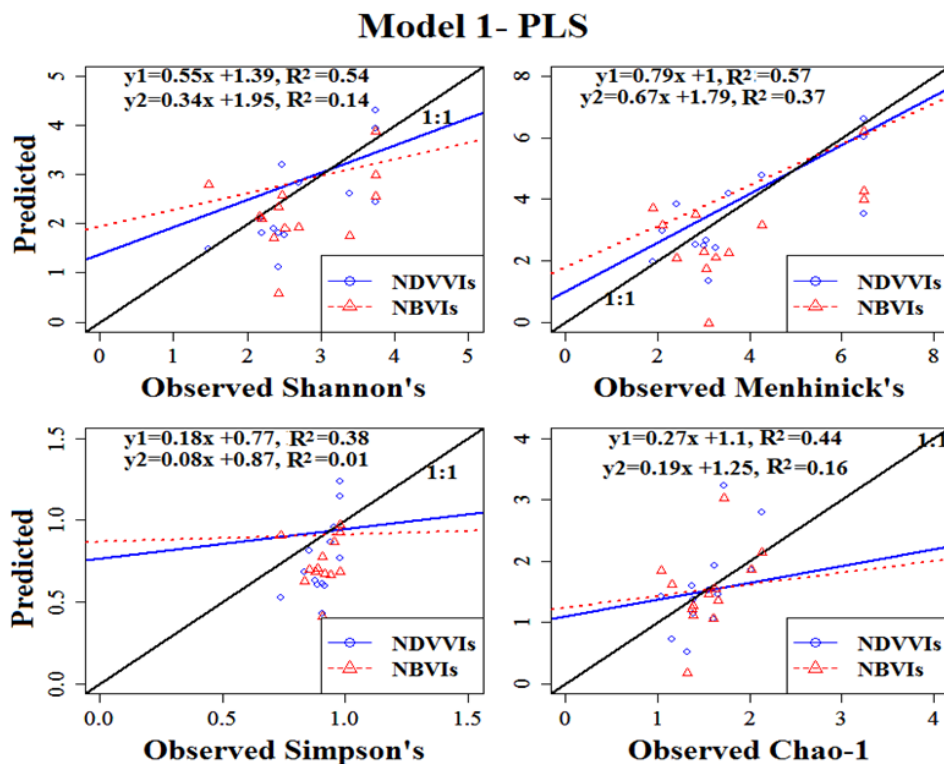
Figure 6.11: Observed versus predicted plots for the various PLS models. For each species diversity index, scatterplots of observed values versus the NDVVI variants (blue) and NBVIs (red) predicted values are shown (n = 13). The regression equations are also shown with the R^2 values, y1 = response to NDVVI variants, y2 = response to NBVIs. The line of best fit for each model is plotted to compare with the 1:1 line (in black).
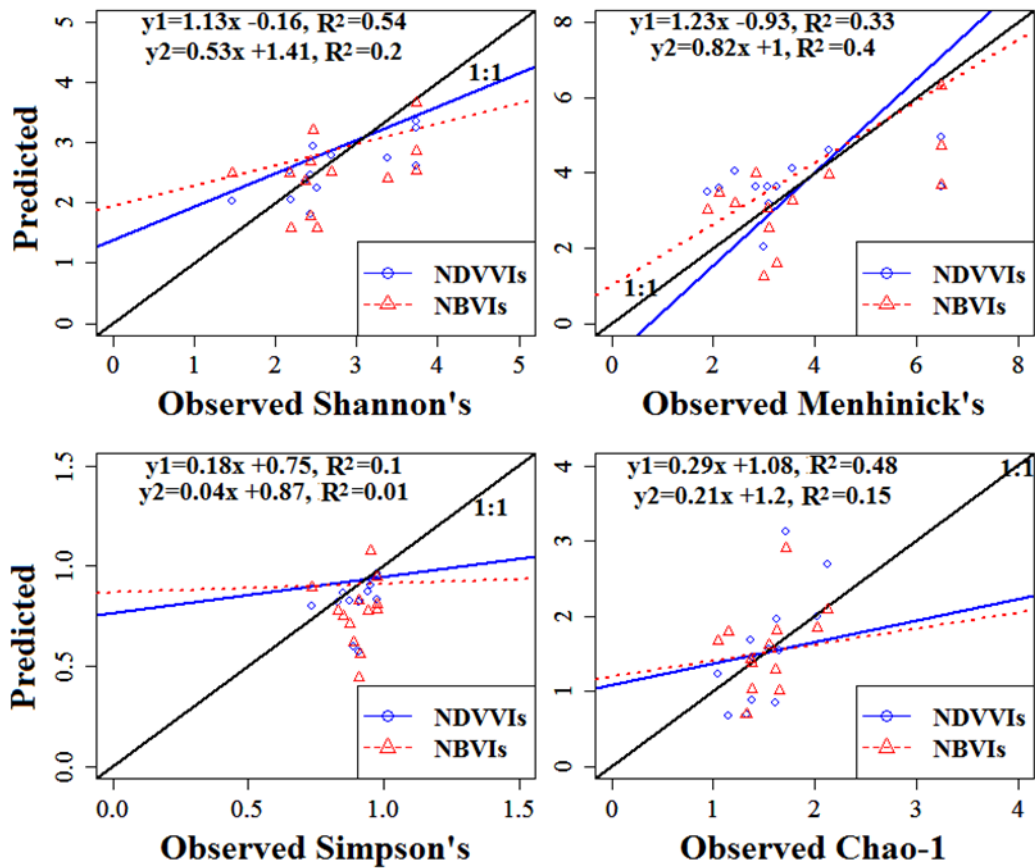
Figure 6.12: Observed versus predicted plots for the NPM models. For each species diversity index, scatterplots of observed values versus the NDVVI variants (blue) and NBVIs (red) predicted values are shown (n = 13). The regression equations are also shown with the R^2 values, y1 = response to NDVVI variants, y2 = response to NBVIs. The line of best fit for each model is plotted to compare with the 1:1 line (in black).

All models clearly distinguished between polluted and control transects with the diversity estimates; however, the NDVVI-based models performed better. The residual versus predicted scatterplot in Figure 6.13 show that the NDVVI-based model is a good fit for Shannon's index and the SPAD chlorophyll estimates. However, this goodness of fit was absent for the other indices.
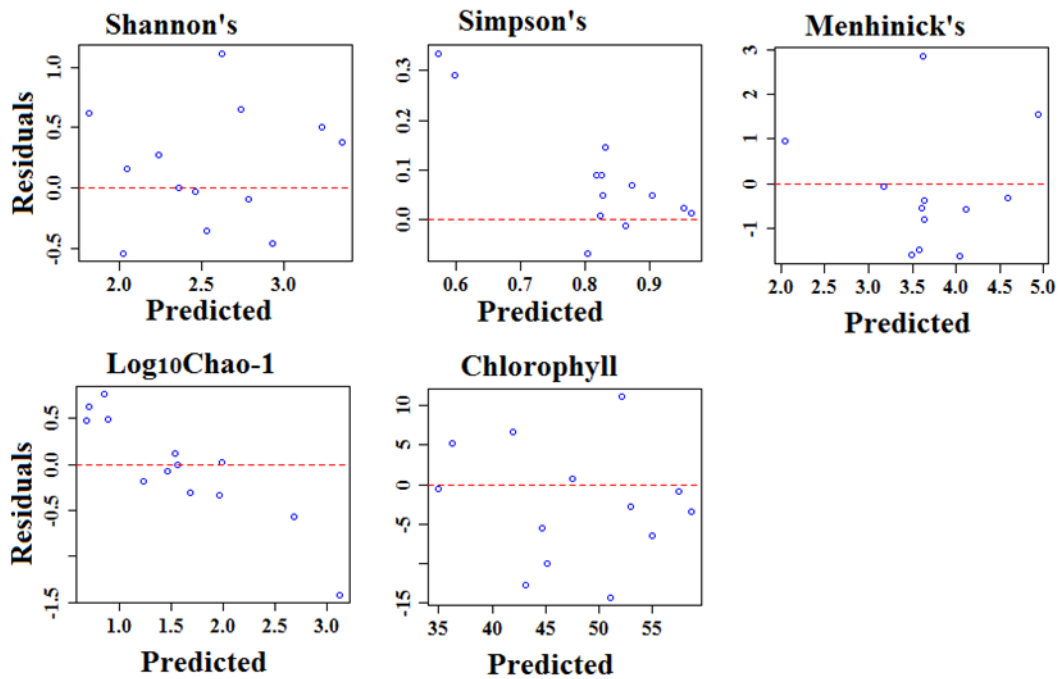
Figure 6.13: Scatterplots of residual versus predicted values of NDVVI -based model. Predicted values are from the NPM regression using test data (n = 13). The charts clearly show that the model was a good fit for Shannon's diversity index and SPAD chlorophyll estimates.

Using the model equations from the NDVVI PLS model, spatial maps of vascular plant species diversity were created for the investigated area (Figure 6.14).
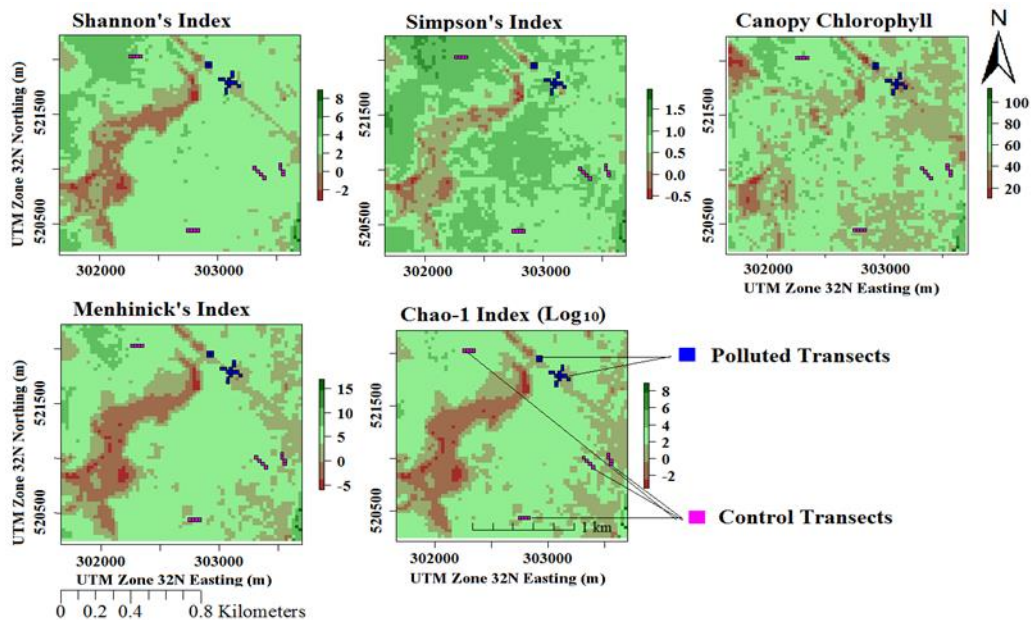
Figure 6.14: Spatial maps of vascular plant species diversity estimated from NDVVI PLS model. Location of control and polluted transects on the maps correspond with the estimated diversity index and chlorophyll content. From the images, polluted transects are seen to have low diversity and canopy chlorophyll values while control transects have high diversity and canopy chlorophyll values. This result further emphasises the linear relationship between vegetation productivity indicated by canopy chlorophyll content and vascular plant species diversity.

A glance at the maps of estimated Shannon's or Simpson's diversity and the canopy chlorophyll content shows that pixels with high diversity index were also high in canopy chlorophyll.

6.3.6.3 Model Implementation and Evaluation Using Random Pixels

The new dataset of derived spectral metrics (preddata) was used as predictors in the NPM model in order to estimate the Shannon's, Simpson's, Menhinick's and Chao-1 index values for the predsites. Estimations were done separately for each variable, and average predicted values for each land cover type visible from a high-resolution image available on Google Earth is shown in Table 6.13. Expectedly predicted values were high for forests and mixed vegetation, low for swamps and waterbodies and moderate for farmlands.

Table 6.13: Average diversity values predicted for randomly selected pixels according to the observed land cover type. N = number of 30 m pixels in each class, L8-NDVI = NDVI derived from Landsat 8 image and S2A-NDVI = NDVI derived from Sentinel 2A image. Due to its higher spatial resolution, average NDVI values were calculated using a 3×3 pixel window from the S2A-NDVI.

Land Cover Type	Farmland	Forested	Mixed	Swamp	Waterbody
N	7	5	10	6	2
L8-NDVI	0.17	0.2	0.18	0.13	0.11
S2A-NDVI	0.11	0.12	0.11	0.05	0.06
Predictor variables					
$NDVVI_{844,447}$	0.48	0.57	0.49	0.29	0.27
$NDVVI_{814,437}$	0.73	0.83	0.76	0.61	0.57
$NDVVI_{824,427}$	0.5	0.58	0.51	0.3	0.28
$NDVVI_{752,630}$	0.44	0.53	0.46	0.25	0.23
$NDVVI_{773,641}$	0.71	0.80	0.73	0.56	0.53
$NDVVI_{844,630}$	0.85	0.94	0.88	0.73	0.7
Response Variables					
Shannon's	2.59	3.42	2.77	0.88	0.94
Simpson's	0.82	0.95	0.87	0.25	0.3
Menhinick's	3.64	5.34	4.13	1.41	1.16
LogChao-1	2.16	2.79	2.4	1	1.06
Canopy Chlorophyll	56.12	64.8	56.46	39.57	34.09

NDVI values computed from both Landsat and Sentinel 2A images and extracted for the predsites were generally low for the different land cover types compared to the NDVVI

values. NDVVI values for forested pixels ranged from 0.53 to 0.94 while NDVI values were 0.2 and 0.12 respectively for L8-NDVI and S2A-NDVI. Similarly, NDVVI values were higher than NDVI values in pixels categorised as farmland and mixed. Despite the large margin between NDVVI and NDVI values, the pattern of vascular plant species diversity estimation was similar. As evident in Table 6.13, the higher the index value, the higher the estimated species diversity value and vice versa.

Additional evaluation of NDVVI-based model performance involved using NDVI using as surrogates for the vascular plant species diversity index. Presumably, the relationship between NDVI values and predicted vascular species diversity indices is positively linear as NDVI correlates strongly with species diversity in literature. Due to the higher spatial resolution of the Sentinel 2A image, average NDVI values were computed for each segment using a 2×2 pixel window. The result of the correlation analysis in Table 6.14 suggests that the estimated values have a strong linear relationship with NDVI values from both images. The correlation coefficients ranged from 0.73 to 0.85 for the diversity indices.

Table 6.14: Spearman's rank correlation coefficients of NDVI and estimated species diversity indices for predsites. All the results are significant ($p < 0.05$).

Diversity Index	L8-NDVI	S2A-NDVI
Shannon's	0.77	0.78
Simpson's	0.73	0.75
Menhinick's	0.78	0.79
Chao-1	0.84	0.84

Visual evaluation of high-resolution Google Earth imagery (Figure 6.15) shows that most predicted values correspond with the land cover type on the ground surface. For instance, the predsites located on swamps and water bodies had low estimated values for vascular plant species diversity. However, the location of the predsite P2 with predicted Shannon diversity index of 2.68 appears to be bare soil in this image (acquired by Digital Globe in December 2006), the most current image acquired in January 2016 (not used due to cloud obstruction) shows the presence of vegetation regrowth at the location, hence the predicted high diversity values for the pixel.
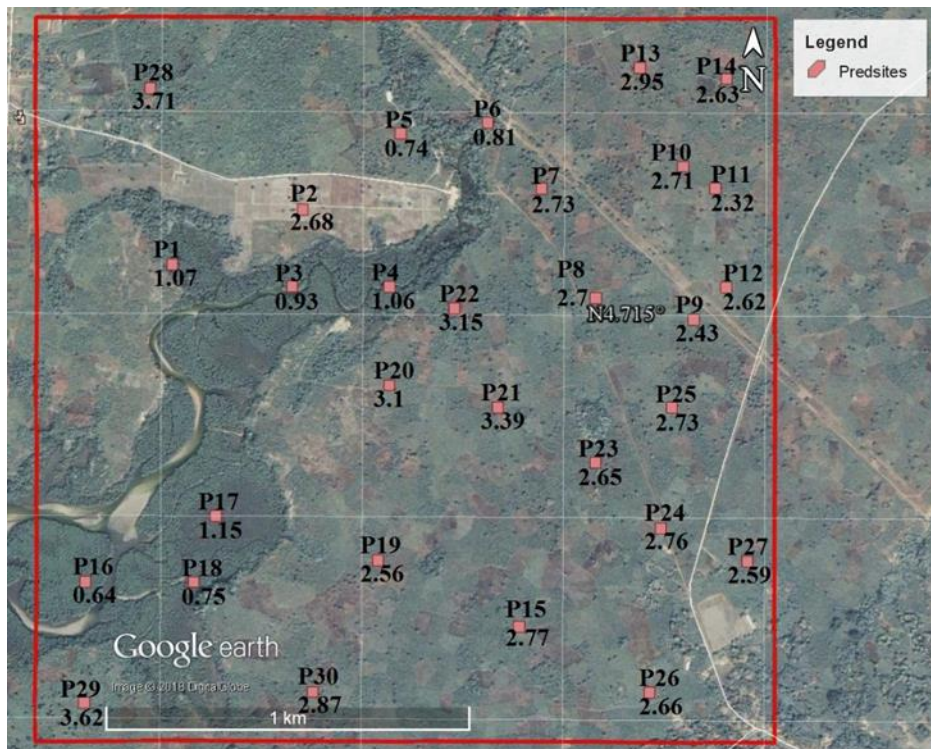
Figure 6.15: A high-resolution Digital Globe 2006 true colour image of the study area extracted from Google Earth showing the location of predsites. This image was selected because it depicted the land cover types in the study area better than more recent high-resolution images. From the estimated Shannon's diversity index shown next to the predsites, it is evident that most of the predictions correspond with the visible land cover type.

6.4 Discussion

Among biologists, ecologists and conservationists there is firm persuasion to develop a standardised methodology for monitoring biodiversity at regional and global scales (Yoccoz, Nichols and Boulinier, 2001; Kerr and Ostrovsky, 2003; Muchoney, 2008; Lindenmayer and Likens, 2010; Han *et al.* 2014). More importantly, vulnerable ecosystems like the Niger Delta region of Nigeria subjected to oil pollution require standard and accessible methods for regular biodiversity monitoring. Conventional techniques are limited in several ways due to time and equipment constraints, as well as in coverage (usually carried out at local scales). Hence, researchers advocate for the integration of remote sensing tools into biodiversity monitoring programmes because of the advantages the technology offers (Wulder, 1998; Nagendra, 2001; Boyd and Danson, 2005; Warren *et al.* 2014; Galidaki and Gitas, 2015; Lucas *et al.* 2015).

Results of the analysis confirmed that the effect of oil pollution on vegetation was statistically significant. The characteristics of polluted vegetation reflectance and band

213

depths conformed to expected changes in the spectral signature of stressed vegetation. Stress indicating pigments such as anthocyanin and carotenoids contents increased in polluted transects but remained minimal (relative to chlorophyll pigments) in control transects. However, along polluted transects, decreased vegetation density and diversity affected vegetation reflectance, particularly at the anthocyanin and carotenoids absorption peaks. Apart from the spill epicentre and segment SS1 of all four polluted transects, where vegetation abundance depreciated substantially, anthocyanin and carotenoids reflectance remained relatively constant with increasing concentration of soil TPH.

Furthermore, vegetation productivity a vital ecosystem service, particularly for inhabitants of the Niger Delta region who rely on forest resources for their livelihood, was shown to be vulnerable to oil pollution. The chlorophyll absorption features in polluted vegetation significantly dwindled in comparison to control vegetation. The normalisation of reflectance at these wavelengths using continuum removal revealed the extent of damage to photosynthetic activity in polluted vegetation. While chlorophyll absorption in control vegetation was as high as 0.6, in polluted vegetation, it was as low as -0.1, amounting to a difference of up to 300%.

Perhaps, a clearer illustration of oil pollution impact on vegetation is the different values of the NDVVI from polluted and control transects. The NDVVI derived from a combination of TPH sensitive and TPH insensitive wavelengths from Hyperion image was created to measure the vigour (productivity and health) of vegetation on polluted and control transects for comparison. Prediction of species diversity was significantly improved using the new Hyperion indices when compared to the performance of traditional narrowband vegetation indices (NBVIs).

6.4.1 Effect of Oil Pollution on Vegetation Reflectance

Hydrocarbon contamination in soils interferes with the physiological processes in plants. The interference, which primarily causes stress in plants is usually evident in the spectral signature of affected plants. Similar to several studies (Akubugwo, Elebe and Osuocha, 2016; Udeh, Nwaogazie and Momoh, 2013; Tanee and Albert, 2015; Ugboma, 2014; Okoye and Okunrobo, 2014), there was evidence that increased concentration of petroleum hydrocarbon in the soil induced changes in the soil parameters including the

temperature, pH, nutrients and microorganism in the investigated transects. These changes caused stress in vegetation growing on polluted transects by interfering with the production of chlorophyll and other photosynthetic pigments that absorb solar radiation, and thus affected their reflectance.

Previous studies (Smith, Steven and Colls, 2005; Bammel and Birnie, 1994) reported that spectral changes in vegetation occur mostly in the visible and near infrared regions as well as in the red-edge region (the slope between the red and near infrared regions) of the spectrum. The spectral changes are characterised by increased reflectance in absorption maxima and reduced reflectance at absorption minima. Gitelson, Buschmann and Lichtenthaler (1999) found that in healthy fully developed leaves, there was high absorption in the visible spectral range (400 nm - 700 nm) and higher reflectance as observed in the NIR (700 nm - 800 nm). They also observed that the red edge position of yellowing leaves shifted towards the shorter wavelengths. These postulations agree with the general increase in reflectance of polluted vegetation in the visible region and decrease in the NIR region followed by a shift in the red edge position towards shorter wavelengths ('blue shift') observed in polluted vegetation in the present study. Li, Ustin and Lay (2005) reported similar changes in reflectance of vegetation under oil-induced stress. The implication is the decrease in the chlorophyll content of polluted vegetation since these pigments absorb light for photosynthesis in the visible wavelengths (Mishra *et al.* 2012). The results obtained earlier in section 4.3.4.1 where in-situ chlorophyll content not only decreased significantly in polluted transects (mean = 36.69) in comparison with control transects (mean = 55.32) but also correlated negatively (r = - 0.86) with soil TPH (Section 4.3.4.3) support this connotation. A decrease in chlorophyll content means reduced light absorption in known absorption maxima, which occurred at around 445 nm, and 680 nm in this study, leading to increased reflectance as obtained in the polluted vegetation.

TPH presence in oil also amplified the reflectance difference between polluted and control transects in wavelengths associated with chlorophyll absorption in the blue (440±10 nm) and red (640±10 nm) spectral channels. These wavelengths were the most sensitive to TPH concentration in the soil. Chlorophyll absorption is known to occur within the wavelength range of 430-460 nm (chlorophyll b) and 650-680 nm (chlorophyll a) (Gitelson, Gritz † and Merzlyak, 2003; Carter and Miller, 1994). The identity of the

most sensitive wavelength 447.17 nm (Band 10), shows that TPH in the soil affected the absorption of chlorophyll in vegetation growing on the polluted transects. Contrarily, Carter and Miller (1994) found that reflectance at 420±5nm varied little with stress in plants, but reported increased sensitivity to plant stress for reflectance at 600 nm and 695 nm. Although there was a significant difference in the NIR (700 nm - 900 nm) reflectance of polluted and control vegetation, the sensitivity analysis which is calculated using mean reflectance showed that this region was least sensitive to TPH-induced stress. Other researchers reported a similar pattern in NIR reflectance of stressed vegetation. For instance, Carter and Miller (1994) reported that at 730 nm, the reflectance in stressed plants did not significantly change while Gitelson, Buschmann and Lichtenthaler (1999) also found that NIR reflectance did not vary between healthy leaves and stressed leaves. Gitelson, Buschmann and Lichtenthaler attributed this phenomenon to the increase in the size and length of the assemblages in the spongy parenchyma. Moreover, (Kokaly *et al.* 2013; Kühn, Oppermann and Hörig, 2004; Adamu, Tansey and Ogutu, 2015) analysed polluted substrates and attributed the increased NIR reflectance in polluted vegetation to the presence of hydrocarbons.

Other factors may be responsible for this response. Firstly, as suggested by Rapport, Regier and Hutchinson (1985); Scholten and Leendertse, (1991); Li, Ustin and Lay (2005) and Asner *et al.* (2009) there may be an increased presence of invasive species which are tolerant to hydrocarbon. Secondly, it may also be that the plant assemblages (cell walls, mesophyll cells and intercellular spaces) responsible for NIR reflectance in vegetation were yet to succumb to the stress caused by TPH in the soil. It is most likely that this was the case along polluted transects as soil TPH concentration decreased, thereby delaying the onset of physiological damage in plants tissues. Furthermore, analysis of vegetation data in section 4.3.2 provides evidence of thinning out of plants on polluted transects. Results of the analysis indicate that vegetation parameters (composition, density, abundance, diversity) suffered decrease as TPH concentrations increased in the soil. It appears that TPH was responsible for over 50% loss in species of annual plants growing on polluted transects.

Several researchers have propounded theories on how TPH influences chlorophyll content in affected plants. Omosun, Markson and Mbanasor (2008); (Lopes, da Rosa-Osman and Piedade (2009); Baruah *et al.* (2014) investigated the effect of crude oil on

plant anatomy and discovered structural deformations in the form of thickening of the epicuticular region, compression of the palisade and spongy parenchyma, compression of the vascular bundles, reduction of intercellular air spaces, distortion and reduction of the stomata. These changes generally inhibit chlorophyll synthesis thereby affecting plant growth and productivity (Baruah *et al.* 2014). Considering the response of Chl-a absorption features to soil TPH concentration, it is safe to assume that these physiological effects linked to oil pollution in various environments, caused a decrease in Chl-a production and consequently vegetation growth, health and productivity.

6.4.2 Effect of Oil Pollution on Chlorophyll, Carotenoids and Anthocyanins Absorption

Increased reflectance at chlorophyll absorption maxima and in-situ chlorophyll data from polluted vegetation reveal that chlorophyll absorption in polluted vegetation decreased by up to 300% compared to control vegetation. This reduction is significant and is bound to impact on not only the productivity of vegetation growing on polluted transects but also other living organisms by interfering with the trophic structure of the ecosystem. Arellano *et al.* (2015) reported low levels of chlorophyll in vegetation at oil-polluted sites in the Amazon forests which they attributed to a decrease in photosynthetic activity due to petroleum-induced stress. Whereas Al-Hawas *et al.* (2012) also observed that jojoba plants grown on crude oil contaminated soils suffered a significant decrease in chlorophyll content. Similarly, Agbogidi, Eruotor and Akparobi (2007) after experimenting with maize plants grown on polluted soils reported the presence of chlorosis in plants subjected to 20.8 mL of crude oil, which they attributed to destruction of chlorophyll pigments and cell injury. Earlier works by Baker (1970), Baudze and Kvesitadze (1997) and Odjegba and Sadiq (2002) suggested that hydrocarbons in crude oil cause structural and functional changes in the chloroplast that negatively affects the photosynthetic apparatus.

Also, the reflectance at the red edge position (REP) which strongly correlates with chlorophyll content in vegetation (Tian *et al.* 2011; Jong and Meer, 2006; Peñuelas and Filella, 1998), notwithstanding the variations of ground cover, showed a similar pattern. The first derivative of the red edge slope illustrated the rate of change in reflectance from the red to the NIR regions of the spectrum. Figure 6.7 showed that vegetation growing on the control transects had higher reflectance increment than vegetation on polluted

transects. Tian *et al.* (2011) reported a drastic increase in reflectance of healthy plants within the red edge (steep slope) likely because of the presence of leaf pigments, mainly chlorophyll which influence radiance absorption at the red region and leaf structures which influence scattering of radiance at the NIR region. Thus healthier plants expectedly have greater reflectance at the REP (maximum first derivative of the red edge slope). Following the Mann-Whitney test result, the null hypothesis of equivalence was rejected, suggesting that there was greater REP reflectance from vegetation on control transects than there was from polluted vegetation. The difference may be adduced to increased absorption in the red wavelength and increased scattering in the NIR region which are spectral signatures of healthy vegetation.

Another important spectral behaviour of the red edge slope in control vegetation is the observed shift towards longer wavelengths which contradicts the blue-shift (shift towards shorter wavelengths) observed in polluted vegetation. Frazier, Wang and Chen (2014) ascribed this behaviour to the widening of the chlorophyll absorption feature in response to the increase in leaf chlorophyll content.

Results of sensitivity analysis also differentiated the pigments chlorophyll a (Chl-a) and chlorophyll b (Chl-b) response to TPH concentration in soil. The most sensitive wavelength in the blue range occurred at the Chl-a absorption maxima (447.17 nm) while the most sensitive wavelength in the red range occurred at the Chl-b absorption maxima (630.32 nm) (See Figures 6.4 and 6.5 in Chapter 6). Although both these wavelengths showed sensitivity to soil TPH concentrations, Chl-a absorption was most affected as the reflectance difference between polluted and controlled vegetation at that wavelength was up to 300%. In contrast, Sims and Gamon (2002) found that the spectral channel around 650 nm was more sensitive to chlorophyll content in vegetation than the chlorophyll absorption features in the blue range. Since Chl-a is the principal pigment for photosynthesis, this may explain the severe effect associated with oil pollution in plants. Al-Hawas *et al.* (2012), Baruah *et al.* (2014) and Arellano *et al.* (2015) in their various studies reported that increasing crude oil contamination caused a significant decrease in the chlorophyll content which sometimes led to plant mortality in impacted vegetation.

The continuum-removed reflectance (CRR) of vegetation from polluted and control transects revealed absorbance at known carotenoids (CaR) and anthocyanins (AnC) features in polluted and control vegetation. CaR and AnC are generally considered as

stress indicators in vegetation (Hatier and Gould, 2008; Gitelson, Chivkunova and Merzlyak, 2009). They are accessory pigments that perform protective functions during photosynthesis in plants. Both AnC and CaR prevent photo-inhibition and photo-damage in plants by absorbing the excessive incident light that would otherwise damage the chlorophyll pigments. Merzlyak *et al.* (2008) stated that AnC occurrence intensifies with environmental factors such as increased solar radiation, extreme temperatures, drought, nutrient deficiency and other stress factors. In this study, CaR absorption increased by up to 300% while AnC absorption increased by less than 100% in polluted vegetation. The negative difference in the CaR and AnC absorption features (Figure 6.6 B) signifies increased synthesis of these accessory pigments in polluted vegetation. Thus, increased AnC and CaR absorption in polluted transects suggest that the presence of soil TPH induced stress in polluted which was either absent or minimal in control vegetation. Although there are diverse opinions on the location of maximum carotenoid absorption in the spectrum, previous studies established that this occurs between 470 nm to 500 nm (Chappelle, Kim and McMurtrey, 1992; Blackburn, 1998). Contrarily, there is some consensus on the absorption peak of AnC in the leaf spectrum as was reported by Merzlyak *et al.* (2008) and Gitelson *et al.* (2001) to be around 540 nm to 550 nm. Results of the present study are consistent with the literature in terms of the wavelength of maximum absorption of AnC and CaR. The central wavelength for the anthocyanins absorption feature was found to be at 559.09 nm while that of carotenoids centred at 457.34 nm.

Band depths indicate that chlorophyll absorption in polluted vegetation did not vary significantly along transects but somewhat differed in their response to the concentration of TPH in the soil. The band depth of known chlorophyll absorption features in the blue channel (447.17 nm) which showed the most sensitivity to soil TPH increased as TPH concentration decreased along polluted transects. The decrease may be due to the higher species abundance observed along polluted transects (please see Section 4.3.2.4 of Chapter 4) or diminishing TPH effect on chlorophyll synthesis as TPH concentration decreased. In any case, the result is consistent with earlier reports such as Baruah *et al.* (2014); Agbogidi, Eruotor and Akpoborie (2007) and Baker (1970) who maintained that as the concentration of crude oil in the soil increased, the chlorophyll content in leaves decreased. Hence, implying that higher doses of crude oil are more damaging to plants

than lower doses due to increased anaerobic processes that inhibit the growth of enzymes necessary for synthesising chlorophyll.

In segments along polluted transects, carotenoids (CaR) and anthocyanins (AnC) absorption varied greatly (coefficient of variation = 40 - 55). Interestingly, the anthocyanins and carotenoids correlated negatively with soil TPH rather than the expected positive correlation. The correlation coefficients were -0.382, -0.34, -0.19 for CaR1-3 respectively and -0.22 for AnC1 and 2. The result may mean that the concentration of TPH in the soil did not increase the production of these pigments in plants; however, it may also have resulted from the reduced vegetation of the polluted transects, particularly the spill epicentre where vegetation presence was near zero due to fire. From the above, we can infer that AnC and CaR spectral behaviour is dependent on vegetation abundance on polluted transects, and hence may not provide accurate information on vegetation stress.

6.4.3 Effect of Oil Pollution on Vegetation Vigour

The NDVVI values obtained from this study provide further evidence of the deleterious effect of oil pollution on vegetation. Vegetation productivity is linked to species richness and diversity (Cardinale *et al.* 2012; Hooper *et al.* 2012; Cardinale *et al.* 2011; Vihervaara *et al.* 2014; Mace, Norris and Fitter, 2012); hence these effects are likely to influence the biodiversity of the polluted transects. Oil contamination affects vegetation through various physical and chemical mechanisms. The intensity and extent of the adverse effect of oil on vegetation depend on the type of oil, soil type and exposure, contact method with vegetation, TPH concentration in the soil and the season (Hester *et al.* 2016; Michel and Rutherford, 2014; Lin and Mendelssohn, 2012). Pezeshki *et al.* (2000) maintained that the impact of oil pollution on vegetation increase with the volume of oil in contact with vegetation. Hester *et al.* (2016) noted that there is an inflexion point at which increased level of pollution results to irreversible damage to the plant. This pattern was observed on the polluted transects in the present study where vegetation characteristics such as taxa (species number), frequency, abundance and density increased along transects as TPH concentration decreased.

Results of the species diversity and distribution analysis in Chapter Four established that oil pollution significantly decreased species number, frequency, abundance and density

of vegetation on impacted transects. Further proof of this adverse effect was evident in the low NDVVI values extracted from polluted transects, affirming that the physical changes in vegetation characteristics observed during the field study were reflected in the spectral behaviour and detected remotely by the Hyperion sensor. The extraction of higher NDVVI values from control transects than from the polluted transects resulted in a significant difference ($p<0.05$) between them. Low NDVVI values indicate decreasing chlorophyll absorption at the blue and red wavelength which may be attributed to reduced species composition, abundance and health on transects while high NDVVI values indicate the reverse. Since vegetation vigour characterises vegetation productivity and health (Munyati and Ratshibvumo, 2011), it follows that the presence of TPH in polluted transects adversely affected both traits in vegetation. Previous studies have shown that changes in vegetation productivity and species diversity are common symptoms of ecosystem distress. Rapport, Regier and Hutchinson (1985) noted that environmental stress which includes oil pollution induce changes "in the size of dominant species, species diversity and a shift in species dominance to opportunistic shorter-lived forms". Evaluation of the importance value index (IVI) of vegetation on polluted and control transects (see section 4.3.2.6 of Chapter Four) supported this assertion. The IVI for herbs and shrubs (annual plants) was higher on polluted transects than on control transects, whereas more tree species had higher IVI values on control transects than on polluted transects (Figure 4.11). Noomen *et al.* (2012) reported changes in vegetation pattern in polluted fields, while Robson *et al.* (2004) found lower diversity indices for contaminated sites than for uncontaminated sites.

As vascular plants are common biodiversity indicators in the ecosystem, any condition that brings about drastic changes in vegetation (such as oil pollution) is bound to interfere with the ecosystem composition, structure and functions. The modelling results of vascular plants species diversity indices provide strong evidence of a relationship with narrowband chlorophyll-related vegetation indices. This relationship is stronger with NDVVI derived from hyperspectral wavelengths sensitive to soil TPH, hence, emphasising the need for incorporating the new index in biodiversity monitoring and conservation schemes. NDVVI is indicative of chlorophyll content and is hence a critical plant biochemical parameter for vegetation productivity and health (Baruah *et al.* 2014; Mishra *et al.* 2012; Curran, Dungan and Gholz, 1990). Not only did NDVVI significantly differ between polluted and control transects, but it also strongly correlated with the

vascular plants' species diversity. This result is consistent with Noomen *et al.* (2012) and Robson *et al.* (2004), as well as Arellano *et al.* (2017), Behl, Donval and Stibor (2011) (Arellano *et al.* 2017; Behl, Donval and Stibor, 2011; Carlson *et al.* 2007) were in agreement with our results. Hence, the low NDVVI values found over polluted transects can be attributed to reduced species composition, reduced abundance and deteriorating health of the vegetation.

The need to clarify the mechanism defining relationships between vegetation reflectance and species diversity remains primal, and several researchers have linked it to variations in vegetation biochemical parameters. For instance, Asner *et al.* (2009) following their study on airborne spectranomics reported that plant species have unique chemical fingerprints which correspond with spectral and species diversity. The chemical fingerprints are exhibited via differences in photosynthetic and photoprotective pigments, water and leaf structure and remotely measurable. Similarly, Aneece, Epstein and Lerdau, (2017) observed that interspecific variability in pigment (chlorophyll, anthocyanins, and carotenoids) levels in plants contributed to species differentiation using spectral metrics. Additionally, Clark and Roberts (2012) successfully classified seven tree species using hyperspectral metrics derived from wavelengths sensitive to vegetation chemistry and structure. Given these, the conclusion is that the superior performance of the NDVVI variants in estimating vascular plants species diversity is due to the selection of particular wavelengths that were sensitive to changes in vegetation biochemical parameters (pigments) responding to oil pollution. This procedure not only extracted relevant wavelengths from hundreds of hyperspectral wavelengths that are potentially redundant but also reduced the presence of noise from the data. Jacquemoud *et al.* (1996) stated that plant spectra might contain additional information unrelated to pigment concentration.

High NDVVI values of predsites contrasted with the low NDVI values and suggest that the new index is better at detecting vegetation presence than the NDVI in oil-polluted regions. Due to the adverse effect of oil pollution on vegetation such as reduced growth (Ogbo, Zibigha and Odogu, 2009; Chima and Vure, 2014; Lin and Mendelssohn, 2012) and increased mortality (Kinako, 1981; Baruah and Sarma, 1996; Tanee and Albert, 2015); the NDVVI designed to have maximum sensitivity to soil TPH, detects even sparse areas of vegetative growth/presence. Furthermore, the NDVVI variants successfully

predicted the diversity indices for the randomly selected sites from the satellite image of the study area. The low index values predicted for the swamps and water bodies are consistent with expectations. According to Orji (2013), the waterways of the Niger delta harbour invasive species, particularly the water hyacinth (*Eichornia crassipes* (Mart.) Solms). In their work, (Hejda, PyÅ¡ek and JaroÅ¡Ãk, 2009) asserted that invasive species adversely affect species richness, diversity and composition of invaded habitats. Hence, it is not surprising that the diversity indices are low for those pixels even though green vegetation is abundant.

Due to its ability to detect oil-induced stress in vegetation, the new NDVVI has potential as a spectral metric for measuring changes in ecosystem functions, an essential biodiversity variable as well as providing information about the condition and vulnerability of ecosystems, a biodiversity indicator. These are valuable information for effective biodiversity monitoring and protection. When incorporated in a temporal analysis, the NDVVI can reveal the extent of habitat degradation resulting from oil pollution. Since the variants were derived from remote sensing data, their application is standardised, scalable and repeatable making it a handy tool to achieve some of the Aichi 2020 targets set by the United Nations Convention on Biological Diversity (CBD) (Convention on Biological Diversity, 2010a). At local or regional scales, routine application of the NDVVI over areas with oil installations will facilitate detection of oil seepages, unreported spills and illegal bunkering activities. In essence, the index will facilitate effective biodiversity monitoring and conservation by providing decision-makers with relevant information on areas of high or low biodiversity. This information will ensure the efficient management of meagre resources by reducing the frequency and scale of cost-intensive field surveys.

6.5 Summary

This chapter focused on assessing the usefulness of Hyperion data (a hyperspectral sensor onboard NASA's EO-1 satellite) in biodiversity monitoring schemes. In other words, the study evaluated the performance of species diversity prediction models developed using spectral indices derived from Hyperion data. Achieving this task required tackling the research questions RQ2, RQ3 and RQ4 (listed in Chapter 2 Section 2.11.1, page 41). The answer to these questions involved a diversity study of vegetation; an analysis of the Hyperion image and regression analysis of both data sets. Non-parametric statistics were

employed as the data did not fit the assumptions of a normal distribution. The preceding analysis and results showed strong links between concentrations of soil TPH and the biochemical and spectral properties of vegetation. Hyperion data analysis provided evidence of crucial changes in the contents of leaf pigments necessary for photosynthetic activities in plants, changes in vegetation health and productivity (vigour) and successfully predicted the species richness and diversity indices of the study area.

7 General Discussion, Conclusions and Future Research

7.1 Introduction

This research has investigated applications of remote sensing to biodiversity monitoring in oil-polluted areas within the Niger Delta region of Nigeria. As a biodiversity hotspot, the degradation of the Niger Delta environment due to oil pollution is of major concern (Oluduro, 2012; Ngoran, 2011), as it leads to the loss of livelihoods, properties and national revenue (Ebegbulam *et al.* 2013; Nwachukwu, 2015; Oshienemen *et al.* 2018). Most importantly, the youth restiveness and militancy of people in the Delta associated with oil pollution-induced environmental degradation led to fatalities in recent years (Watts, 2004; Obi, 2009; Orji, 2012; Adams and Ogbonnaya, 2014; Oshienemen *et al.* 2018). Members of affected communities feel disfranchised and dissatisfied with the 'lacklustre efforts' of oil companies and the Nigerian government to remedy the situation (Okwoche, 2011; Aliyu and Ammani, 2011; Orji, 2012; Odoeme, 2013).

The overarching goal here was to develop tools for biodiversity monitoring, which are standardised, replicable, scalable and accessible to all interested parties. With vascular plant species as biodiversity indicators, four research questions (RQs) were investigated. RQ1 tested the hypothesis that oil pollution adversely affected vascular plant species composition (richness and diversity) and productivity (abundance and chlorophyll content). RQ2 hypothesised that satellite sensors could detect vascular plants susceptibility to oil pollution. RQ3 investigated the relationship between species diversity and spectral diversity metrics derived from satellite data, and finally, RQ4 sought to model the relationship between spectral metrics and species diversity to estimate vascular plants species diversity in polluted locations.

7.2 General Discussion

Achieving the overarching aim of this study required a three-dimensional approach. This included the application and evaluation of conventional field methods, analysis of multispectral (MS) data and analysis of hyperspectral (HS) data. The conventional methods provided useful field data, from which essential information including species abundance, richness and diversity, soil properties and chlorophyll content) was deducted,

encountered serious challenges (discussed in detail in Section 7.4.1.) during application (vegetation survey and sample collection). Analysis of multispectral data yielded limited information mainly on vegetation structure and distribution but lacked a detailed representation of subtle changes in vegetation reflectance. The analysis of hyperspectral data provided an in-depth revelation of vegetation response to oil pollution by highlighting the changes in pigment concentration, thus overcoming the limitations of MS data. The preceding sections present an all-encompassing discussion on the processes, techniques and approaches adopted in developing remote sensing tools for monitoring biodiversity in oil-polluted regions.

7.2.1 Application of Conventional Methods for Detecting Oil Pollution

Laboratory analysis of physicochemical properties in soil samples collected form spill locations revealed extreme levels of TPH (RQ1, RO1) which, also influenced other soil properties including phosphorus, lead, organic matter and heterotrophic bacteria populations in the soil. Oil pollution increases soil acidity (pH in polluted soil range from 6.15 to 8.02 according to Obire and Nwaubeta, 2002; Udeh, Nwaogazie and Momoh, 2013; Wang *et al.* 2013) and temperature by 1^0 to 2^0 C (Akubugwo, Elebe and Osuocha, 2016, Wang *et al.* 2013). The result from this study showed that the differences in pH and temperature of polluted and control soils were insignificant. The more significant effect of TPH on soil properties is in the depletion of nutrients such as phosphorus and nitrates in polluted soil. Both electrical conductivity and phosphorus concentration in polluted soil decreased substantially. This process renders the soil infertile for both agricultural and conservation programmes, a factor that exacerbated poverty in the region (United Nations Environmental Programme, 2011; Oluduro, 2012)

7.2.2 Application of Conventional Methods for Detecting the Effects of Oil Pollution on Vegetation

The study commenced with a vegetation survey to determine the vascular plant species diversity and create a baseline record for the study area (RQ1 and RO1). Comparing diversity indices of polluted and control transects revealed significant differences and validated the hypothesis that oil pollution adversely affects species diversity in the region.

226

Oil pollution effects on soil properties were detrimental to vegetation growth and productivity as significant differences were observed in frequency, abundance, richness, diversity and chlorophyll content of vegetation between polluted and control transects. Other researchers reported similar observations on oil polluted sites (Ogbo, Zibigha and Odogu, 2009; Chima and Vure, 2014). Some vegetation losses were immediate due to smothering by oil while others occurred over time due to nutrient depletion in soil supporting their growth consistent with previous reports (e.g. Njoku, Akinola and Oboh, 2008; Ogbo, Zibigha and Odogu, 2009). The high number of rare plant species observed in the study area is consistent with reports of biological endemism of the Niger Delta (Emoyan, Akpoborie and Akporhonor, 2008), and re-emphasises the need for biodiversity monitoring using indicator species. The acquisition of spectral signatures of such rare or indicator species will facilitate the development of remote sensing tools for managing biodiversity in the Niger Delta. The decrease in ecological importance of some plant species following oil pollution triggered both ecosystem services and economic losses, and in extreme cases, species extinction. Biodiversity loss is unacceptable globally and has led to international treaties to protect biodiversity and the ecosystem services they provide such as the United Nations Convention on Biodiversity (CBD) (United Nations General Assembly, 2000)

Plant lifeform was a crucial factor in determining the vegetation response to oil pollution. This study revealed that herbaceous perennial species were the most tolerant while herbaceous annuals were the most vulnerable to TPH. Several tree species observed on investigated transects were in secondary growth stages due to the presence of vast oil distribution pipelines that criss-cross the study area (United Nations Environmental Programme, 2011; Oluduro, 2012). The fragmentation of the ecosystem portends additional danger for biodiversity in the region as organisms that rely on matured and fully-grown tree species are forced to migrate to other areas, which may not be conducive for their survival, hence accelerating extinction rates and increasing poverty among their inhabitants. The food crop *Manihot esculenta* and creeping plant *Paullinia pinnata* were dominant in all locations investigated, however, certain species performed better in abundance on polluted transects than on control transects, which we attributed to the reduced competition for resources. Considering the economic importance of *Manihot esculenta* as a food and cash crop, further research into its survivability on polluted transects and the impact of its consumption on human health becomes pertinent. Ifemeje

and Egbuna (2016) showed that both the nutritional quality and shelf life of cassava fruit from polluted transects decreased substantially. Oil pollution triggered a process of resource partitioning for surviving species such that their importance value on polluted and control transect did not differ significantly. Ecologists have demonstrated that plants can extract and stabilise pollutants, which they store in their biomass (Glick, 2010; Ma *et al.* 2011). This knowledge formed the basis for the practice of phytoremediation, that is the removal of pollutants from soil using plant species (Wang *et al.* 2008; Nwaichi *et al.* 2015). Herbaceous species such as *Perotis indica, Kyllinga erecta*, *Sida cordifolia* were revealed to have potentials for phytoremediation of polluted sites in this study.

7.2.3 Analysis of Multispectral (MS) Data for Detecting Oil Pollution

Analysis of the MS dataset proved useful for detecting the presence of TPH in the soil. Spectral metrics derived from high-resolution MS data revealed the adverse effect of TPH on soil fertility measured as phosphorus and electrical conductivity. These metrics also showed sensitivity to TPH as the relationship was stronger on polluted transects than on control transects; however, the sensitivity of band metrics was greater, possibly due to the influence of RGB bands on plant photosynthetic processes. TPH influence on reflectance controlled the spectral diversity of the entire study area as demonstrated in the significant negative correlation between spectral metrics and species diversity indices of the study area. The increased habitat heterogeneity associated with oil spills may have contributed to this phenomenon.

7.2.4 Analysis of Multispectral (MS) Data for Detecting the Effects of Oil Pollution on Vegetation

Integrating remote sensing tools with field measurements yielded exciting results and highlighted its potentials for biodiversity monitoring. Analyses of multispectral Sentinel 2A imagery using open-source software revealed the intricate connection between vegetation biochemical parameters and their spectral signatures. Beginning with a test of the spectral variability hypothesis (SVH), the study demonstrated its validity and applicability in oil-polluted areas. However, results also revealed that the SVH is sensitive to oil pollution effects on vegetation, given the linear relationship observed between spectral diversity metrics and species diversity indices on both polluted and control transects. On control transects, this relationship was expected because of the high

species diversity, whereas, on polluted transects, an inverse relationship was expected due to low species diversity. This interesting result was attributed to the increased habitat heterogeneity following vegetation removal, waterlogging, and even burning of contaminated surfaces (habitat disturbance). Previous studies (Arellano *et al.* 2015; Pysek and Pysek, 1989; Jan Douda *et al.* 2012) show that these factors, measurable via remote sensing, influence species diversity. On control transects, the variations in the internal structures of different species such as pigments and tissues that produce unique spectral signatures controlled the relationship between spectral metrics and species diversity (Heumann, Hackett and Monfils, 2015). Previous studies testing the SVH achieved success with one set of metrics (Warren *et al.* 2014; Hall *et al.* 2012; Rocchini, Hernández-Stefanoni and He 2015; Schmidtlein and Fassnacht 2017). This study, however, demonstrated that a combination of metrics derived from different statistical computations significantly strengthened the spectral diversity-species diversity relationship enough to estimate the Simpson's and Shannon's indices for the study area successfully.

7.2.5 Implications for Biodiversity Monitoring in the Niger Delta region.

Oil pollution in the Niger Delta region of Nigeria poses an existential threat to the people as well as the vast and diverse species of flora and fauna that inhabit the region. Results of the present study demonstrated the relevance of incorporating remote sensing technology in tackling critical environmental issues caused by oil pollution. The strength of relationships between spectral diversity metrics and field measured species diversity data can be exploited to develop solutions to environmental problems such as halting species extinction through proper monitoring and conservation policies. The peculiar condition of the Niger Delta region also demands alternative methods to traditional field survey practices that endanger lives. The SVH lends itself to several applications including regular inspection of ecosystem services and biodiversity. Warren *et al.* (2014) noted that plant species diversity is an essential indicator of ecosystem health, which is monitorable via the SVH.

The combination of spectral metrics showing strong relationships with species richness and diversity measures may be useful for mapping the species distribution of a given ecosystem. Schmidtlein and Fassnacht (2017) successfully implemented a similar project

(2017) in mapping species occurrences in southern Germany using multispectral data. Species distribution maps enhance conservation decisions such as site prioritisation based on the structure and composition of plant communities revealed in the spectral variability of the maps (Rocchini, Chiarucci and Loiselle, 2004).

Most importantly, the SVH is applicable in oil spill monitoring programmes to detect occurrences. The result of this study showed a clear distinction in species composition of polluted and control transects and this difference was apparent in the vegetation reflectance. Such definitive characterisation will enhance the monitoring of changes in polluted vegetation over time and space by applying the SVH over an area of interest. Warren *et al.* (2014) detected changes in species composition of a habitat subjected to different levels of disturbances.

7.2.6 Analysis of Hyperspectral (HS) Data for Detecting Oil Pollution

Hyperspectral indices successfully detected TPH in the soil. Sensitivity analysis revealed that in many wavelengths the response to oil pollution was significantly different between polluted and control transects. Band depths of absorption maxima of pigments, NDVVIs and red edge position (REP) index were inversely related to soil TPH. Greater R^2 values existed between these indices and TPH than other field measurements including chlorophyll content, vegetation abundance and diversity. The strength of this relationship reflects the susceptibility of vegetation to TPH, which interferes with the spectral signature. Models of this relationship are useful for detecting spill points and estimating TPH concentration in the soil (Zhu *et al.* 2013). The REP indices successfully discriminated between polluted and control transects with an overall accuracy of 84%.

7.2.7 Analysis of Hyperspectral (HS) Data for Detecting the Effects of Oil Pollution on Vegetation

The development of prediction models for biodiversity monitoring in oil-polluted fields from satellite imagery produced two distinctive outcomes. Firstly, with proof that vegetation biochemical parameters are linearly related to spectral reflectance and intricately linked to species diversity, models based on this relationship were validated and implemented with reasonable success. Asner *et al.* (2009) and Aneece, Epstein and Lerdau (2017) linked the mechanism driving the species-spectral diversity relationship

to specific chemical fingerprints expressed as differences in plants photosynthetic and photoprotective pigments, water and leaf structure. Secondly, oil pollution disrupts these relationships substantially due to its deleterious effects (Scholten and Leendertse, 1991; Beaubien *et al.* 2008; Noomen *et al.* 2012; Njoku, Akinola and Oboh, 2008; Chima and Vure, 2014). This occurrence was apparent in the superior performance of NDVVI-based models for predicting species diversity and productivity. Sensitivity analysis confirmed that differences between polluted and control vegetation were amplified in chlorophyll absorption maxima in the blue (440±10 nm) and red (640±10 nm) spectral channels. These wavelengths were the most sensitive to TPH concentration in the soil. Although abnormal levels of hydrocarbon in the soil cause detectable changes in the mineralogical composition of the soil, this phenomenon was not investigated in this study as spectral wavelength evaluated were limited to the VIS and NIR regions.

Improving remote sensing applications for biodiversity monitoring relies on the availability of affordable hyperspectral and hyperspatial imagery. For low- and middle-income countries such as Nigeria to achieve their biodiversity targets, the availability of free or low-cost satellite data is imperative. Such valuable resources will ensure that scarce funds are directed towards meeting the needs of other crucial aspects of the National Biodiversity Strategy and Action Plans such as creating awareness amongst the population on the importance of biodiversity.

7.2.8 Monitoring Oil Pollution Impact on Vegetation in Kporghor Spill Area

The new hyperspectral indices derived from the Hyperion image performed not only firmly in predicting the species diversity of the investigated area of study, but also much better than the traditional narrowband indices (NBVIs). The overall best performing model depended on indices that measured chlorophyll content in vegetation. This result is consistent with previous reports such as Asner, Martin and Suhaili (2012) as well as Clark and Roberts (2012), who found strong links between the spectral diversity and biochemical variations in vegetation. Clark and Roberts (2012) notably reported that hyperspectral metrics, which respond to vegetation chemistry and structure, achieved the highest accuracies in discriminating tree species in a tropical rainforest.

The study is further proof of the strong relationship between species diversity and vegetation productivity in an ecosystem and offers a valuable resource for biodiversity monitoring. Although the mechanism by which species diversity influences ecosystem productivity is still a subject of much debate, what is sure is that the degradation of one leads to the loss of the other (Chapin *et al.* 2000; Mace, Norris and Fitter, 2012; Mori, Furukawa and Sasaki, 2013). Therefore, it is imperative that a uniform standard procedure for monitoring biodiversity that provides valuable information to policymakers remains a research focus among scientists.

The spatial map, which portrays the state of vegetation in the investigated area, is an essential tool for monitoring biodiversity in the Niger Delta region, as well as on a larger scale in areas prone to oil pollution. Considering the deleterious effects of oil pollution on vegetation, as reported in previous literature, and confirmed by the results of the present study, a combination of the derived hyperspectral metrics and baseline field study will provide to investigators adequate information on how much the biodiversity of the area is changing. These variables can be integrated into a time series analysis to detect oil spill sites and areas worst affected by oil pollution. Such realistic approaches to monitoring and preventing environmental degradation and loss of livelihood for inhabitants of affected areas can help ameliorate the restiveness associated with oil spill impacts. Change detection analysis can help to quantify in monetary terms the ecosystem services lost to oil pollution and environmental degradation.

7.3 Conclusions

This section presents the overall findings from investigating the research questions outlined in Chapter 2 Section 2.10.1 for each results chapter.

7.3.1 Effect of Oil Pollution on Vascular Plant Species in Rivers State (RQ1 and RQ2)

The main conclusion from this research is that oil pollution adversely affects biodiversity and ecosystem services in Rivers State of Nigeria (RQ1, RO1, RQ2, RO2, C-4). Evidence of this effect abounds in reduced vegetation physical (species abundance and diversity) and biochemical (leaf chlorophyll) parameters observed on polluted transects, some of which were measurable via remote sensing tools. Giving due consideration to these losses when compensatory policies are implemented is highly recommended as it will go a long

way in ameliorating the suffering of the indigenous population following oil spill incidents, thereby reducing militancy and restiveness in the Niger Delta region of Nigeria. Consequently, it is imperative that the rate and extent of oil spills are drastically reduced to avoid further damage in the Niger Delta ecosystem. Furthermore, environmental friendly remediation methods are encouraged to restore polluted areas to their pre-spill status without further damaging the vegetation. These methods include phytoremediation using TPH tolerant species such as revealed in this study.

7.3.2 Spectral Diversity Metrics for Detecting Effect of Oil Pollution on Biodiversity (RQ2, RQ3)

Spectral metrics from Sentinel 2A validated the SVH and revealed the adverse effect of TPH on vegetation (RQ2, RQ3, RO2, RO3, C-5). Models based on these metrics estimated soil and vegetation parameters successfully. However, the species-spectral diversity relationship was influenced by the presence of TPH in the soil, which challenged the SVH as originally proposed in the literature. The results of the present study imply that estimation of TPH concentration in polluted soil is possible remotely without going to the field to obtain soil samples. This potential is very crucial in the Niger Delta region of Nigeria where insecurity is a significant consideration in any field activity. With the successful discrimination of polluted and control vegetation using spectral diversity metrics, biodiversity monitoring over time and space is enhanced with satellite data.

7.3.3 Species Diversity Models for Monitoring Biodiversity (RQ4)

Hyperspectral data revealed subtle changes in vegetation reflectance that were inconspicuous in the multispectral data (RQ2, RO2 C-4). These changes may have resulted from oil pollution effect on pigment concentration including chlorophyll, anthocyanins, and carotenoids, which appeared to have interfered with vegetation spectra. The new index (NDVVI) derived from TPH sensitive Hyperion wavelengths outperformed traditional NBVIs in predicting the species diversity of the area (RQ4, RO4, C-6). The index provides an essential tool for monitoring biodiversity in oil-producing areas that are always at risk of pollution thereby limiting the need for time-consuming and cost-intensive field surveys. It also serves as a tool for early detection of spills when carried out routinely. The red-edge position (REP) index, also computed from

hyperspectral data, revealed vegetation response to oil pollution. There were obvious significant differences in red-edge reflectance of polluted and control vegetation attributable to the effect of hydrocarbon on chlorophyll absorption in the red channel of the spectrum.

Furthermore, oil pollution adversely affected vegetation characteristics such as abundance, and reduced reflectance at the REP. Despite the linear relationship between REP reflectance and vegetation abundance and chlorophyll estimate, the regression analysis showed that REP decreased for these parameters in the presence of soil TPH. Finally, the REP index successfully classified investigated transects as polluted or control with an overall accuracy of 84% which renders it a useful tool for detecting oil spills in inaccessible vegetated terrestrial areas.

7.4 Challenges

7.4.1 Data Availability

One of the major challenges encountered in this study was the unavailability of appropriate satellite data for the study area. Initially, very high-resolution data were intended for use; however, the prohibitive cost of acquiring this type of dataset discouraged their use. The Hyperion sensor acquired the only free hyperspectral data; however, the spatial resolution of 30 m limited its usefulness.

7.4.2 Field Work

The human conflicts in the study area during the fieldwork campaign also hindered data collection. The lack of support from the oil companies, despite a directive from the regulatory agency, put the fieldwork team at risk of kidnapping and other dangers. Attempts to collect as much as data as possible within short periods made species identification in the field challenging; hence photographs were taken to herbariums for their determination. This type of difficult conditions generally hinders academic research in Nigeria. It is recommended that oil companies and other corporate organisations support researchers as part of their social responsibility to society. Furthermore, the regulatory agency should enforce commensurate penalties for companies failing to adhere to directives to provide support for research.

7.4.3 Image Processing Tools

Conscientious effort to utilise free software for most of the image processing demanded the acquisition of new analytical skills. Most of the resources were available online and through funded workshops. However, in reality, this is a severe challenge for local researchers or stakeholders interested in applying remote sensing tools in monitoring the effect of oil pollution on biodiversity. The internet connectivity and funding problems are a significant hindrance to assessing these important analytical skill set.

7.5 Contribution to Knowledge

This research provides an overview of vascular plant species composition in Rivers State. The vegetation survey of 20 locations in five LGAs across the State in difficult terrain and insecure localities present a unique dataset that fills a gap in knowledge. This species inventory is crucial for biodiversity conservation and management in the region. The research in Chapter 4 identifies, on the one hand, oil-tolerant indicator species that are essential for biodiversity monitoring of polluted areas and on the other hand, the vulnerable species requiring protection through conservation policies. Vegetation species with potential for phytoremediation in oil-polluted sites also were identified. Phytoremediation is an environmentally friendly alternative clean-up method for impacted locations.

The evaluation of remote sensing tools integrated with field data revealed the mechanism through which oil pollution impact on vegetation productivity. The continuum removal and band depth analysis in Chapter 6 Section 6.3.4 demonstrated that oil pollution inhibits chlorophyll synthesis and radiance absorption, which triggers the production of photoprotective pigments such as the anthocyanins manifested in the increased band depth at the absorption maxima. Processing of satellite data also yielded indices (for instance, the normalised difference vegetation vigour index computed from TPH-sensitive Hyperion wavelengths) that may contribute to the development of essential biodiversity variables (EBVs) for biodiversity monitoring. Analysis of the spectral variability hypothesis (SVH) revealed the limitations of its application in environmentally degraded highly diverse regions. The results supported the hypothesis that habitats with higher species diversity have higher spectral diversity, but also that habitat heterogeneity associated with oil pollution also supports high spectral diversity.

This revelation is essential for efficient monitoring and management of biodiversity at local, regional and global scales. Additionally, the study demonstrated that the estimation of soil TPH is possible with a combination of spectral metrics in prediction models. This may serve as a useful tool in monitoring oil pollution in hard to reach areas of the Niger Delta region.

7.6 Future Research

Based on the results of the present research, there is potential to improve biodiversity monitoring using satellite data. Future research projects may involve implementing the species diversity models in other regions subjected to oil pollution to determine species identification using very high spectral and spatial resolution imagery. Spectral library of the indicator and dominant species in the study area can be acquired using the field spectrometer provided the area is secured. The acquisition of spectral signatures of the indicator and dominant species across the Niger Delta region of Nigeria will facilitate biodiversity conservation and monitoring and help the country meet its National Biodiversity Strategy and Action Plans. An area of hyperspectral remote sensing of vegetation currently under-researched is the estimation of TPH from vegetation reflectance. With the high dimensional hyperspectral data, investigating the shortwave infrared (SWIR) where water and atmospheric absorption maxima occur may yield interesting tools for oil spill detection on forested areas. Additionally, the proximate chemical composition of major food crops grown in the region needs investigating to determine their safety for consumption, and links between these and general wellbeing of inhabitants determined to facilitate the provision of health care services.

8 Appendix

8.1 Description of Vegetation and Biodiversity Measures

8.1.1 Species Taxa

Taxa is a measure of the counts of species occurring in each segment along investigated transects. It provides an estimate of the species richness and diversity of the segments. Determined from species inventory tally sheets.

8.1.2 Sorenson's Similarity Index of Transects

Similarity index measures the degree of association or agreement of two entities or variables, in this case, vegetation data from polluted and control transects (Warrens, 2008). In this study, segments of polluted and control transects across the entire study area were clustered into groups based on their similarity index which, quantifies their level of association concerning species composition. The formula for Sorenson's similarity index (IS) is:

$$IS = \frac{2MW}{MA+MB} * 100$$

Where
MW = Sum of the smaller numbers of plant species common to the control and test transects
MA = the sum of all plant species in the transect A
MB = the sum of plant species in the transect B

8.1.3 Number of Individual Plants

This is a measure of the abundance of each species observed per segment. The number of individual plants per species was determined from tally sheets

8.1.4 Frequency

This is the probability of a plant species occurring in a given number of segments (Bonham, 2013a). Frequency of species occurrence was used to detect any changes in vegetation composition of polluted and control transects. Vegetation frequency was calculated from species inventory data as:-

$$\text{Frequency} \ = \ \frac{number\ of\ segments\ in\ which\ species\ occured}{number\ of\ segments\ investigated}$$

8.1.5 Density

Also a measure of abundance defined as the number of individuals of a given species occurring in a given sample unit. Density estimate are relevant for monitoring plant responses to environmental disturbances (Bonham, 2013b). Density estimates for observed species in the study area were calculated to identify vegetation responses to oil pollution using the following formula:-

$$\text{Density} = \frac{number\ .of\ individuals\ of\ the\ species\ in\ all\ the\ segments}{Total\ number\ of\ segments\ studied}$$

8.1.6 Importance Value Index

This is a measure of the ecological importance of a given species in an ecosystem. It is frequently used to prioritise species for conservation purposes (Zegeye, Teketay and Kelbessa, 2006), however, in this study, the IVI of species was used to determine the effect of oil pollution on vegetation structure by comparing the IVI of species on polluted and control transects. IVI was calculated by summing the relative values of frequency and density where

$$\text{Relative frequency} = \frac{frequency\ of\ a\ given\ species}{sum\ frequency\ of\ all\ species} * 100$$

And

$$\text{Relative density} = \frac{number\ of\ individuals\ of\ a\ species}{totalnumber\ of\ individuals} * 100$$

8.1.7 Indicator Species

Indicator species are organisms whose presence, absence or abundance provides an ecological indication of community or habitat types, environmental conditions or environmental changes (Cáceres *et al.* 2012). They can provide important information on the type and volume of environmental pollution and other stressors. A good indicator species is one that is both abundant in a specific type of habitat (specificity) and predominantly found in this type of habitat (fidelity).

Indicator values of a species (i) at a given site (j) is calculated as

$\text{IndVal}_{ij} = \text{Specificity}_{ij} * \text{Fidelity}_{ij} * 100$

Where

IndVal$_{ij}$ = indicator value of a given species (i) in relation to a (j) type of site

Specificity$_{ij}$ = proportion of sites 'j' in which occurred species 'i'

Fidelity$_{ij}$ = the proportion of the number of individuals (abundance) of species 'i' that occurred in site 'j'

In this study, indicator value of species was calculated in *R* using the *indicspecies* package developed by De Cáceres and Jansen (2016), to identify species whose presence or absence reveal the occurrence of oil pollution in the study area.

8.1.8 Species Occurrence Curve (SOC)

This is a measure of how individuals of a species are distributed among the sampling units (segments). Species occurrence curve was used to visualise the distribution of species in polluted and control segments and to determine the most frequently occuring species. The curve is derived by plotting the cumulative count of species on the x-axis and the number of plots on the y-axis.

8.1.9 Species Accumulation Curve (SAC)

Provide estimations of the number of species in a given habitat and is used to compare the richness of different communities at comparable levels of sampling efforts (Dorazio *et al.* 2006). In this study, the SAC was plotted to illustrate the differences in the species richness of polluted and control transects.

8.2 Description of Vegetation Indices

8.2.1 Normalised Difference Vegetation Index (NDVI)

The NDVI originally derived by Pearson and Miller (1972) is a non-linear transformation of the visible (red) and near-infrared bands of vegetation signals captured by remote sensors. It is useful for the assessment of vegetation characteristics such as biomass (AGB), leaf area index (LAI), the percentage of vegetation cover and the fraction of absorbed photosynthetic active radiation intercepted (fPAR) (Pettorelli *et al.* 2005; Adoki, 2012). Although factors including soil colour, atmospheric effects, illumination and observation geometry affect the index, it remains the most widely used vegetation index for analysing remotely sensed data. The NDVI can serve as a functional biotic

indicator in biodiversity monitoring schemes (de Bello *et al*, 2010) NDVI is calculated from the following formulae for broadband and narrowband respectively:

$$NDVI = \frac{(NIR-Red)}{(NIR+Red)}$$

(5)

$$NDV I = \frac{(R_{800}-R_{670})}{(R_{800}-R_{670})}$$

(6)

Where

NIR is the reflectance from the near-infrared band
Red/R is the reflectance from the visible red band(s)

8.2.2 Soil Adjusted Vegetation Index (SAVI)

The vegetation index adjusted for soil reflectance is for use in areas of sparse vegetation. According to Huete (1988), the SAVI minimises "soil brightness influences from spectral vegetation indices involving red and near-infrared (NIR) wavelengths" using the parameter L. SAVI is calculated from the following formula for narrowband

$$SAVI = (1 + L) * \frac{(R_{800}-R_{670})}{(R_{800}+R_{670}+L)}$$

(7)

And for broadband

$$SAVI = NIR - \frac{RED}{NIR + RED + L} * (1 + L)$$

(8)

Where

R is the reflectance at the listed waveband
NIR is the reflectance from the near-infrared band
L is the constant 0.5

8.2.3 Red Edge Position (REP)

The Red Edge Position (REP) determines spectral vegetation reflectance by correlating chlorophyll content with reflectance (Noomen, Van der Meer and Skidmore, 2005). It is the inflexion point on the slope between the red absorption and the near-infrared reflectance. Factors that affect plant health affect the chlorophyll content in leaves and lead to increased reflectance in the red region. Studies show that decreasing leaf chlorophyll causes the red edge position to shift towards shorter wavelengths (Noomen and Skidmore, 2009). Whereas increasing chlorophyll content results in REP shifting towards longer wavelengths in plants growing on polluted soils (Cho and Skidmore, 2006). There are several methods for calculating REP including maximum first derivative, linear four-point interpolation technique, polynomial fitting technique and the inverted Gaussian fitting technique (Noomen *et al.* 2012). In this study, REP determination is from the maximum first derivative and linear interpolation method. The formula for the linear method is based on Clevers (1994) and given as

$$REP \ = \ 700 \ + \ 40 * \frac{(R_{REP} - R_{700})}{(R_{740} - R_{700})}$$

(9)

Where $R_{REP} \ = \frac{R_{670} + R_{780}}{2}$

(10)

700 and 40 = constants resulting from interpolation in the 700 nm – 740 nm interval

R = reflectance at listed waveband.

8.2.4 Anthocyanin Reflectance Index (ARI)

Anthocyanins are water- soluble leaf pigments that determine how plants respond to stress conditions in the environment. (Ustin *et al.* 2009). They frequently occur in higher plants at the epidermal and mesophyll cells and are bio-synthesised in response to soil contamination, extreme temperatures, pathogenic infections, nitrogen and phosphorus deficiencies, wounding or other environmental stress factors occurring in plants. Anthocyanins also screen out excess solar radiation from reaching the reaction centre. They are stress indicators as well as mitigators (Hatier and Gould, 2008). Together with chlorophyll contents in leaves, the anthocyanins provide essential information on the

health status of vegetation (Gitelson, Chivkunova and Merzlyak, 2009). The ARI is a non-destructive method of estimating the leaf anthocyanins using data from remote sensing.

Researchers determine leaf anthocyanin content using both broadband and narrowband derived indices (Gitelson *et al.* 2001; Gitelson *et al.* 2006; Gitelson, Chivkunova and Merzlyak, 2009; van den Berg, Abby K and Perkins, 2005). These indices are a combination of reflectance values from spectral bands, which are sensitive to changes in the anthocyanin content in leaves. Gitelson *et al.* (2008) compared the anthocyanin estimation accuracy of a few prominent indices, and results showed that the anthocyanin reflectance index (ARI) and its modified version (mARI) were most successful with the least root mean square error (RMSE). The following equations are used to estimate both indices

$$ARI \; = \; (\frac{1}{R_{green}} - \frac{1}{R_{red-edge}})$$

(11)

$$mARI \; = \; (\frac{1}{R_{green}} - \frac{1}{R_{red-edge}}) \; * \; R_{NIR}$$

(12)

Where

R_{green} = is reflectance at the green waveband,
$R_{red-edge}$ = reflectance at the red waveband.
R_{NIR} = reflectance at the near infrared

8.2.5 Carotenoid Reflectance Index (CRI)

Carotenoids are plant pigments that help to protect plants from harmful and excessive solar radiation and essential for photosynthetic functions in green plants. Unhealthy vegetation contains higher concentrations of carotenoids, hence is an indicative measure of stress in plants. Carotenoids strongly absorb light in the blue band and exhibit varying degrees of reflectance at longer wavelengths (Gitelson *et al.* 2002). Several studies assessing the sensitivity of spectral bands to pigment content have been carried out with various indices suggested for estimating carotenoid content in plants (Chappelle, Kim and McMurtrey, 1992; Blackburn, 1998; Peñuelas and Filella, 1998) However, Gitelson

et al. (2002) identified the limitations in these indices and proposed the following formula for deriving carotenoid contents

$$CRI2 = (\lambda_{510}^{-1}) - (\lambda_{700}^{-1})$$
(13)

Where
λ_{510} is reflectance at 510nm +/- 5
λ_{700} is reflectance at 700nm +/- 7.5

Other important indices relevant to measuring total petroleum hydrocarbon effect (TPH) effect on plant biochemical parameters include

Pigment Specific Simple Ration (PSSR)

Pigment Specific Normalised Difference (PSND)

Modified Chlorophyll Absorption Ratio Index (MCARI)

Transformed Chlorophyll Absorption Ratio Index (TCARI)

Maximum First Derivative Spectrum (deRES)

And so on (Zhu *et al.* 2013).

8.3 Supplementary Data

8.3.1 Laboratory Analytical Methods

This section describes the analytical methods utilized by the International Energy Services Limited laboratory located at 34 Old Aba Road, Port Harcourt, Rivers State, Nigeria to determine the various soil physico-chemical properties.

8.3.1.1 General Health and Safety Observations

A.   Health Safety and Environment

- **Hazards**
  - Toxic chemicals
  - Glass breakage
  - Chemical burns
  - Generation of waste
- **Personal protective equipment**

  All personnel must be aware of chemical handling technique. Wear the appropriate personal protective equipment at all times in the work area. PPEs shall

include laboratory coats, coverall, safety shoes, hand gloves and respiratory masks.

8.3.1.2 Total Petroleum Hydrocarbons: EPA 8015

https://www.epa.gov/sites/production/files/2015-12/documents/8015d_r4.pdf

8.3.1.3 Determination of Arsenic Ion in Water

A.   Purpose

This document describes the determination of arsenic ion in water in water

B.   Scope

This document covers the determination of arsenic ion in fresh water, waste water and sea water, associated hazards, personal protective equipment required and quality control.

C.   Methods

Atomic Absorption Graphite furnace, ASTM D 2972

D.   Summary of Method

Water adjusted to approximately pH 8.3 is titrated with silver nitrate solution in the presence of potassium chromate indicator. The end point is indicated by persistence of brick red silver chromate color.

E.   Apparatus

- **Equipment**
  - Weighing balance
  - Weighing boat
  - Magnetic stirring bar
  - Pipette filler
  - Filter paper
  - Graphite furnace
- **Glassware**
  - Volumetric flask, 1L
  - Graphite tubes
  - Conical flask
  - Burette
  - Beakers
  - Glass funnel

F.   Reagents and Solutions

- **Reagents**
  - Arsenic solution intermediate (1m=10μg As); Arsenic standard solution. Dilute 10ml of arsenic intermediate solution and 1ml of HNO_3 to 100ml, this standard is used to prepare working standards at the same time of analysis.
  - Hydrogen peroxide (30%)-H_2O_2.
  - Nickel Nitrate solution –dissolve 5g of Nickel nitrate (Ni(NO3)2.6H20) in water and dilute to 100ml.

- Nitric acid-concentration nitric acid. Nitric acid (1+9) –add 1ml of HNO_3 to 9ml of water.
- Purified argon is the usual support gas though nitrogen may be used if recommended by the instrument manufacturer.

G.   Procedure

- All glass wares should be cleaned and rinsed with HNO_3 (1+1) and with water.
- Add 8.0ml of filtered and acidified sample to a beaker or flask.
- Then add 1ml of HNO_3 (1+9) and 1.0ml of Nickel nitrate solution. Mix thoroughly and inject a measured aliquot of sample into the furnace device.

H.   Calibration

- Prepare calibration standards by diluting stock solution at the time of analysis for best result, prepare these calibration standard solutions daily, or as required, and discard after use.
- Prepare a blank and at least 3 calibration standard in graduated amounts in the appropriate range. Space the calibration standard evenly in concentrations from 0 to 20% greater than the highest expected value.
- Prepare the calibration standards with same acid and at the same acid concentration as will result in the sample to be analysed either directly or after processing.
- Beginning with the blank and working towards the highest standard, analyze the solutions and record the readings. Repeat the operation and record the readings.
- Repeat the operations with both the calibration standards and the samples a number of times to get a reliable average reading for each solution.
- Construct an analytical curve by plotting the absorbance of standards versus their conc. on linear graph paper. Alternatively, read direct in conc. if the capability is provided with instrument.
- Prepare a new analytical curve for each series of samples or whenever a new Graphite Tube is used.

I.   Reporting Results

Record results directly into analyst notebook before transferring to the relevant test/analysis result.

8.3.1.4 Determination of Lead Ion in Water

A.   Purpose

This document describes the determination of lead ion in water in water

B.   Scope

This document covers the determination of lead ion in fresh water, waste water and sea water, associated hazards, personal protective equipment required and quality control.

C.   **Methods**

Direct Atomic Absorption ASTM D 3559
        Summary of Method
Determination of lead in water/soil samples.

D.   **Apparatus**

- **Equipment**
  - Weighing balance
  - Weighing boat
  - AAS
  - Pipette filler
  - Filter paper
- **Glassware**
  - Volumetric flask, 1L
  - Pipette
  - Conical flask
  - Burette
  - Beakers
  - Glass funnel

E.   **Reagents and Solutions**

- **Reagents**
  - Lead stock solution (1ml=1mg Pb)
    Dissolve 1.5999g of lead nitrate ($Pb(NO_3)_2$) in a mixture of 10ml of HNO_3 and 100ml of water. Dilute to 1L of water.
    (Warning: lead salts are toxic, handle with care to avoid personal contamination)
  - Lead standard solution (1ml=0.1mg Pb)
    Dilute 100ml of stock lead solution to 1L with HNO_3 (1+499), store all solutions in polyethylene bottles.
  - Nitrate acid (1+499)
    Add 1 volume of HNO_3 to 499 volumes of water.

F.   **Procedure**

  - Measure 100ml or less of the sample into a 125ml conical flask or beaker.
  - Aspirate each filtered and acidified sample and determine its absorbance to concentration at 283.3 nm.
  - Aspirate HNO_3 (1+499) between samples.

G.   **Calibration**

  - Prepare 100ml each of a blank and at least four standard solutions by diluting the lead standard solution with HNO_3 (1+499). Prepare the standard each time the test is to be performed.
  - Aspirate the blank and standards and record the instruments readings.
  - Aspirate HNO_3 (1+499) between standards.
  - Prepare an analytical curve by plotting the absorbance versus the concentration for each standard on linear graph paper.

Record results directly into analyst notebook before transferring to the relevant test/analysis result

8.3.1.5 Determination of Cadmuim Ion in Water

A.   Purpose

This document describes the determination of cadmuim ion in water in water

B.   Scope

This document covers the determination of cadmuim ion in fresh water, waste water and   sea water, associated hazards, personal protective equipment required and quality control.

C.   Methods

Direct Atomic Absorption ASTM D 3557

❖ **Summary of Method**
Determination of cadmium in water/soil samples.

D.   Apparatus

- **Equipment**
    - Weighing balance
    - Weighing boat
    - AAS
    - Pipette filler
    - Filter paper
- **Glassware**
    - Volumetric flask, 1L
    - Pipette
    - Conical flask
    - Burette
    - Beakers
    - Glass funnel

E.   Reagents and Solutions

- Calcium solution: Dissolve 630 mg calcium carbonate, $CaCO_3$, in 50 mL of 1 + 5 HCl. If necessary, boil gently to obtain complete solution. Cool and dilute to 1000 mL with water.
- Hydrochloric acid, HCl, 1%, 10%, 20% (all v/v), 1 + 5, 1 + 1, and conc.
- Lanthanum solution: Dissolve 58.65 g lanthanum oxide, La_2O_3, in 250 mL conc HCl. Add acid slowly until the material is dissolved and dilute to 1000 mL with water.
- Hydrogen peroxide, 30%.
- Nitric acid, HNO_3, 2% (v/v), 1 + 1, and conc.
- Aqua regia: Add 3 volumes conc HCl to 1 volume conc HNO_3.
- Cadmium: Dissolve 0.100 g cadmium metal in 4 mL conc HNO_3. Add 8.0 mL conc HNO_3 and dilute to 1000 mL with water; 1.00 mL = 100 µg Cd.

-

F.   Procedure

- Measure 100ml or less of the sample into a 125ml conical flask or beaker.
- Aspirate each filtered and acidified sample and determine its absorbance to concentration at 396 nm.
- Aspirate HNO_3 (1+1) between samples.

G.   Calibration

- Prepare 100ml each of a blank and at least four standard solutions by diluting the cadmuim standard solution with HNO_3 (1+1). Prepare the standard each time the test is to be performed.
- Aspirate the blank and standards and record the instruments readings.
- Aspirate HNO_3 (1+1) between standards.
- Prepare an analytical curve by plotting the absorbance versus the concentration for each standard on linear graph paper.

H.   Reporting Results

Record results directly into analyst notebook before transferring to the relevant test/analysis result

8.3.1.6 Digestion of Sample for Metals Analysis with Mineral Acids and Heating at Atmospheric Pressure (METHOD: ASTM D 1971B)

A.   Apparatus:

Steam bath or hot plate

B.   Reagents and Materials:

- Hydrochloric Acid (Sp Gr 1.19) – Concentrated Hydrochloric Acid (Hcl)
- Nitric Acid (Sp Gr 1.42) – Concentrated Nitric Acid (HNO_3)
- Filter Paper – Fine Textured, Acid Washed, Ash-less.

C.   Procedure:

- **Preparation for liquid sample (acidification),**
  - Measure 100ml of well mixed sample into a 125ml beaker or flask and add 0.5ml of Conc HNO_3.
  - If the sample has been preserved at a recommended level of 0.5ml of Conc HNO_3 per litre of sample, the addition of acid at this step can be omitted.
- **Preparation for solid or semi-solid sample,**
  - Sample should be homogenous and solid samples should be finely ground (samples are first dried at $<60^oC$, then ground and sieved through a 20mm/10mesh sieve). The sample should not be digested as received (wet)
  - Weigh out accurately to the nearest milligram, 0.5g or otherwise and place in a 125ml (or larger) beaker or flask and add 100ml of distilled water and 0.5ml of HNO_3.
- **Finishing (Digestion)**

- Add 5ml of HCl to the beaker or flask and heat the samples on a stream bath or hot plate in a well ventilated hood until the volume has been reduced to 15 to 20ml making certain that the sample does not boil. (Alternatively the sample mixture with acids is heated at 90ºC for 2hrs)
- When analyzing samples containing appreciable amount of solid matter, the actual amount of reduction in volume is left to the discretion of the analyst.
- Cool and remove solids (filter), quantitatively transfer sample to 100ml volumetric flask or other suitable size and Adjust to volume. (The digested sample is filtered/ washed and diluted as the case may be with water to appropriate volume and then;
- Proceed with assay of digested sample by atomic absorption spectrophotometry (flame atomization or plasma emission spectroscopy).

Note: This procedure presents a digestion technique widely used for water, influent and effluent, sludge, soil, sediment as well as plant and animal tissue etc samples to give what is defined as total recoverable metals. The metals digestion procedure of the USEPA for total recoverable metals is similar, but uses one-half the amount of HCl that is specified in this practice.

D.   Interferences

- In some samples, the metals of interest are bounds or occluded in a matrix that is impervious to dissolution by the acids. This is most frequently encountered in geological samples.
- The complete dissolution of a metal may not occur due to the digestion conditions being insufficiently rigorous for a particular metal. In other instances, the chemical makeup of the sample may render the digestion acids ineffective.

8.3.1.7 Total Heterotrophic Plate Count

A.   Purpose

This document describes the determination of Total Heterotrophic Bacteria (THB) in water.

B.   Scope

This document covers the determination of Total Heterotrophic Bacteria (THB) in fresh water, waste water and sea water, associated hazards, personal protective equipment required and quality control.

C.   Methods

APHA 9215 B Pour Plate Method
❖ **Summary of Method**
Determination of total hetrotrophic bacteria (THB) water/soil samples.

D.   Apparatus

- **Equipment**
  - Bags, Whirl-Pak with declorinating agent, sterile, 180-mL
  - Bags, Whirl-Pak without declorinating agent, sterile, 205-mL and 710-mL
  - Clamp, Test Tube Colony Counter, Quebec, 110 VAC, 60 Hz.
  - Colony Counter, Quebec, 220 VAC, 50 Hz

- Counter, hand tally
- Germicidal ClothsHot Plate, 120 VAC, 50/60 Hz
- Hot Plate, 240 VAC, 50/60 Hz
- Incubator, Culture, Low-Profile, 120 VAC, 50/60 Hz
- Incubator, Culture, Low-Profile, 220 VAC, 50/60 Hz
- Thermometer -10 to 110 °C
- **Glassware**
  - Pipets, Serological, 1 mL, sterile, disposable
  - Pipets, Serological, 10-11 mL, sterile, disposable
  - Beaker, 250-mL
  - Bottle, sample, glass, with cap, 118-mL
  - Dish, Petri, 100 x 15 mm, sterile, disposable
  - Dish, Petri, 100 x 15 mm, sterile, disposable

E.   Reagents and Solutions

8.3.1.7.E.1 Dechlorinating Reagent Powder Pillows

8.3.1.7.E.2 Dilution Water, Buffered, sterile, 99-mL

8.3.1.7.E.3 Plate Count Agar (Tryptone glucose yeast agar) Tubes

F.   Procedures

8.3.1.7.F.1 Preparation: Thoroughly mix samples using a mechanical shaker for 15 seconds

8.3.1.7.F.2 Dilution: serial dilution using sterile water so that the total number of colonies on aplate will be between 30-300.

- Pipet 0.1 ml of diluted sample into sterile petri dish before adding melted culture nmeduinm and mix carefully
- Solid agar is melted in boiling water and maintained at temperatures of 44 to 46 0C
- Place solidified plates in an incubatoir

G.   Incubation:-

- 35^0C for 48 hours

H.   Reporting Results

Count all colonies on selected plates promptly after incubation. If count must be delayed temporarily, store plates at 5 to 10 °C for no more than 24 hours, but avoid routine delays.

8.3.1.8 Determining the pH of samples

❖ **Apparatus**
- Electrometric titrator
- Titration vessel (020-mL, tall-form Berzelius beaker with a three-hole stopper or a 125-mL or 250-mL erlenmeyer flask with a two-hole stopper.
- Magnetic stirrer.
- Pipets, volumetric.
- Flasks, volumetric, 1000-, 200-, 100-mL.

- Burets, borosilicate glass, 50-, 25-, 10-mL.
- Polyolefin bottle, 1-L.

❖ **Reagents and Solutions**
- **Reagents**
  - Carbon dioxide-free water: distilled or deionized water boiled for 15 minutes and cooled to room temperature with pH $\geq$ 6.0 and conductivity <2 µmhos/cm.
  - Potassium hydrogen phthalate solution, approximately 0.05N
  - Standard sodium hydroxide titrant, 0.1N
  - Standard sodium hydroxide titrant, 0.02N
  - Hydrogen peroxide, H2O2, 30%.
- **Solutions**
  - Bromphenol blue indicator solution, pH 3.7 indicator
  - Metacresol purple indicator solution, pH 8.3 indicator
  - Phenolphthalein indicator solution, alcoholic, pH 8.3 indicator.
  - Sodium thiosulfate, 0.1M4.
  -

❖ **Procedure**
- **Hot peroxide treatment**:
  - Pipet a suitable sample into titration flasks.
  - Measure pH. If pH is above 4.0 add 5-mL increments of 0.02N sulfuric acid (H2SO4) to reduce pH to 4 or less.
  - Remove electrodes.
  - Add 5 drops 30% H_2O_2 and boil for 2 to 5 min.
  - Cool to room temperature and titrate with standard alkali to pH 8.3.
- **Potentiometric titration curve**:
  - Measure sample pH.
  - Add standard alkali in increments of 0.5 mL or less, such that a change of less than 0.2 pH units occurs per increment.
  - After each addition, mix thoroughly but gently with a magnetic stirrer. Avoid splashing. Record pH when a constant reading is obtained.
  - Continue adding titrant and measure pH until pH 9 is reached.
  - Construct the titration curve by plotting observed pH values versus cumulative millilitres titrant added.
  - Determine acidity relative to a particular pH from the curve.

❖ **Reporting Results**
- Report pH of the endpoint used, as follows: ''The acidity to pH _____ = _____ mg CaCO3/L.'' If a negative value is obtained, report the value as negative. The absolute value of this negative value should be equivalent to the net alkalinity.

8.3.1.9 Determination of Nitrate ion in water

A.   Purpose

This document describes the determination of Nitrate ion in water.

B.   Scope

This document covers the determination of Nitrate ion in fresh water, waste water and sea water, associated hazards, personal protective equipment required and quality control.

C.   Methods

APHA 4500 Nitrate Electrode Method

❖   **Summary of Method**

Determination of nitrate ion (NO_3^+) water/soil samples.

❖   **Apparatus**

- **pH meter, expanded-scale or digital, capable of 0.1 mV resolution.**
- **Double-junction reference electrode. Fill outer chamber with (NH4)2SO4 solution.**
- **Nitrate ion electrode: Carefully follow manufacturer's instructions regarding care and storage.**
- **Magnetic stirrer: TFE-coated stirring bar.**

D.   Reagents and Solutions

- Nitrate-free water: Use for all solutions and dilutions.
- Stock nitrate solution:
- Standard nitrate solutions: Dilute 1.0, 10, and 50 mL stock nitrate solution to 100 mL with water to obtain standard solutions of 1.0, 10, and 50 mg NO3–-N/L, respectively.
- Buffer solution: Dissolve 17.32 g Al2(SO4)318H2O, 3.43 g Ag2SO4, 1.28 g H3BO3, and 2.52 g sulfamic acid (H2NSO3H), in about 800 mL water. Adjust to pH 3.0 by slowly adding 0.10N NaOH. Dilute to 1000 mL and store in a dark glass bottle.
- Sodium hydroxide, NaOH, 0.1N.
- Reference electrode filling solution: Dissolve 0.53 g (NH4)2SO4 in water and dilute to 100 mL.

E.   Procedure

- **Preparation of calibration curve:**
  - Transfer 10 mL of 1 mg NO_3^--N/L standard to a 50-mL beaker, add 10 mL buffer, and stir with a magnetic stirrer. Immerse tips of electrodes and record millivolt reading when stable (after about 1 min).
  - Remove electrodes, rinse, and blot dry.
  - Repeat for 10-mg NO_3^--N/L and 50-mg NO_3^--N/L standards.
  - Plot potential measurements against NO3–-N concentration on semilogarithmic graph paper, with NO3–-N concentration on the logarithmic axis (abscissa) and potential (in millivolts) on the linear axis (ordinate). A straight line with a slope of +57 ±3 mV/decade at 25°C should result.
  - Recalibrate electrodes several times daily by checking potential reading of the 10 mg NO3–-N standard and adjusting the calibration control until the reading plotted on the calibration curve is displayed again.

- **Measurement of sample:**
  - Transfer 10 mL sample to a 50-mL beaker, add 10 mL buffer solution, and stir (for about 1 min) with a magnetic stirrer.
  - Measure standards and samples at about the same temperature. Immerse electrode tips in sample and record potential reading when stable (after about 1 min).
  - Read concentration from calibration curve.
- **Precision**
  - Over the range of the method, precision of ±0.4 mV, corresponding to 2.5% in concentration, is expected.

8.3.1.10 Determination of Total Dissolved Phosphorus ion in water

A. Purpose

This document describes the determination of Phosphorus ion in water.

B. Scope

This document covers the determination of Phosphorus ion in fresh water, waste-water and sea water, associated hazards, personal protective equipment required and quality control.

C. Methods

APHA 4500 Vanadomolybdophosphoric Acid Colorimetric Method

❖ **Summary of Method**

Determination of total dissolved phosphorus ion (PO_4^+) water/soil samples.

❖ **Apparatus**
  - Autoclave or pressure cooker, capable of operating at 98 to 137 kPa.
  - Hot plate: A 30- $\times$ 50-cm heating surface is adequate.
  - Safety shield.
  - Safety goggles.
  - Erlenmeyer flasks, 125-mL, acid-washed and rinsed with distilled water
  - Colorimetric equipment: One of the following is required:
  - Spectrophotometer, for use at 400 to 490 nm.
  - Acid-washed glassware
  - Filtration apparatus and filter paper

❖ **Reagents**
  - Phenolphthalein indicator aqueous solution.
  - Strong acid solution: Slowly add 300 mL conc H_2SO_4 to about 600 mL distilled water.
  - When cool, add 4.0 mL conc HNO3 and dilute to 1 L.
  - Sodium hydroxide, NaOH, 6N.
  - Nitric acid, HNO_3, conc.
  - Perchloric acid, $HClO_4 \cdot 2H_2O$, purchased as 70 to 72% $HClO_4$, reagent-grade.
  - Sodium hydroxide, NaOH, 6N.
  - Methyl orange indicator solution.
  - Phenolphthalein indicator aqueous solution.
  - Phenolphthalein indicator aqueous solution.

- Hydrochloric acid, HCl, 1 + 1. H_2SO_4, $HClO_4$, or HNO_3 may be substituted for HCl. The acid concentration in the determination is not critical but a final sample concentration of 0.5N is recommended.
- Activated carbon
- Vanadate-molybdate reagent:
- Solution A: Dissolve 25 g ammonium molybdate, $(NH_4)6Mo_7O_{24}\cdot4H_2O$, in 300 mL distilled water.
- Solution B: Dissolve 1.25 g ammonium metavanadate, NH_4VO_3, by heating to boiling in 300 mL distilled water. Cool and add 330 mL conc HCl. Cool Solution B to room temperature, pour Solution A into Solution B, mix, and dilute to 1 L.
- Standard phosphate solution: Dissolve in distilled water 219.5 mg anhydrous KH2PO4 and dilute to 1000 mL; 1.00 mL = 50.0 µg PO43–-P.

❖ Procedure

• Preliminary Filtration

- Filter samples for determination of dissolved reactive phosphorus, dissolved acid-hydrolyzable phosphorus, and total dissolved phosphorus through 0.45-µm membrane filters. A glass fiber filter may be used to prefilter hard-to-filter samples.
- Wash membrane filters by soaking in 2 L distilled water for 24 h before use because they may contribute significant amounts of phosphorus to samples containing low concentrations of phosphate.

• Preliminary Acid Hydrolysis

- To 100-mL sample or a portion diluted to 100 mL, add 0.05 mL (1 drop) phenolphthalein indicator solution. If a red color develops, add strong acid solution dropwise, to just discharge the color. Then add 1 mL more.
- Boil gently for at least 90 min, adding distilled water to keep the volume between 25 and 50 mL. Cool, neutralize to a faint pink color with NaOH solution, and restore to the original 100-mL volume with distilled water.
- Prepare a calibration curve by carrying a series of standards containing orthophosphate through the hydrolysis step. Do not use orthophosphate standards without hydrolysis, because the salts added in hydrolysis cause an increase in the color intensity in some methods.
- To calculate its content of acid-hydrolyzable phosphorus, determine reactive phosphorus in a sample portion that has not been hydrolyzed, using the same colorimetric method as for treated sample, and subtract.

• Perchloric Acid Digestion

Caution: Heated mixtures of $HClO_4$ and organic matter may explode violently. Avoid this hazard by taking the following precautions:
- Do not add $HClO_4$ to a hot solution that may contain organic matter.
- Always initiate digestion of samples containing organic matter with HNO_3. Complete digestion using the mixture of HNO_3 and $HClO_4$.
- Do not fume with HClO4 in ordinary hoods. Use hoods especially constructed for $HClO_4$ fuming or a glass fume eradicator connected to a water pump.
- Never let samples being digested with $HClO_4$ evaporate to dryness.

- Measure sample containing the desired amount of phosphorus into a 125-mL erlenmeyer flask.
- Acidify to methyl orange with conc HNO_3, add another 5 mL conc HNO_3, and evaporate on a steam bath or hot plate to 15 to 20 mL.
- Add 10 mL each of conc HNO_3 and $HClO_4$ to the 125-mL conical flask, cooling the flask between additions.
- Add a few boiling chips, heat on a hot plate, and evaporate gently until dense white fumes of $HClO_4$ just appear.
- If solution is not clear, cover neck of flask with a watch glass and keep solution barely boiling until it clears. If necessary, add 10 mL more HNO_3 to aid oxidation.
- Cool digested solution and add 1 drop aqueous phenolphthalein solution. Add 6N NaOH
- solution until the solution just turns pink. If necessary, filter neutralized solution and wash filter liberally with distilled water. Make up to 100 mL with distilled water.
- Determine the PO_4^{3-}–P content of the treated sample by Method C, D, or E.
- Prepare a calibration curve by carrying a series of standards containing orthophosphate

- **Vanadomolybdophosphoric Acid Colorimetric Method**
  - **Sample pH adjustment**: If sample pH is greater than 10, add 0.05 mL (1 drop) phenolphthalein indicator to 50.0 mL sample and discharge the red color with 1 + 1 HCl before diluting to 100 mL.
  - **Color removal from sample**: Remove excessive color in sample by shaking about 50 mL with 200 mg activated carbon in an erlenmeyer flask for 5 min and filter to remove carbon.
  - Check each batch of carbon for phosphate because some batches produce high reagent blanks.
  - **Color development in sample:** Place 35 mL or less of sample, containing 0.05 to 1.0 mg P, in a 50-mL volumetric flask.
  - Add 10 mL vanadate-molybdate reagent and dilute to the mark with distilled water.
  - Prepare a blank in which 35 mL distilled water is substituted for the sample.
  - After 10 min or more, measure absorbance of sample versus a blank at a wavelength of 400 to 490 nm, depending on sensitivity desired. The color is stable for days and its intensity is unaffected by variation in room temperature.
  - **Preparation of calibration curve**: Prepare a calibration curve by using suitable volumes of standard phosphate solution.
  - When ferric ion is low enough not to interfere, plot a family of calibration curves of one series of standard solutions for various wavelengths. This permits a wide latitude of concentrations in one series of determinations.
  - Analyze at least one standard with each set of samples.

8.3.2 Soil Properties Data (2017)

IESL — INTERNATIONAL ENERGY SERVICES LIMITED

COMPREHENSIVE ANALYSIS RESULTS FOR PROJECT SAMPLES

Project Ref. No: IESL/NKEIRU/PROJECT/09042017/001
No. of Samples: 190 Soil Samples
Date Received 9th April – 5th May 2017

A, Results of Analysis for Soil Samples

S/N	SAMPLE POINT ID.	PO_3 APHA 4500 (mg/kg)	Pb ASTM D3559 (mg/kg)	TPH EPA 8015 (mg/kg)	TOM ASTM D7573-09 %
1	OMOIGWOR SS0	9.02	42.9	13263	5.21
2	OMOIGWOR ASS1	7.38	65.7	8275	5.13
3	OMOIGWOR A SS3	4.92	86.3	4480	4.98
4	OMOIGWOR A SS5	2.05	96.5	391	5.39
5	OMOIGWOR B SS1	2.05	33.7	7626	7.33
6	OMOIGWOR B SS3	6.35	53.9	3552	8.92
7	OMOIGWOR B SS5	1.23	41.3	561	7.43
8	OMOIGWOR CSS1	6.47	53.9	7681	6.55
9	OMOIGWOR CSS3	7.36	67.8	3318	7.25
10	OMOIGWOR CSS5	5.22	69.5	764	6.47
11	OMOIGWOR DSS1	3.66	45.2	8839	8.11
12	OMOIGWOR DSS3	7.12	55.3	4627	6.37
13	OMOIGWOR DSS5	5.35	64.4	672	7.35
14	OMOIGWOR A C1SS0	11.07	1.31	50.5	6.82
15	OMOIGWOR A C1SS1	15.3	0.92	61	6.22
16	OMOIGWOR A C1SS3	24.1	0.78	59	5.16
17	OMOIGWOR A C1SS5	17.3	2.14	100	7.39
18	OMOIGWOR A C2SS0	18.2	1.12	34	6.82
19	OMOIGWOR A C2SS1	15.9	0.63	72	5.97
20	OMOIGWOR A C2SS3	17.6	0.38	56	7.11
21	OMOIGWOR A C2SS5	12.5	0.97	45	8.31
22	UMUOKPABA SS0	5.58	29.1	15504	6.13
23	UMUOKPABA A SS1	6.71	42.8	7452	5.34
24	UMUOKPABA A SS3	5.66	33.2	1736	6.09
25	UMUOKPABA A SS5	6.29	24.2	806	4.61
26	UMUOKPABA B SS1	7.42	15.7	5236	6.24
27	UMUOKPABA B SS3	5.81	11.3	3112	7.22
28	UMUOKPABA B SS5	0.82	16.2	631	6.33
29	UMUOKPABA C SS1	2.46	21.8	7490	5.78
30	UMUOKPABA C SS3	7.32	24.6	4143	5.34
31	UMUOKPABA C SS5	3.62	23.2	1323	6.09
32	UMUOKPABA D SS1	4.18	36.1	8029	4.61
33	UMUOKPABA D SS3	4.42	26.2	5582	6.24
34	UMUOKPABAD SS5	6.36	18.3	573	7.22
35	UMUOKPABA C1SS0	20.82	1.13	31	6.33

S/N	SAMPLE POINT ID.	PO₃ APHA 4500 (mg/kg)	Pb ASTM D3559 (mg/kg)	TPH EPA 8015 (mg/kg)	TOM ASTM D7573-09 %
36	UMUOKPABA C1SS1	12.46	2.13	44	5.78
37	UMUOKPABA C1SS3	18.46	0.75	57	7.34
38	UMUOKPABA C1SS5	15.39	0.92	100	8.25
39	UMUOKPABA C1SS0	17.38	1.05	63	6.29
40	UMUOKPABA C2SS1	21.3	0.79	38	6.76
41	UMUOKPABA C2SS3	18.35	0.63	36	8.32
42	UMUOKPABA C2SS5	15.28	1.36	54	7.54
43	EGBALOR SS0	4.51	7.74	8520	6.84
44	EGBALOR A SS1	5.74	29.6	3722	7.59
45	EGBALOR A SS3	6.28	18.22	1758	6.11
46	EGBALOR A SS5	4.1	32.6	435	7.13
47	EGBALOR B SS1	4.51	103	4491	7.43
48	EGBALOR B SS3	4.26	43.4	988	5.34
49	EGBALOR B SS5	2.96	78.6	507	6.83
50	EGBALOR C SS1	5.65	22.5	5633	5.65
51	EGBALOR C SS3	3.72	56.3	1940	6.38
52	EGBALOR C SS5	6.34	26.4	566	4.57
53	EGBALOR D SS1	5.72	28.3	5722	6.39
54	EGBALOR D SS3	5.86	22.1	1056	4.78
55	EGBALOR D SS5	6.35	16.23	723	6.38
56	EGBALOR C1 SS0	19.04	1.83	53	8.15
57	EGBALOR C1 SS1	15.23	1.95	24	7.39
58	EGBALOR C1 SS3	21.23	2.16	31	6.35
59	EGBALOR C1 SS5	17.34	5.66	46	8.49
60	EGBALOR C2 SS0	16.67	4.53	56	7.33
61	EGBALOR C2 SS1	19.54	2.34	42	7.29
62	EGBALOR C2 SS3	21.36	5.46	63	8.38
63	EGBALOR C2 SS5	16.73	2.17	38	7.92
64	ANYU SS0	2.43	150	6772	6.13
65	ANYU ASS1	3.69	41.3	708	6.03
66	ANYU ASS3	6.56	124	721	5.72
67	ANYU ASS5	0.82	17.1	800	5.04
68	ANYU BSS1	5.17	35	6334	5.81
69	ANYU BSS3	4.24	28	1083	8.17
70	ANYU BSS5	7.22	44.2	853	4.38
71	ANYU CSS1	2.63	31.7	799	6.2
72	ANYU CSS3	3.72	17.1	800	7.22
73	ANYU CSS5	6.25	40	8871	5.31
74	ANYU DSS1	7.17	36	937	6.39
75	ANYU DSS3	6.38	24	675	5.57
76	ANYU DSS5	3.41	29	708	5.38

S/N	SAMPLE POINT ID.	PO_3 APHA 4500 (mg/kg)	Pb ASTM D3559 (mg/kg)	TPH EPA 8015 (mg/kg)	TOM ASTM D7573-09 %
77	ANYU C1SS0	20.22	2.11	109	9.23
78	ANYU C1SS1	17.28	1.47	33	8.54
79	ANYU C1SS3	19.36	3.16	17	6.57
80	ANYU C1SS5	15.24	3.21	29	6.94
81	ANYU C2SS0	17.33	2.55	22	8.22
82	ANYU C2SS1	19.39	1.86	17	8.56
83	ANYU C2SS3	22.14	4.28	16.5	6.77
84	ANYU C2SS5	19.25	1.89	18.3	8.68
86	ALIMINI ASS0	2.05	78.6	1891	6.62
87	ALIMINI ASS1	5.74	91	974	8.7
88	ALIMINI ASS3	1.64	5.87	529	7.81
89	ALIMINI ASS5	6.15	62.2	345	7.25
90	ALIMINI BSS1	3.69	91.5	1039	8.69
91	ALIMINI BSS3	4.71	52.1	938	5.77
92	ALIMINI BSS5	6.02	60.5	674	7.35
93	ALIMINI CSS1	3.98	53.8	1322	8.29
94	ALIMINI CSS3	7.36	61.3	835	4.78
95	ALIMINI CSS5	8.42	30.4	547	8.36
96	ALIMINI DSS1	5.25	38.3	1738	6.47
97	ALIMINI DSS3	7.34	72	788	9.56
98	ALIMINI DSS5	4.21	53.4	521	6.82
99	ALIMINI C1SS0	13.61	13.2	18.6	7.93
100	ALIMINI C1SS1	24.66	6.44	15.9	8.21
101	ALIMINI C1SS3	12.71	3.06	21.3	9.33
102	ALIMINI C1SS5	13.78	7.37	19.3	5.82
103	ALIMINI C2SS0	15.28	4.27	25.1	7.77
104	ALIMINI C2SS1	23.44	1.92	19.5	9.27
105	ALIMINI C2SS3	17.28	5.87	28.3	5.61
106	ALIMINIC2SS5	12.31	2.62	16.7	7.67
107	KPORGHOR16 SS0	5.33	99.5	39,425	6.24
108	KPORGHOR16 A SS1	1.23	21.5	42,530	5.83
109	KPORGHOR16 A SS3	5.74	163	44,873	6.09
110	KPORGHOR16 A SS5	9.02	18.6	52,238	5.11
111	KPORGHOR16 B SS1	2.87	45	4377	9.33
112	KPORGHOR16 B SS3	9.43	43.5	1694	7.12
113	KPORGHOR16 B SS5	6.56	76.1	5295	4.96
114	KPORGHOR16 C SS1	6.15	51.5	23,901	6.21
115	KPORGHOR16 C SS3	5.33	14.4	3657	5.77
116	KPORGHOR16 C SS5	4.51	10.2	4,829	6.74
117	KPORGHOR16 D SS1	6.37	44.5	45,799	7.82
118	KPORGHOR16 D SS3	5.08	52.4	5,921	3.11

258

S/N	SAMPLE POINT ID.	PO₃ APHA 4500 (mg/kg)	Pb ASTM D3559 (mg/kg)	TPH EPA 8015 (mg/kg)	TOM ASTM D7573-09 %
119	KPORGHOR16 D SS5	4.28	36.2	6,638	4.28
120	KPORGHOR16 C1SS0	18.2	1.18	56.4	4.08
121	KPORGHOR16 C1SS1	15.26	2.88	33	5.05
122	KPORGHOR16 C1SS3	18.24	2.1	26	5.79
123	KPORGHOR16 C1SS5	19.17	1.92	59	6.18
124	KPORGHOR16 C2SS0	21.2	1.56	46	7.21
125	KPORGHOR16 C2SS1	29.31	4.24	37	6.33
126	KPORGHOR16 C2SS3	16.15	3.61	28	8.37
127	KPORGHOR16 C2SS5	17.26	4.73	34	6.92
128	OBUA SS0	1.14	36.65	10,151	5.69
129	OBUA ASS1	7.11	97.49	5,317	8.66
130	OBUA ASS3	6.74	80.44	1,971	5.31
131	OBUA ASS5	10.06	41.52	745	6.45
132	OBUA BSS1	5.15	29.82	7,291	6.19
133	OBUA BSS3	2.41	33.46	3,465	7.26
134	OBUA BSS5	4.63	26.98	827	6.14
135	OBUA CSS1	9.33	54.72	9,301	8.18
136	OBUA CSS3	9.11	49.42	4,461	7.49
137	OBUA CSS5	1.31	77.35	985	9.12
138	OBUA DSS1	8.23	56.79	8,689	7.87
139	OBUA DSS3	9.21	40.63	3,705	5.49
140	OBUA DSS5	8.24	78.67	854	7.45
141	OBUA C1SS0	31.32	8.43	15	5.57
142	OBUA C1SS1	28.22	1.37	79	4.12
143	OBUA C1SS3	23.27	8.07	25	5.89
144	OBUA C1SS5	30.25	2.71	40	7.11
145	OBUA C2SS0	33.16	3.07	47	7.23
146	OBUA C2SS1	28.21	3.49	53	3.41
147	OBUA C2SS3	17.22	1.14	46	5.71
148	OBUA C2SS5	15.62	6.31	56	6.84
149	AMURUTO SS0	2.03	40.63	99,390	7.09
150	AMURUTO ASS1	1.32	44.78	83,752	8.25
151	AMURUTO ASS3	2.21	37.29	61,476	4.93
152	AMURUTO ASS5	1.55	33.28	42,829	8.22
153	AMURUTO BSS1	11.4	26.47	89,158	4.31
154	AMURUTO BSS3	1.65	54.7	72,165	5.59
155	AMURUTO BSS5	5.17	72.1	51,312	6.17
156	AMURUTO CSS1	7.23	49.31	78,420	5.25
157	AMURUTO CSS3	9.21	42.32	62,938	4.91
158	AMURUTO CSS5	3.14	29.77	40,719	5.83
159	AMURUTO DSS1	1.12	40.44	79,778	6.03
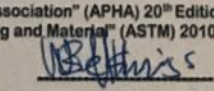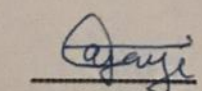
S/N	SAMPLE POINT ID.	PO₃ APHA 4500 (mg/kg)	Pb ASTM D3559 (mg/kg)	TPH EPA 8015 (mg/kg)	TOM ASTM D7573-09 %
160	AMURUTO DSS3	2.44	41.87	62,272	8.94
161	AMURUTO DSS5	6.76	52.69	35,997	6.88
162	AMURUTO C1SS0	15.7	2.91	22	8.17
163	AMURUTO C1SS1	31.19	4.33	67	6.04
164	AMURUTO C1SS3	19.62	1.47	57	7.28
165	AMURUTO C1SS5	16.32	2.48	42	4.99
166	AMURUTO C2SS0	18.72	6.91	29	5.27
167	AMURUTO C2SS1	21.71	1.64	55	6.92
168	AMURUTO C2SS3	23.51	4.11	32	8.32
169	AMURUTO C2SS5	20.25	5.94	63	6.79
170	RUMUEKPE SS0	2.25	37.33	10,822	5.41
171	RUMUEKPE ASS1	5.32	28.46	6,631	6.13
172	RUMUEKPE ASS3	3.66	89.47	1,477	7.17
173	RUMUEKPE ASS5	8.24	31.72	548	7.08
174	RUMUEKPE BSS1	4.2	15.44	5,352	5.03
175	RUMUEKPE BSS3	1.62	17.33	1,708	7.39
176	RUMUEKPE BSS5	1.46	16.66	363	5.66
177	RUMUEKPE CSS1	2.56	34.4	7,892	4.78
178	RUMUEKPE CSS3	6.13	49.29	3,460	7.51
179	RUMUEKPE CSS5	1.18	41.43	1,046	3.2
180	RUMUEKPE DSS1	2.14	36.92	8,847	8.25
181	RUMUEKPE DSS3	7.21	56.34	3,357	6.32
182	RUMUEKPE DSS5	1.91	46.19	1,570	5.86
183	RUMUEKPE C1SS0	29.33	1.26	23	4.16
184	RUMUEKPE C1SS1	32.3	1.52	64	7.39
185	RUMUEKPE C1SS3	21.26	6.55	49	5.02
186	RUMUEKPE C1SS5	15.82	7.09	35	5.54
187	RUMUEKPE C2SS0	15.27	5.02	56	6.27
188	RUMUEKPE C2SS1	17.19	6.86	42	5.81
189	RUMUEKPE C2SS3	25.28	2.18	47	8.74
190	RUMUEKPE C2SS5	22.2	4.13	11	3.88

Method Source: "American Public Health Association" (APHA) 20th Edition 2005
"American Society for Testing and Material" (ASTM) 2010

NWACHUKWU.P
LAB. COORDINATOR

BELLA WILLIAMS.
OPERATIONS MANAGER

AJAYI O. B.
PHC BASE MANAGER

8.3.3 Soil Properties Data (2016)

INTERNATIONAL ENERGY SERVICES LIMITED

COMPREHENSIVE ANALYSIS RESULTS FOR PROJECT SAMPLES

Project Ref. No: IESL/NKEIRU/PROJECT/18022016/002
No. of Samples: 31 Soil Samples
Date Received: 15-16/02/2016

A, Results of Analysis for Soil Samples

SI N	SAMPLE POINT ID.	Temp. APHA 2550 A, °C	pH ASTM D 293 B	E. Cond ASTM D 1125, µS/cm	PO_3 APHA 4500 (mg/kg)	NO_3 APHA 4500 (mg/kg)	Pb ASTM D3559 (mg/kg)	Cd ASTM D3557 (mg/kg)	As ASTM D2972 (mg/kg)	TPH EPA 8015 (mg/kg)	TOC ASTM D7573-09 %	TOM ASTM D7573-09 %	TOTAL HETEROTROPHIC BACTERIA (THB) APHA 9215B, (cfu/mL)
1	Line A SS0	29.1	4.4	35.9	4.67	0.01	2.27	0.01	0.001	16,063	7.12	21.08	5.63×10^6
2	Line A SS1	28.2	4.9	5.1	2.27	<0.01	5.23	1.07	0.001	1851	2.58	7.64	1.37×10^6
3	Line A SS2	29.8	4.5	5.6	1.63	<0.01	7.54	1.51	0.001	1655	2.83	8.38	1.12×10^6
4	Line A SS3	29.2	4.7	9.9	2.14	<0.01	20.8	2.34	0.001	767	1.64	4.86	1.02×10^6
5	Line A SS4	29.0	4.4	6.4	3.12	<0.01	17.8	2.11	0.001	562	0.95	1.34	0.93×10^6
6	Line A SS5	29.1	4.5	7.8	3.35	<0.01	11.4	1.86	0.001	498	0.84	1.18	0.52×10^6
7	Line B SS1	30.1	4.4	3.6	1.42	<0.01	33.4	3.89	0.001	1365	1.46	4.32	1.36×10^6
8	Line B SS2	29.2	4.3	4.9	1.72	0.01	59.0	1.53	0.001	1383	1.48	4.38	1.32×10^6
9	Line B SS3	28.6	4.3	2.0	1.89	<0.01	5.36	3.42	0.001	996	1.22	3.61	0.86×10^6
10	Line B SS4	29.0	4.5	3.8	2.08	<0.01	4.85	2.05	0.001	605	1.03	1.44	0.66×10^6
11	Line B SS5	29.0	4.3	5.2	2.38	<0.01	2.16	1.37	0.001	326	0.55	0.78	0.38×10^4
12	Line C SS1	28.7	4.1	3.6	2.56	<0.01	28.6	5.84	0.001	875	0.54	1.60	0.62×10^6
13	Line C SS2	29.0	4.2	8.0	1.67	0.01	40.1	2.75	0.001	1319	0.93	2.75	0.45×10^6
14	Line C SS3	28.8	4.0	44.2	3.09	0.02	8.30	1.76	0.001	933	0.75	2.22	1.08×10^6
15	Line C SS4	29.1	4.2	17.7	3.21	<0.01	4.42	1.42	0.001	771	1.31	1.83	1.02×10^6
16	Line C SS5	29.1	4.1	11.6	3.45	<0.01	2.33	1.08	0.001	424	0.72	1.01	0.74×10^6
17	Line D SS1	29.1	4.0	16.3	2.11	<0.01	6.23	4.54	0.001	1381	1.39	4.12	1.41×10^6
18	Line D SS2	28.7	4.3	26.1	2.04	0.01	10.87	1.30	0.001	1043	3.09	9.15	1.70×10^6
19	Line D SS3	29.9	4.3	10.6	3.65	0.01	25.5	2.38	0.001	1030	2.74	8.11	1.26×10^6
20	Line D SS4	29.4	4.4	8.3	3.69	<0.01	15.7	2.04	0.001	846	1.43	2.01	1.1×10^6
21	Line D SS5	29.1	4.2	6.5	3.80	<0.01	9.82	1.71	0.001	529	0.90	1.26	1.09×10^6
22	Con 1 SS1	29.1	4.4	25.4	32.5	<0.01	11.9	0.001	0.001	3.75	0.11	2	1.41×10^6
23	Con 1 SS2	29.3	4.4	28	28.6	<0.01	15	0.002	0.001	2.1	0.16	1.8	1.46×10^6
24	Con 1 SS3	29.5	4.4	25	30.3	<0.01	13.5	0.01	0.001	2.6	0.23	2.2	1.45×10^6
25	Con 1 SS4	28.1	4.4	28	29	<0.01	14.2	0.003	0.001	4	0.13	2.1	1.43×10^6
26	Con 1 SS5	29	4.4	30	35	<0.01	13	0.04	0.001	3.9	0.24	1.9	1.42×10^6
27	Con2 SS1	29.2	4.1	17	27.5	<0.01	8	0.001	0.001	1.9	0.15	28.3	1.46×10^6
28	Conl 2 SS2	28.9	4.1	14	28	<0.01	7.6	0.022	0.001	1.3	0.18	26	1.43×10^6

IESL PHC Laboratory Analysis Results

PROJECT SAMPLES (RECEIVED: 15/02/2016 and 16/02/2016)

Page 1

INTERNATIONAL ENERGY SERVICES LIMITED

Sl N	SAMPLE POINT ID.	Temp. APHA 2550 A, °C	pH ASTM D 293 B	E. Cond ASTM D 1125, µS/cm	PO₃ APHA 4500 (mg/kg)	NO₃ APHA 4500 (mg/kg)	Pb ASTM D3559 (mg/kg)	Cd ASTM D3557 (mg/kg)	As ASTM D2972 (mg/kg)	TPH EPA 8015 (mg/kg)	TOC ASTM D7573-09 %	TOM ASTM D7573-09 %	TOTAL HETEROTROPHIC BACTERIA (THB) APHA 9215B, (cfu/mL)
29	Con 2 SS3	29.5	4.1	27	29	<0.01	7.2	0.001	0.001	1.8	0.26	30	1.41×10^6
30	Con2 SS4	29.2	4.1	20	30	<0.01	6.5	0.015	0.001	1.5	0.15	25	1.44×10^6
31	Con 2 SS5	29.3	4.1	10	25	<0.01	8.5	0.001	0.001	1.62	0.18	35	1.4×10^7

Method Source: "American Public Health Association" (APHA) 20ᵗʰ Edition 2005
"American Society for Testing and Material" (ASTM) 2010

NWACHUKWU.P
LAB. COORDINATOR

BELLA WILLIAMS.
OPERATIONS MANAGER

AJAYI O. B.
PHC BASE MANAGER

8.4 Sample R codes
8.4.1 Indicator Species for Locations

#Calculate Indicator Species for Different Locations
library(indicspecies)

```
#read vegetation abundance data from directory
abd<-read.csv('abdt.csv')
head(abd)
dim(abd)

#extract site data
env1<-abd[,1:32]
#extract vegetation data
veg1<-abd[,33:195]
#replace NA's with 0 value
veg1[is.na(veg1)]<-0
#check to see dataframe is okay
head(veg1)
head(env1)
attach(env1)

#subset dataframe by variables
grp<-env1[,3]#groups
grsg<-env1[,7]#segments
grlc<-env1[,5]#locations

#calculate indicator species for locations
indval3<-multipatt(veg1,grlc,control=how(nperm=10))
summary(indval3)
```

8.4.2 Spectral Diversity Hypothesis Testing

```
#spectral diversity analysis
library(np)
library(Metrics)
#read data files
bdtr<-read.csv('bds4rgrtr.csv')#band metrics training data
bdts<-read.csv('bds4rgrts.csv')#band metrics test data
idtr<-read.csv('idx4rgrtr.csv')#index metrics training data
idts<-read.csv('idx4rgrts.csv')#index metrics test data


#predicting TPH from spectral metrics

#band-based
#model; calibration using training data
Mbtpc=npregbw(formula=lgtphr~b3sd+b3sh+b3qcv+hb3+db3+b3pc3+b4mn+b4sd+b4
qcv+hb4+db4+b5sd+b5qcv+hb5+db5+b6sd+b6qcv+hb6+db6+b7sd+b7qcv+hb7+db7+
b8sd+hb8+db8+b8asd+b8aqcv+hb8a+db8a+pc3+pc4+pc5,regtype='ll',bwmethod='cv.ai
c',data=bdtr)
mbtpc<-npreg(bws=mbtpc)
summary(mbtpc)

#validation using test data
fttp<-predict(mbtpc,newdata=bdts)
```

```
write.csv(fttp,'bdtph.csv')
rttp<-bdts$tphr-fttp
write.csv(rttp,'brestph.csv')
pttp<-mean((bdts$tphr-fttp)^2)
rmtp<-rmse(bdts$tphr,fttp)

#plot residual graphs
plot(bdts$tphr,rttp,cex.main=1.5,cex.axis=1.5,cex.lab=1.5,
    font.lab=2,font.axis=2,family='serif',xlab='Predicted',ylab='Residual')
plot(bdts$tphr,fttp,cex.main=1.5,cex.axis=1.5,cex.lab=1.5,
    font.lab=2,font.axis=2,family='serif',xlab='Observed',ylab='Predicted')
abline(rtp3, col="blue",lwd=2)
rtp<-cor(bdts$tphr,fttp)


#index-based
#model; calibration using training data
mtp=npregbw(formula=lgtphr~arpc3+gmmn+gmsd+gmpc1+gndmn+gndsh+gndpc1+gn
dpc3+lcqcv+ndvmd+ndipc1+psmn+pssd+reimnn+reish+rp2mn+rp2sd+rp2pc1+rp2pc3
+sppc2+svsh+hsv,regtype='ll',bwmethod='cv.aic',data=idtr)
mtpr<-npreg(bws=mtp)
summary(mtpr)

#validation using test data
ftp<-predict(mtpr,newdata=idts)
write.csv(ftp,'idtph.csv')
rstp<-idts$lgtphr-ftp
pstp<-mean((idts$lgtphr-ftp)^2)
rmtp<-rmse(idts$lgtphr,ftp)

plot(ftp,rstp,cex.main=1.5,cex.axis=1.5,cex.lab=1.5,
    font.lab=2,font.axis=2,family='serif',xlab='Predicted',ylab='Residual')
abline(h=0,lty=2,col='red')
rtp2<-lm(idts$lgtphr~ftp)
plot(idts$lgtphr,ftp,cex.main=1.5,cex.axis=1.5,cex.lab=1.5,
    font.lab=2,font.axis=2,family='serif',xlab='Observed',ylab='Predicted')
abline(rtp2, col="blue",lwd=2)
rtp<-(cor(idts$lgtphr,ftp)^2)

#phosphorus
#model; calibration using training data
mpr=npregbw(formula=pr~b2sd+b2pc3+b3sd+b3pc3+b5sd+b5sh+b7sd+pc3+pc4,regty
pe='ll',bwmethod='cv.aic',data=bdtr)
mprr<-npreg(bws=mpr)
summary(mprr)

#validation using test data
fpr<-predict(mprr,newdata=bdts)
rpf<-bdts$pr-fpr
pspr<-mean((bdts$pr-fpr)^2)
```

```
rmpr<-rmse(bdts$pr,fpr)

plot(fpr,rpf,cex.main=1.5,cex.axis=1.5,cex.lab=1.5,
    font.lab=2,font.axis=2,family='serif',xlab='Predicted',ylab='Residual')
abline(h=0,lty=2,col='red')
rpr2<-lm(bdts$pr~fpr)
plot(bdts$pr,fpr,cex.main=1.5,cex.axis=1.5,cex.lab=1.5,
    font.lab=2,font.axis=2,family='serif',xlab='Observed',ylab='Predicted')
abline(rpr2, col="blue",lwd=2)
rpr<-(cor(bdts$pr,fpr)^2)

#index-based

#model; calibration using training data
Mp=npregbw(formula=pr~armn+arsd+sipi+gmsh+gmqcv+gndmn+gndmd+dgnd+lcmd
+lcpc3+mcsd+mcsh+ndvsd+ndvsh+nd2sh+psmn+pssd+pssh+pspc2+reipc3+rp2sd+svp
c2,regtype='ll',bwmethod='cv.aic',data=idtr)
mpr<-npreg(bws=mp)
summary(mpr)

#validation using test data
fp<-predict(mpr,newdata=idts)
rsp<-idts$pr-fp
psp<-mean((idts$pr-fp)^2)
rmp<-rmse(idts$pr,fp)

plot(fp,rsp,cex.main=1.5,cex.axis=1.5,cex.lab=1.5,
    font.lab=2,font.axis=2,family='serif',xlab='Predicted',ylab='Residual')
abline(h=0,lty=2,col='red')
rp2<-lm(idts$pr~fp)
plot(idts$pr,fp,cex.main=1.5,cex.axis=1.5,cex.lab=1.5,
    font.lab=2,font.axis=2,family='serif',xlab='Observed',ylab='Predicted')
abline(rp2, col="blue",lwd=2)
rp<-(cor(idts$pr,fp)^2)

#lead
mpb<-npregbw(formula=pbr~b2pc3+b3pc2+b4sd+b4sh+db4+b4pc1+b7sd+b8asd,
        regtype='ll',bwmethod='cv.aic',data=bdtr)
mpbr<-npreg(bws=mpb)
summary(mpbr)

#validation using test data
fpb<-predict(mpbr,newdata=bdts)
rpb<-bdts$pbr-fpb
pspb<-mean((bdts$pbr-fpb)^2)
rmpb<-rmse(bdts$pbr,fpb)

plot(fpb,rpb,cex.main=1.5,cex.axis=1.5,cex.lab=1.5,
    font.lab=2,font.axis=2,family='serif',xlab='Predicted',ylab='Residual')
abline(h=0,lty=2,col='red')
```

```
rpb2<-lm(bdts$pbr~fpb)
plot(bdts$pbr,fpb,cex.main=1.5,cex.axis=1.5,cex.lab=1.5,
    font.lab=2,font.axis=2,family='serif',xlab='Observed',ylab='Predicted')
abline(rpb2, col="blue",lwd=2)
rpb<-(cor(bdts$pbr,fpb)^2)

#index-based
mpp<-npregbw(formula=pbr~arsd+lcqcv+lcpc3+ndvsd+ndvpc1+ndvpc2+dnd2
        +ndimn+pssd+pssh+pspc1+reimd+reipc2+rp2qcv+rp2pc2+sph+spmd+spqcv
        +svmd+svqcv+dsv,regtype='ll',bwmethod='cv.aic',data=idtr)
mppr<-npreg(bws=mpp)
summary(mppr)

fpp<-predict(mppr,newdata=idts)
rspp<-idts$pbr-fpp
pspp<-mean((idts$pbr-fpp)^2)
rmpp<-rmse(idts$pbr,fpp)

plot(fpp,rspp,cex.main=1.5,cex.axis=1.5,cex.lab=1.5,
    font.lab=2,font.axis=2,family='serif',xlab='Predicted',ylab='Residual')
abline(h=0,lty=2,col='red')
rpp2<-lm(idts$pbr~fpp)
plot(idts$pbr,fpp,cex.main=1.5,cex.axis=1.5,cex.lab=1.5,
    font.lab=2,font.axis=2,family='serif',xlab='Observed',ylab='Predicted')
abline(rpp2, col="blue",lwd=2)
rpp<-(cor(idts$pbr,fpp)^2)

#total organic matter

#band-based
mtm=npregbw(formula=tomr~b3sh+b4sh+b5pc2+db8+b8aqcv,regtype='ll',bwmethod='
cv.aic',data=bdtr)
mtmr<-npreg(bws=mtm)
summary(mtmr)

ftm<-predict(mtmr,newdata=bdts)
rstm<-bdts$tomr-ftm
pstm<-mean((bdts$tomr-ftm)^2)
rmtm<-rmse(bdts$tomr,ftm)

plot(ftm,rstm,cex.main=1.5,cex.axis=1.5,cex.lab=1.5,
    font.lab=2,font.axis=2,family='serif',xlab='Predicted',ylab='Residual')
abline(h=0,lty=2,col='red')
rtm2<-lm(bdts$tomr~ftm)
plot(bdts$tomr,ftm,cex.main=1.5,cex.axis=1.5,cex.lab=1.5,
    font.lab=2,font.axis=2,family='serif',xlab='Observed',ylab='Predicted')
abline(rtm2, col="blue",lwd=2)
rtm<-(cor(bdts$tomr,ftm)^2)

#index-based
```

```
mto=npregbw(formula=tomr~arsd+sipi+ccqcv+ccpc3+gmsh+gmpc3+hndv+ndvpc2+nd
2md+ndimd+ndiqcv+ndipc2+reipc3+rp2sd+rp2sh+hrp2+rp2pc2+rp2pc3+spqcv+hspi
+sppc3+svpc2+sv2sd+sv2md+hsv2,regtype='lc',bwmethod='cv.aic',data=idtr)
mtom<-npreg(bws=mto)
summary(mtom)

fto<-predict(mtom,newdata=idts)
rsto<-idts$tomr-fto
psto<-mean((idts$tomr-fto)^2)
rmto<-rmse(idts$tomr,fto)
plot(fto,rsto,cex.main=1.5,cex.axis=1.5,cex.lab=1.5,
    font.lab=2,font.axis=2,family='serif',xlab='Predicted',ylab='Residual')
abline(h=0,lty=2,col='red')
rto2<-lm(idts$tomr~fto)

plot(idts$tomr,fto,cex.main=1.5,cex.axis=1.5,cex.lab=1.5,
    font.lab=2,font.axis=2,family='serif',xlab='Observed',ylab='Predicted')
abline(rto2, col="blue",lwd=2)
rto2
rto<-(cor(idts$tomr,fto)^2)

#predicting diversity indices from spectral metrics
#simpson

mbtr=npregbw(formula=simr~b2mn+b2md+b2pc1+b4mn+b4sd+b4md+hb4+db4+b4pc
1+b5mn+b5sd+b5md+b5qcv+b5pc1+b6sd+hb6+db6+b7sd+b7qcv+b8asd+pc3,regtype
='ll',bwmethod='cv.aic',data=bdtr)
mbtr<-npreg(bws=mbtr)
summary(mbtr)

ftsi<-predict(mbtr,newdata=bdts)
rssi<-bdts$simr2-ftsi
pssi<-mean((bdts$simr2-ftsi)^2)
rmsi<-rmse(bdts$simr2,ftsi)

plot(bdts$simr2,rssi,cex.main=1.5,cex.axis=1.5,cex.lab=1.5,
    font.lab=2,font.axis=2,family='serif',xlab='Predicted',ylab='Residual')
abline(h=0,lty=2,col='red')
rsi2<-lm(bdts$simr2~ftsi)
plot(bdts$simr2,ftsi,cex.main=1.5,cex.axis=1.5,cex.lab=1.5,
    font.lab=2,font.axis=2,family='serif',xlab='Observed',ylab='Predicted')
abline(rsi2, col="blue",lwd=2)
rsi<-(cor(bdts$simr2,ftsi)^2)
summary(rsi2)

#index-based simpson
mis=npregbw(formula=simr~arpc1+sipi+ccmn+ccsh+ccmd+ccqcv+ccpc3+gmqcv+lcm
d+hlc+ndvmd+ndvpc3+hndi+dndi+pssd+psqcv+dps+spsd+spqcv+sppc2+sv2pc2,regty
pe='ll',bwmethod='cv.aic',data=idtr)
misi<-npreg(bws=mis)
```

```
summary(misi)

fts<-predict(misi,newdata=idts)
rss<-idts$simr-fts
pss<-mean((idts$simr-fts)^2)
rms<-rmse(idts$simr,fts)

plot(fts,rss,cex.main=1.5,cex.axis=1.5,cex.lab=1.5,
    font.lab=2,font.axis=2,family='serif',xlab='Predicted',ylab='Residual')
abline(h=0,lty=2,col='red')
rs2<-lm(idts$simr~fts)
plot(idts$simr,fts,cex.main=1.5,cex.axis=1.5,cex.lab=1.5,
    font.lab=2,font.axis=2,family='serif',xlab='Observed',ylab='Predicted')
abline(rs2, col="blue",lwd=2)
rs<-cor(idts$simr,fts)
write.csv(fts,'presim.csv')

#shannon
mstr=npregbw(formula=shar~b2mn+b2md+b2pc1+b4mn+b4sd+b4md+hb4+db4+b4pc
1+b5mn+b5sd+b5md+b5qcv+b5pc1+b6sd+hb6+db6+b7sd+b7qcv+b8asd+pc3,regtype
='ll',bwmethod='cv.aic',data=bdtr)
mstr<-npreg(bws=mstr)
summary(mstr)

ftsh<-predict(mstr,newdata=bdts)
rssh<-bdts$shar-ftsh
pssh<-mean((bdts$shar-ftsh)^2)
rmsh<-rmse(bdts$shar,ftsh)

plot(ftsh,rssh,cex.main=1.5,cex.axis=1.5,cex.lab=1.5,
    font.lab=2,font.axis=2,family='serif',xlab='Predicted',ylab='Residual')
abline(h=0,lty=2,col='red')
rsh2<-lm(bdts$shar~ftsh)
plot(bdts$shar,ftsh,cex.main=1.5,cex.axis=1.5,cex.lab=1.5,
    font.lab=2,font.axis=2,family='serif',xlab='Observed',ylab='Predicted')
abline(rsh2, col="blue",lwd=2)
rsh<-(cor(bdts$shar,ftsh)^2)

#index-based shannon
msh=npregbw(formula=shar~arpc2+ccpc2+gmqcv+gmpc1+gmpc2+gndpc3+lcmd+dlc
+nd2sh+hndi+dndi+pssd+psqcv+reimd+rp2sh+h2sr+d2sr+spsd+sph+svpc1+svpc2
+sv2qcv,regtype='ll',bwmethod='cv.aic',data=idtr)
mish<-npreg(bws=msh)
summary(mish)

ftshr<-predict(mish,newdata=idts)
rsshr<-idts$shar-ftshr
psshr<-mean((idts$shar-ftshr)^2)
rmshr<-rmse(idts$shar,ftshr)
```

```r
plot(ftshr,rsshr,cex.main=1.5,cex.axis=1.5,cex.lab=1.5,
    font.lab=2,font.axis=2,family='serif',xlab='Predicted',ylab='Residual')
abline(h=0,lty=2,col='red')
rshr2<-lm(idts$shar~ftshr)
plot(idts$shar,ftshr,cex.main=1.5,cex.axis=1.5,cex.lab=1.5,
    font.lab=2,font.axis=2,family='serif',xlab='Observed',ylab='Predicted')
abline(rshr2, col="blue",lwd=2)
rshr<-cor(idts$shar,ftshr)

#menhinick
Mmtr=npregbw(formula=menr~b2mn+b2md+b2pc1+b4mn+b4sd+b4md+hb4+db4+b4
pc1+b5mn+b5sd+b5md+b5qcv+b5pc1+b6sd+hb6+db6+b7sd+b7qcv+b8asd+pc3,regty
pe='ll',bwmethod='cv.aic',data=bdtr)
mmtr<-npreg(bws=mmtr)
summary(mmtr)

ftm<-predict(mmtr,newdata=bdts)
rsm<-bdts$menr-ftm
psm<-mean((bdts$menr-ftm)^2)
rmm<-rmse(bdts$menr,ftm)

plot(ftm,rsm,cex.main=1.5,cex.axis=1.5,cex.lab=1.5,
    font.lab=2,font.axis=2,family='serif',xlab='Predicted',ylab='Residual')
abline(h=0,lty=2,col='red')
rm2<-lm(bdts$menr~ftm)
plot(bdts$menr,ftm,cex.main=1.5,cex.axis=1.5,cex.lab=1.5,
    font.lab=2,font.axis=2,family='serif',xlab='Observed',ylab='Predicted')
abline(rm2, col="blue",lwd=2)
rm<-cor(bdts$menr,ftm)

#index-based menhinick
me<-npregbw(formula=menr~sipi+ccqcv+gmqcv+gmpc2+dgnd+lcmd+pssd+rp2pc2
        +spsd+spqcv+svsd+svpc1,regtype='ll',bwmethod='cv.aic',data=idtr)
mehr<-npreg(bws=me)
summary(mehr)

fme<-predict(mehr,newdata=idts)
rsme<-idts$menr-fme
psme<-mean((idts$menr-fme)^2)
rmsm<-rmse(idts$menr,fme)

plot(fme,rsme,cex.main=1.5,cex.axis=1.5,cex.lab=1.5,
    font.lab=2,font.axis=2,family='serif',xlab='Predicted',ylab='Residual')
abline(h=0,lty=2,col='red')
rmms2<-lm(idts$menr~fme)
plot(idts$menr,fme,cex.main=1.5,cex.axis=1.5,cex.lab=1.5,
    font.lab=2,font.axis=2,family='serif',xlab='Observed',ylab='Predicted')
abline(rmms2, col="blue",lwd=2)
rmms<-cor(idts$menr,fme)
```

8.4.3 Distance Decay

```
#distance decay in polluted and control transects using presence-absence data
library(betapart)
library(quantreg)
library(vegan)
#read vegetation data file from directory
psc<-read.csv('pscsorted.csv')
dim(psc)
head(psc)
#split data into polluted and control groups
vcn<-split(psc,psc$Group)
vcon<-vcn$con
vpol<-vcn$pol
#Extracat site data
dim(vcon)
sct<-vcon[,9:14]
spl<-vpol[,9:14]
#Extract species data
vct<-vcon[,33:194]
vpl<-vpol[,33:194]

#read band data file from directory
abb<-read.csv('albds.csv')
head(abb)
#Extract only band values
abs<-abb[,1:74]
#split data into polluted and control groups
abbs<-split(abs,abs$Group)
abcon<-abbs$Con
abpol<-abbs$Pol
dim(abcon)
#Extract only band values
abct<-abcon[,3:74]
abpl<-abpol[,3:74]

#distance analysis for control transects
bcbt<-vegdist(abct,method='jaccard',diag=FALSE)
vcbt<-vegdist(vct,method='jaccard',diag=FALSE)
scds<-vegdist(sct,method='jaccard',diag=FALSE)

#convert to matrix
bcbt1<-as.matrix(bcbt)
vcbt1<-as.matrix(vcbt)
scds1<-as.matrix(scds)

#save distances
write.csv(bcbt1,'bcbt1.csv')
write.csv(vcbt1,'vcbt1.csv')
#compute similarities
```

```
vcsm=1-vcbt1
btsm=1-bcbt1
scsm=1-scds1

#plot distance decay graphs
plot(bcbt1,vcsm,cex.lab=1.5,cex.main=2,cex.axis=1.5,
    font.lab=2,font.axis=2,family='serif',
    xlab='Species Similarity',ylab='Spectral Distance')
plot(bcbt1,vcbt1,cex.lab=1.5,cex.main=2,cex.axis=1.5,
    font.lab=2,font.axis=2,family='serif',
    xlab='Species Dissimilarity',ylab='Spectral Distance')
plot(bcbt1,scsm)
plot(bcbt1,scds1)
rgcn<-cor(bcbt1,vcbt1)
summary(rgcn)
rgcn3<-cor(bcbt1,scds1)

#distance analysis for polluted transects
bpds<-vegdist(abpl,method='jaccard',diag=FALSE)
vpds<-vegdist(vpl,method='jaccard',diag=FALSE)
spds<-vegdist(spl,method='jaccard',diag=FALSE)

#convert to matrix
bpdss1<-as.matrix(bpdss)
vpdss1<-as.matrix(vpdss)
spds1<-as.matrix(spds)

#compute similarity
vpssm=1-vpdss1
bpssm=1-bpdss1
spsm=1-spds1

#plot distance decay graphs
plot(bpdss1,vpssm,cex.lab=1.5,cex.main=2,cex.axis=1.5,
    font.lab=2,font.axis=2,family='serif',
    xlab='Species Similarity',ylab='Spectral Distance')
abline(rgp2,col='blue', lty=1,lwd=2)
plot(bpds1,vpds1,cex.lab=1.5,cex.main=2,cex.axis=1.5,
    font.lab=2,font.axis=2,family='serif',
    xlab='Species Dissimilarity',ylab='Spectral Distance')

#to regress the variables, first convert matrices to vectors
#and combine to a single dataframe

#polluted
da1<-as.data.frame(as.vector(bpds1))
da2<-as.data.frame(as.vector(vpds1))
da3<-as.data.frame(as.vector(spds1))
da4<-as.data.frame(as.vector(bpsm))
da5<-as.data.frame(as.vector(vpsm))
```

```
da6<-as.data.frame(as.vector(spsm))
da7<-cbind(da1,da2,da3,da4,da5,da6)
head(da7)
#rename columns
colnames(da7)[1]<-'bpds'
colnames(da7)[2]<-'vpds'
colnames(da7)[3]<-'spds'
colnames(da7)[4]<-'bpsm'
colnames(da7)[5]<-'vpsm'
colnames(da7)[6]<-'spsm'

#find regression intercept (similarity at zero distance) and coefficient (decay rate)
rgp1<-lm(da7$bpds~da7$vpsm)
summary(rgp1)
lines(lowess(da7$bpds,da7$vpds),col='blue')
crp<-cor(da7$bpds,da7$vpsm,method='spearman')

#control
dc1<-as.data.frame(as.vector(bcbt1))
dc2<-as.data.frame(as.vector(vcbt1))
dc3<-as.data.frame(as.vector(scds1))
dc4<-as.data.frame(as.vector(btsm))
dc5<-as.data.frame(as.vector(vcsm))
dc6<-as.data.frame(as.vector(scsm))
dc7<-cbind(dc1,dc2,dc3,dc4,dc5,dc6)
head(dc7)
#rename columns
colnames(dc7)[1]<-'bcds'
colnames(dc7)[2]<-'vcds'
colnames(dc7)[3]<-'scds'
colnames(dc7)[4]<-'bcsm'
colnames(dc7)[5]<-'vcsm'
colnames(dc7)[6]<-'scsm'

#find regression intercept (similarity at zero distance) and coefficient (decay rate)
rgc1<-lm(dc7$bcds~dc7$vcsm)
summary(rgc1)
crc<-cor(dc7$bcds,dc7$vcsm,method='spearman')

#plots
attach(dc7)
attach(da7)
par(mfrow=c(2,2),cex.lab=2,cex.main=2,cex.axis=2,
    font.lab=2,font.axis=2,family='serif')
plot(bpds1,vpsm,xlab='Spectral Distance',ylab='Species Similarity')
abline(rgp1,col='blue', lty=1,lwd=2)
plot(bpds,vpds,xlab='Spectral Diversity',ylab='Betadiversity')
plot(bpds,spds,xlab='Spectral Diversity',ylab='Ecosystem Diversity')
plot(spds,vpds,xlab='Ecosystem Diversity',ylab='Betadiversity')
```

```
plot(dc7$bcds,dc7$vcsm,xlab='Spectral Distance',ylab='Species Similarity')
abline(rgc1,col='blue', lty=1,lwd=2)
plot(dc7$bcsm,dc7$vcds,xlab='Spectral Diversity',ylab='Betadiversity')
plot(bcds,dc7$scds,xlab='Spectral Diversity',ylab='Ecosystem Diversity')
plot(vcds,dc7$scds,xlab='Betadiversity',ylab='Ecosystem Diversity')
max(dc7$bcds)
max(dc7$vcsm)
```

9 Bibliography

Abdikan, S., Balik Sanli, F., Sunar, F. and Ehlers, M. (2014) 'A comparative data-fusion analysis of multi-sensor satellite images', *International Journal of Digital Earth,* 7(8), pp. 671-687.

Abrams, P. (1983) 'The Theory of Limiting Similarity', *Annual Review of Ecology and Systematics,* 14(1), pp. 359-376.

Adamu, B., Tansey, K. and Ogutu, B. (2018) 'Remote sensing for detection and monitoring of vegetation affected by oil spills', *International Journal of Remote Sensing,* 39(11), pp. 3628-3645.

Adegbehin, J.O. and Nwaigbo, L.C. (1990) 'Mangrove resources in Nigeria: Use and Management Perspectives', *Nature and Resources,* 26(2), pp. 13-25.

Adishi, E., Hunga and M. O. (2017) 'Oil Theft, Illegal Bunkering and Pipeline Vandalism: Its Impact on Nigeria Economy, 2015 - 2016', *International Journal of Economics and Business Management,* 3(2), pp. 47-65.

Adler-Golden, S., Richtsmeier, S., Conforti, P. & Bernstein, L. (2013) 'Spectral image destriping using a low-dimensional model', Sylvia S. Shen, Paul E Lewis (ed.) *SPIE Defense, Security, and Sensing,* Baltimore, Maryland, United States, 18 May 2013 Baltimore, Maryland, United States: SPIE.

Agbagwa, I.O. and Ekeke, C. (2011) 'Structure and Phytodiversity of Freshwater Swamp Forest in Oil-rich Bonny, Rivers State, Nigeria', *Research Journal of Forestry,* 5(2), pp. 66-77.

Agbogidi, O.M., Eruotor, P.G. and Akparobi, S.O. (2007) 'Effects of Crude Oil Levels on the Growth of Maize (Zea mays L.)', *American Journal of Food Technology,* 2(6), pp. 529-535.

Akinnibosun, H. A., Omatsola and M. E. (2011) 'Baseline Studies Of The Floral Biodiversity Of A Proposed Crude Oil Exploration Field In Edo State, Nigeria.', *Science world,* 6(1), pp. 27-32.

Alam, M., Abedi, V., Bassaganya-Riera, J., Wendelsdorf, K., Bisset, K., Deng, X., Eubank, S., Hontecillas, R., Hoops, S. and Marathe, M. (2016) 'Chapter 6 - Agent-Based Modeling and High Performance Computing', in Bassaganya-Riera, J. (ed.) *Computational Immunology.* Elsevier Inc.: Academic Press, pp. 79-111.

Albek, E. (2003) 'Estimation of Point and Diffuse Contaminant Loads to Streams by Non-Parametric Regression Analysis of Monitoring Data', *Water, air, and soil pollution,* 147(1), pp. 229-243.

Albert, O.N., Amaratunga, D. and Haigh, R.P. (2018b) 'Evaluation of the Impacts of Oil Spill Disaster on Communities and Its Influence on Restiveness in Niger Delta, Nigeria', *Procedia Engineering,* 212, pp. 1054-1061.

Al-Hawas, G. H. S., Shukry, W. M., Azzoz, M. M., Al-Moaik, R. M. S. (2012) 'The effect of sublethal concentrations of crude oil on the metabolism of Jojoba (*Simmodsia chinensis*) seedlings', *International Research Journal of Plant Science,* 3(4), pp. 54-62.

Anderson, M.J., Ellingsen, K.E. and McArdle, B.H. (2006) 'Multivariate dispersion as a measure of beta diversity', *Ecology Letters,* 9(6), pp. 683-693.

Aneece, I.P., Epstein, H. and Lerdau, M. (2017) 'Correlating species and spectral diversities using hyperspectral remote sensing in early-successional fields', *Ecology and Evolution,* 7(10), pp. 3475-3488.

Ansgar Kahmen, Carsten Renker, Sybille B. Unsicker and Nina Buchmann (2006) 'Niche Complementarity for Nitrogen: An Explanation for the Biodiversity and Ecosystem Functioning Relationship?', *Ecology,* 87(5), pp. 1244-1255.

Arellano, P., Tansey, K., Balzter, H. and Tellkamp, M. (2017) 'Plant Family-Specific Impacts of Petroleum Pollution on Biodiversity and Leaf Chlorophyll Content in the Amazon Rainforest of Ecuador', *PLOS ONE,* 12(1), pp. e0169867.

Asa Gholizadeh, Jan Misurec, Veronika Kopackova, Christian Mielke and Christian Rogass (2016) 'Assessment of Red-Edge Position Extraction Techniques: A Case Study for Norway Spruce Forests Using HyMap and Simulated Sentinel-2 Data', *Forests,* 7(10), pp. 226.

Asner, G.P. and Martin, R.E. (2011) 'Canopy phylogenetic, chemical and spectral assembly in a lowland Amazonian forest', *The New phytologist,* 189(4), pp. 999-1012.

Asner, G.P., Martin, R.E. and Suhaili, A.B. (2012) 'Sources of Canopy Chemical and Spectral Diversity in Lowland Bornean Forest', *Ecosystems,* 15(3), pp. 504-517.

Asner, G.P., Jones, M.O., Martin, R.E., Knapp, D.E. and Hughes, R.F. (2008) 'Remote sensing of native and invasive species in Hawaiian forests', *Remote Sensing of Environment,* 112(5), pp. 1912-1926.

Asner, G.P., Scurlock, J.M. and Hicke Jeffrey, A. (2003) 'Global synthesis of leaf area index observations: implications for ecological and remote sensing studies', *Global Ecology and Biogeography,* 12(3), pp. 191-205.

Atlas, R.M. (1981) 'Microbial degradation of petroleum hydrocarbons: an environmental perspective', *Microbiological reviews,* 45(1), pp. 180-209.

Atuma, M.I. and Ojeh, V.N. (2013) 'Effect of Gas Flaring on Soil and Cassava Productivity in Ebedei, Ukwuani Local Government Area, Delta State, Nigeria', *Journal of Environmental Protection,* 4(10), pp. 1054-1066.

Ayotamuno, M.J., Kogbara, R.B., Ogaji, S.O.T. and Probert, S.D. (2006) 'Bioremediation of a crude-oil polluted agricultural-soil at Port Harcourt, Nigeria', *Applied Energy,* 83(11), pp. 1249-1257.

Baker, J.M. (1970) 'The effects of oils on plants', *Environmental Pollution (1970),* 1(1), pp. 27-44.

Balvanera, P., Pfisterer, A.B., Buchmann, N., He, J., Nakashizuka, T., Raffaelli, D. and Schmid, B. (2006) 'Quantifying the evidence for biodiversity effects on ecosystem functioning and services', *Ecology Letters,* 9(10), pp. 1146-1156.

Bammel, B.H. & Birnie, R.W. (1994) 'Spectral Reflectance response of Big Sagebrush to Hydrocarbon-Induced Stress in Bighorn Basin, Wyoming', *Thematic Conference on Geologic Remote Sensing,* Pasadena CA, USA, 08-02-1993American Society for Photogrammetry and Remote Sensing, pp. 87.

Barati, S., Rayegani, B., Saati, M., Sharifi, A. and Nasri, M. (2011) 'Comparison the accuracies of different spectral indices for estimation of vegetation cover fraction in sparse vegetated areas', *The Egyptian Journal of Remote Sensing and Space Sciences,* 14(1), pp. 49-56.

Bargain, A., Robin, M., Méléder, V., Rosa, P., Le Menn, E., Harin, N. and Barillé, L. (2013) 'Seasonal spectral variation of Zostera noltii and its influence on pigment-based Vegetation Indices', *Journal of Experimental Marine Biology and Ecology,* 446, pp. 86-94.

Barry, P. 2001 *EO1/Hyperion Science data User's Guide Level 1_B*, NASA, California, US.

Baruah, D. and Sarma, S.K. (1996) 'Impact of crude oil pollution on species number and live standing herbaceous crop biomass', *Environmentalist,* 16(4), pp. 291-295.

Baruah, P., Saikia, R., Baruah, P. and Deka, S. (2014) 'Effect of Crude Oil Contamination on the Chlorophyll Content and Morpho-Anatomy of *Cyperus brevifolius (Rottb.) Hassk*', *Environmental Science and Pollution Research,* 21(21), pp. 12530-12538.

Baselga, A. and Orme, C.D.L. (2012) 'Betapart: an R package for the study of beta diversity', *Methods in Ecology and Evolution,* 3(5), pp. 808-812.

Baselga, A., Orme, D., Villeger, S., De Bortoli, J. and Leprieur, F. (eds.) (2018) *Betapart: Partitioning Beta Diversity into Turnover and Nestedness Components.*.CRAN, Betapart Documentation. Available at: https://rdrr.io/cran/betapart/

Basorun, J.O. and Olamiju, I.O. (2013) 'Environmental Pollution and Refinery Operations in an Oil Producing Region of Nigeria: A Focus on Warri Petrochemical Company', *IOSR Journal of Environmental Science, Toxicology and Food Technology,* 2(6), pp. 18-23.

Baudze, O. and Kvesitadze, G. (1997) 'Effect of Low-Molecular-Weight Alkanes on the PLant Cell Photosynthetic Apparatus', *Ecotoxicology and Environmental Safety,* 38, pp. 36-44.

Bayrak, M.M. and Marafa, M.L. (2016) 'Ten Years of REDD+: A Critical Review of the Impact of REDD+ on Forest-Dependent Communities', *Sustainability,* 8(7), pp. 620.

Beadle, C.L. and Long, S.P. (1985) 'Photosynthesis — is it limiting to biomass production?', *Biomass,* 8(2), pp. 119-168.

Beaubien, S.E., Ciotoli, G., Coombs, P., Dictor, M.C., Krüger, M., Lombardi, S., Pearce, J.M. and West, J.M. (2008) 'The impact of a naturally occurring CO2 gas vent on the shallow ecosystem and soil chemistry of a Mediterranean pasture (Latera, Italy)', *International Journal of Greenhouse Gas Control,* 2(3), pp. 373-387.

Behl, S., Donval, A. and Stibor, H. (2011) 'The relative importance of species diversity and functional group diversity on carbon uptake in phytoplankton communities', *Limnology and Oceanography,* 56(2), pp. 683-694.

Benka-Coker, M. and Ekundayo, J.A. (1995) 'Effects of an oil spill on soil physicochemical properties of a spill site in the Niger Delta Area of Nigeria', *Environmental monitoring and assessment,* 36(2), pp. 93-104.

Bhandari, A.K., Kumar, A. and Singh, G.K. (2012) 'Feature Extraction using Normalized Difference Vegetation Index (NDVI): A Case Study of Jabalpur City', *Procedia Technology,* 6, pp. 612-621

Blackburn, G.A. (1998) 'Quantifying Chlorophylls and arotenoids at Leaf and Canopy Scales: An Evaluation of Some Hyperspectral Approaches', *Remote Sensing of Environment,* 66(3), pp. 273-285.

Blackburn, G.A. and Ferwerda, J.G. (2008) 'Retrieval of Chlorophyll Concentration from Leaf Reflectance Spectra Using Wavelet Analysis', *Remote Sensing of Environment,* 112(4), pp. 1614-1632.

Bock, C.E., Jones, Z.F. and Bock, J.H. (2007) 'Relationships between Species Richness, Evenness, and Abundance in a Southwestern Savanna', *Ecology,* 88(5), pp. 1322-1327.

Bockheim, J.G., Gennadiyev, A.N., Hartemink, A.E. and Brevik, E.C. (2014) 'Soil-forming factors and Soil Taxonomy', *Geoderma,* 226-227, pp. 231-237.

Bonham, C.D. (2013a) 'Density', in Anonymous *Measurements for Terrestrial Vegetation.* Second edition. edn. GB: Wiley-Blackwell, pp. 153-162.

Bonham, C.D. (2013b) 'Frequency', in Anonymous *Measurements for Terrestrial Vegetation.* Second edition. edn. GB: Wiley-Blackwell, pp. 99-102.

Bot, A. and Benites, J. 2005 *The Importance of Soil Organic Matter: Key to Drought-Resistant Soil and Sustained Food and Production*, Food and Agriculture Organization of the United Nations, Rome.

Bowman, W.D., Gartner, J.R., Holland, K. and Wiedermann, M. (2006) 'Nitrogen Critical Loads For Alpine Vegetation And Terrestrial Ecosystem Response: Are We There Yet?', *Ecological Applications,* 16(3), pp. 1183-1193.

Boyd, D.S. and Danson, F.M. (2005) 'Satellite Remote Sensing of Forest Resources: Three Decades of Research Development', *Progress in Physical Geography,* 29(1), pp. 1-26.

Braak, T., Cajo J.F and Verdonschot, P.F.M. (1995) 'Canonical correspondence analysis and related multivariate methods in aquatic ecology', *Aquatic Sciences,* 57(3), pp. 255-289.

Brian S. Cade and Barry R. Noon (2003) 'A Gentle Introduction to Quantile Regression for Ecologists', *Frontiers in Ecology and the Environment,* 1(8), pp. 412-420.

Brooks, T.M., Mittermeier, R.A., da Fonseca, G A B, Gerlach, J., Hoffman, M., Lamoreux, J.F., Mittermeier, C.G., Pilgrim, J.D. and Rodrigues, A.S.L. (2006) 'Global Biodiversity Conservation Priorities', *Science,* 313(58), pp. 58-61.

Brown, K.L. (2003) 'From teacher-centered to learner-centered curriculum: improving learning in diverse classrooms', *Education,* 124, pp. 49+.

Brown, L. (1992) 'A survey of image registration techniques', *ACM Computing Surveys (CSUR),* 24(4), pp. 325-376.

Brundtland Commission *Our Common Future.* Available at: http://www.un-documents.net/our-common-future.pdf (Accessed: 01/20 2015).

Buckland, S.T., Borchers, D.L., Johnston, A., Henrys, P.A. and Marques, T.A. (2007) 'Line Transect Methods for Plant Surveys', *Biometrics,* 63(4), pp. 989-998.

Buddhiraju, K.M. and Porwal, A. (2015) *Hyperspectral image processing and analysis.*

Bunce, R.G.H., Bogers, M.M.B., Evans, D., Halada, L., Jongman, R.H.G., Mucher, C.A., Bauch, B., de Blust, G., Parr, T.W. and Olsvig-Whittaker, L. (2013) 'The significance of habitats as indicators of biodiversity and their links to species', *Ecological Indicators,* 33, pp. 19-25.

Burgman, M.A. and Lindenmayer, D.B. (1998) *Conservation Biology for the Australian Environment.* New South Wales, Australia: Surrey Beaty and Sons.

Burk, J.C. (1977) 'A Four Year Analysis of Vegetation Following an Oil Spill in a Freshwater Marsh', *Journal of Applied Ecology,* 14(2), pp. 515-522.

Burley, W.F. (1988) 'Monitoring Biological Diversity for Setting Priorities in Conservation', in Wilson, E.O. and Peter, F.M. (eds.) *Biodiversity.* Washington DC: National Academy Press, pp. 277-230.

Butchart, S.H.M., Walpole, M., Collen, B., van Strien, A., Scharlemann, J.P.W., Almond, R.E.A., Baillie, J.E.M., Bomhard, B., Brown, C., Bruno, J., Carpenter, K.E., Carr, G.M., Chanson, J., Chenery, A.M., Csirke, J., Davidson, N.C., Dentener, F., Foster, M., Galli, A., Galloway, J.N., Genovesi, P., Gregory, R.D., Hockings, M., Kapos, V., Lamarque, J., Leverington, F., Loh, J., McGeoch, M.A., McRae, L., Minasyan, A., Morcillo, M.H., Oldfield, T.E.E., Pauly, D., Quader, S., Revenga, C., Sauer, J.R., Skolnik, B., Spear, D., Stanwell-Smith, D., Stuart, S.N., Symes, A., Tierney, M., Tyrrell, T.D., Vié, J. and Watson, R. (2010) 'Global Biodiversity: Indicators of Recent Declines', *Science,* 328(5982), pp. 1164-1168.

Cáceres, M., Legendre, P., Wiser, S.K., Brotons, L. and O'Hara, R.B. (2012) 'Using species combinations in indicator value analyses', *Methods in Ecology and Evolution,* 3(6), pp. 973-982.

Cacuci, D.G., Ionescu-Bujor, M. and Navon, I.M. (2005) *Sensitivity and uncertainty analysis.* 1st edn. Boca Raton [u.a.]: Chapman & Hall/CRC Press.

Cadotte, M.W., Cardinale, B.J. and Oakley, T.H. (2008) 'Evolutionary history and the effect of biodiversity on plant productivity', *Proceedings of the National Academy of Sciences,* 105(44), pp. 17012-17017.

Cain, S.A. and Castro, G.M. (1959) *Manual of vegetation analysis.* New York: Harper.

Cantarello, E. and Newton, A.C. (2008) 'Identifying Cost-Effective Indicators to Assess the Conservation Status of Forested Habitats in Natura 2000 Sites', *Forest Ecology and Management,* 256(4), pp. 815-826.

Cao, M. and Zhang, J. (1997) 'Tree species diversity of tropical forest vegetation in Xishuangbanna, SW China', *Biodiversity and Conservation,* 6(7), pp. 995-1006.

Caratti, J.F. (2006) 'Line Intercept (LI)', in Lutes, D.C. (ed.) *FIREMON: Fire effects monitoring and inventory system.* Fort Collins, CO: U.S. Dept. of Agriculture, Forest Service, Rocky Mountain Research Station, pp. 1-13.

Caravaca, F. and Roldán, A. (2003) 'Assessing changes in physical and biological properties in a soil contaminated by oil sludges under semiarid Mediterranean conditions', *Geoderma,* 117(1–2), pp. 53-61.

Cardinale, B.J., Duffy, J.E., Gonzalez, A., Hooper, D.U., Perrings, C., Venail, P., Narwani, A., Mace, G.M., Tilman, D., Wardle, D.A., Kinzig, A.P., Daily, G.C., Loreau, M., Grace, J.B., Larigauderie, A., Srivastava, D.S. and Naeem, S. (2012) 'Biodiversity loss and its impact on humanity', *Nature,* 486, pp. 59.

Cardinale, B.J., Matulich, K.L., Hooper, D.U., Byrnes, J.E., Duffy, E., Gamfeldt, L., Balvanera, P., O'Connor, M.I. and Gonzalez, A. (2011) 'The functional role of producer diversity in ecosystems', *American Journal of Botany,* 98(3), pp. 572-592.

Carlson, K.M., Asner, G.P., Hughes, F.R., Ostertag, R. and Martin, R.E. (2007) 'Hyperspectral Remote Sensing of Canopy Biodiversity in Hawaiian Lowland Rainforests', *Ecosystems,* 10(4), pp. 536-549.

Carpenter, S.R., DeFries, R., Dietz, T., Mooney, H.A., Polasky, S., Reid, W.V. and Scholes, R.J. (2006) 'Millennium Ecosystem Assessment: Research Needs', *Science,* 314(5797), pp. 257-258.

Carter, G.A. (1994) 'Ratios of leaf reflectances in narrow wavebands as indicators of plant stress', *International Journal of Remote Sensing,* 15(3), pp. 697-703.

Carter, G.A. (1993) 'Responses of Leaf Spectral Reflectance to Plant Stress', *American Journal of Botany,* 80(3), pp. 239-243.

Carter, G.A. and Miller, R.L. (1994) 'Early detection of plant stress by digital imaging within narrow stress-sensitive wavebands', *Remote Sensing of Environment,* 50(3), pp. 295-302.

Carwardine, J., Klein, C.J., Wilson, K.A., Pressey, R.L. and Possingham, H.P. (2009) 'Hitting the Target and Missing the Point: Target -based Consertvation Planning in Context', *Conservation Letters,* 2, pp. 3-10.

Ceccato, P., Flasse, S., Tarantola, S., Jacquemoud, S. and Grégoire, J. (2001) 'Detecting vegetation leaf water content using reflectance in the optical domain', *Remote Sensing of Environment,* 77(1), pp. 22-33.

Central Intelligence Agency (2015) *The World FactBook: Nigeria.* Available at: https://www.cia.gov/library/publications/the-world-factbook/geos/ni.html(Accessed: 04/03 2015).

Centre for Remote Imaging, Sensing and Processing (CRISP) (2015) *What is Remote Sensing?* Available at:

http://www.crisp.nus.edu.sg/~research/tutorial/intro.htm (Accessed: 03/05 2015).

Chambers, J.C. and Brown, R.W. (1983) *Methods for Vegetation Sampling and Analysis on Revegetated Mined Lands.* Ogden, Utah: U.S. Dept. of Agriculture, Forest Service, Intermountain Forest and Range Experimental Station.

Chandra, A. and Idrisova, A. (2011) 'Convention on Biological Diversity: a Review of National Challenges and Opportunities for Implementation', *Biodiversity and Conservation,* 20(14), pp. 3295-3316.

Chao, A., Chazdon, R.L., Colwell, R.K. and Shen, T. (2006) 'Abundance-Based Similarity Indices and Their Estimation When There Are Unseen Species in Samples', *Biometrics,* 62(2), pp. 361-371.

Chao, A., Chiu, C. (2016) 'Species Richness Estimation and Comparison', in N. Balakrishnan, T. Colton, B. Everitt, W. Piegorsch, F. Ruggeri and J. L. Teugels (ed.) *Wiley StatsRef: Statistics Reference Online.* 1st edn. Online: Wiley.

Chapin, F.S., Zavaleta, E.S., Eviner, V.T., Naylor, R.L., Vitousek, P.M., Reynolds, H.L., Hooper, D.U., Lavorel, S., Osvaldo, E.S., Hobbie, S.E., Mack, M.C. and Díaz, S. (2000) 'Consequences of Changing Biodiversity', *Nature,* 405, pp. 234-242.

Chappelle, E.W., Kim, M.S. and McMurtrey, J.E. (1992) 'Ratio analysis of reflectance spectra (RARS): An algorithm for the remote estimation of the concentrations of chlorophyll A, chlorophyll B, and carotenoids in soybean leaves', *Remote Sensing of Environment,* 39(3), pp. 239-247.

Chen, P.Y., Fedosejevs, G., Tiscareno-Lopez, M. and Arnold, J.G. (2006) 'Assessment of MODIS-EVI, MODIS-NDVI and VEGETATION-NDVI composite data using agricultural measurements: an example at corn fields in western Mexico', *Environmental monitoring and assessment,* 119(1-3), pp. 69-82.

Chen, W. and Henebry, G.M. (2009) 'Change of spatial information under rescaling: A case study using multi-resolution image series', *ISPRS Journal of Photogrammetry and Remote Sensing,* 64(6), pp. 592-597.

Chen, Z., Elvidge, C.D. & Jansen, W.T. (1993) 'Description of derivative-based high-spectral-resolution (AVIRIS) green vegetation index', *Optical Engineering and Photonics in Aerospace Sensing, 1993 * Florida, United States, 23 September 1993 United States: SPIE, pp. 43.

Chima, U.D. and Vure, G. (2014) 'Implications of crude oil pollution on natural regeneration of plant species in an oil-producing community in the Niger Delta Region of Nigeria', *Journal of Forestry Research,* 25(4), pp. 915-921.

Cho, M.A., Skidmore, A., Corsi, F., van Wieren, S.E. and Sobhan, I. (2007) 'Estimation of green grass/herb biomass from airborne hyperspectral imagery using spectral indices and partial least squares regression', *International Journal of Applied Earth Observations and Geoinformation,* 9(4), pp. 414-424.

CITES (1975) *Convention on International Trade in Endangered Species of Wild Fauna and Flora Document.* Available at:

http://www.cites.org/sites/default/files/eng/disc/E-Text.pdf (Accessed: 01/19 2015).

Clark, M.L. and Roberts, D.A. (2012) 'Species-Level Differences in Hyperspectral Metrics among Tropical Rainforest Trees as Determined by a Tree-Based Classifier', *Remote Sensing,* 4(12), pp. 1820-1855.

Clark, R.N. and Roush, T.L. (1984) 'Reflectance spectroscopy - Quantitative analysis techniques for remote sensing applications', *Journal of Geophysical Research: Solid Earth,* 89(B7), pp. 6329-6340.

Clark, R.N., Swayze, G.A., Leifer, I., Livo, K.E., Kokaly, R., Hoefen, T., Lundeen, S., Eastwood, M., Green, R.O., Pearson, N., Sarture, C., McCubbin, I., Roberts, D., Bradley, E., Steele, D., Ryan, T., Dominguez, R. & and the Air borne Visible/Infrared Imaging Spectrometer (AVIRIS) Team 2010 *A method for quantitative mapping of thick oil spills using imaging spectroscopy: U.S. Geological Survey Open-File Report* , U.S. Department of the Interior, U.S. Geological Survey, Reston Virginia.

Clevers, J G P W and Büker, C. (1991) 'Feasibility of the red edge index for the detection of nitrogen deficiency', *Int. Coll. Physical Measurements and Signatures in Remote Sensing;* Courchevel, France, 14th - 18th January, 1991 France: European Space Agency (ESA).

Clevers, J. G. P. W., De Jong, S. M., Epema, G. F., Van Der Meer, F. D., Bakker, W H, Skidmore, A. K., Scholte and K H (2002) 'Derivation of the red edge index using the MERIS standard band setting', *International Journal of Remote Sensing,* 23(16), pp. 3169-3184.

Connell, J.H. (2008) 'Diversity in Tropical Rainforests and Coral Reefs (1978)', *Science,* 199(4335).

Convention on Biodiversity (2017) *How Nigeria Strives to Achieve Biodiversity ConservationTargets;* Available at: https://www.environewsnigeria.com/nigeria-strives-achieve-biodiversity-conservation-targets-cbd/ (Accessed: 15/09/2018).

Convention on Biological Diversity (2010) *Strategic Plan for Biodiversity 2011-2020.* Available at: https://www.cbd.int/sp/default.shtml (Accessed: 20/02/2018).

Corcoran, E., Ravilious, C. & Skuja, M. 2007 *Mangroves of Western and Central Africa*, UNEP-WCMC/UNEP, Cambridge, United Kingdom.

Cowell, E.B. (1971) 'Some Effects of Oil Pollution in Milford Haven, United Kingdom', *International Oil Spill Conference Proceedings,* 1971(1), pp. 429-436.

Cummings, J., Smith & D. (2000) 'The Line-Intercept Method: A Tool for Introductory Plant Ecology Laboratories', *Association for Biology Laboratory Education (ABLE)* South Carolina, USA, 2000 Clemson University: Association for Biology Laboratory Education (ABLE), pp. 234.

Curran, P.J., Dungan, J.L. and Gholz, H.L. (1990) 'Exploring the relationship between reflectance red edge and chlorophyll content in slash pine', *Tree physiology,* 7(1_2_3_4), pp. 33-48.

Curran, P.J., Dungan, J.L. and Peterson, D.L. (2001) 'Estimating the foliar biochemical concentration of leaves with reflectance spectrometry', *Remote Sensing of Environment,* 76(3), pp. 349-359.

Dalponte, M., Bruzzone, L., Vescovo, L. and Gianelle, D. (2009) 'The Role of Spectral Resolution and Classifier Complexity in the Analysis of Hyperspectral Images of Forest Areas', *Remote Sensing of Environment,* 113(11), pp. 2345-2355.

Daniel, K.S., Jacob, D.E. and Udeagha, A.U. (2015) 'Tree Species Composition in Selected sacred Forests in Nigeria', *International Journal of Mol. Ecol. and Conserv 2015, Vol.5, No.7, 1-10,* 5(7), pp. 1-10.

Daniel-Kalio, L. and Braide, S.A. (2002) 'The Impact of Accidental Oil Spill on Cultivated and Natural Vegetation in a Wetland Area of Niger Delta, Nigeria', *AMBIO: A Journal of the Human Environment,* 31(5), pp. 441-442.

Danielsen, F., Mendoza, M.M., Alviola, P., Balete, D.S., Poulsen, M.K. and Jenson, A.E. (2003) 'Biodiversity Monitoring in Developing Countries: What Are We Trying To Achieve', *Oryx,* 37(4), pp. 407-409.

Das, N. and Chandra, P. (2011) 'Microbial Degradation of Petroleum Hydrocarbon Contaminants: An Overview', *Biotechnology Research International,* Article ID 941810, pp 13.

Das, N. (2009) 'A comparison study of three non-parametric control charts to detect shift in location parameters', *The International Journal of Advanced Manufacturing Technology,* 41(7), pp. 799-807.

Datt, B., McVicar, T.R., Van Niel, T.G., Jupp, D.L.B. and Pearlman, J.S. (2003) 'Preprocessing EO-1 Hyperion hyperspectral data to support the application of

agricultural indexes', *IEEE Transactions on Geoscience and Remote Sensing,* 41(6), pp. 1246-1259.

Datt, B. (1999) 'A New Reflectance Index for Remote Sensing of Chlorophyll Content in Higher Plants: Tests using Eucalyptus Leaves', *Journal of Plant Physiology,* 154(1), pp. 30-36.

Daughtry, C.S.T., Walthall, C.L., Kim, M.S., de Colstoun, E.B. and McMurtrey, J.E. (2000) 'Estimating Corn Leaf Chlorophyll Concentration from Leaf and Canopy Reflectance', *Remote Sensing of Environment,* 74(2), pp. 229-239.

David U Hooper, E Carol Adair, Bradley J Cardinale, Jarrett E K Byrnes, Bruce A Hungate, Kristin L Matulich, Andrew Gonzalez, J Emmett Duffy, Lars Gamfeldt and Mary I O'Connor (2012) 'A global synthesis reveals biodiversity loss as a major driver of ecosystem change', *Nature,* 486(7401), pp. 105.

De Cáceres, M., Legendre, P. and Moretti, M. (2010) 'Improving indicator species analysis by combining groups of sites', *Oikos,* 119(10), pp. 1674-1684.

de Jong, W. (1997) 'Developing swidden agriculture and the threat of biodiversity loss', *Agriculture, Ecosystems & Environment,* 62(2–3), pp. 187-197.

Deák, M., Telbisz, T., Árvai, M., Mari, L., Horváth, F., Kohán, B., Szabó, O. and Kovács, J. (2017) 'Heterogeneous forest classification by creating mixed vegetation classes using EO-1 Hyperion', *International Journal of Remote Sensing,* 38(18), pp. 5215-5231.

Denes, S.L., Miksis-Olds, J.L., Mellinger, D.K. and Nystuen, J.A. (2014) 'Assessing the Cross Platform Performance of Marine Mammal Indicators between Two Collocated Acoustic Recorders', *Ecological Informatics,* 21, pp. 74-80.

Dengler, J. (2009) 'A Flexible Multi-Scale Approach for Standardised Recording of Plant Species Richness Patterns ', *Ecological Indicators,* 9(6), pp. 1169-1178.

DENR-NORDECO (2001) *Biodiversity Monitoring System Manual for Protected Areas.* 2nd edn. Manila: NORDECO-DENR.

Department of Petroleum Resources, (DPR) 2002 *Environmental Guidelines and Standards for the Petroleum Industry in Nigeria*, Department of Petroleum Resources (DPR), Lagos.

Dickson, U.J. and Udoessien, E.I. (2012) 'Physicochemical studies of Nigeria's Crude Blend', *Petroleum and Coal,* 54(3), pp. 243-251.

Dobson, A. (2005) 'Monitoring Global Rates of Biodiversity Change: Challenges That Arise in Meeting the Convention on Biological Diversity (CBD) 2010 goals', *Philosophical Transactions of the Royal Society B: Biological Sciences,* 360(1454), pp. 229-241.

Dorazio, R.M., Royle, J.A., Söderström, B. and Glimskär, A. (2006) 'Estimating Species Richness and Accumulation by Modeling Species Occurrence and Detectability', *Ecology,* 87(4), pp. 842-854.

Duelli, P. and Obrist, M.K. (2003) 'Biodiversity Indicators: the Choice of Values and Measures', *Agriculture, Ecosystems and Environment,* 98(1-3), pp. 87-98.

Duffield, C. (2010) *Nigeria: 'World Oil Pollution Capital'.* Available at: http://www.bbc.co.uk/news/10313107 (Accessed: 15/02 2015).

Dung, N.T. and Webb, E.L. (2008) 'Combining Local Ecological knowledge and Quantitative Forest Surveys to Select Indicator Species for Forest Condition Monitoring in Central Viet Nam', *Ecological Indicators,* 8(5), pp. 767-770.

Dunn, O.J. (1964) 'Multiple Comparisons Using Rank Sums', *Technometrics,* 6(3), pp. 241-252.

Duro, D.C., Coops, N.C., Wulder, M.A. and Han, T. (2007) 'Development of a Large Area Biodiversity Monitoring System Driven by Remote Sensing', *Progress in Physical Geography,* 31(3), pp. 235-260.

Dymond, C.C., Mladenoff, D.J. and Radeloff, V.C. (2002) 'Phenological Differences in Tasseled Cap Indices Improve Deciduous Forest Classification ', *Remote Sensing of Environment,* 80(3), pp. 460-472.

Eastwood, J.A., Yates, M.G., Thomson, A.G. and Fuller, R.M. (1997) 'The Reliability of Vegetation Indices for Monitoring Saltmarsh Vegetation Cover', *International Journal of Remote Sensing,* 18(18), pp. 3901-3907.

Ebegbulem, J.C., Ekpe, D. and Adejumo, T.O. (2013) 'Oil Exploration and Poverty in the Niger Delta Region of Nigeria: A Critical Analysis', *International Journal of Business and Social Science,* 4(3), pp. 279-287.

Ebeku, K.S.A. (2006) *Oil and the Niger Delta People in International Law: Resource Rights, Environmental and Equity Issues.* Cologne: Rüdiger Köppe Verlag.

Ebigwa, J.K. and Akomaye, F. (2014) 'Species Diversity and Regeneration Potential of Some Mixed Mangrove Forests in Escravos Communities Delta State Nigeria', *Research Journal of Forestry,* 8(2), pp. 34-47.

Edgar, G.J. and Barrett, N.S. (2000) 'Impact of the Iron Baron Oil Spill on Subtidal Reef Assemblages in Tasmania', *Marine pollution bulletin,* 40(1), pp. 36-49.

Ehrlich, P.R. (1988) *The Loss of Diversity Causes and Consequences in Biodiversity by Wilson, E. O. (Ed).* Available at:

http://site.ebrary.com/lib/leicester/reader.action?docID=10068400 (Accessed: 01/06 2015).

Eigemeier, E., Heiskanen, J., Rautiainen, M., Vesanto, V., Majasalmi, T. and Stenberg, P. (2012) 'Narrowband Vegetation Indices for Estimating Boreal Forest Leaf Area Index', *Remote Sensing - Applications,* Available at:

https://www.openaire.eu/search/publication?articleId=intech_____::14f9238abeaf 507c5916be876b19e81.

Eisenhauer, N., Beßler, H., Engels, C., Gleixner, G., Habekost, M., Milcu, A., Partsch, S., Sabais, A.C.W., Scherber, C., Steinbeiss, S., Weigelt, A., Weisser, W.W. and Scheu, S. (2010) 'Plant diversity effects on soil microorganisms support the singular hypothesis', *Ecology,* 91(2), pp. 485-496.

Elenwo, E. and Akankali, J. (2014) 'Impact of Climate Change on Aquatic Fauna of Economic Importance in Niger Delta, Nigeria.', *Atmospheric and Climate Sciences,* 4(4), pp. 710-720.

El-Nemr, A. (2006) *Petroleum contamination in warm and cold marine environments.* 1st edn. New York: Novinka Books.

Elvidge, C.D. and Chen, Z. (1995) 'Comparison of broad-band and narrow-band red and near-infrared vegetation indices', *Remote Sensing of Environment,* 54(1), pp. 38-48.

Elzinga, C.L., Willoughby, J.W. and Salzer, D.W. (1998) *Measuring and Monitoring Plant Populations.* Denver, Colo.] : Arlingtion, Va.]: U.S. Dept. of the Interior, Bureau of Land Management ; Nature Conservancy.

Emoyan, O.O., Akpoborie, I.A. and Akporhonor, E.E. (2008) 'The Oil and Gas Industry and the Niger Delta: Implications for the Environment', *Journal of Applied Science and Environmental Management,* 12(3), pp. 29-37.

Encyclopedia of the Earth (2015) *Niger Delta Swamp Forests.* Available at: http://www.eoearth.org/view/article/154853/ (Accessed: 03/10 2015).

Eneje, R.C., Nwagbara, C. and Uwumarongie-Ilori, E.G. (2012) 'Amelioration of Chemical Properties of Crude Oil Contaminated Soil using Compost from *Calapoigonium mucunoides* and Poultry Manure ', *International Research Journal of Agricultural Science and Soil Science',* 2(6), pp. 246-251.

Eniscuola (2015) *Biodiversity.* Available at:

http://www.eniscuola.net/en/argomento/biodiversity1/ (Accessed: 03/10 2015).

Environmental Resources Managers Limited, (ERML) 1997 *Environmental and Social Characteristics of the Niger Delta. Phase 1: A Report Submitted by Environmental Resources Managers Limited to the* , Niger Delta Environmental Survey (NDES), Lagos.

Ereba, P., Pyagbara, S.L., Draper, T.L. & Emmanuel, E.O.S. 2010 *Shell in the Niger Delta: A Framework for Change*, The Ecunemical Council for Corporate Responsibility, Oxford.

Escuin, S., Navarro, R. and Fernández, P. (2008) 'Fire severity assessment by using NBR (Normalized Burn Ratio) and NDVI (Normalized Difference Vegetation Index) derived from LANDSAT TM/ETM images', *International Journal of Remote Sensing,* 29(4), pp. 1053-1073.

Essien, O. and John, I. (2011) 'Impact of Crude-Oil Spillage Pollution and Chemical Remediation on Agricultural Soil Properties and Crop Growth', *Journal of Applied Sciences and Environmental Management,* 14(4).

European Space Agency (2018) *STEP: Science Toolbox Exploitation Platform.* Available at: http://step.esa.int/main/toolboxes/snap/ (Accessed: 18/01/2018).

European Space Agency 2015 *Sentinel-2 User Handbook*, ESA, Frascati, Italy.

Ewers, R.M. and Rodrigues, A.S.L. (2006) 'Speaking Different Languages on Biodiversity', *Nature,* 443(7111), pp. 506.

Fagbami, A.A., Udo, E.J. and Odu, C.T.I. (2009) 'Vegetation Damage in an Oilfield in the Niger Delta of Nigeria', *Journal of Tropical Ecology,* 4, pp. 75.

Faith, D.P. and Walker, P.A. (1996) 'How do Indicator Groups Provide Information about the Relative Biodiversity of Different Sets of Areas?; on Hotspot, Complementary and Pattern-based Approaches', *Biodiversity Letters,* 3(1), pp. 18-25.

Fangliang, H. and Hu Xin-Sheng (2005) 'Hubbell's fundamental biodiversity parameter and the Simpson diversity index', *Ecology Letters,* 8(4), pp. 386-390.

Fatoba, P.O., Ogunkunle, C.O., Folarin, O.O. and Oladele, F.A. (2016) 'Heavy metal pollution and ecological geochemistry of soil impacted by activities of oil industry in the Niger Delta, Nigeria', *Environmental Earth Sciences,* 75(4), pp. 1-9.

Fatoyinbo, T.E. and Simard, M. (2013) 'Height and biomass of mangroves in Africa from ICESat/GLAS and SRTM', *International Journal of Remote Sensing,* 34(2), pp. 668-681.

Feilhauer, H., He, K.S. and Rocchini, D. (2012) 'Modeling Species Distribution Using Niche-Based Proxies Derived from Composite Bioclimatic Variables and MODIS NDVI.', *Remote Sensing.,* 4(7).

Felde, G.W., Anderson, G.P., Cooley, T.W., Matthew, M.W., adler-Golden, S.M., Berk, A. & Lee, J. (2003a) 'Analysis of Hyperion data with the FLAASH atmospheric correction algorithm', *International Geoscience and Remote Sensing Symposium, 2003. IGARSS '03. * Toulouse, France, 21-25 July, 2003 Toulouse, France: IEEE, pp. 90.

Féret, J. and Asner, G.P. (2014) 'Mapping tropical forest canopy diversity using high-fidelity imaging spectroscopy', *Ecological Applications,* 24(6), pp. 1289-1296.

Fern, K., Fern, A. & Morris, R. (2015) *Useful Tropical Plants: Symphonia globulifera L.f. CLUSIACEAE.* Available at:

http://tropical.theferns.info/viewtropical.php?id=Symphonia+globulifera (Accessed : 03/04 2015).

Flombaum, P. and Sala, O.E. (2007) 'Higher effect of plant species diversity on productivity in natural than artificial ecosystems', *Proceedings of the National Academy of Sciences of the United States of America,* 105(16), pp. 6087-6090.

Foody, G.M. and Ajay Mathur (2004) 'A relative evaluation of multiclass image classification by support vector machines', *Geoscience and Remote Sensing, IEEE Transactions on,* 42(6), pp. 1335-1343.

Foody, G.M. and Cutler, M.E.J. (2003) 'Tree biodiversity in protected and logged Bornean tropical rain forests and its measurement by satellite remote sensing', *Journal of Biogeography,* 30(7), pp. 1053-1066.

Franco, José Luiz de Andrade (2013) 'The Concept of Biodiversity and the History of Conservation Biology: from Wilderness Preservation to Biodiversity Conservation.', *História,* 32(2), pp. 48.

Frazier, A.E., Wang, L. and Chen, J. (2014) 'Two new hyperspectral indices for comparing vegetation chlorophyll content', *Geo-spatial Information Science,* 17(1), pp. 17-25.

Fricker, G.A., Wolf, J.A., Saatchi, S.S. and Gillespie, T.W. (2015) 'Predicting spatial variations of tree species richness in tropical forests from high-resolution remote sensing', *Ecological Applications,* 25(7), pp. 1776-1789.

Friedel, M.J., Buscema, M., Vicente, L.E., Iwashita, F. and Koga-Vicente, A. (2018) 'Mapping fractional landscape soils and vegetation components from Hyperion satellite imagery using an unsupervised machine-learning workflow', *International Journal of Digital Earth,* 11(7), pp. 670-690.

Fu, X., Cui, Z. and Zang, G. (2014) 'Migration, speciation and distribution of heavy metals in an oil-polluted soil affected by crude oil extraction processes', *Environmental Science: Processes & Impacts,* 16(7), pp. 1737-1744.

Fund, W. (2014) *Niger Delta Swamp Forests.* Available at: http://www.eoearth.org/view/article/154853 (Accessed: January/14 2015).

Galidaki, G. and Gitas, I. (2015) 'Mediterranean Forest Species Mapping Using Classification of Hyperion Imagery', *Geocarto International,* 30(1), pp. 48-61.

Gallardo-Cruz, J.A., Meave, J.A., Gonzalez, E.J., Lebrija Trejos, E.E., Romero-Romero, M.A., Perez-Garcia, E.A., Gallardo-Cruz, R., Hernandez-Stefanoni, J.L. and Martorell, C. (2012) 'Predicting Tropical Dry Forest Successional Attributes from Space: Is the Key Hidden in Image Texture?', *PLoS One,* 7(2), pp. e30506.

Galvao, L.S., Roberts, D.A., Formaggio, A.R., Numata, I. and Breunig, F.M. (2009) 'View angle effects on the discrimination of soybean varieties and on the relationships between vegetation indices and yield using off-nadir Hyperion data', *Remote Sensing of Environment,* 113(4), pp. 846-856.

Gamon, J.A., Serrano, L. and Surfus, J.S. (1997) 'The photochemical reflectance index: an optical indicator of photosynthetic radiation use efficiency across species, functional types, and nutrient levels', *Oecologia,* 112(4), pp. 492-501.

Gamon, J.A. and Surfus, J.S. (1999) 'Assessing leaf pigment content and activity with a reflectometer', *New Phytologist,* 143(1), pp. 105-117.

Gao, B. (1996) 'NDWI—A normalized difference water index for remote sensing of vegetation liquid water from space', *Remote Sensing of Environment,* 58(3), pp. 257-266.

Gersman, R., Ben-Dor, E., Beyth, M., Avigad, D., Abraha, M. and Kibreab, A. (2008) 'Mapping of hydrothermally altered rocks by the EO-1 Hyperion sensor, Northern Danakil Depression, Eritrea', *International Journal of Remote Sensing,* 29(13), pp. 3911-3936.

Gilabert, M.A., González-Piqueras, J., García-Haro, F.J. and Meliá, J. (2002) 'A Generalized Soil-Adjusted Vegetation Index', *Remote Sensing of Environment,* 82(2–3), pp. 303-310.

Gitelson, A.A., Kaufman, Y.J., Stark, R. and Rundquist, D. (2002) 'Novel Algorithms for Remote Estimation of Vegetation Fraction', *Remote Sensing of Environment,* 80(1), pp. 76-87.

Gitelson, A.A. and Merzlyak, M.N. (1996) 'Signature analysis of leaf reflectance spectra: Algorithm development for remote sensing of chlorophyll', *Journal of Plant Physiology,* 148(3-4), pp. 494-500.

Gitelson, A.A., Merzyl Yak, M.N., Zur, Y., Stark, R. and Gritz, U. (2001) 'Non-Destructive and Remote Sensing Techniques for Estimation of Vegetation Status', *Papers in Natural Resource,* 273, pp. 205.

Gitelson, A.A., Peng, Y., Masek, J.G., Rundquist, D.C., Verma, S., Suyker, A., Baker, J., Hatfield, J.L. and Meyers, T. (2012) 'Remote Estimation of Crop Gross Primary Production with Landsat Data', *Remote Sensing of Environment,* 121(0), pp. 404-414.

Gitelson, A.A., Viña, A., Arkebauer, T.J., Rundquist, D.C., Keydan, G. and Leavitt, B. (2003) 'Remote Estimation of Leaf Area Index and Green Leaf Biomass in Maize Canopies', *Geophysical Research Letters,* 30(5).

Gitelson, A.A., Viña, A., Verma, S.B., Rundquist, D.C., Arkebauer, T.J., Keydan, G., Leavitt, B., Ciganda, V., Burba, G.G. and Suyker, A.E. (2006) 'Relationship between Gross Primary Production and Chlorophyll Content in Crops: Implications for the Synoptic Monitoring of Vegetation Productivity', *Journal of Geophysical Research: Atmospheres,* 111(D8).

Gitelson, A., Kaufman, Y. and Merzylak, M. (1996) 'Use of a Green Channel in Remote Sensing of Global Vegetation from EOS-MODIS', *Remote Sensing of Environment,* 58, pp. 289-298.

Gitelson, A.A., Chivkunova, O.B. and Merzlyak, M.N. (2009) 'Nondestructive estimation of anthocyanins and chlorophylls in anthocyanic leaves', *American Journal of Botany,* 96(10), pp. 1861-1868.

Gitelson, A.A., Gritz †, Y. and Merzlyak, M.N. (2003) 'Relationships between leaf chlorophyll content and spectral reflectance and algorithms for non-destructive chlorophyll assessment in higher plant leaves', *Journal of Plant Physiology,* 160(3), pp. 271-282.

Gitelson, A.A. and Merzlyak, M.N. (1998) 'Remote sensing of chlorophyll concentration in higher plant leaves', *Advances in Space Research,* 22(5), pp. 689-692.

Gitelson, A.A., Viña, A., Ciganda, V., Rundquist, D.C. and Arkebauer, T.J. (2005) 'Remote estimation of canopy chlorophyll content in crops', *Geophysical Research Letters,* 32(8), pp. n/a.

Glenn, E.P., Huete, A.R., Nagler, P.L. and Nelson, S.G. (2008) 'Relationship Between Remotely-sensed Vegetation Indices, Canopy Attributes and Plant Physiological Processes: What Vegetation Indices Can and Cannot Tell Us About the Landscape', *Sensors,* 8, pp. 2136-2160.

Glick, B.R. (2010) 'Using soil bacteria to facilitate phytoremediation', *Biotechnology Advances,* 28(3), pp. 367-374.

Global Biodiversity Information Facility, (GBIF) (2015) *Global Biodiversity Information Facility (GBIF).* Available at: http://www.gbif.org/ (Accessed: 20th March, 2016).

Global Environment Facility (2013) *Global environment Facility: Investing in our Planet.* Available at: http://www.thegef.org/gef/whatisgef (Accessed: 01/20 2015).

Goetz, S., Steinberg, D., Dubayah, R. and Blair, B. (2007) 'Laser remote sensing of canopy habitat heterogeneity as a predictor of bird species richness in an eastern temperate forest, USA', *Remote Sensing of Environment,* 108(3), pp. 254-263.

Gong, P., Pu, R., Biging, G.S. and Larrieu, M.R. (2003) 'Estimation of Forest Leaf Area Index Using Vegetation Indices Derived from Hyperion Hyperspectral Data', *Geoscience and Remote Sensing,* 41(6), pp. 1355-1362.

Goodenough, D.G., Dyk, A., Niemann, K.O., Pearlman, J.S., Hao Chen, Tian Han, Murdoch, M. and West, C. (2003) 'Processing Hyperion and ALI for forest classification', *Geoscience and Remote Sensing, IEEE Transactions on,* 41(6), pp. 1321-1331.

Gosselin, F. (2006) 'An assessment of the dependence of evenness indices on species richness', *Journal of theoretical biology,* 242(3), pp. 591-597.

Gould, W. (2000) 'Remote Sensing of Vegetation, Plant Species Richness, and Regional Biodiversity Hotspots', *Ecological Applications,* 10(6), pp. 1861-1870.

Green, A.A., Berman, M., Switzer, P. and Craig, M.D. (1988) 'A transformation for ordering multispectral data in terms of image quality with implications for noise removal', *IEEE Transactions on Geoscience and Remote Sensing,* 26(1), pp. 65-74.

Gregorius, H. and Gillet, E.M. (2008) 'Generalized Simpson-diversity', *Ecological Modelling,* 211(1–2), pp. 90-96.

Griffin, J.N. and Silliman, B.R. (2011) 'Resource Partitioning and Why It Matters', *Nature Education Knowledge,* 3(10), pp. 49.

Group on Earth Observations Biodiversity Observation Network, (GEO BON) 2011 *Adequacy of Biodiversity Observation Systems to support the CBD 2020 Targets.*

Gu, Y., Wylie, B.K., Howard, D.M., Phuyal, K.P. and Ji, L. (2013) 'NDVI saturation adjustment: A new approach for improving cropland performance estimates in the Greater Platte River Basin, USA', *Ecological Indicators,* 30, pp. 1-6.

Guyon, D., Guillot, M., Vitasse, Y., Cardot, H., Hagolle, O., Delzon, S. and Wigneron, J. (2011) 'Monitoring elevation variations in leaf phenology of deciduous broadleaf forests from SPOT/VEGETATION time-series', *Remote Sensing of Environment,* 115(2), pp. 615-627.

Haines-Young, R., Potschin, M. and Kienast, F. (2012) 'Indicators of Ecosystem Service Potential at European Scales: Mapping Marginal Changes and Trade-Offs', *Ecological Indicators,* 21(0), pp. 39-53.

Hall, K., Reitalu, T., Sykes, M.T. and Prentice, H.C. (2012) 'Spectral heterogeneity of QuickBird satellite data is related to fine-scale plant species spatial turnover in semi-natural grasslands', *Applied Vegetation Science,* 15(1), pp. 145-157.

Hammer, Ø and Harper, D. A. T., Ryan, P. D. (2001) 'PAST: Paleontological Statistics Software Package for Education and Data Analysis', *Palaentol Electronica,* 4(1), pp. 4-9.

Han, X., Smyth, R.L., Young, B.E., Brooks, T.M., Sánchez de Lozada, A., Bubb, P., Butchart, S.H.M., Larsen, F.W., Hamilton, H., Hansen, M.C. and Turner, W.R. (eds.) (2014) *A Biodiversity Indicators Dashboard: Addressing Challenges to Monitoring Progress towards the Aichi Biodiversity Targets Using Disaggregated Global Data.* - Public Library of Science.

Harrop, S.R. and Pritchard, D.J. (2011) 'A Hard Instrument Goes Soft: The Implications of the Convention on Biological Diversity's Current Trajectory ', *Global Environmental Change,* 21(2), pp. 474-480.

Hatier, J.B. and Gould, K.S. (2008) 'Foliar anthocyanins as modulators of stress signals', *Journal of Theoretical Biology,* 253(3), pp. 625-627.

Hayfield, T. and Racine, J.S. (2008) 'Nonparametric Econometrics: The np Package', *Journal Of Statistical Software,* 27(5), pp. 1-32.

He, K.S., Zhang, J. and Zhang, Q. (2009) 'Linking variability in species composition and MODIS NDVI based on beta diversity measurements', *Acta Oecologica,* 35(1), pp. 14-21.

Hector, A., Schmid, B., Beierkuhnlein, C., Caldeira, M.C., Diemer, M., Dimitrakopoulos, P.G., Finn, J.A., Freitas, H., Giller, P.S., Good, J., Harris, R., Högberg, P., Huss-Danell, K., Joshi, J., Jumpponen, A., Körner, C., Leadley, P.W., Loreau, M., Minns, A., Mulder, C.P.H., O'Donovan, G., Otway, S.J., Pereira, J.S., Prinz, A., Read, D.J.,

Scherer-Lorenzen, M., Schulze, E.-., Siamantziouras, A.-.D., Spehn, E.M., Terry, A.C., Troumbis, A.Y., Woodward, F.I., Yachi, S. and Lawton, J.H. (1999) 'Plant Diversity and Productivity Experiments in European Grasslands', *Science,* 286(5442), pp. 1123-1127.

Hector, A. (1998) 'The Effect of Diversity on Productivity: Detecting the Role of Species Complementarity', *Oikos,* 82(3), pp. 597-599.

Hejcmanovā-Nežerková, P. and Hejcman, M. (2006) 'A canonical correspondence analysis (CCA) of the vegetation–environment relationships in Sudanese savannah, Senegal', *South African Journal of Botany,* 72(2), pp. 256-262.

Hejda, M., PyÅ¡ek, P. and JaroÅ¡Ãk, V. (2009) 'Impact of invasive plants on the species richness, diversity and composition of invaded communities', *Journal of Ecology,* 97(3), pp. 393-403.

Hester, M.W., Willis, J.M., Rouhani, S., Steinhoff, M.A. and Baker, M.C. (2016) 'Impacts of the Deepwater Horizon oil spill on the salt marsh vegetation of Louisiana', *Environmental pollution (Barking, Essex: 1987),* 216, pp. 361-370.

Hestir, E.L., Khanna, S., Andrew, M.E., Santos, M.J., Viers, J.H., Greenberg, J.A., Rajapakse, S.S. and Ustin, S.L. (2008) 'Identification of Invasive Vegetation Using Hyperspectral Remote Sensing in The California Delta Ecosystem ', *Remote Sensing of Environment,* 112(11), pp. 4034-4047.

Heumann, B.W., Hackett, R.A. and Monfils, A.K. (2015) 'Testing the spectral diversity hypothesis using spectroscopy data in a simulated wetland community', *Ecological Informatics,* 25, pp. 29-34.

Hill, D., Fasham, M., Tucker, G., Shewry, M. and Shaw, P. (eds.) (2005) *Handbook of Biodiversity Methods: Survey, Evaluation and Monitoring.* Cambridge: Cambridge University Press.

Hoel, B.O. (1998) 'Use of a hand-held chlorophyll meter in winter wheat: Evaluation of different measuring positions on the leaves', *Acta Agriculturae Scandinavica, Section B — Soil & Plant Science,* 48(4), pp. 222-228.

Holt, A. (2006) 'Biodiversity Definitions Vary Within the Discipline', *Nature,* 444(146).

Hooper, D.U., Chapin, F.S., Ewel, J.J., Hector, A., Inchausti, P., Lavorel, S., Lawton, J.H., Lodge, D.M., Loreau, M., Naeem, S., Schmid, B., Setälä, H., Symstad, A.J., Vandermeer, J. and Wardle, D.A. (2005) 'Effects of Biodiversity on Ecosystem Functioning: A Consensus of Current Knowledge', *Ecological Monographs,* 75(1), pp. 3-35.

Horler, D.N.H., Dockray, M., Barber, J. and Barringer, A.R. (1983) 'Red edge measurements for remotely sensing plant chlorophyll content', *Advances in Space Research,* 3(2), pp. 273-277.

Houborg, R. and Boegh, E. (2008) 'Mapping Leaf Chlorophyll and Leaf Area Index Using Inverse and Forward Canopy Reflectance Modeling and SPOT Reflectance Data', *Remote Sensing of Environment,* 112(1), pp. 186-202.

Hu, Q., Wu, W., Xia, T., Yu, Q., Yang, P., Li, Z. and Song, Q. (2013) 'Exploring the Use of Google Earth Imagery and Object-Based Methods in Land Use/Cover Mapping', *Remote Sensing,* 5(11), pp. 6026-6042.

Huete, A.R. (2012) 'Vegetation Indices, Remote Sensing and Forest Monitoring', *Geography Compass,* 6(9), pp. 513-532.

Huete, A.R. (1988) 'A Soil-Adjusted Vegetation Index (SAVI)', *Remote Sensing of Environment,* 25(3), pp. 295-309.

Human Rights Watch, (. 1999 *The Price of Oil: Corporate Responsibility and Human Right Violations in Nigeria's Oil Producing Communities*, HRW, New York.

Hunter, P.R. and Gaston, M.A.'Numerical Index of theDiscriminatory Ability of Typing Systems: An Application of Simpson's Index of Diversity', *Journal of Clinical Microbiology,* 26(11).

Hurlbert, S.H. (1971) 'The Nonconcept of Species Diversity: A Critique and Alternative Parameters', *Ecology,* 52(4), pp. 577-586.

Hurvich, C.M., Simonoff, J.S. and Tsai, C. (1998) 'Smoothing parameter selection in nonparametric regression using an improved Akaike information criterion', *Journal of the Royal Statistical Society: Series B (Statistical Methodology),* 60(2), pp. 271-293.

Huston, M. (1979) 'A General Hypothesis of Species Diversity', *The American Naturalist,* 113(1), pp. 81-101.

Ibezue, V.C. (2013) 'Effects of Fossil Fuel Extraction on Gokana Environment, Ogoni land, Nigeria', *2nd International Conference on Energy Systems and Technologies* Cairo, Egypt.

Ifemeje, J. and Egbuna, C. (2016) 'Effect of Crude Oil Pollution on Soil and Proximate Composition of Cassava from Owaza in Ukwa West Local Government Area of Abia State, Nigeria.*', International Journal of Innovation and Applied Studies, 15(1), pp. 72.*

International Institute for Environment and Development *IIED.* Available at: http://www.iied.org/about-us (Accessed: November/24 2014).

IUCN *World Conservation Strategy.* Available at: https://portals.iucn.org/library/efiles/documents/WCS-004.pdf (Accessed: 01/19 2015).

Jacob, D.E., Eniang, E.A., Nelson, I.U. and Udoakpan, U.I. (2015) 'Vegetation Assessment of Sclater's Guenon Habitat in Ikot Uso Akpan Forest, ITU, South-Eastern Nigeria', *International Journal of Mol. Ecol. and Conserv,* 5(1), pp. 1-7.

Jacquemoud, S., Ustin, S.L., Verdebout, J., Schmuck, G., Andreoli, G. and Hosgood, B. (1996) 'Estimating leaf biochemistry using the PROSPECT leaf optical properties model', *Remote Sensing of Environment,* 56(3), pp. 194-202.

Jan Douda, Jana Doudová-Kochánková, Karel Boublík and Alena Drašnarová (2012) 'Plant species coexistence at local scale in temperate swamp forest: test of habitat heterogeneity hypothesis', *Oecologia,* 169(2), pp. 523-534.

Jinru Xue and Baofeng Su (2017) 'Significant Remote Sensing Vegetation Indices: A Review of Developments and Applications', *Journal of Sensors,* 2017(1), pp. 11-21.

John, R., Ntino, E. and Essien, J. (2016) 'Ammonium Oxidizing Bacteria Activity and Nitrification Rate in Oil-Contaminated Wetland Soil under Remediation with Nutrient Supplements and Leguminous Plants', *Journal of Environmental Protection,* 7(4).

Johnson, D.D.P., Hay, S.I. and Rogers, D.J. (1998) 'Contemporary Environmental Correlates of Endemic Bird Areas Derived from Meteorological Satellite Sensors', *Proceedings: Biological Sciences,* 265(1400), pp. 951-959.

Jong, S.M.d. and Meer, F.v.d. (eds.) (2006) *Remote sensing image analysis.* 2nd edn. Dordrecht: Springer.

Jørgensen, U., Mortensen, J. and Ohlsson, C. (2003) 'Light Interception and Dry Matter Conversion Efficiency of Miscanthus Genotypes Estimated from Spectral Reflectance Measurements', *New Phytologist,* 157(2), pp. 263-270.

Joseph, L.N., Field, S.A., Wilcox, C. and Possingham, H.P. (2006) 'Presence-Absence versus Abundance Data for Monitoring Threatened Species; Datos de Presencia-Ausencia versus Abundancia para el Monitoreo de Especies Amenazadas', *Conservation Biology,* 20(6), pp. 1679-1687.

Jost, L. (2010) 'The Relation between Evenness and Diversity', *Diversity,* 2(2), pp. 207-232.

K.N. Aroh, I.U. Ubong, C.L. Eze, I.M. Harry, J.C. Umo-Otong and A.E. Gobo (2010) 'Oil Spill Incidents and Pipeline Vandalization in Nigeria', *Disaster Prev and Management,* 19(1), pp. 70-87.

Kaimaris, D., Georgoula, O., Patias, P. and Stylianidis, E. (2011) 'Comparative analysis on the archaeological content of imagery from Google Earth', *Journal of Cultural Heritage,* 12(3), pp. 263-269.

Kamaljit Bawa, Joseph Rose, K.N. Ganeshaiah, Narayani Barve, M.C. Kiran and R. Umashaanker (2002) 'Assessing Biodiversity from Space', *Conservation Ecology,* 6(2), pp. 7.

Kanke, Y., Raun, W., Solie, J., Stone, M. and Taylor, R. (2012) 'Red Edge as a Potential Index for Detecting Differences in Plant Nitrogen Status in Winter Wheat', *Journal of Plant Nutrition,* 35(10), pp. 1526-1541.

Karthikeyan, N., Shashikkumar, M.C. & Ramanamurthy, J. (2010) 'A study on vegetation vigour as affected by soil properties using remote sensing approach', *RSTSCC-2010* Chennai, India, 13-15 November 2010IEEE, pp. 107.

Kathryn, M.E., Tancredi, C., Buscot François, Markus, F., Christine, H., Maier, T.S., Torsten, M., Müller Caroline, Elisabeth, O., Daniel, P., Socher, S.A., Ilja, S., Wäschke Nicole, Tesfaye, W., Susanne, W. and Rillig, M.C. (2014) 'Choosing and using diversity indices: insights for ecological applications from the German Biodiversity Exploratories', *Ecology and Evolution,* 4(18), pp. 3514-3524.

Kennish, M.J. (1991) *Ecology of Estuaries: Anthropogenic Effects.* Florida: CRC Press.

Kercher, S.M., Frieswyk, C.B. and Zedler, J.B. (2003) 'Effects of sampling teams and estimation methods on the assessment of plant cover', *Journal of Vegetation Science,* 14(6), pp. 899-906.

Kerr, J.T. and Ostrovsky, M. (2003) 'From space to species: ecological applications for remote sensing', *Trends in Ecology & Evolution,* 18(6), pp. 299-305.

Khanna, S., Santos, M.J., Ustin, S.L., Koltunov, A., Kokaly, R.F. and Roberts, D.A. (2013) 'Detection of Salt Marsh Vegetation Stress and Recovery after the Deepwater Horizon Oil Spill in Barataria Bay, Gulf of Mexico Using AVIRIS Data', *PLoS ONE,* 8(11), pp. e78989.

Khanna, S., Santos, M.J., Ustin, S.L., Shapiro, K., Haverkamp, P.J. and Lay, M. (2018) 'Comparing the Potential of Multispectral and Hyperspectral Data for Monitoring Oil Spill Impact', *Sensors (Basel, Switzerland),* 18(2).

Kinako, P.D.S. (1981) 'Short-term effects of oil pollution on species numbers and productivity of a simple terrestrial ecosystem', *Environmental Pollution Series A, Ecological and Biological,* 26(2), pp. 87-91.

Kisic, I., Mesic, S., Basic, F., Brkic, V., Mesic, M., Durn, G., Zgorelec, Z. and Bertovic, L. (2009) 'The effect of drilling fluids and crude oil on some chemical characteristics of soil and crops', *Geoderma,* 149(3–4), pp. 209-216.

Klokk, T. (1984) 'Effects of oil pollution on the germination and vegetative growth of five species of vascular plant', *Oil and Petrochemical Pollution,* 2(1), pp. 25-30.

Koenker, R., Portnoy, S., Ng, P.T., Zeileis, A., Grosjean, P. and Ripley, B.D. (eds.) (2018) *Quantile Regression.* CRAN.R: .

Kokaly, R.F. and Clark, R.N. (1999) 'Spectroscopic determination of leaf biochemistry using band-depth analysis of absorption features and stepwise multiple linear regression', *Remote Sensing of Environment,* 67(3), pp. 267-287.

Kokaly, R.F., Couvillion, B.R., Holloway, J.M., Roberts, D.A., Ustin, S.L., Peterson, S.H., Khanna, S. and Piazza, S.C. (2013) 'Spectroscopic remote sensing of the distribution and persistence of oil from the Deepwater Horizon spill in Barataria Bay marshes', *Remote Sensing of Environment,* 129, pp. 210-230.

Kokaly, R.F., Despain, D.G., Clark, R.N. and Livo, K.E. (2003) 'Mapping vegetation in Yellowstone National Park using spectral feature analysis of AVIRIS data', *Remote Sensing of Environment,* 84(3), pp. 437-456.

Krebs, C.J. (2002) 'Two Complementary Paradigms for Analysing Population Dynamics', *The Royal Society,* B(357), pp. 1211-1219.

Kromrey, J.D., Hogarty, K.Y., Ferron, J.M., Hines, V.C. & Hess, M.R. (2005) 'Robustness in Meta-Analysis: An Empirical Comparison of Point and Interval Estimates of Standardized Mean Differences and Cliff's Delta', *Joint Statistical Meetings*, August 7 - 11 2005 Minneapolis:

Kuenzer, C. and Knauer, K. (2013) 'Remote Sensing of Rice Crop Areas', *International Journal of Remote Sensing,* 34(6), pp. 2101-2139.

Kuenzer, C., van Bejima, S., Gessner, U. and Dech, S. (2014) 'Land Surface Dynamics and Environmental Challenges of the Niger Delta, Africa: Remote Sensing- Based Analyses Spanning Three Decades (1986-2013)', *Applied Geography,* 53, pp. 354-368.

Kühn, F., Oppermann, K. and Hörig, B. (2004) 'Hydrocarbon Index – an algorithm for hyperspectral detection of hydrocarbons', *International Journal of Remote Sensing,* 25(12), pp. 2467-2473.

le Maire, G., François, C. and Dufrêne, E. (2004) 'Towards Universal Broad Leaf Chlorophyll Indices Using PROSPECT Simulated Database and Hyperspectral Reflectance Measurements', *Remote Sensing of Environment,* 89(1), pp. 1-28.

Legendre, P. (2007) 'Studying beta diversity: ecological variation partitioning by multiple regression and canonical analysis', 1(1), pp. 3-8.

Legendre, P. and Legendre, L. (2012) *Numerical ecology.* 3. engl. ed. edn. Amsterdam [u.a.]: Elsevier.

Levin, N., Shmida, A., Levanoni, O., Tamari, H. and Kark, S. (2007) 'Predicting Mountain Plant Richness and Rarity from Space Using Satellite-Derived Vegetation Indices', *Diversity and Distributions,* 13(6), pp. 692-703.

Li, L., Ustin, S.L. and Lay, M. (2005) 'Application of AVIRIS data in detection of oil-induced vegetation stress and cover change at Jornada, New Mexico', *Remote Sensing of Environment,* 94(1), pp. 1-16.

Lichtenthaler, H.K. (1996) 'Vegetation Stress: an Introduction to the Stress Concept in Plants', *Journal of Plant Physiology,* 148(1), pp. 4-14.

Lin, Q. and Mendelssohn, I.A. (2012) 'Impacts and Recovery of the Deepwater Horizon Oil Spill on Vegetation Structure and Function of Coastal Salt Marshes in the Northern Gulf of Mexico', *Environmental science & technology,* 46(7), pp. 3737-3743.

Lindén, O. and Pålsson, J. (2013) 'Oil Contamination in Ogoniland, Nigeria', *Ambio,* 42(6), pp. 685-701.

Lindenmayer, D.B. and Likens, G.E. (2010) 'The Science and Application of Ecological Monitoring', *Biological Conservation,* 143(6), pp. 1317-1328.

Lindenmayer, D.B., Margules, C.R. and Botkin, D.B. (2000) 'Indicators of Biodiversity for Ecologically Sustainable Forest Management', *Conservation Biology,* 14(4), pp. 941-950.

Ling, Q., Huang, W. and Jarvis, P. (2011) 'Use of a SPAD-502 meter to measure leaf chlorophyll concentration in Arabidopsis thaliana', *Photosynthesis Research,* 107(2), pp. 209-214.

Linhai Zhu, Xuechun Zhao, Liming Lai, Jianjian Wang, Lianhe Jiang, Jinzhi Ding, Nanxi Liu, Yunjiang Yu, Junsheng Li, Nengwen Xiao, Yuanrun Zheng and Glyn M Rimmington (2013) 'Soil TPH Concentration Estimation Using Vegetation Indices in an Oil Polluted Area of Eastern China', *PLoS One,* 8(1), pp. e54028.

Liu, Z., Liu, G., Fu, B. and Zheng, X. (2008) 'Relationship between plant species diversity and soil microbial functional diversity along a longitudinal gradient in temperate grasslands of Hulunbeir, Inner Mongolia, China', *Ecological Research,* 23(3), pp. 511-518.

Lopes, A., da Rosa-Osman, S.M. and Piedade, M.T.F. (2009) 'Effects of crude oil on survival, morphology, and anatomy of two aquatic macrophytes from the Amazon floodplains', *Hydrobiologia,* 636(1), pp. 295-305.

López-Serrano, P., Corral-Rivas, J., Díaz-Varela, R., Álvarez-González, J. and López-Sánchez, C. (2016) 'Evaluation of Radiometric and Atmospheric Correction Algorithms for Aboveground Forest Biomass Estimation Using Landsat 5 TM Data', *Remote Sensing,* 8(5), pp. 369.

Lucas, R., Blonda, P., Bunting, P., Jones, G., Inglada, J., Arias, M., Kosmidou, V., Petrou, Z.I., Manakos, I., Adamo, M., Charnock, R., Tarantino, C., Mücher, C.A., Jongman, R.H.G., Kramer, H., Arvor, D., Honrado, J.P. and Mairota, P. (2015) 'The Earth Observation Data for Habitat Monitoring (EODHaM) system', *International Journal of Applied Earth Observations and Geoinformation,* 37, pp. 17-28.

Lugo, A.E. (1988) 'Estimating Reductions in the Diversity of Tropical Forest Species', in Anonymous *Biodiversity.* National Academies Press, pp. 58-70.

Luo, G., Chen, G., Tian, L., Qin, K. and Qian, S. (2016) 'Minimum Noise Fraction versus Principal Component Analysis as a Preprocessing Step for Hyperspectral Imagery Denoising', *Canadian Journal of Remote Sensing,* 42(2), pp. 106-116.

Ma, Y., Prasad, M.N.V., Rajkumar, M. and Freitas, H. (2011) 'Plant growth promoting rhizobacteria and endophytes accelerate phytoremediation of metalliferous soils', *Biotechnology Advances,* 29(2), pp. 248-258.

MacArthur, R.H. and MacArthur, J.W. (1961) 'On Bird Species Diversity', *Ecology,* 42(3), pp. 594-598.

Mace, G.M. and Baillie, J.E.M. (2007) 'The 2010 Biodiversity Indicators: Challenges for Science and Policy; Los Indicadores de Biodiversidad al 2010: Retos para la Ciencia y la Política', *Conservation Biology,* 21(6), pp. 1406-1413.

Mace, G.M., Norris, K. and Fitter, A.H. (2012) 'Biodiversity and Ecosystem Services: a Multi-Layered Relationship', *Trends in Ecology and Evolution,* 27(1).

Madonsela, S., Cho, M.A., Ramoelo, A., Mutanga, O. and Naidoo, L. (2018) 'Estimating tree species diversity in the savannah using NDVI and woody canopy cover', *International Journal of Applied Earth Observations and Geoinformation,* 66, pp. 106-115.

Magurran, A.E. (2010) *Ecological Diversity and Its Measurement.* Dordrecht: Springer Netherlands.

Mandoloma, L., Kazembe, J. and Moyo, B. (2014) 'Testing the Ecosystem Productivity-Diversity Hypothesis in a Grassland', *International Journal of Sciences: Basic and Applied Research,* 14(2), pp. 305-322.

Manuel Jonas Steinbauer, Klara Dolos, Björn Reineking and Carl Beierkuhnlein (2012) 'Current measures for distance decay in similarity of species composition are influenced by study extent and grain size', *Global Ecology and Biogeography,* 21(11/12), pp. 1203-1212.

Mapfumo, R.B., Murwira, A., Masocha, M. and Andriani, R. (2016) 'The relationship between satellite-derived indices and species diversity across African savanna ecosystems', *International Journal of Applied Earth Observation and Geoinformation,* 52, pp. 306-317.

Mark N. Merzlyak, Olga B. Chivkunova, Alexei E. Solovchenko and K. Razi Naqvi (2008) 'Light absorption by anthocyanins in juvenile, stressed, and senescing leaves', *Journal of Experimental Botany,* 59(14), pp. 3903-3911.

Marinescu, M., Toti, M., Tanase, V., Carabulea, V., Plopeanu, G. and Calciu, I. (2010) 'An Assessment of the Effects of Crude Oil Pollution on Soil Properties', *Annals: Food Science and Technology,* 11(1), pp. 94.

Marques, A., Pereira, H.M., Krug, R.M., Krug, C., Leadley, P.W., Visconti, P., Januchowski-Hartley, S.R., Alkemade, R., Bellard, C., Cheung, W.W.L., Christensen, V., Cooper, H.D., Hirsch, T., Hoft, R., van Kolck, J., Newbold, T., Noonan-Mooney, K., Regan, E.C., Rondinini, C., Sumaila, U.R., Teh, L.S.L. and Walpole, M. (2014) 'A framework to identify enabling and urgent actions for the 2020 Aichi Targets', *Basic and Applied Ecology,* 15(8), pp. 633-638.

Maselli, F. (2004) 'Monitoring forest conditions in a protected Mediterranean coastal area by the analysis of multiyear NDVI data', *Remote Sensing of Environment,* 89(4), pp. 423-433.

Maslova, S.P. (2014) ' Structure and Metabolism of Underground Shoots in Perennial Rhizome-Forming Plants', in Pessarakli, M. (ed.) *Handbook of Plant and Crop Physiology.* 3rd edn. Florida, USA: Taylor and Francis Group.

McKendry, P. (2002) 'Energy production from biomass (part 1): overview of biomass', *Bioresource technology,* 83(1), pp. 37-46.

McNaughton, S.J. (1977) 'Diversity and Stability of Ecological Communities: A Comment on the Role of Empiricism in Ecology', *The American Naturalist,* 111(979), pp. 515-525.

Meer, F. D. Van der, Jong and S. M. de (2002) *Imaging Spectrometry. Basic Principles and Prospective Applications : Basic Principles and Prospective Applications.* Hingham: Springer.

Meine, C., Soule, M. and Noss, F.R. (2006) 'A Mission-Driven Discipline? the Growth of Conservation Biology', *Conservation Biology,* 20(3), pp. 631-651.

Melillo, J.M., McGuire, A.D., Kicklighter, D.W., Moore, B., Vorosmarty, C.J. and Schloss, A.L. (1993) 'Global climate change and terrestrial net primary production', *Nature,* 363, pp. 234.

Merriam-Webster Dictionary (2017) *Vigour (vegetation).* (Accessed: January, 2017).

Merzlyak, M.,N., Chivkunova, O.,B., Solovchenko, A.,E. and Naqvi, K.,Razi (2008) 'Light absorption by anthocyanins in juvenile, stressed, and senescing leaves', 59(14), pp. 3903-3911.

Michel, J. and Rutherford, N. (2014) 'Impacts, recovery rates, and treatment options for spilled oil in marshes', *Marine Pollution Bulletin,* 82(1-2), pp. 19-25.

Mirzaie, F. S., Ghorbani, R. and Montajami, S. (2013) 'A Comparative Study of Different Biological Indices Sensitivity: A Case Study of Macro invertebrates of Gomishan Wetland, Iran', *World Journal of Fish and Marine Sciences,* 5(6), pp. 611-615.

Mielke, M.S., Schaffer, B. and Schilling, A.C. (2012) 'Evaluation of Reflectance Spectroscopy Indices for Estimation of Chlorophyll Content in Leaves of a Tropical Tree Species', *Photosynthetica,* 50(3), pp. 343-352.

Millennium Ecosystem Assessment (2005) *Millennium Ecosystem Assessment.* Available at: http://www.millenniumassessment.org/en/About.html (Accessed: 01/20 2015).

Mishra, D.R., Mishra, S., Cho, H.J., Ghosh, S., Fox, A., Downs, C., Merani, P.B.T., Kirui, P. and Jackson, N. (2012) 'Post-spill state of the marsh: Remote estimation of the ecological impact of the Gulf of Mexico oil spill on Louisiana Salt Marshes', *Remote Sensing of Environment,* 118, pp. 176-185.

Mmom, P.C. and Arokoyu, S.B. (2010) 'Mangrove Forest Depletion, Biodiversity Loss and Traditional Resources Management Practices in the Niger Delta, Nigeria', *Research Journal of Applied Sciences, Engineering and Technology,* 2(1), pp. 28-34.

Mohammadi, J. and Shataee, S. (2010) 'Possibility investigation of tree diversity mapping using Landsat ETM+ data in the Hyrcanian forests of Iran', *Remote Sensing of Environment,* 114(7), pp. 1504-1512.

Mori, A.S., Furukawa, T. and Sasaki, T. (2013) 'Response diversity determines the resilience of ecosystems to environmental change', *Biological Reviews,* 88(2), pp. 349-364.

Morlon, H., Chuyong, G., Condit, R., Hubbell, S., Kenfack, D., Thomas, D., Valencia, R. and Green, J.L. (2008) 'A general framework for the distance-decay of similarity in ecological communities', *Ecology Letters,* 11(9), pp. 904-917.

Morris, E.K., Caruso, T., Buscot, F., Fischer, M., Hancock, C., Maier, T.S., Meiners, T., Müller, C., Obermaier, E., Prati, D., Socher, S.A., Sonnemann, I., Wäschke, N., Wubet, T., Wurst, S. and Rillig, M.C. (2014) 'Choosing and using diversity indices: insights for ecological applications from the German Biodiversity Exploratories', *Ecology and Evolution,* 4(18), pp. 3514-3524.

Muchoney, D.M. (2008) 'Earth Observations for Terrestrial Biodiversity and Ecosystems', *Remote Sensing of Environment,* 112, pp. 1909-1911.

MuellerWilm, U., Devignot, O. and Pessiot, L. (eds.) (2016) *Sen2Cor Configuration and User Manual.* ESA Frascati, Italy: ESA.

Munyati, C. and Ratshibvumo, T. (2011) 'Characterising vegetation cover in relation to land use in the Inkomati catchment, South Africa, using Landsat imagery', *Area,* 43(2), pp. 189-201.

Musa, Z.N., Popescu, I. and Mynett, A. (2014) 'The Niger Delta's vulnerability to river floods due to sea level rise', *Natural Hazards and Earth System Sciences,* 14(12), pp. 3317-3329.

Musila, W., Todt, H., Uster, D. and Dalitz, H. (2005) 'Is Geodiversity Correlated to Biodiversity? A Case Study of the Relationship Between Spatial Heterogeneity of Soil Resources and Tree Diversity in a Western Kenyan Rainforest', in Anonymous Springer US, pp. 405-414.

Mutanga, O., Skidmore, A.K. and Prins, H.H.T. (2004) 'Predicting in situ pasture quality in the Kruger National Park, South Africa, using continuum-removed absorption features', *Remote Sensing of Environment,* 89(3), pp. 393-408.

Mutanga, O. and Skidmore, A.K. (2004) 'Narrow band vegetation indices overcome the saturation problem in biomass estimation', *International Journal of Remote Sensing,* 25(19), pp. 3999-4014.

Naeem, S., Thompson, L.J., Lawler, S.P., Lawton, J.H. and Woodfin, R.M. (1994) 'Declining biodiversity can alter the performance of ecosystems', *Nature,* 368, pp. 734.

Nagendra, H. (2002) 'Opposite Trends in Response for the Shannon and Simpson Indices of Landscape Diversity', *Applied Geography,* 22(2), pp. 175-186.

Nagendra, H. (2001) 'Using Remote Sensing to Assess Biodiversity ', *International Journal of Remote Sensing,* 22(12), pp. 2377-2400.

Naidoo, G. and Naidoo, K. (2018) 'Uptake and accumulation of polycyclic aromatic hydrocarbons in the mangroves Avicennia marina and Rhizophora mucronata', *Environmental Science and Pollution Research,* 25(29), pp. 28875-28883.

National Population Commission, N. (2015) *National Census, 2006.* Available at: http://www.population.gov.ng/images/Vol03TableDSxLGAPopbySDistrict-PDF.pdff (Accessed: 03/10 2015).

Netherlands Engineering Consultants, (. 1959 *Niger and Benue Investigation: Final Report*, NEDECO, The Hague.

Ng, J.P., Hollister, E.B., González-Chávez, C.A., Hons, F.M., Zuberer, D.A., Aitkenhead-Peterson, J.A., Loeppert, R. and Gentry, T.J. (2012) 'Impacts of Cropping Systems and Long-Term Tillage on Soil Microbial Population Levels and Community Composition in Dryland Agricultural Setting', *ISRN Ecology,* 2012, pp. 1-11.

Njoku, K., Akinola, M. and Oboh, B. (2008) 'Growth and Performance of Glycine max L. (Merrill) Grown in Crude Oil Contaminated Soil Augmented With Cow Dung', *Life Science Journal,* 5(3), pp. 89-93.

Nkwocha, E.E. and Duru, P.O. (2010) 'Micro-Analytic Study on the Effect of Oil Pollution on Local Plant Species and Food Crops', *Advances in Bioresearch,* 1(1), pp. 189-198.

Noomen, M.F. and Skidmore, A.K. (2009) 'The Effects of High Soil CO_2 Concentrations on Leaf Reflectance of Maize Plants', *International Journal of Remote Sensing,* 30(2), pp. 481-497.

Noomen, M.F., van der Werff, H. M. A, van der Meer, F. D. and F.D. (2012) 'Spectral and spatial indicators of botanical changes caused by long-term hydrocarbon seepage', *Ecological Informatics,* 8(1), pp. 55-64.

Noomen, M., Van der Meer, F. & Skidmore, A. (2005) 'Hyperspectral Remote Sensing for Detecting the Effects of Three Hydrocarbon Gases on Maize Reflectance', *Proceedings of the 31st International Symposium on Remote Sensing of Environment: Global Monitoring for Sustainability and Security*, June 20-14, 2005 St. Petersburg Russia: International Centre for Remote Sensing of Environment.

Norris, K. (2012) 'Biodiversity in the Context of Ecosystem Services: the Applied Need for Systems Approaches', *Philosophical Transactions of the Royal Society B: Biological Sciences,* 367(1586), pp. 191-199.

NOSDRA (2015) *Nigerian Oil Spill Monitor.* Available at: https://oilspillmonitor.ng/ (Accessed: 5th October, 2015).

Noss, R.F. (1999) 'Assessing and Monitoring Forest Biodiversity: A Suggested Framework and Indicators', *Forest Ecology and Management,* 115(2–3), pp. 135-146.

Noss, R.F. (1990) 'Indicators for Monitoring Biodiversity: A Hierarchical Approach', *Conservation Biology,* 4(4), pp. 355-364.

Novák, V. and Vidovič, J. (2003) 'Transpiration and nutrient uptake dynamics in maize (Zea mays L.)', *Ecological Modelling,* 166(1–2), pp. 99-107.

Nwaichi, E.O., Frac, M., Nwoha, P.A. and Eragbor, P. (2015) 'Enhanced Phytoremediation of Crude Oil-Polluted Soil by Four Plant Species: Effect of Inorganic and Organic Bioaugumentation', *International Journal of Phytoremediation,* 17(12), pp. 1253-1261.

Nwilo, P.C. and Badejo, O.T. (2005) 'Oil Spill Problems and Management in the Niger Delta', *International Oil Spill Conference Proceedings,* 2005(1), pp. 567-570.

Nwoko, C.O., Okeke, P.N., Agwu, O.O., Akpan, I.E. and Akpan (2007) 'Performance of Phaseolus vulgaris L. in a soil contaminated with spent-engine oil', *African Journal of Biotechnology,* 6(16), pp. 1922-1925.

Nzeadibe, T.C., Egbule, C.L., Chukwuone, N.A. and Agu, V.C. (eds.) (2011) *Climate Change Awareness and Adaptation in the Niger Delta Region of Nigeria.* Niger Delta/ Nigeria: African Technology Policy Studies Network.

Obi, C. (2009) 'Nigeria's Niger Delta: Understanding the Complex Drivers of Violent Oil-Related Conflict', *Africa Development,* 34(2), pp. 103-128.

OBIRE, O. and NWAUBETA, O. (2002) 'Effects of Refined Petroleum Hydrocarbon on Soil Physicochemical and Bacteriological Characteristics', *Journal of Applied Sciences & Environmental Management,* 6(1), pp. 39-44.

Odjegba, V. and Sadiq, A.O. (2002) 'Effects of spent engine oil on the growth parameters, chlorophyll and protein levels of Amaranthus hybridus L', *Environmentalist,* 22(1), pp. 23-28.

Odoeme, V.C. (2013) 'Corporate Accountability in the Nigerian Oil and Gas Sector: Coping With Uncertainties', *Commonwealth Law Bulletin,* 39(4), pp. 741-765.

OECD (2006) *Test No. 227: Terrestrial Plant Test: Vegetative Vigour Test.* Organisation for Economic Co-operation and Development.

Ogbo, M.E., Zibigha, M. and Odogu, G. (2009) 'The Effect of Crude Oil on Growth of the Weed (*Paspalum scrobiculatum L.*) -Phytoremediation Potential of the Plant', *African Journal of Environmental Science and Technology,* 3(9), pp. 229-233.

Ohimain, E.I. (2004) 'Environmental Impacts of Dredging in the Niger Delta; Options for Sediment Relocation That Will Mitigate Acidification and Enhance Natural Mangrove Restoration.', *Terra et Aqua,* 97, pp. 19.

Ohimain, E.I. (2003) 'Environmental Impacts of Oil Mining Activities in the Niger Delta Mangrove Ecosystem.', Armstrong, D., de Villiers, A.B., Kleinmann, R.L.P., *et al* (eds.) *Proceedings of the 8th International Mine Water Association (IMWA) Congress,* Johannesburg, South Africa Johannesburg: International Mine Water Association (IMWA), pp. 503.

Okonokhua, B.O., Ikhajiagbe, B., Anoliefo, G.O. and Emede, T.O. (2007) 'The Effects of Spent Engine Oil on Soil Properties and Growth of Maize (Zea mays L.)', *Journal of Applied Science and Environmental Management,* 11(3).

Okoye, C.O. and Okunrobo, L.A. (2014) 'Impacts of Oil Spill on Land and Water and its Health Implications in Odu-Gboro Community, Sagamu, Ogun State, Nigeria', *World Journal of Environmental Sciences & Engineering,* 1(1).

Oksanen, J., Blanchet, F.G., Friendly, M., Kindt, R., Legendre, P., Minchin, P.R., Simpson, G.L., Stevens, H., Wagner, H., McGlinn, D., O'Hara, R.B., Solymos, P. and Szoecs, E. (eds.) (2018) *Vegan: Community Ecology Package.*

Okwoche, P. (2011) *Nigeria Ogoniland Oil Clean-up 'Could Take 30 Years'.* Available at: http://www.bbc.co.uk/news/world-africa-14398659 (Accessed: 02/15 2015).

Olajire, A.A., Altenburger, R., Küster, E. and Brack, W. (2005) 'Chemical and Ecotoxicological Assessment of Polycyclic Aromatic Hydrocarbon—Contaminated Sediments of the Niger Delta, Southern Nigeria', *Science of the Total Environment,* 340(1–3), pp. 123-136.

Oldeland, J., Wesuls, D., Rocchini, D., Schmidt, M. and Jürgens, N. (2010) 'Does Using Species Abundance Data Improve Estimates of Species Diversity from Remotely Sensed Spectral Heterogeneity?', *Ecological Indicators,* 10(2), pp. 390-396.

Oluduro, O. (2012) 'Oil Exploration and Ecological Damage: The Compensation Policy in Nigeria', *Canadian Journal of Development Studies,* 33(2), pp. 164-179.

Omo-Irabor, O.O., Olobaniyi, S.B., Akunna, J., Venus, V., Maina, J.M. and Paradzayi, C. (2011) 'Mangrove Vulnerability Modelling in Parts of Western Niger Delta, Nigeria Using Satellite Images, GIS Techniques and Spatial Multi-Criteria Analysis (SMCA)', *Environmental Monitoring and Assessment,* 178(1-4), pp. 39-51.

Omosun, G., Markson, A.,A. and Mbanasor, O. (2008) *Growth and anatomy of Amaranthus hybridus as affected by different crude oil concentrations.*

O'Neill, N.T., Zagolski, F., Bergeron, M., Royer, A., Miller, J.R. and Freemantle, J. (1997) 'Atmospheric Correction Validation of CASI Images Acquired over the Boreas Southern Study Area', *Canadian Journal of Remote Sensing,* 23(2), pp. 143-162.

Onwuka, E.C. (2005) 'Oil Extraction, Environmental Degradation and Poverty in the Niger Delta Region of Nigeria: A Viewpoint', *International Journal of Environmental Studies,* 62(6), pp. 655-662.

Onyekwelu, J.C., Mosandl, M.B. & Stimm, B. (2013) 'Tree species diversity and soil status of two natural forest ecosystems in lowland humid tropical rainforest region of Nigeria. Utilisation of diversity inland use systems: Sustainable and organic approaches to meet human needs', *Conference on International Agricultural Research for Development *, October 9-11, 2007 University of Göttingen: Witzenhausen Selbstverlag.

Onyia, N., Balzter, H. and Berrio, J. (2018) 'Normalized Difference Vegetation Vigour Index: A New Remote Sensing Approach to Biodiversity Monitoring in Oil Polluted Regions', *Remote Sensing,* 10(6), pp. 897.

Oosting, H.J. (1948) *The Study of Plant Communities, an Introduction to Plant Ecology.* san Francisco: W. H. Freeman.

Opukri, C.O. and Ibaba, S.I. (2008) 'Oil Induced Environmental Degradation and Internal Population Displacement in the Nigeria's Niger Delta', *Journal of Sustainable Development in Africa,* 10(1), pp. 173-193.

Orji, F. (2013) 'Bioremediation of Petroleum Hydrocarbon-Polluted Mangrove Swamps Using Nutrient Formula Produced From Water Hyacinth (*Eicchornia Crassipes*)', *American Journal of Environmental Sciences,* 9(4), pp. 348-366.

Orji, U.J. (2012) 'An Appraisal of the Legal Frameworks for the Control of Environmental Pollution in Nigeria', *Commonwealth Law Bulletin,* 38(2), pp. 321-346.

Ortenberg, F. (2012) 'Hyperspectral Sensor Systems', in Thenkabail, P.S., Lyon, J.G. and Huete, A. (eds.) *Hyperspectral Remote Sensing of Vegetation.* 1st edn. Boca Raton, Florida: CRC Press, pp. 39-68.

Osam, M.U., Wegwu, M.O. and Uwakwe, A.A. (2011) 'The Omoku old pipeline oil spill: Total hydrocarbon content of affected soils and the impact on the nutritive value of food crops ', *Archives of Applied Science Research*: 3(3),pp 514-521

Osuagwu, E.S. and Olaifa, E. (2018) 'Effects of oil spills on fish production in the Niger Delta', *PloS one,* 13(10), pp. e0205114.

Osuji, L.C., Adesiyan, S.O. and Obute, G.C. (2004) 'Post-Impact Assessment of Oil Pollution in Agbada West Plain of Niger Delta, Nigeria: Field Reconnaissance and Total Extractable Hydrocarbon Content', *Chemistry and Biodiversity,* 1(10), pp. 1569-1578.

Osuji, L.C. and Ezebuiro, P.E. (2006) 'Hydrocarbon contamination of a typical mangrove floor in Niger Delta, Nigeria', *International Journal of Environmental Science & Technology,* 3(3), pp. 313-320.

Osuji, L.C., Ndukwu, B.C., Obute, G.C. and Agbagwa, I. (2006) 'Impact of Four-Dimensional Seismic and Production Activities on the Mangrove Systems of the Niger Delta, Nigeria.', *Chemistry and Ecology,* 22(5), pp. 424.

Osuji, L.C. and Nwoye, I. (2007) 'An Appraisal of the Impact of Petroleum Hydrocarbons on Soil Fertility: The Owaza Experience', *African Journal of Agriculural Research,* 2(7), pp. 318-324.

Oyebadejo, O. and Ugbaja, V. (1995) '"Oil as Threat; Well Blowouts, Pipeline Failures and Spills"', *Nigeria Oil and Gas Monthly,* 1(9).

Oyedeji, A.A., Adebiyi, A.O., Omotoyinbo, M.A. and Ogunkunle, C.O. (2012) 'Effect of Crude Oil-Contaminated Soil on Germination and Growth Performance of Abelmoschus esculentus L. Moench—A Widely Cultivated Vegetable Crop in Nigeria', *American Journal of Plant Sciences,* 3(10), pp. 1451-1454.

Oyeshola, D., Fayomi, I. and Ifedayo, T.E. (2011) 'Education, Stability, and Security in Niger Delta', *Democracy and Security,* 7(1), pp. 1-17.

Oyinloye, M.A. and Olamiju, O.I. (2013) 'An Assessment of the Physical Impact of Oil Spillage Using GIS and Remote Sensing Technologies: Empirical Evidence from Jesse Town, Delta State, Nigeria', *British Journal of Arts and Social Sciences,* 12(11), pp. 235-252.

Pachavo, G. and Murwira, A. (2014) 'Land-Use and Land Tenure Explain Spatial and Temporal Patterns in Terrestrial Net Primary Productivity (NPP) in Southern Africa', *Geocarto International,* 29(6), pp. 671-687.

Palmer, M.A., Bernhardt, E.S., Allan, J.D., Lake, P.S., Alexander, G., Brooks, S., Carr, J., Clayton, S., Dahm, C.N., Follstad Shah, J., Galat, D.L., Loss, S.G., Goodwin, P., Hart, D.D., Hassett, B., Jenkinson, R., Kondolf, G.M., Lave, R., Meyer, J.L., O'Donnell, T.K., Pagano, L. and Sudduth, E. (2005a) 'Standards for ecologically successful river restoration', *Journal of Applied Ecology,* 42(2), pp. 208-217.

Palmer, M.W., Earls, P.G., Hoagland, B.W., White, P.S. and Wohlgemuth, T. (2002) 'Quantitative tools for perfecting species lists', *Environmetrics,* 13(2), pp. 121-137.

Pande, H., Tiwari, P. and Dobhal, S. (2009) 'Analyzing hyper-spectral and multi-spectral data fusion in spectral domain', *Journal of the Indian Society of Remote Sensing,* 37(3), pp. 395-408.

Parviainen, M., Luoto, M. and Heikkinen, R.K. (2009) 'The role of local and landscape level measures of greenness in modelling boreal plant species richness', *Ecological Modelling,* 220(20), pp. 2690-2701.

Paz-Kagan, T., Caras, T., Herrmann, I., Shachak, M. and Karnieli, A. (2017) 'Multiscale mapping of species diversity under changed land use using imaging spectroscopy', *Ecological Applications,* 27(5), pp. 1466-1484.

Pearlman, J., Carman, S., Segal, C., Jarecke, P., Clancy, P. & Browne, W. (2001) 'Overview of the Hyperion Imaging Spectrometer for the NASA EO-1 mission', *IGARSS 2001. Scanning the Present and Resolving the Future. Proceedings. IEEE 2001 International Geoscience and Remote Sensing Symposium (Cat. No.01CH37217)* Sydney, NSW, Australia, Australia, 9-13 July 2001 Piscataway, New Jersey: IEEE, pp. 3036.

Pearson, R. L. & Miller, L.D. (1972) 'Remote mapping of standing crop biomass for estimation of the productivity of the short-grass Prairie, Pawnee National Grasslands, Colorado', *8th Int. Symp. on Remote Sens.of Environment* Ann Arbor, Michigan USA, October 2-6, 1972 University of Michigan, USA: Environmental Research Institute of Michigan, pp. 1357.

Peet, R.K. (1974) 'The Measurement of Species Diversity', *Annual Review of Ecology and Systematics,* 5, pp. 285-307.

Peng Gong, Ruiliang Pu, G. S. Biging and M. R. Larrieu (2003) 'Estimation of forest leaf area index using vegetation indices derived from Hyperion hyperspectral data', *IEEE Transactions on Geoscience and Remote Sensing,* 41(6), pp. 1355-1362.

Peng, Y., Fan, M., Song, J., Cui, T. and Li, R. (2018a) 'Assessment of plant species diversity based on hyperspectral indices at a fine scale', *Scientific Reports,* 8(1), pp. 4776.

Peñuelas, J., Filella, I., Biel, C., Serrano, L. and Savé, R. (1993) 'The reflectance at the 950–970 nm region as an indicator of plant water status', *International Journal of Remote Sensing,* 14(10), pp. 1887-1905.

Peñuelas, J., Filella, I. and Gamon, J.A. (1995) 'Assessment of photosynthetic radiation-use efficiency with spectral reflectance', *New Phytologist,* 131(3), pp. 291-296.

Peñuelas, J. and Filella, I. (1998) 'Visible and near-infrared reflectance techniques for diagnosing plant physiological status', *Trends in plant science,* 3(4), pp. 151-156.

Pereira, H.M. and Cooper, D.H. (2006) 'Towards the Global Monitoring of Biodiversity Change', *Trends in Ecology and Evolution,* 21(3), pp. 123-129.

Pereira, H.M., Ferrier, S., Walters, M., Geller, G.N., Jongman, R.H.G., Scholes, R.J., Bruford, M.W., Brummitt, N., Butchart, S.H.M., Cardoso, A.C., Coops, N.C., Dulloo, E., Faith, D.P., Freyhof, J., Gregory, R.D., Heip, C., Höft, R., Hurtt, G., Jetz, W., Karp, D.S., McGeoch, M.A., Obura, D., Onoda, Y., Pettorelli, N., Reyers, B., Sayre, R., Scharlemann, J.P.W., Stuart, S.N., Turak, E., Walpole, M. and Wegmann, M. (2013) 'Essential Biodiversity Variables', *Science,* 339(6117), pp. 277-278.

Perring, M.P., Jonson, J., Freudenberger, D., Campbell, R., Rooney, M., Hobbs, R.J. and Standish, R.J. (2015) 'Soil-vegetation type, stem density and species richness influence biomass of restored woodland in south-western Australia', *Forest Ecology and Management,* 344, pp. 53-62.

Perry, E.M. and Davenport, J.R. (2007) 'Spectral and Spatial Differences in Response of Vegetation Indices to Nitrogen Treatments on Apple', *Computers and Electronics in Agriculture,* 59(1–2), pp. 56-65.

Peterson, A. and Soberón, J. (2018) 'Essential biodiversity variables are not global', *Biodiversity and Conservation,* 27(5), pp. 1277-1288.

Petit, C., Scudder, T. and Lambin, E. (2001) 'Quantifying Processes of Land-Cover Change by Remote Sensing: Resettlement and Rapid Land-Cover Changes in South-Eastern Zambia', *International Journal of Remote Sensing,* 2015(01/21).

Petrovic, A., Jurisic, A. and Rajkovic, D. (2010) 'Seasonal Distribution and Species Association among Spider Mites (Acari: *Tetranychidae*) and Predatory Mites (Acari: *Phytoseiidae* and Acari: *Stigmaeidae*) in Serbian Apple Orchards', *International Journal of Acarology,* 36(6), pp. 519-526.

Pettorelli, N., Laurance, W.F., O'Brien, T.G., Wegmann, M., Nagendra, H. and Turner, W. (2014) 'Satellite Remote Sensing for Applied Ecologists: Opportunities and Challenges', *Journal of Applied Ecology,* 51(4), pp. 839-848.

Pettorelli, N., Vik, J.O., Mysterud, A., Gaillard, J., Tucker, C.J. and Stenseth, N.C. (2005) 'Using the Satellite-Derived NDVI to Assess Ecological Responses to Environmental Change', *Trends in Ecology & Evolution,* 20(9), pp. 503-510.

Pezeshki, S.R., Hester, M.W., Lin, Q. and Nyman, J.A. (2000) 'The effects of oil spill and clean-up on dominant US Gulf coast marsh macrophytes: a review', *Environmental pollution (Barking, Essex : 1987),* 108(2), pp. 129-139.

Philip, D. (2009) 'VEGAN, a package of R functions for community ecology', *Journal of Vegetation Science,* 14(6), pp. 927-930.

Philips, E.A. (1959) *Methods of Vegetation Study.* USA: Henry Holt and Company.

Pitman, C.R.S. (1953) 'The Balance of Nature', *Oryx,* 2(01), pp. 9-15.

Pohl, C. and Van Genderen, J.L. (1998) 'Review article Multisensor image fusion in remote sensing: Concepts, methods and applications', *International Journal of Remote Sensing,* 19(5), pp. 823-854.

Powers, R.P., Coops, N.C., Morgan, J.L., Wulder, M.A., Nelson, T.A., Drever, C.R. and Cumming, S.G. (2013) 'A Remote Sensing Approach to Biodiversity Assessment and Regionalization of the Canadian Boreal Forest', *Progress in Physical Geography,* 37(1), pp. 36-62.

Pu, R., Bell, S. and English, D. (2015) 'Developing Hyperspectral Vegetation Indices for Identifying Seagrass Species and Cover Classes', *Journal of Coastal Research,* , pp. 595-615.

Pu, R., Gong, P. and Yu, Q. (2008) 'Comparative Analysis of EO-1 ALI and Hyperion, and Landsat ETM+ Data for Mapping Forest Crown Closure and Leaf Area Index', *Sensors (Basel, Switzerland),* 8(6), pp. 3744-3766.

Purevdorj, T., Tateishi, R., Ishiyama, T. and Honda, Y. (1998) 'Relationships between Percent Vegetation Cover and Vegetation Indices', *International Journal of Remote Sensing,* 19(18), pp. 3519-3535.

Purvis, A. and Hector, A. (2000) 'Getting the Measure of Biodiversity', *Nature,* 405(6783), pp. 212-219.

Pysek, P. and Pysek, A. (1989) 'Veränderungen der Vegetation durch experimentelle Erdgasbehandlung', *Weed Research,* 29(3), pp. 193-204.

Rai, V., Khatoon, S., Bisht, S.S. and Mehrotra, S. (2005) 'Effect of cadmium on growth, ultramorphology of leaf and secondary metabolites of Phyllanthus amarus Schum. and Thonn.', *Chemosphere,* 61(11), pp. 1644-1650.

Rapport, D.J., Regier, H.A. and Hutchinson, T.C. (1985) 'Ecosystem Behavior Under Stress', *The American Naturalist,* 125(5), pp. 617-640.

Rasche, M.E., Hyman, M.R. and Arp, D.J. (1990) 'Biodegradation of Halogenated Hydrocarbon Fumigants by Nitrifying Bacteria', *Applied and Environmental Microbiology,* 56(8), pp. 2568-2571.

Reddy, C.S., Khuroo, A.A., Krishna, P.H., Saranya, K.R.L., Jha, C.S. and Dadhwal, V.K. (2014) 'Threat Evaluation for Biodiversity Conservation of Forest Ecosystems Using Geospatial Techniques: A Case Study of Odisha, India', *Ecological Engineering,* 69, pp. 287-303.

Reynolds, S.C., Marston, C.G., Hassani, H., King, G.C.P. and Bennett, M.R. (2016) 'Environmental hydro-refugia demonstrated by vegetation vigour in the Okavango Delta, Botswana', *Scientific reports,* 6(1), pp. 35951.

Rich, T. (2005) *Habitat Requirements and Issues; Handbook of Biodiversity Methods.* Cambridge: Cambridge University Press.

Ricotta, C. (2017) 'Of beta diversity, variance, evenness, and dissimilarity', *Ecology and Evolution,* 7(13), pp. 4835-4843.

Ringnér, M. (2008) 'What is principal component analysis?', *Nature Biotechnology,* 26(3), pp. 303-304.

Rivero, C., Chirenje, T., Ma, L.Q. and Martinez, G. (2004) 'Influence of compost on soil organic matter quality under tropical conditions', *Geoderma,* 123(3–4), pp. 355-361.

Roberts, D.W. (ed.) (2016) *Ordination and Multivariate Analysis for Ecology.* Open Source: CRAN.

Robson, D.B., Knight J.D. , Farrell, R.E. and Germida, J.J. (2004) 'Natural revegetation of hydrocarbon-contaminated soil in semi-arid grasslands', *Canadian Journal of Botany,* 82(1), pp. 22-30.

Rocchini, D. and Cade, B.S. (2008) 'Quantile Regression Applied to Spectral Distance Decay', *IEEE Geoscience and Remote Sensing Letters,* 5(4), pp. 640-643.

Rocchini, D. (2007a) 'Effects of spatial and spectral resolution in estimating ecosystem α-diversity by satellite imagery', *Remote Sensing of Environment,* 111(4), pp. 423-434.

Rocchini, D., Balkenhol, N., Carter, G.A., Foody, G.M., Gillespie, T.W., He, K.S., Kark, S., Levin, N., Lucas, K., Luoto, M., Nagendra, H., Oldeland, J., Ricotta, C., Southworth, J. and Neteler, M. (2010) 'Remotely sensed spectral heterogeneity as a proxy of species diversity: Recent advances and open challenges', *Ecological Informatics,* 5(5), pp. 318-329.

Rocchini, D., Boyd, D.S., Féret, J., Foody, G.M., He, K.S., Lausch, A., Nagendra, H., Wegmann, M. and Pettorelli, N. (2016) 'Satellite remote sensing to monitor species diversity: potential and pitfalls', *Remote Sensing in Ecology and Conservation,* 2(1), pp. 25-36.

Rocchini, D., Chiarucci, A. and Loiselle, S.A. (2004) 'Testing the spectral variation hypothesis by using satellite multispectral images', *Acta Oecologica,* 26(2), pp. 117-120.

Rocchini, D., Hernández-Stefanoni, J.L. and He, K.S. (2015) 'Advancing species diversity estimate by remotely sensed proxies: A conceptual review', *Ecological Informatics,* 25, pp. 22-28.

Rock, B.N., Vogelmann, J.E., Williams, D.L., Vogelmann, A.F. and Hoshizaki, T. (1986) 'Remote Detection of Forest Damage', *Bioscience,* 36(7), pp. 439-445.

Rock, B.N., Hoshizaki, T. and Miller, J.R. (1988) 'Comparison of in situ and airborne spectral measurements of the blue shift associated with forest decline', *Remote Sensing of Environment,* 24(1), pp. 109-127.

Rodriguez, I.R. and Miller, G.L. (2000) 'Using a Chlorophyll Meter to Determine the Chlorophyll Concentration, Nitrogen Concentration, and Visual Quality of St. Augustine grass', *HortScience,* 35(4), pp. 751.

Rondeux, J. and Sanchez, C. (2010) 'Review of Indicators and Field Methods for Monitoring Biodiversity within National Forest Inventories. Core Variable: Deadwood', *Environmental Monitoring and Assessment,* 164(1-4), pp. 617-630.

Rosso, P.H., Pushnik, J.C., Lay, M. and Ustin, S.L. (2005) 'Reflectance Properties and Physiological Responses of *Salicornia virginica* to Heavy Metal and Petroleum Contamination', *Environmental Pollution,* 137(2), pp. 241-252.

Rouse, J., Haas, R., Schell, J. & Deering, D. (1974) '*Monitoring Vegetation Systems in the Great Plains with ERTS*', *Third Earth Resources Technology Satellite-1 Symposium- Volume I: Technical Presentations. NASA SP-351* Washington, D.C., pp. 309.

Roy, D.P., Wulder, M.A., Loveland, T.R., C.E., W., Allen, R.G., Anderson, M.C., Helder, D., Irons, J.R., Johnson, D.M., Kennedy, R., Scambos, T.A., Schaaf, C.B., Schott, J.R., Sheng, Y., Vermote, E.F., Belward, A.S., Bindschadler, R., Cohen, W.B., Gao, F., Hipple, J.D., Hostert, P., Huntington, J., Justice, C.O., Kilic, A., Kovalskyy, V., Lee, Z.P., Lymburner, L., Masek, J.G., McCorkel, J., Shuai, Y., Trezza, R., Vogelmann, J., Wynne, R.H. and Zhu, Z. (2014) 'Landsat-8: Science and Product Vision for Terrestrial Global Change Research', *Remote Sensing of Environment,* 145, pp. 154-172.

Saatchi, S., Buermann, W., ter Steege, H., Mori, S. and Smith, T.B. (2008) 'Modeling distribution of Amazonian tree species and diversity using remote sensing measurements', *Remote Sensing of Environment,* 112(5), pp. 2000-2017.

Salem, B.B. (2003) 'Application of GIS to Biodiversity Monitoring', *Journal of Arid Environments,* 54(1), pp. 91-114.

Salinas-Zavala, C.A., Douglas, A.V. and Diaz, H.F. (2002) 'Interannual variability of NDVI in northwest Mexico. Associated climatic mechanisms and ecological implications', *Remote Sensing of Environment,* 82(2), pp. 417-430.

Sapijanskas, J., Paquette, A., Potvin, C., Kunert, N. and Loreau, M. (2014) 'Tropical tree diversity enhances light capture through crown plasticity and spatial and temporal niche differences', *Ecology,* 95(9), pp. 2479-2492.

Sattout, E. and Caligari, P.D.S. (2011) 'Forest Biodiversity Assessment in Relic Ecosystem: Monitoring and Management Practice Implications', *Diversity,* 3(3), pp. 531-546.

Savitzky, A. and Golay, M.J.E. (1964) 'Smoothing and Differentiation of Data by Simplified Least Squares Procedures', *Analytical Chemistry,* 36(8), pp. 1627-1639.

Scheffler, D. & Karrasch, P. (Oct 17, 2013) 'Preprocessing of hyperspectral images: a comparative study of destriping algorithms for EO1-hyperion', Lorenzo & Bruzzone (eds.) *SPIE Remote Sensing* Dresden, Germany, 23-26 September, 2013 Dresden, Germany: SPIE.

Schmeller, D.S., Weatherdon, L.V., Loyau, A., Bondeau, A., Brotons, L., Brummitt, N., Geijzendorffer, I.R., Haase, P., Kuemmerlen, M., Martin, C.S., Mihoub, J., Rocchini, D., Saarenmaa, H., Stoll, S. and Regan, E.C. (2018) 'A suite of essential biodiversity variables for detecting critical biodiversity change', *Biological Reviews,* 93(1), pp. 55-71.

Schmidtlein, S. and Fassnacht, F.E. (2017) 'The spectral variability hypothesis does not hold across landscapes', *Remote Sensing of Environment,* 192, pp. 114-125.

Scholes, R.J., Walters, M., Turak, E., Saarenmaa, H., Heip, C.H., Tuama, ÉÓ, Faith, D.P., Mooney, H.A., Ferrier, S., Jongman, R.H., Harrison, I.J., Yahara, T., Pereira, H.M., Larigauderie, A. and Geller, G. (2012) 'Building a Global Observing System for Biodiversity', *Current Opinion in Environmental Sustainability,* 4(1), pp. 139-146.

Scholten, M.C.T. and Leendertse, P.C. (1991) 'The impact of oil pollution on salt marsh vegetation', in Rozema, J. and Verkleij, J.A.C. (eds.) *Ecological responses to environmental stresses.* Dordrecht: Springer Netherlands, pp. 184-190.

Schott, J.R. (2007) *Remote Sensing : The Image Chain Approach.* Cary, NC, USA: Oxford University Press.

Seak, S., Schmidt-Vogt, D. and Thapa, G.B. (2012) 'Biodiversity Monitoring at the Tonle Sap Lake of Cambodia: A Comparative Assessment of Local Methods', *Environmental management,* 50(4), pp. 707-720.

Seibert, J., Stendahl, J. and Sørensen, R. (2007) 'Topographical influences on soil properties in boreal forests', *Geoderma,* 141(1-2), pp. 139.

Serrano, L., Filella, I. and Peñuelas, J. (2000) 'Remote sensing of biomass and yield of winter wheat under different nitrogen supplies', *Crop Science,* 40(3), pp. 723-731.

Sewelam, N., Oshima, Y., Mitsuda, N. and Ohme-Takagi, M. (2014) 'A step towards understanding plant responses to multiple environmental stresses: a genome-wide study', *Plant, Cell & Environment,* 37(9), pp. 2024-2035.

Shafr, H.Z., Salleh, M.A. and Ghiyamat, A. (2006) 'Hyperspectral Remote Sensing of Vegetation Using Red Edge Position Techniques', *American Journal of Applied Sciences,* 3(6), pp. 1864-1871.

Shah, A. (2014) *Global Issues: Why Is Biodiversity Important? Who Cares?* Available at: http://www.globalissues.org/article/170/why-is-biodiversity-important-who-cares (Accessed: January 24th 2015).

Shalaby, A. and Tateishi, R. (2007) 'Remote Sensing and GIS for Mapping and Monitoring Land Cover and Land Use Changes in the Northwestern Coastal Zone of Egypt', *Applied Geography,* 27, pp. 28-41.

Sheil, D. (2001) 'Conservation and Biodiversity Monitoring in the Tropics: Realities, Priorities, and Distractions', *Conservation Biology,* 15(4), pp. 1179-1182.

Sheil, D., Sayer, J.A. and O'Brien, T.G. (1999) 'Tree Species Diversity in Logged Rainforests', *Science,* 284(5420), pp. 1587.

Short, K.C. and Stauble, A.J. (1967) 'Outline of Geology of Niger Delta', *AAPG Bulletin,* 51(5), pp. 761-779.

Siegel, S. and Castellan, N.J. (1989) *Nonparametric statistics for the behavioral sciences.* 2. ed., 2. print. edn. New York u.a: McGraw-Hill.

Sims, D.A. and Gamon, J.A. (2002) 'Relationships between Leaf Pigment Content and Spectral Reflectance across a Wide Range of Species, Leaf Structures and Developmental Stages', *Remote Sensing of Environment,* 81(2-3), pp. 337-354.

Skidmore, A.K., Pettorelli, N., Coops, N.C., Geller, G., Hansen, M., Lucas, R., Muncher, C.A., O'Connor, B., Paganini, M., Pereira, H.M., Schaepman, M.E., Turner, W., Wang, T. and Wegman, M. (2015) 'Environmental science : agree on biodiversity metrics to track from space', *Nature,* 523(7561), pp. 403-405.

Small, C. (2004) 'The Landsat ETM+ spectral mixing space', *Remote Sensing of Environment,* 93(1), pp. 1-17.

Smith, K.L., Steven, M.D. and Colls, J.J. (2005a) 'Plant spectral responses to gas leaks and other stresses', *International Journal of Remote Sensing,* 26(18), pp. 4067-4081.

Smith, K.L., Steven, M.D. and Colls, J.J. (2004) 'Use of hyperspectral derivative ratios in the red-edge region to identify plant stress responses to gas leaks', *Remote Sensing of Environment,* 92(2), pp. 207-217.

Smith, K.L., Steven, M.D. and Colls, J.J. (2004b) 'Spectral responses of pot-grown plants to displacement of soil oxygen', *International Journal of Remote Sensing,* 25(20), pp. 4395-4410.

Soininen, J., McDonald, R. and Hillebrand, H. (2007a) 'The distance decay of similarity in ecological communities', *Ecography,* 30(1), pp. 3-12.

Soininen, J., Passy, S. and Hillebrand, H. (2012) 'The relationship between species richness and evenness: a meta-analysis of studies across aquatic ecosystems', *Oecologia,* 169(3), pp. 803-809.

Spellerberg, I.F. and Fedor, P.J. (2003) 'A tribute to Claude Shannon (1916-2001) and a plea for more rigorous use of species richness, species diversity and the Shannon-Wiener- Index', *Global Ecology and Biogeography,* 12(3), pp. 177-179.

Spies, R.B. (2006) *Long-Term Ecological Change in the Northern Gulf of Alaska.* Amsterdam, NLD: Elsevier Science & Technology.

Sripada, R.P., Heiniger, R.W., White, J.G. and Meijer, A.D. (2006) 'Aerial Color Infrared Photography for Determining Early In-Season Nitrogen Requirements in Corn This project was supported in part by Initiative for Future Agriculture and Food Systems Grant no. 00-52103-9644 from the USDA Cooperative State Research, Education, and Extension Service', *Agronomy Journal,* 98, pp. 968-977.

Steinauer, K., Tilman, D., Wragg, P.D., Cesarz, S., Cowles, J.M., Pritsch, K., Reich, P.B., Weisser, W.W. and Eisenhauer, N. (2015) 'Plant diversity effects on soil microbial functions and enzymes are stronger than warming in a grassland experiment', *Ecology,* 96(1), pp. 99-112.

Stirling, G. and Wilsey, B.J. (2001) 'Empirical Relationships between Species Richness, Evenness, and Proportional Diversity', *The American Naturalist,* 158(3), pp. 286-299.

Stohlgren, T.J., Falkner, M.B. and Schell, L.D. (1995) 'A Modified-Whittaker Nested Vegetation Sampling Method', *Vegetation,* 117(2), pp. 113-121.

Stork, N.E. (1996) *Measuring Global Biodiversity and its Decline, In: Biodiversity II: Understanding and Protecting Our Biological Resources.* Washington, DC, USA: Joseph Henry Press.

Stow, D.A., Hope, A., McGuire, D., Verbyla, D., Gamon, J., Huemmrich, F., Houston, S., Sturm, M., Sturm, M., Tape, K., Hinzman, L., Yoshikawa, K., Tweedie, C., Noyle, B., Silapaswan, C., Douglas, D., Griffith, B., Jia, G., Epstein, H., Walker, D., Daeschner, S., Petersen, A., Zhou, L. and Myneni, R. (2004) 'Remote Sensing of Vegetation and Land-Cover Change in Arctic Tundra Ecosystems', *Remote Sensing of Environment,* 89(3), pp. 281-308.

Tanee, F.B.G. and Albert, E. (2015) 'Reconnaissance Assessment of Long-Term Effects of Crude Oil Spill on Soil Chemical Properties and Plant Composition at Kwawa, Ogoni, Nigeria', *Journal of Environmental Science and Technology,* 8(6), pp. 320-329.

Teillet, P.M., Staenz, K. and William, D.J. (1997) 'Effects of spectral, spatial, and radiometric characteristics on remote sensing vegetation indices of forested regions', *Remote Sensing of Environment,* 61(1), pp. 139-149.

The Ecumenical Council for Corporate Responsibility, (ECCR) 2010 *Shell in the Niger Delta: A Framework for Change-Five Case Studies from Civil Society*, ECCR, Oxford, United Kingdom.

Thenkabail, P.S., Enclona, E.A., Ashton, M.S., Legg, C. and de Dieu, M.J. (2004a) 'Hyperion, IKONOS, ALI, and ETM+ Sensors in the Study of African Rainforests', *Remote Sensing of Environment,* 90(1), pp. 23-43.

Thenkabail, P.S. and Lyon, J.G. (2016) *Hyperspectral Remote Sensing of Vegetation.* CRC Press.

Thenkabail, P.S., Mariotto, I., Gumma, M.K., Middleton, E.M., Landis, D.R. and Huemmrich, K.F. (2013) 'Selection of Hyperspectral Narrowbands (HNBs) and Composition of Hyperspectral Twoband Vegetation Indices (HVIs) for Biophysical Characterisation and Discrimination of Crop Types Using Field Reflectance and Hyperion/EO-1 Data', *IEEE Journal of Selected Topics in Applied Earth Observations and Remote Sensing,* 6(2), pp. 427-439.

Thenkabail, P., S., Enclona, E.A., Ashton, M.S. and Van Der Meer, B. (2004b) 'Accuracy Assessments of Hyperspectral Waveband Performance for Vegetation Analysis Applications', *Remote Sensing of Environment,* 91(3–4), pp. 354-376.

Tian, Y., Yao, X., Yang, J., Cao, W. and Zhu, Y. (2011) 'Extracting Red Edge Position Parameters from Ground- and Space-Based Hyperspectral Data for Estimation of Canopy Leaf Nitrogen Concentration in Rice', *Plant Production Science,* 14(3), pp. 270-281.

Tilman, D. (1996) 'Biodiversity: Population Versus Ecosystem Stability', *Ecology,* 77(2), pp. 350-363.

Tim Newbold, Lawrence N Hudson, Samantha L L Hill, Sara Contu, Igor Lysenko, Rebecca A Senior, Luca Börger, Dominic J Bennett, Argyrios Choimes, Ben Collen, Julie Day, Adriana De Palma, Sandra Díaz, Susy Echeverria-Londoño, Melanie J Edgar, Anat Feldman, Morgan Garon, Michelle L K Harrison, Tamera Alhusseini, Daniel J Ingram, Yuval Itescu, Jens Kattge, Victoria Kemp, Lucinda Kirkpatrick, Michael Kleyer, David Laginha Pinto Correia, Callum D Martin, Shai Meiri, Maria Novosolov, Yuan Pan, Helen R P Phillips, Drew W Purves, Alexandra Robinson, Jake Simpson, Sean L Tuck, Evan Weiher, Hannah J White, Robert M Ewers, Georgina M Mace, Jörn P W Scharlemann and Andy Purvis (2015) 'Global effects of land use on local terrestrial biodiversity', *Nature,* 520(7545), pp. 45-50.

Tovo, A. and Favretti, M. (2018) 'The distance decay of similarity in tropical rainforests. A spatial point processes analytical formulation', *Theoretical Population Biology,* 120, pp. 78-89.

Tran, T.H., Mayzlish Gati, E., Eshel, A. and Winters, G. (2018) 'Germination, physiological and biochemical responses of acacia seedlings *(Acacia raddiana* and *Acacia tortilis*) to petroleum contaminated soils', *Environmental Pollution,* 234, pp. 642-655.

Treitz, P.M. and Howarth, P.J. (1999) 'Hyperspectral Remote Sensing for Estimating Biophysical Parameters of Forest Ecosystems', *Progress in Physical Geography,* 23(3), pp. 359-390.

Treitz, P.M., Howarth, P.J. and Gong, P. (1992) 'Application of Satellite and GIS Technologies for Land-Cover and Land-Use Mapping at the Rural- Urban Fringe: A Case Study', *Photogrammetric Engineering and Remote Sensing,* 58(4), pp. 439-448.

Tucker, C.J. (1979) 'Red and photographic infrared linear combinations for monitoring vegetation', *Remote Sensing of Environment,* 8(2), pp. 127-150.

Tuomisto, H. (2010) 'A diversity of beta diversities: straightening up a concept gone awry. Part 1. Defining beta diversity as a function of alpha and gamma diversity', *Ecography,* 33(1), pp. 2-22.

Turner, W., Spector, S., Gardiner, N., Fladeland, M., Sterling, E. and Steininger, M. (2003) 'Remote sensing for biodiversity science and conservation', *Trends in Ecology & Evolution,* 18(6), pp. 306-314.

Ubom, R.M. (2010) 'Ethnobotany and Biodiversity Conservation in the Niger Delta, Nigeria', *International Journal of Botany,* 6(3), pp. 310-322.

Uddling, J., Gelang-Alfredsson, J. and Piikki, K. (2007) 'Evaluating the Relationship between Leaf Chlorophyll Concentration and SPAD-502 Chlorophyll Meter Readings', *Photosynthesis Research,* 91.

Udeh, N.U., Nwaogazie, I.L. and Momoh, Y. (2013) 'Bio-remediation of a Crude Oil Contaminated Soil Using Water Hyacinth *(Eichornia crassipes)*', *Advances in Applied Science Research,* 4(2).

Udoh, B.T. and Chukwu, E.D. (2014) 'Post-Impact Assessment of Oil Pollution on Some Soil Characteristics in Ikot Abasi, Niger Delta Region Nigeria', *Journal of Biology, Agriculture and Healthcare,* 4(24).

Ugboma, P.P. (2014) 'Effects of Oil Spillage on Soil Fertility in Udu Local Government Area in Delta State', *International Journal of Science and Technology,* 3(3).

Ugochukwu, C.N.C. and Ertel, J. (2008) 'Negative Impacts of Oil Exploration on Biodiversity Management in the Niger Delta Area of Nigeria', *Impact Assessment and Project Appraisal,* 26(2), pp. 139-147.

United Nations (2013) *The Millennium Development Goals Report.* Available at: http://www.un.org/millenniumgoals/pdf/report-2013/mdg-report-2013-english.pdf (Accessed: 01/2/2015).

United Nations (1997) *UN Conference on Environment and Development.* Available at: http://www.un.org/geninfo/bp/enviro.html (Accessed: 01/2/2015).

United Nations 1987 *Our Common Future:Report of the World Commission on Environment and Development (Brudtland Report)*, WCED, New York.

United Nations (1982) *World Charter for Nature.* Available at: http://www.un.org/documents/instruments/docs_en.asp?year=1980 (Accessed: November/24 2014).

United Nations Development Programme 2010 *UNDP Project Document on Niger Delta Biodiversity Project*, UNDP GEF.

United Nations Development Programme 2006 *Niger Delta Human Development Report*, UNDP, Abuja, Nigeria.

United Nations Environment Programme 1972 *Report of the United Nations Conference on the Human Environment*, United Nations Environment Programme, Stockholm.

United Nations Environmental Programme 2011 *Environmental Assessment of Ogoniland Report*, UNEP, Nairobi, Kenya.

United Nations Environmental Programme (1992) *Rio Declaration: Report of the United Nations Conference on Environment and Development.* Available at: http://www.unep.org/Documents.Multilingual/Default.asp?documentid=78&articleid=1163 (Accessed: November/24 2014).

United Nations General Assembly (2000) *Resolutions 55/201: Convention on Biological Diversity.* Available at: http://www.un.org/en/ga/search/view_doc.asp?symbol=A/55/PV.87 (Accessed: 2015).

United States Agency for International Development 2014 *Biodiversity Conservation and Forestry Programs, 2014 Report*, USAID, Washington DC.

United States Department of Agriculture- Natural Resource Conservation Service (2016) *Plants Database.* Available at: https://plants.usda.gov/ (Accessed: March 2017).

United States Environment Protection Agency, (USEPA) 2012 *Ecological Effects Test Guidelines: OCSPP 850.4150: Vegetation Vigour*, USEPA, United States.

United States Environment Protection Agency & U. S. EPA 2003 *Method 8015D (SW-846): Nonhalogenated Organics Using GC/FID*, U. S. EPA, Washington, DC.

United States Geological Survey, USGS (2016) *Landsat Science Products.* Available at: https://landsat.usgs.gov/landsat-science-data-products (Accessed: 23/02/2016).

Ustin, S.L., Gitelson, A.A., Jacquemoud, S., Schaepman, M., Asner, G.P., Gamon, J.A. and Zarco-Tejada, P. (2009) 'Retrieval of foliar information about plant pigment systems from high resolution spectroscopy', *Remote Sensing of Environment,* 113, Supplement 1, pp. S77.

Vaiphasa, T., Vaiphasa, C., Skidmore, A.K. and de Boer, W.F. (2007) 'A hyperspectral band selector for plant species discrimination', *ISPRS Journal of Photogrammetry and Remote Sensing,* 62(3), pp. 225-235.

Valderrama, L., Troche, C., Rodriguez, T.M., Marquez, D., Vazquez, B., Velazquez, S., Vazquez, A., Cruz, I.M. and Ressl, R. (2014) 'Evaluation of Mangrove Cover Changes in Mexico during the 1970-2005 Period', *Wetlands,* 34(4), pp. 747-758.

van den Berg, Abby K and Perkins, T.D. (2005) 'Nondestructive Estimation of Anthocyanin Content in Autumn Sugar Maple Leaves', *HortScience,* 40(3), pp. 685.

Vasilevich, V.I. (2009) 'Species Diversity of Plants', *Contemporary Problems of Ecology,* 2(4), pp. 297-303.

Vihervaara, P., Mononen, L., Auvinen, A., Virkkala, R., Lu, Y., Pippuri, I., Packalen, P., Valbuena, R. and Valkama, J. (2014) 'How to Integrate Remotely Sensed Data and Biodiversity for Ecosystem Assessments at Landscape Scale', *Landscape Ecology,* 30(3), pp. 501.

Vincini, M., Frazzi, E. and D'Alessio, P. (2008) 'A broad-band leaf chlorophyll vegetation index at the canopy scale', *Precision Agriculture,* 9(5), pp. 303-319.

Vogelmann, J.E., Rock, B.N. and Moss, D.M. (1993) 'Red edge spectral measurements from sugar maple leaves', *International Journal of Remote Sensing,* 14(8), pp. 1563-1575.

Vrieling, A. (2006) 'Satellite remote sensing for water erosion assessment: A review', *Catena,* 65(1), pp. 2-18.

Waide, R.B., Willig, M.R., Steiner, C.F., Mittelbach, G., Gough, L., Dodson, S.I., Juday, G.P. and Parmenter, R. (1999) 'The Relationship between Productivity and Species Richness', *Annual Review of Ecology and Systematics,* 30(1), pp. 257-300.

Wallace, A.R. (1862) 'On the Physical Geography of the Malay Archipelago', *Proceedings of the Royal Geographical Society of London,* 7(5), pp. 206-213.

Wallis, W.A. and Kruskal, W.H. (1952) 'Use of Ranks in One-Criterion Variance Analysis', *Journal of the American Statistical Association,* 47(257), pp. 583.

Wang, J., Zhang, Z., Su, Y., He, W., He, F. and Song, H. (2008) 'Phytoremediation of petroleum polluted soil', *Petroleum Science,* 5(2), pp. 167-171.

Wang, Y., Feng, J., Lin, Q., Lyu, X., Wang, X. and Wang, G. (2013) 'Effects of Crude oil Contamination on Soil Physical and Chemical Properties in Momoge Wetland of China', *Chinese Geographical Science,* 23(6), pp. 708-715.

Wang, Y., Zhu, H. and Tam, N.F.Y. (2014a) 'Effect of a polybrominated diphenyl ether congener (BDE-47) on growth and antioxidative enzymes of two mangrove plant species, Kandelia obovata and Avicennia marina, in South China', *Marine Pollution Bulletin,* 85(2), pp. 376-384.

Warren, S.D., Alt, M., Olson, K.D., Irl, S.D.H., Steinbauer, M.J. and Jentsch, A. (2014) 'The Relationship between the Spectral Diversity of Satellite Imagery, Habitat Heterogeneity, and Plant Species Richness', *Ecological Informatics,* 24, pp. 160-168.

Warrens, M.J. (2008) 'On Similarity Coefficients for 2X2 Tables and Correction for Chance', *Psychometrika,* 73(3), pp. 487-502.

Watts, M. (2004) 'Resource Curse? Governmentality, Oil and Power in the Niger Delta, Nigeria', *Geopolitics,* 9(1), pp. 50-80.

Whittaker, R.H. (1960) 'Vegetation of the Siskiyou Mountains, Oregon and California', *Ecological Monographs,* 30(3), pp. 279-338.

Wiesmair, M., Otte, A. and Waldhardt, R. (2017) 'Relationships between plant diversity, vegetation cover, and site conditions: implications for grassland conservation in the Greater Caucasus', *Biodiversity and Conservation,* 26(2), pp. 273-291.

Wilfong, B.N., Gorchov, D.L. and Henry, M.C. (2009) 'Detecting an Invasive Shrub in Deciduous Forest Understories Using Remote Sensing', *Weed Science,* 57(5), pp. 512-520.

Wilsey, B.J., Chalcraft, D.R., Bowles, C.M. and Willig, M.R. (2005) 'Relationships Among Indices Suggest That Richness is an Incomplete Surrogate for Grassland Biodiversity', *Ecology,* 86(5).

Wilson, E.O. and Peter, F.M. (eds.) (1996) *Biodiversity.* 13th edn. Washington, DC, USA: National Academies Press.

World Bank 1995 *Defining an Environmental Development Strategy for the Niger Delta. Vol. 1*, World Bank, Washington DC.

World Health Organisation (2015) *World Summit on Sustainable Development.* Available at: http://www.who.int/trade/glossary/story097/en/ (Accessed: 01/20 2015).

Wu, C., Niu, Z., Tang, Q. and Huang, W. (2008) 'Estimating Chlorophyll Content from Hyperspectral Vegetation Indices: Modeling and Validation ', *Agricultural and Forest Meteorology,* 148(8–9), pp. 1230-1241.

Wuana, R.A. and Okieimen, F.E. (2011) 'Heavy Metals in Contaminated Soils: A Review of Sources, Chemistry, Risks and Best Available Strategies for Remediation', *ISRN Ecology,* 2011(Article ID 402647).

Wulder, M. (1998) 'Optical Remote-Sensing Techniques for the Assessment of Forest Inventory and Biophysical Parameters', *Progress in Physical Geography,* 22(4), pp. 449-476.

Wulf, H., Mulder, T., Schaepman, M.E., Keller, A. and Jörg, P.C. (2015) *Remote Sensing of Soils.* 5.2nd edn. Zurich: University of Zurich.

Xiao, J., Shen, Y., Ge, J., Tateishi, R., Tang, C., Liang, Y. & Huang, Z. (2006) *Evaluating Urban Expansion and Land Use Change in Shijiazhuang, China, by Using GIS and Remote Sensing.* Available at:

http://www.sciencedirect.com/science/article/pii/S0169204605000058 (Accessed: 01/21 2015).

Xiao, X., Boles, S., Frolking, S., Salas, W., Moore, B., Li, C., He, L. and Zhao, R. (2002) 'Landscape-scale characterization of cropland in China using Vegetation and

Landsat TM images', *International Journal of Remote Sensing,* 23(18), pp. 3579-3594.

Xu, C., Li, Y., Hu, J., Yang, X., Sheng, S. and Liu, M. (2012) 'Evaluating the difference between the normalized difference vegetation index and net primary productivity as the indicators of vegetation vigor assessment at landscape scale', *Environmental monitoring and assessment,* 184(3), pp. 1275-1286.

Xue, J. and Su, B. (2017) 'Significant Remote Sensing Vegetation Indices: A Review of Developments and Applications', *Journal of Sensors,* 2017, pp. 1-17.

Yan, B., Wang, R., Wang, Z. and Gan, F. (2010) 'Minerals mapping of the lunar surface with Clementine UVVIS/NIR data based on spectra unmixing method and Hapke model', *Icarus,* 208(1), pp. 11-19.

Yang, L.Y., Gao, X.H., Zhang, W., Shi, F.F., He, L.H. and Jia, W. (2016) 'Estimating heavy metal concentrations in topsoil from vegetation reflectance spectra of Hyperion images: A case study of Yushu County, Qinghai, China', *Ying yong sheng tai xue bao = The journal of applied ecology,* 27(6), pp. 1775-1784.

Yoccoz, N.G., Nichols, J.D. and Boulinier, T. (2001) 'Monitoring of Biological Diversity in Space and Time', *Trends in Ecology & Evolution,* 16(8), pp. 446-453.

Yu, L. and Gong, P. (2012) 'Google Earth as a virtual globe tool for Earth science applications at the global scale: progress and perspectives', *International Journal of Remote Sensing,* 33(12), pp. 3966-3986.

Yuan, F., Sawaya, K.E., Loeffelholz, B.C. and Bauer, M.E. (2005) 'Land Cover Classification and Change Analysis of the Twin Cities (Minnesota) Metropolitan Area by Multitemporal Landsat Remote Sensing', *Remote Sensing of Environment,* 98, pp. 317-328.

Yussufu, B.A. (2010) 'Biodiversity and Ecosystem Services', *Economics for Ecology; 16th International Scientific Conference* Sumy, Ukraine.

Zak, D.R., Holmes, W.E., White, D.C., Peacock, A.D. and Tilman, D. (2003) 'Plant Diversity, Soil Microbial Communities, and Ecosystem Function: are There any Links?', *Ecology,* 84(8), pp. 2042-2050.

Zarco-Tejada, P.J., Berjón, A., López-Lozano, R., Miller, J.R., Martín, P., Cachorro, V., González, M.R. and de Frutos, A. (2005) 'Assessing vineyard condition with hyperspectral indices: Leaf and canopy reflectance simulation in a row-structured discontinuous canopy', *Remote Sensing of Environment,* 99(3), pp. 271-287.

Zegeye, H., Teketay, D. and Kelbessa, E. (2006) 'Diversity, regeneration status and socio-economic importance of the vegetation in the islands of Lake Ziway, south-central Ethiopia', *Flora,* 201(6), pp. 483-498.

Zeide, B. (1994) 'Big Projects, Big Problems', *Environmental Monitoring and Assessment,* 33, pp. 115-133.

Zha, Y., Gao, J. and Ni, S. (2003) 'Use of normalized difference built-up index in automatically mapping urban areas from TM imagery', *International Journal of Remote Sensing,* 24(3), pp. 583-594.

Zhang, B. (2010) 'Hyperspectral remote sensing of vegetation growing condition and regional environment', *2010 2nd Workshop on Hyperspectral Image and Signal Processing: Evolution in Remote Sensing*, pp. 1.

Zhang, C.G., Leung, K.K., Wong, Y.S. and Tam, N.F.Y. (2007) 'Germination, growth and physiological responses of mangrove plant (Bruguiera gymnorrhiza) to lubricating oil pollution', *Environmental and experimental botany,* 60(1), pp. 127-136.

Zhang, H., John, R., Peng, Z., Yuan, J., Chu, C., Du, G. and Zhou, S. (2012) 'The Relationship between Species Richness and Evenness in Plant Communities along a Successional Gradient: A Study from Sub-Alpine Meadows of the Eastern Qinghai-Tibetan Plateau, China', *PLoS ONE,* 7(11), pp. e49024.

Zhang, S., Huang, Y., Shen, C., Ye, H. and Du, Y. (2012) 'Spatial prediction of soil organic matter using terrain indices and categorical variables as auxiliary information', *Geoderma,* 171-172, pp. 35-43.

Zhang, Y., Chen, J.M., Miller, J.R. and Noland, T.L. (2008) 'Leaf Chlorophyll Content Retrieval from Airborne Hyperspectral Remote Sensing Imagery', *Remote Sensing of Environment,* 112(7), pp. 3234-3247.

Zhao, D., Huang, L., Li, J. and Qi, J. (2007) 'A Comparative Analysis of Broadband and Narrowband Derived Vegetation Indices in Predicting LAI and CCD of a Cotton Canopy', *ISPRS Journal of Photogrammetry and Remote Sensing,* 62(1), pp. 25-33.

Zhou, Y., Zhang, L., Xiao, J., Chen, S., Kato, T. and Zhou, G. (2014) 'A Comparison of Satellite-Derived Vegetation Indices for Approximating Gross Primary Productivity of Grasslands', *Rangeland Ecology & Management,* 67(1), pp. 9-18.

Zhu, L., Zhao, X., Lai, L., Wang, J., Jiang, L., Ding, J., Liu, N., Yu, Y., Li, J., Xiao, N., Zheng, Y. and Rimmington, G.M. (2013) 'Soil TPH concentration estimation using vegetation indices in an oil polluted area of eastern China', *PloS one,* 8(1), pp. e54028.

Zhu, Y., Yao, X., Tian, Y., Liu, X. and Cao, W. (2008) 'Analysis of common canopy vegetation indices for indicating leaf nitrogen accumulations in wheat and rice', *International Journal of Applied Earth Observation and Geoinformation,* 10(1), pp. 1-10.